UNIVERSITY OF SOUTHAMPTON

A Microscopic Simulation Model of Merging Operation at Motorway On-ramps

Pengjun Zheng

A thesis submitted in partial fulfilment of the requirements for the degree of Doctor of Philosophy in Transportation

Transportation Research Group
Department of Civil and Environmental Engineering
University of Southampton
Highfield,
Southampton
SO17 1BJ

June 2003

UNIVERSITY OF SOUTHAMPTON

ABSTRACT

FACULTY OF ENGINEERING AND APPLIED SCIENCE
DEPARTMENT OF CIVIL AND ENVIRONMENTAL ENGINEERING

Doctor of Philosophy

A MICROSCOPIC SIMULATION MODEL OF MERGING OPERATION AT MOTORWAY ON-RAMPS

by Pengjun Zheng

This thesis presents the development and application of a microscopic simulation model of merging operation at motorway on-ramps. At the core of the simulation model are several behavioural models of driver-vehicle system; each is capable of mimicking one of driving sub-tasks such as merging, car following etc. The simulation of merging operation is achieved through programming many driver-vehicle systems to interact according to the behavioural models within a simulated network. Two behavioural models developed and validated in this research are the model of car following behaviour and the model of merging behaviour.

Time-series data of merging manoeuvres and related motorway driving has been derived from the time-space trajectories of interacting vehicles. These have been based on detailed data collected in a large-scale, long-term observation using a combination of camera technology and the TRG instrumented vehicle. Data reduction and processing techniques have been developed and the accuracy of the data is discussed.

In this research, the fundamental understanding of merging behaviour has been improved by examining the merging process using accurate time-series data and incorporating driver's eye-movement analysis. The merging behaviour analysis has been extended to cover slip road upstream of the merge and passing vehicles on the shoulder lane of the motorway. The merging behaviour was analysed based on data on gap leaders, merging vehicles and gap followers, covering dynamic control behaviour of following gaps and gap acceptance behaviour etc. The model of merging behaviour achieved by treating two interacting traffic streams, the merging and passing traffic as an entity, shows a satisfactory performance. The model of car following behaviour has been developed based on an extensive investigation of possible model formulations using a data-driven approach. Detailed results from the model calibration and validation process are presented. The behavioural models have been implemented in a computer simulation program, and has been applied to evaluate the impacts of ramp metering on traffic operations. Results indicate that the simulation model reproduces realistic merging operations and can be used as a stand-alone simulation program for merging related applications. Alternatively, it could be implemented as a module in a network-wide traffic simulation model to replace the existing merging logic.

Contents

List of Figures

List of Tables

Acknowledgements

I am deeply indebted to Professor Mike McDonald who supervised the work, for his guidance and encouragement over many years; also, for providing a marvellous research environment and giving me the opportunity to come which eventually resulted in this work.

The work presented in this thesis would not have been possible without the contributions of many other people.

I would like to express my thanks to Dr. Jianping Wu and Dr. Mark Brackston for their help, advice and feedback on a variety of topics throughout this research.

Thanks to Brian for developing the time event logger and keeping the instrumented vehicle working properly, and to Eamon and Doug for their considerable efforts in making the behaviour experiment a success. Thanks also go to TRG staff and PhD students for their participation in the early morning experiment, to Melanie and Karen for their secretarial work.

Last, but not least, I would like to thank my wife, Qi and my son, Yifan, and all of my friends and colleagues in Southampton not mentioned so far, who have made living and studying in this city an enjoyable experience.

The author was supported by a scholarship from University of Southampton. Part of work was conducted on the TRG instrumented vehicle, funding for the construction of which has been provided by the Engineering and Physical Sciences Research Council in the U.K., the University of Southampton, and Lucas-TRW. Loop data was made available through Highway Agency.

Photos used in Figure 2.1, 2.4 and 2.7 were taken by Doug. Figure 2.9 and 2.14(a) was still shots from roadside and IV camera recordings. The copyright was therefore owned by Transportation Research Group of University of Southampton.

Chapter 1 Introduction

1.1 Background

Merging at on-ramps is one of the most complicated and important aspects of motorway operation. The combination of driver behaviour and vehicle capability under particular geometry configurations influences the operational performance such as delay, capacity and safety etc., for both merging and through traffic. Empirical evidence has suggested that merging operation is closely related to motorway flow breakdown, an increasingly common phenomenon with the increase in the traffic congestion in recent years (refer to [40], [41], [85]).

Early studies on merging operation focused on determining the relationships between geometric configurations and operational performance of on-ramp junctions using analytical and empirical methods. Several analytical models developed in the 1960s were used to study the problem of delay to the ramp traffic (e.g. [10], [69], [75]). However, they were based on assumptions that often required oversimplification and representations. Many empirical studies have also been conducted over the past half-century, to establish empirical models for design purposes (e.g. [57], [90]). However, empirical methods require the use of a high level resource and the results are not necessarily transferable to scenarios with significant differences in control strategies (e.g. ramp metering) and traffic composition etc. The alternative approach of microscopic simulation is increasingly able to model complex traffic behaviour. Such modelling is based on describing individual driver's behaviour in performing such driving tasks as car following, lane changing and gap-acceptance, and enables traffic operation to be investigated with great flexibility and in detail. Many simulation models have been developed to simulate the merging operation, e.g. Paramics, VISSIM, CORSIM, FRESIM, SISTM etc. [8]. However, because of the inherent complexity of merging behaviour and the difficulties of collecting the necessary detailed data for calibration, these models often demonstrate a poor ability to reproduce realistic merging operations. Most models only use some simple logic to describe very complex merging behaviour, typically gap-acceptance logic. A detailed understanding of driver behaviour under merging scenario is necessary and a microscopic merging behaviour model is essential for a more realistic evaluation of merging operation related issues.

The merging operations may influence conditions upstream, downstream and across lanes. This can be achieved in a simulation model using driver behaviour models for car following, lane changing, etc. However, as will be seen from the review detailed in Chapter 3, there is a lack of consistency of clear empirical or model findings in car following behaviour. This may result from the difficulties in collecting sufficiently accurate time series data in the past. Because of the importance of car following behaviour, there is a necessity to undertake further empirical observations and modelling.

1.2 Objectives

The objectives of this research have been to:

I. Develop fundamental understandings of driver behaviour during and adjacent to the motorway merging situations.
II. Develop a behavioural car following model for use in a microscopic simulation model.
III. Determine mathematical models of the merging process for use in a microscopic simulation model.
IV. Develop a microscopic simulation model incorporating the best available understanding of behaviour from the new empirical results and from previously published research findings.
V. Apply the model to determine new understandings of the effects of ramp metering measures on motorway merge operations.

The simulation model should enable a wide range of alternative Intelligent Transportation System (ITS) measures to be evaluated in future applications.

1.3 Terms and Definitions

Merging is the process by which two separate traffic streams moving in the same direction, i.e. entering ramp traffic and motorway traffic interact with each other and form a single stream. The complete process of merging involves a highly dynamic human decision and control process. The possible decision choices for merging drivers include accepting or rejecting a gap and speed choices. The driver of a motorway vehicle may choose to change lane or change speed to facilitate merging or to gain an advantage. The final performance of a merging operation is the result of a combined effect of the behaviour of the different drivers involved, the vehicle dynamics and the geometric characteristics of the merge.

There are different types of merge, e.g. normal (taper) merge, parallel lane merge, ghost island merge etc. Common to all merges is the interacting area where and only where ramp traffic can move into a

gap in motorway traffic. Using taper merge as an example (Figure 1.1), some relevant terms and definitions are given as follows (refer to [52], [88]):

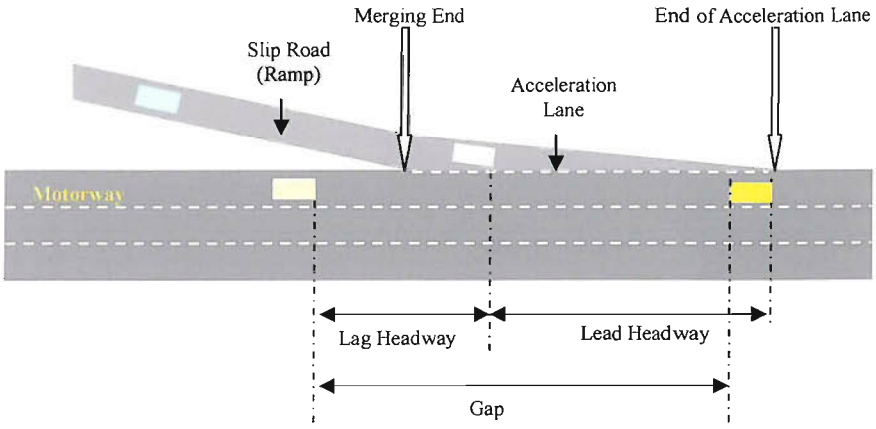

Figure 1.1 A Typical Taper Merge

- **Ramp or Slip Road**: A connecting roadway between two intersecting or parallel roadways, one end of which joins in such a way as to produce a merging operation. In this research, a ramp (slip road) is the section of roadway ended at the point where the left edge of the ramp intersects the left edge of the motorway (including acceleration lane).
- **Merging End**: The point where the right edge of the ramp intersects the left edge of the motorway or where transition of vehicle to motorway is first possible.
- **Acceleration Lane**: The section of roadway from merging end to where the left edge of the ramp intersects the left edge of the motorway.
- **End of Acceleration Lane**: The point where the left edge of the acceleration lane intersects the left edge of the motorway.
- **Ramp (merging) Traffic**: Vehicles originated from the slip road and joining the main traffic.
- **Motorway (passing) Traffic**: Vehicles originally on the motorway upstream before approaching merging area.
- **Merging**: The process by which vehicles in two separate traffic streams moving in the same direction to form a single stream.
- **Multiple Merging**: When two or more vehicles merge into a single motorway gap.
- **Motorway Gap**: The time or distance interval between successive motorway vehicles moving in the same direction with respect to a reference point. An inter-vehicular gap is measured from the rear-bumper of the leading vehicle to the front-bumper of the corresponding following vehicle.
- **Motorway Gap Follower**: The motorway vehicle which forms the end of a motorway gap.
- **Motorway Gap Leader**: The motorway vehicle which forms the start of a motorway gap.

- **Headway**: The distance from the front bumper of the leading vehicle to the front bumper of the following vehicle (bumper-to-bumper headway) or the distance from the rear bumper of the leading vehicle to the front bumper of the following vehicle (rear-to-front headway). In this research, the headway refers to bumper-to-bumper headway unless otherwise stated.
- **Time Headway**: The time interval of passing a reference point between two consecutive vehicles. In this research, the time headway refers to bumper-to-bumper time headway unless otherwise stated.
- **Lag Headway**: The headway between a merging vehicle and the corresponding motorway gap follower.
- **Lag Time**: The time headway between a merging vehicle and the corresponding motorway gap follower.
- **Lead Headway**: The distance headway between a merging vehicle and the corresponding motorway gap leader.
- **Lead Time**: The time headway between a merging vehicle and the corresponding motorway gap leader.
- **Start of Merging**: The time at which the right front wheel of a merging vehicle passes the separation line between acceleration lane and motorway shoulder lane.
- **End of Merging**: The time at which the left front wheel of a merging vehicle passes separation line between acceleration lane and motorway shoulder lane.

1.4 Modelling Approaches

Motorway merging may be modelled using microscopic simulation, in which the individual behaviour of each driver is represented, or through a variety of other analytical models. This section considers the different modelling approaches to justify the use of simulation, and the need for improved simulation, as appropriate for this study. The detailed review of car following is given in Chapter 3.

1.4.1 Analytical Models

Analytical models have largely been focused on the problem of delay to merging vehicles in a merging situation. The modelling approach was a direct extension to the work on the gap acceptance problem at the stop intersections. Typical configuration of problem has been described like this [69]:
When a merging vehicle arrived at the merging end at a speed of $v(0)$, the driver observed a gap (t) in the motorway traffic, which was distributed with a known probability density function (pdf) of $\varphi(t)$. The driver accepted it with probability $\alpha[t, v(0)]$ (the gap acceptance function). If he/she rejected the gap, he/she immediately proceeded onto the acceleration lane. After a time τ he/she was passed by a

vehicle on the motorway, and at this instant he/she observed a new gap of length t, which was accepted with a probability $\alpha[t,v(\tau)]$. In this way, the merging problem was converted to a gap acceptance problem in a moving coordinate with the same speed as the merging vehicle. If the length of the acceleration lane was infinitive and the speed of the merging vehicle did not equal to the speed of motorway vehicles, the number of gaps presented to the merging vehicle was infinitive and there would always be a gap that a merging vehicle could accept. If the length of the acceleration lane was limited, as assumed by Blumenfeld et al. [10], the number of gaps presented to the merging vehicle while he/she was moving was finite. It was assumed that the merging vehicle would stop at the end of acceleration lane if no gap were accepted during movement. New gaps would continuously be presented to the stopped merging vehicle until he/she could accept one (In general, the problem was reduced to that of a simple intersection).

Under the framework of the above simplification of merging operation, operational performance such as delay to ramp traffic and probability of merging at the acceleration lane could be addressed analytically. The determining factors were:

1) motorway gap distribution, $\varphi(t)$
2) motorway traffic speed, V
3) ramp traffic speed function, $v(\tau)$
4) gap acceptance function $\alpha(v(\tau),t)$
5) acceleration lane length, L.

Further simplifications were made in deriving mathematical expressions. In work reported in [10], the speeds of both merging and motorway vehicles were assumed to be constant, namely v and V respectively. The gap of motorway traffic was assumed to be distributed negative exponentially:

$$\varphi(t) = \lambda \exp(-\lambda t)$$

The step function was chosen as the gap acceptance function, for moving and stopped merging vehicle, they were:

$$\alpha_m(t) = H(t - T_m) \text{ and}$$

$$\alpha_s(t) = H(t - T_s)$$

where t denotes gap size, T_m and T_s is the critical gap size for moving vehicle and stopped vehicles respectively .

Three possibilities existed as to the gap acceptance of the merging vehicle:

1) Merging vehicle accepted a gap when he/she arrived at the merging end.
2) Merging vehicle accepted a gap at time τ during travelling on the acceleration lane.
3) Merging vehicle stopped at the end of acceleration lane and accepted a gap later.

The availabilities of new gaps to a moving merging vehicle were determined solely by the speed difference between the merging vehicle and the motorway traffic volume. The gap distribution viewed from a moving co-ordinate was:

$\varphi_1(t) = \beta\lambda \exp(-\beta\lambda t)$, where $\beta = 1 - v/V$

If $v=V$, the mean time headway would be infinitive, i.e., no new gap would be presented to a merging vehicle except the original one.

The expected total delay could be calculated with known moving gap acceptance function $\alpha_m(t)$ (merging vehicle not stopped), stopped gap acceptance function $\alpha_s(t)$ (merging vehicle stopped), gap density $\varphi(t)$ and moving headway density, $\varphi_1(t)$.

Similar research by Mine et al. was based on the assumption that the length of the acceleration lane was infinitive [69], where the speed of merging vehicle on acceleration lane was expressed as a function $v(\tau)$, and the gap acceptance function was dependent on $v(\tau)$, that was $\alpha[t,v(\tau)]$. The probability density function of the delay to the merging vehicle could be obtained analytically.

The advantage of an analytical model is that the relationship between delay and contributing factors such as motorway flow rate (λ), length of acceleration lane (L) and gap acceptance parameters (T_s, T_m) are directly expressed in a functional form. The effects of contributing factors can be evaluated efficiently and completely. However, it is based on several assumptions that may be unrealistic. Firstly, the model does not consider the arrival condition of ramp traffic. The delay distribution is derived based on one merging vehicle, and possible multiple-merge situations are excluded. Thus, the model is only valid when ramp flow rate is low. Secondly, the gap-acceptance function is based on rational, homogenous and consistent driver behaviour, i.e., drivers are assumed to merge into main traffic as soon as there is a suitable gap, and differences between and within drivers are not taken into account. Thirdly, the assumption of constant (or time function) speed of merging vehicle and constant speed of motorway traffic is not realistic as both ramp and motorway drivers are able to dynamically control their speed in merging processes. Also, the rationale of using gap size as the only criteria in gap acceptance is doubtful.

Several later studies attempted to partly relax the assumptions of the above-mentioned models by using more complicated form of gap acceptance function, e.g. Polus et al, Kita etc. (refer to [48], [76]) However, the observation of gap-acceptance behaviour with moving coordinates was very difficult. Instead, gap acceptance functions were usually derived based on observation at a fixed reference point.

In the analytical approach, it was not found possible to relax many assumptions and achieve a more realistic model. In addition, analytical models were unable to address the impacts of merging operation

in changed situations, particularly, under advanced telematics, such as ramp metering. Apart from their theoretical value, the application of analytical models was limited.

1.4.2 Simulation Models

Simulation has gained popularity with the rapid advances in computer technology. A simulation model contains several behavioural models mimicking the behaviour of basic traffic elements, the driver-vehicle system. The traffic system is treated as an aggregation of individual driver-vehicle elements, which is entirely consistent with the nature of the problem to be modelled. In the context of merging operation, a number of microscopic behavioural models have been developed.

Although merging operation involved two interacting traffic streams, most studies have only modelled ramp traffic behaviour based on the assumption that merging behaviour had no influence on the motorway traffic. Typical of this approach is the research of Michaels and Fazio [67]. For merging vehicles, the merging process was divided into five sub-tasks:

1) Ramp curve tracking;
2) Steering from the ramp curvature onto Speed-Change-Lane (SCL);
3) Accelerating from the ramp controlling speed up to a speed closer to the freeway speed;
4) Searching for an acceptable gap;
5) Steering from the acceleration lane onto the motorway lane 1 or aborting.

Sub-tasks 3 and 4 could be repeated several times as necessary. The merging model then addressed two aspects of merging driver's behaviour on the acceleration lane: the speed control and gap acceptance. Michaels et al. used an angular velocity threshold in describing gap acceptance behaviour (angular velocity model). The model assumed that there was an iterative process of gap search and acceleration. The iteration continued until the merging vehicle speed equalled or exceeded motorway speed or the merging vehicle ran out of acceleration lane. The decision to merge was determined entirely by the angular velocity of the lag vehicle. A driver would accept a gap if he/she were below an angular velocity threshold, If not, he/she would accelerate at a constant rate which could lead him/her to a smaller speed difference with the motorway vehicles. Empirical data was used to derive the angular velocity threshold and test the model. The angular velocity was measured at the start of merging, median was used as the threshold, which was 0.004 rad/sec. No speed function was given.

Many other models took similar approaches although the iteration process was not considered. Emphasis was specially paid to gap acceptance behaviour, described by a gap-acceptance function. As a result of extensive empirical observations, a number of gap acceptance functions were developed. Two main varieties emerged from different researches. The first was the form of function, which included the step function using a fixed threshold, and probabilistic distribution function for accepting

a gap. The second was the argument of the gap acceptance function, which included gap size, lag time, angular velocity or some combination. For example, Michaels, et al. [67] modelled gap acceptance behaviour using angular velocity while Skabardonis [88] used a step function based on a lag time:

$H(t-L_{cr})=1 \quad t>L_{cr}$

$=0 \quad t<L_{cr}$,

where L_{cr} is the critical lag time, which was assumed to vary between drivers and also depend on the relative speed. Three kinds of distributions, normal, log-normal and exponential, had been assumed to represent the variability between the drivers. Szwed also reported a similar treatment, where critical gap was assumed to be log-normally distributed between drivers [90].

More complicated forms of gap acceptance function have also been used in simulation models. Kou devised a binary logit gap acceptance function with perceived merging driver angular velocity to a corresponding motorway lag vehicle, and the remaining distance to the acceleration lane end as decision criteria [52].

For the speed control behaviour of the ramp traffic, common assumptions have included constant speed and constant acceleration ([32] and [74]) or iterative steps of constant acceleration [67]. Several models have used car following theory to describe the movement of merging vehicle, which was especially pertinent to a platoon of merging vehicles. Of the few models that described the acceleration behaviour of merging vehicles on the acceleration lane in detail, Kou et al proposed a microscopic model based on stimulus-response car following theory [53]. In the approach, the acceleration rate of merging vehicles was decided by the relative location and speed to the gap leaders and gap followers on the motorway as well the distance to the end of the acceleration lane. The model was expressed using a distance scale, because the directly reduced data was based on several reference positions. The parameters of the model were obtained by non-linear regression, and the goodness of fit, in terms of an R value, was poor. Further efforts were made to improve the validity of the model by separating different acceleration regimes. A multinomial probit model, using speed differentials, distance separations of merging vehicles to corresponding motorway and merging vehicles, distance to the end of acceleration lane etc. as attributes, was devised to predict merging driver acceleration, deceleration, or constant speed choice. The magnitudes of the acceleration/deceleration rates of merging vehicles in each regime were predicted by a family of exponential curves using merging vehicle speed as variable. An improved correlation was reported.

Skabardonis [89] used a different procedure where acceleration behaviour was associated with gap acceptance choice. He assumed a constant acceleration/deceleration rate of the merging driver, which was situation dependent and generated from a distribution. Once a merging driver arrived at the acceleration lane, if immediate gap-structure was available, he/she merged accelerating at a rate f_m

depending on his speed, which was assumed to be normally or log-normally distributed. Otherwise, a theoretically required acceleration rate in order to create an acceptable lag was computed, if it was less than f_m, then the driver accelerated to create an acceptable gap. If not, driver decelerated at a constant rate that could ensure a safe stop at the end of acceleration lane.

Basically, the above models only covered part of the merging operation, i.e., the behaviour of ramp traffic. Motorway traffic was not considered so that the possible influences of merging operation on motorway traffic could not be addressed within the modelling framework.

Besides the explicit assumptions made in each model, there were underlying assumptions common to these modelling approaches that the merging behaviour was not interactive and dynamic. Implicitly, merging vehicle was assumed to have no influence on the behaviour of other merging/passing traffic. Only the gap-structure of motorway traffic, which was flow-rate dependent, could affect the gap-acceptance behaviour of merging drivers. Speed control and gap-acceptance was treated as totally separate behaviour in most models. With the very limited choice of speed control strategy, either keeping a constant speed, or a fixed rate of acceleration/deceleration, the merging driver behaviour was implicitly assumed not to be dynamic.

From the above introductory background it may be seen that available behavioural models of merging behaviour are incomplete, the behaviour of one of the interacting traffic streams involved in merging operation, the motorway traffic, was not modelled under merging scenarios. Also, the behavioural model of ramp traffic was established on several simplifying assumptions, the rationale of these assumptions had not been properly justified.

1.5 Scope of Study

The merging operation involves two interacting traffic streams that perform nearly every driving sub-tasks, e.g., follow-the-leader, gap acceptance, lane changing etc. To make the problem more complicated, it is not easy to find a clear boundary within which a driver's behaviour can be associated with one sub-task. For example, both ramp and motorway vehicles normally need to follow the leader before, during and after merging. Therefore, it was necessary to define a scope for this study in order to make the work manageable.

It has been neither possible nor practical to develop all the behavioural models necessary to simulate all aspects of a merging situation in this research. At the Transportation Research Group (TRG) of University of Southampton, research on the microscopic simulation of driver behaviour on motorways

has been carried out in the past decade. Several behavioural models such as car following and lane changing etc. have been developed and validated (refer to [9], [62], [87], [103]). It is possible to implement some of them directly into the simulation model. For this research, it was decided to focus on the development of two behaviour models, the merging behaviour model and the car following behaviour model.

1.6 Thesis Overview

Chapter 1 has introduced the problem framework and objectives of this thesis research, defined the scope of study and discussed related work.

Chapter 2 introduces the experiment for empirical data collection; presents data reduction procedure, data accuracy analysis results and data integration method.

Chapter 3 introduces the development of a fuzzy logic car following behaviour model and presents improved performance obtained.

Chapter 4 introduces the development of the merging behaviour model, discusses the dynamic aspects in merging behaviour and presents the results of merging behaviour analysis and model validation.

Chapter 5 introduces implementation of the computer simulation and provides an application of the model in evaluating the local impact of ramp metering.

Chapter 6 summarises the work and contributions presented in this research and discusses directions for future research.

Chapter 2 Data

Empirical data is essential to develop understandings, calibrate and validate models. This Chapter introduces the data collection and reduction procedures. The long-term large-scale experiment at a motorway junction is described as well as the comprehensive database of merging and car following behaviour. The empirical database was collected as part of a study of ramp metering for the Highway Agency, and was focused to enable this research to be included.

2.1 Data Collection

The literature review described in Section 1.4 has revealed that studies on quantitative modelling of merging operation were few, especially for behaviour of dynamic interactions between merging and motorway vehicles. A comprehensive observation covering both merging traffic and motorway traffic will be necessary for a better understanding of microscopic interactions under merging scenario. This requires time series data to be collected for relevant vehicles during merging process at representative sites.

In this research, merging behaviour was observed at Junction 11 on the M27 near Southampton in UK, one of the ramp metering test sites (Figure 2.1). This site was suitable for merging behaviour observation because:

- At this site, the merging traffic on offside ramp lane joins the main carriageway through a taper merge, this kind of merge is typical in UK.
- The motorway is in a cutting and an elevated bank makes it suitable for setting up video cameras
- Congestion occurred regularly at this site and the upstream junction (Junction 10) in the morning peak, so that merging operation can be observed at a wide range of traffic scenarios.

The experiment was carried out in the morning peak hours from 7 a.m. to 9 a.m., when the interactions between ramp and motorway traffic is frequent. Although the existence of minor slope in approaching this junction may slightly affect the maximum acceleration ability of vehicles, it is believed that the effect will be not significant compared with acceleration capability of modern passenger cars. Drivers are usually able to compensate the slope effect by increasing throttle deployment.

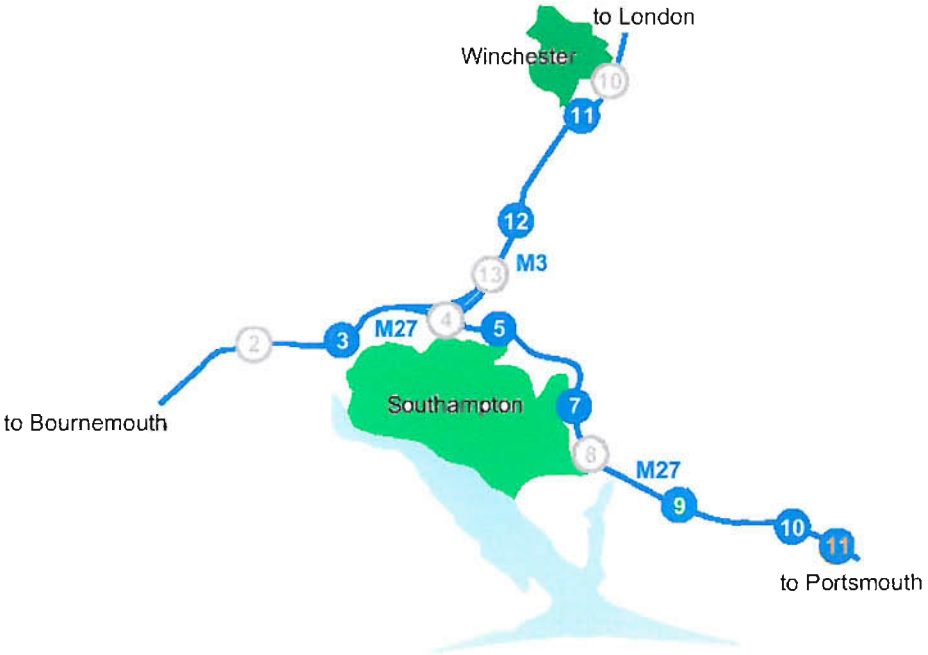

Figure 2.1 Site Location Map

Figure 2.2 Geometry of the Experiment Junction

2.1.1 Geometry

The geometry of the survey junction is shown in Figure 2.2. The junction incorporates Ghost Island merge with an extended nearside lane merge of about 1000 meters. The offside ramp lane joins the main carriageway with a taper merge. At this location, the motorway is in a cutting and an elevated bank makes it suitable for setting up video cameras for observation. The merging behaviour used in this study is based on the data collected at this taper merge. The layout of the taper merge is shown in Figure 2.3.

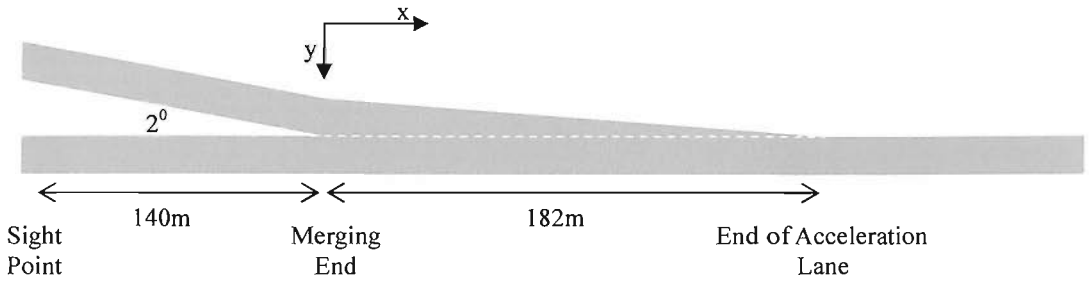

Figure 2.3 Layout of the Taper Merge

The 'sight point' (i.e., the position where the ramp traffic and motorway traffic can view each other) is about 140 meters upstream of the merging end and the acceleration lane is 182 meters long. The observation of merging behaviour was limited to this taper merge because of budget and time constraints.

2.1.2 Instrumentation and Measurements

The measurement requirements to study driver behaviour determine the possible choices of instrumentation. Within the two traffic streams involved in a merging process, microscopic interactions can occur between a ramp vehicle and several other vehicles either on the acceleration lane or adjacent motorway lane. Although many past studies have assumed that a merging vehicle had no influence on motorway traffic, the rationale of this assumption had not been properly justified. Within this research it was decided to include measurement of the merging vehicle and those adjacent vehicles who could be influenced in the merging process as part of the database.

The measurement requirements for car following behaviour are relatively easy to identify. Follow-the-leader behaviour mainly involves the interactions between a pair of vehicles on the same lane, i.e., the leader and the follower.

Drivers are able to control a vehicle with throttle/brake and steering. For any driver-vehicle system, its state can be described by six variables:

- **Longitudinal Position (x)**
- **Longitudinal Speed (x')**
- **Longitudinal Acceleration (x'')**
- **Lateral Position (y)**
- **Lateral Speed (y')**
- **Lateral Acceleration (y'')**

Steering control is more usually associated with lane keeping and curvature tracking behaviour and will not be considered in this research. Lane number will be used to describe the lateral position of a driver-vehicle system. This results in the simplified measurement requirements of **Position (x), Speed (x'), Acceleration (x'') and Lane Number (y).**

In a car following situation, the lane number is of no importance, as a pair of vehicles must be on the same lane according to the definition of car following. All measurements must be made continuously in order to capture dynamic features. In practice, this is achieved through time-series measurements sampled at an appropriate rate. It should be noted that the first three state variables, i.e. position, speed and acceleration may be estimated from each other, as long as measurements are sufficiently accurate. In addition, some time-discrete events, such as drivers' eye-movement, start merging, end merging and lane changing, are important in characterising merging behaviour, and need to be recorded. The measurements fall into two categories:

- Time-series data of driver-vehicle system
- Time-discrete events of interest

Three candidate techniques identified to meet the above requirements of measurement were video camera, radar speedometer and instrumented vehicle (IV). Each is considered below.

2.1.2.1 Video Camera

Previous empirical observations on merging behaviour have made extensive use of camera technology (refer to [1], [52], [91]). It can be effective and easy to implement. Cameras set facing down a merging area enable the recording of time-space trajectories of vehicles. Measurements of interest, such as speed, relative speed and headway, can be obtained through an appropriate data reduction procedure. The main disadvantage of camera technology is that each camera can cover only a short section of road from a fixed location, and the accuracy may be rather limited.

Event times of interest can be identified by playing videotapes frame by frame. The time measurement accuracy is equal to the frame-time-resolution of the video recording/playback system. The precise location of a vehicle within a frame may be difficult to measure, because of the reduced size of image

and optical deformation. A practical way is to draw reference lines of known position on the image. Two raw measurements can be made for each vehicle, the location and the associated time at this location. Other outputs can only be estimated from the raw measurements.

Kou has undertaken a theoretical analysis of error in speed measurement using camera technology [52]. The distribution of speed measurement error was found to be:

$$f(\varepsilon)=[k-\frac{k^2}{v}(\frac{\varepsilon D}{v+\varepsilon})]\frac{D}{(v+\varepsilon)^2}(for \quad 0\le\varepsilon\le\frac{v^2}{kD-v}) \tag{2.1}$$

$$f(\varepsilon)=[k+\frac{k^2}{v}(\frac{\varepsilon D}{v+\varepsilon})]\frac{D}{(v+\varepsilon)^2}(for \quad \frac{-v^2}{kD+v}\le\varepsilon\le 0) \tag{2.2}$$

where: k is the time resolution of a video recorder/playback system

v is the actual speed of car to be measured

D is the distance between two reference lines.

Figure 2.4 shows the speed measurement error when k=25 frames/sec and D=9 m. The error will be within 2 m/s under 95% probability at a typical traffic speed of 25 m/s. Increasing the distance intervals between adjacent reference lines, D, can improve the average speed measurement accuracy. However, D also determines the possible direct measurement points, and accordingly, the sampling rate, which is v/D (Hz). Dynamics of behaviour cannot be captured if the sampling rate is too low. Typical merging processes only last for about a few seconds, and leaves little room for the choice of D. Therefore, the accuracy of average speed measurement using video technology is no better than 2 m/s under typical traffic condition, and point speed measurement is impossible.

The position measurement error at the time-resolution of k is between [-v/2k, v/2k], supposing the reference line position is sufficiently accurate, e.g. about $\pm$1m. Accurate assessment of higher time derivatives such as acceleration is virtually impossible given the low accuracy of speed measurement. Theoretically, the acceleration rate measurement error is:

$$\eta=\frac{\varepsilon_2-\varepsilon_1}{t+D/v} \tag{2.3}$$

where ε is speed measurement error with a distribution of Equation (2.1) and (2.2), v is the actual average speed and t and D are defined above. It is clear that the error will be larger than that of speed measurement at normal traffic speeds, i.e., the acceleration measurement error will be greater than 2 m/s^2 given a speed measurement error of 2 m/s. A measured acceleration rate with an error of 2 m/s^2 will be of little value in this study, as it is larger than typical acceleration/deceleration rates drivers will

use when merging. In conclusion, video camera technology is able to measure position and average speed with limited accuracy.

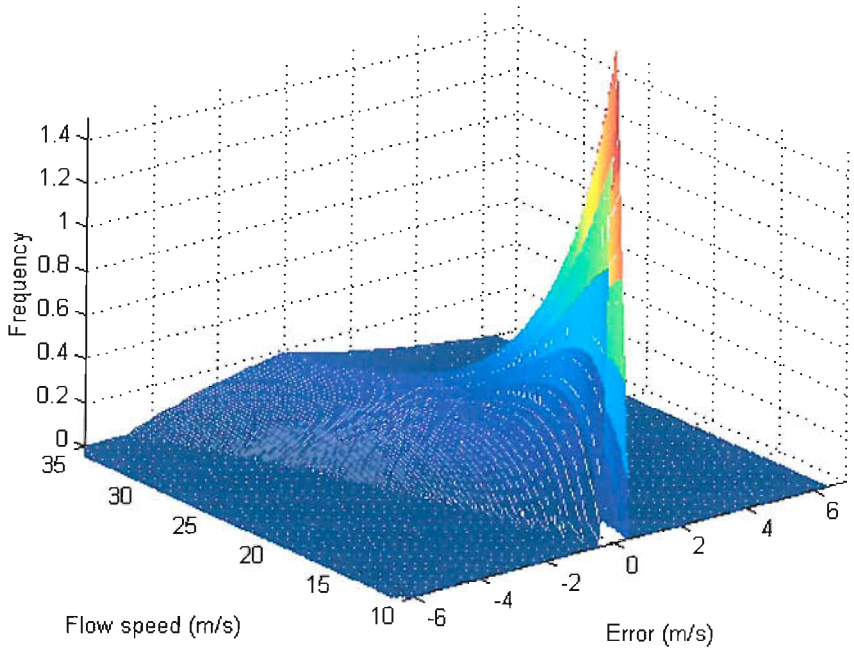

Figure 2.4 Distribution of Speed Measurement Error

2.1.2.2 Radar Speedometer

Huberman had used a radar speedometer technique to measure acceleration on ramps [42]. However, as the relative position of vehicles could not be measured using this technique, it was considered not suitable for a complete measurement of merging behaviour.

2.1.2.3 Instrumented Vehicle

An instrumented vehicle is a conventional car equipped with a variety of sensors. It has been shown to be very powerful in collecting dynamic traffic data accurately at high sampling rates. The instrumentation has been used in a wide range of behavioural research, e.g., car following, lane changing etc (refer to [12], [61], [63], [64]). An instrumented vehicle can enable relevant measurements to be directly taken while moving for at least three vehicles, the IV itself, the direct leader and follower in a straight line. Another important benefit is that close observation of driver

behaviour from inside the vehicle can be made for the subjects. This is not possible using camera technology.

Figure 2.5 TRG Instrumented Vehicle

The TRG instrumented vehicle is shown Figure 2.5. The sensors with which it is equipped include:

- Two Radar, for measuring headway and relative speed of leading and following vehicles.
- A Laser Speedometer, for measuring IV speed and distance travelled.
- A GPS Receiver, for measuring real time position.
- Other Sensors, for measuring brake movement, throttle movement, indicator use, brake light state etc.
- Three Cameras, typically facing front, rear and driver.

All the readings from the sensors can be saved on an in-vehicle computer at a sampling rate of 10 Hz. Video images from cameras superimposed with time synchronised to GMT (GPS provided) can be recorded using two in-vehicle video recorders. One for front facing camera and another for images from a Quad Image Mixer where images from three cameras (facing front, rear and driver) are mixed, each occupying a quarter of the mixed image.

The accuracy of sensors as stated by the manufacturers is:

- Speedometer: 1 km/h (0.278 m/s).

- Radar: 20 cm per 100m for relative distance measurement, 0.5 m/s for relative speed measurement.

GPS positioning error can be affected by a lot of factors other than receiver itself. Without selective availability (SA), it is about 15 meters according to recent field observation [86].

The instrumented vehicle outperforms video camera technology for accuracy of measurement. Although GPS does not enable the measurement of real time position very accurately, the speedometer can be used to estimate position by counting distance travelled from a reference point of known position. Sensor readings from the IV are directly digitised and can be easily exported from the IV computer for further processing. Other benefits of the IV measurement include, for example, the movement of drivers' eyes can be directly observed from an in-vehicle camera facing the driver, brake-movement and throttle-movement can also be measured.

There are also shortcomings associated with IV instrumentation. The radar can only cover the targets within a narrow sector (8^0 for TRG IV) in its direction. In a merging process, even the direct gap leaders and gap followers are not always positioned in such a way as to be within the radar beam. Temporary loss of targets is possible, and information on vehicles other than the direct leader and follower is often desirable. Therefore, merging behaviour of interest cannot be measured completely using an IV alone.

2.1.2.4 Combined Measurements

To overcome the shortcomings of a single data collection method, a combination of Instrumented Vehicle and camera technology was used to observe the whole process of merging. Cameras were able to measure a time-space trajectory of all vehicles within a fixed observation area, including the vehicles outside the coverage of IV Radar. The IV is able to observe its gap leader and follower continuously and accurately whilst moving. It can cover a much longer road section than any camera or cameras. The combination offers a suitable instrumentation for this research.

2.1.3 Route

The experimented route used by the IV is illustrated in Figure 2.6. The subjects drove two predefined routes alternatively. The first is a merging route (B-C-A) in which the IV merges at junction B from the offside taper merge and then returns from downstream junction C, goes to upstream junction A preparing for the next passing trial. The second route is as a passing route (A-C-B). The IV passes junction B on the motorway shoulder lane and then returns from downstream junction, entering junction B in preparation for the next merging trial. Each route involves a period of motorway driving.

The data collected during this motorway driving is used for the study of car following behaviour.

The inclusion of passing route provides the opportunity for a more complete and accurate observation of merging operation, than could be achieved using cameras.

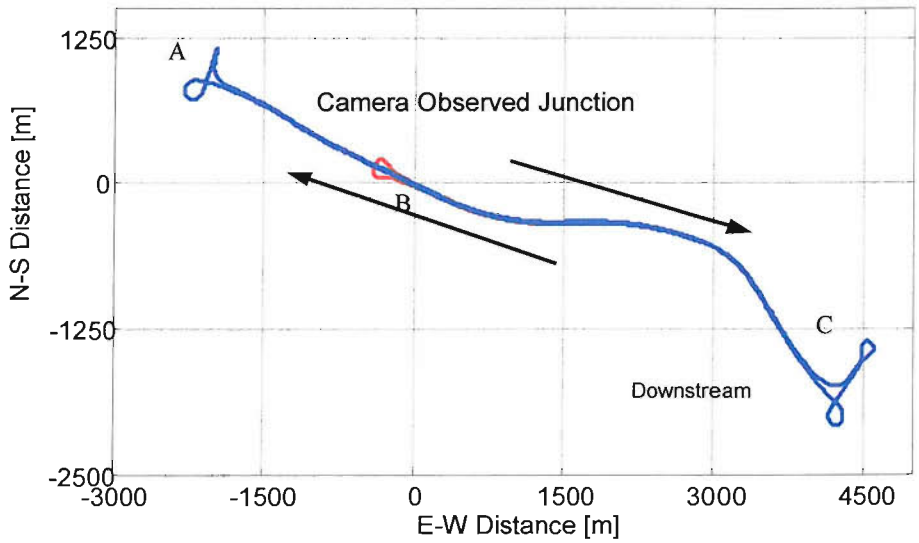

Figure 2.6 Experiment Route (GPS measured)

2.1.4 Arrangement of Cameras

Ten cameras were set on the bank above the slip road at appropriate intervals. The arrangement of cameras was made in such a way that an overlapping area was created between two adjacent cameras (Figure 2.7). This was necessary in order to synchronise time base between cameras in later data reduction stage.

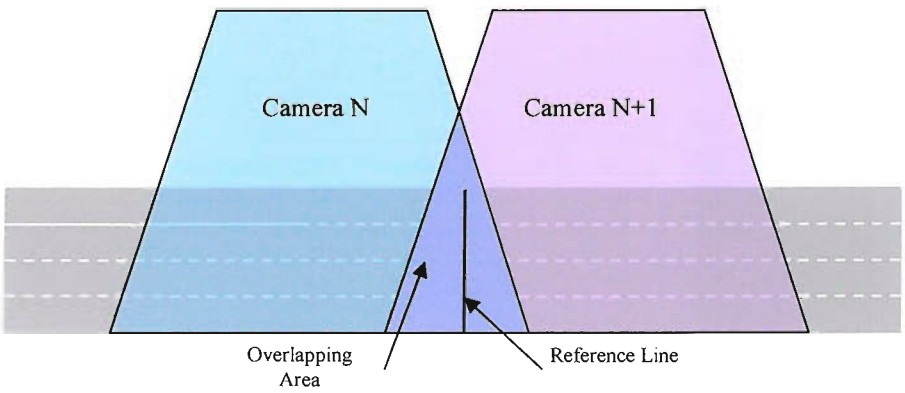

Figure 2.7 Overlapping Between Cameras

Any vehicle passing a reference line inside overlapping area was recorded by adjacent cameras. The difference in the time-base between adjacent cameras can be calculated by comparing the registered event times for the same event. Thus, time-base between adjacent cameras can be synchronised to as accurate as the time resolution of the recorder/playback system.

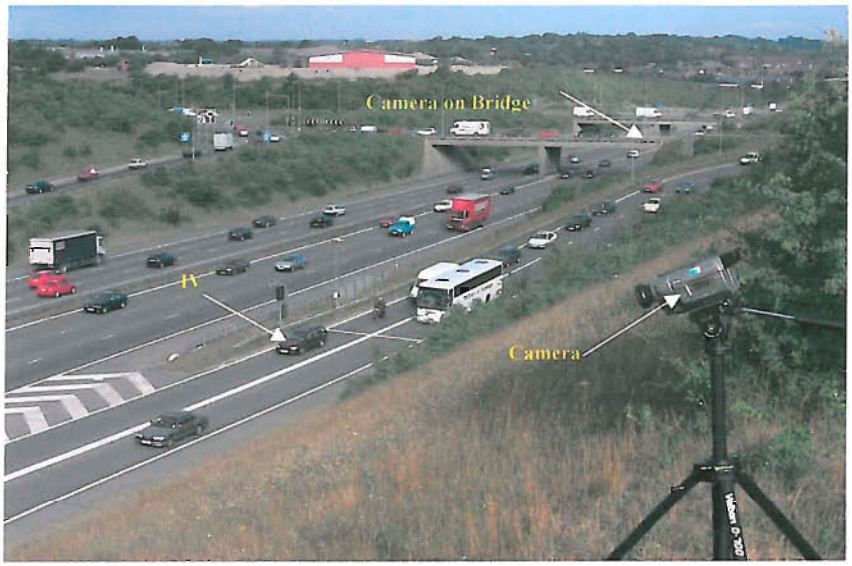

Figure 2.8 Camera Positions

The longitudinal coverage of each camera is determined by the camera itself (horizontal view angle) and the distance between the camera and the road. According to test measurements, each camera could cover a width of about 45 meters. The aim was to monitor the whole merging process from the sight point, i.e., where entering and merging drivers can first see each other, to slightly downstream of the end of acceleration lane. After that, the IV radar was able to track leading and following vehicles on the same lane. Ten cameras were needed to meet the requirements over a length of about 300 meters. An additional camera was set up on the bridge upstream of the merge site to give an overview of the merging and lane changing process (Figure 2.8).

2.1.5 Subjects and Timing of Surveys

The subjects, i.e., IV drivers, were staff of the Transportation Research Group (TRG) who held full driving licence (One subject was from Highway Agency). Participation was voluntary. In total, 19 subjects (18 males/1 female) took part in the survey. Subjects were asked to merge or pass the merge site as they would do in everyday driving. No instructions were given for the motorway driving between the junctions. Subjects were not told that data collected during motorway driving would be used to study car following behaviour to better reflect normal motorway driving.

The experiment was carried out together with Highway Agency research project (Additional Research for the Operational Assessment of the Ramp Metering Pilot Scheme) between 21 May and 17 July of 2001. The experiments were conducted in morning peak hours from 7 a.m. to 9 a.m. on normal working days, when interactions between ramp and motorway traffic was frequent. The survey was divided into two stages, the first stage with ramp-metering-off and second stage with ramp-metering-on.

2.2 Data Reduction

2.2.1 Camera Data Reduction

The raw camera data was a collection of still images (frames) recorded consecutively; each frame associated with a time. The primary task in data reduction was to record the time when certain events of interest happened. These events included driver's eye-movement, start of merging, end of merging, passing merging end, etc. Another task was to estimate a vehicle's position in a still image, so that a time-series position of any vehicle can be determined. However, it is difficult to estimate accurately the position directly from a still image. Alternatively, a set of reference marks with known position on the roadway can be selected so that the position of any vehicle at these reference marks can be derived. The event when a vehicle arrives at a predefined position (a reference mark) is defined as the passing event. For a given vehicle, if the passing time at several reference positions (e.g. 0 m, 10 m, 20 m, etc.) can be determined, the time-series positions of the vehicle is known and the speed can be calculated.

2.2.1.1 Coordinate

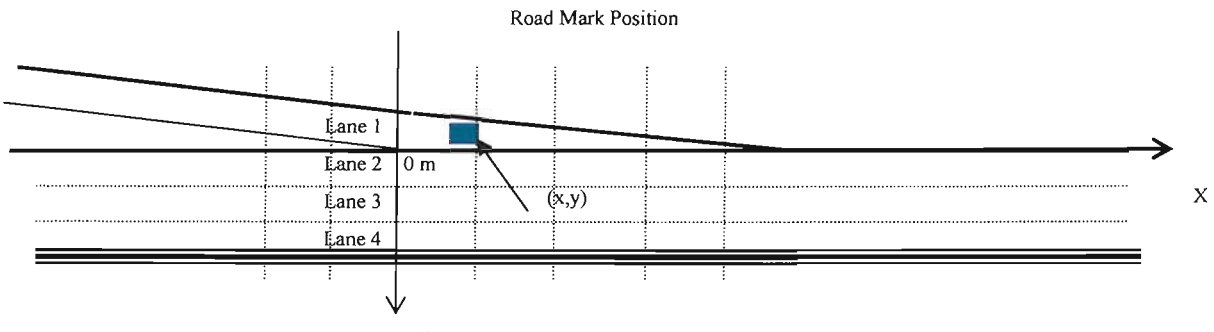

Figure 2.9 Measurement Coordinate

A coordinate is established in order to derive vehicles position (Figure 2.9). The position of vehicle is measured at its right-front corner. The longitudinal position is measured in meters from merging end

while the lane number directly denotes the lateral position. For example, a vehicle's position of (15, 1) denotes that the vehicle is on acceleration lane (lane 1) with a longitudinal offset of 15 m from the merging end.

2.2.1.2 Location Reference Marking

In this research, it was found that lane marking lines on motorway were suitable as the natural distance markings. They were clearly identified on video recording during initial test investigations. By joining two parallel markings on the motorway, a reference line can be drawn on the video display and can be extended to slip road. The natural markings on motorway and reference lines drawn on them are shown in Figure 2.10.

2.2.1.3 Event Time Reduction

An event time logging system developed at the TRG was used for camera data reduction. The core of the system is a Videocassette Recorder (VCR) controlled by a computer program, the Lane Monitor. Figure 2.11 shows the hardware architecture and Figure 2.12 is a screen shot of the Lane Monitor. The operator watches the video screen while playing the video frame by frame. If an event of interest happens, he/she pushes a button. The computer program will register the event time and the button code, which will be saved into a text file at the end of a data reduction session. The system has a time-resolution of 1/25 second (25 frames per second).

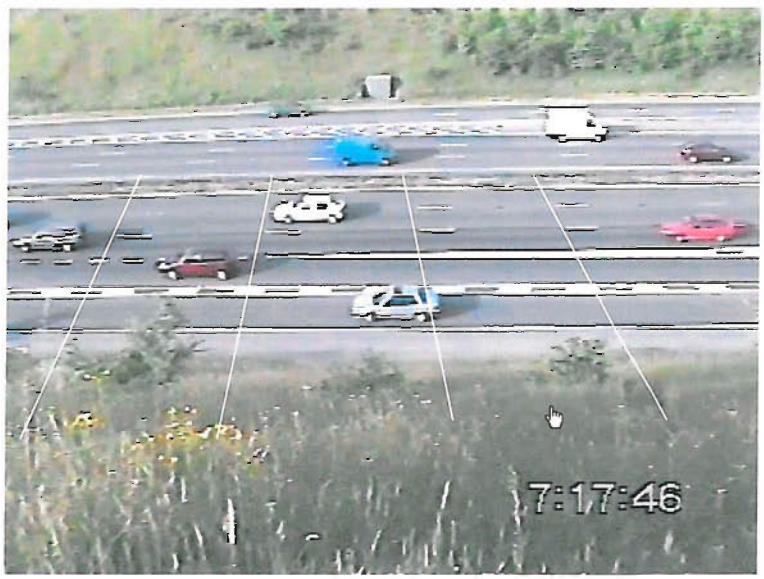

Figure 2.10 Location Reference

Figure 2.11 Hardware Architecture of Event Time Logger

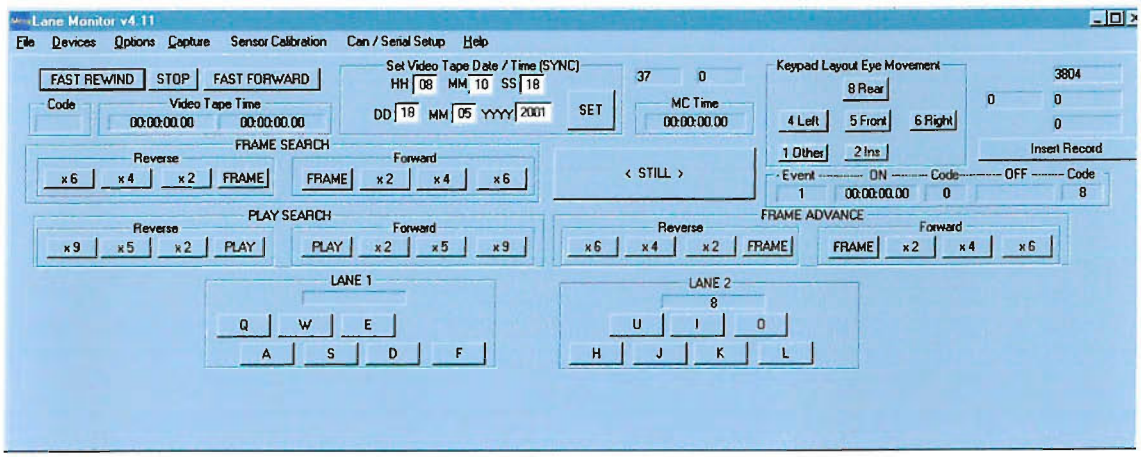

Figure 2.12 A Screenshot of Lane Monitor

2.2.1.4 Vehicle Identification

Vehicle tracking is another important task in data reduction. Different vehicles can be easily identified according to their physical features such as colour, shape etc. A record for each vehicle is established when it appears in the first camera. Each record has four fields that describe the different attributes of **ID, Length, Colour** and **Type**.

The ID is a unique identification number assigned to a vehicle. Vehicles can then be tracked across successive camera records according to their attributes. The length of each vehicle is estimated by comparing the size of the vehicle with the length between two road markings (about 9 m) (The IV has a known length of 4.8 m).

2.2.1.5 Data Organisation

The data was organised for each merging (passing) trial performed by the IV. Any vehicles with time headway of less than 10 second to the IV, either on the ramp or on the motorway shoulder lane, were included. Typically, five vehicles were chosen in a merging (passing) trial.

For those selected vehicles, the event times were reduced using the event time logging system. The result was saved in a text file. The file had two fields, time and event code. Each event is denoted by an alphabetic or numeric code. Typical event time records and the coding scheme are illustrated in Tables 2.1 and 2.2. The maximum number of the reference line covered by one camera is 7, 14 codes can represent all events of passing reference line on both ramp and motorway shoulder lane.

The code was then converted to road mark number and lane number according to the decoding scheme. Each vehicle was assigned a unique number. A program (CamDataSee) was developed for this purpose. The result was saved in a text file with four fields of **time, mark number, lane number** and **car identification number**.

Table 2.1 Event Time Record (generated by **Lane Monitor**)

Time	*Code*
07:02:26.24	H
07:02:27.10	J
07:02:27.20	K

Table 2.3 shows content of a converted file. Time is the elapsed time from midnight (0h00m00s). The camera number is denoted in the file name, e.g., a file named 702cam3mg1.cam indicate that the data contained in the file has been reduced from camera 3 for the first merging trial performed on 2nd of July.

Table 2.2 Coding Table

Code	Meaning
H	Passing road mark 1 on lane 1 (ramp)
J	Passing road mark 2 on lane 1
K	Passing road mark 3 on lane 1
L	Passing road mark 4 on lane 1
U	Passing road mark 5 on lane 1
I	Passing road mark 6 on lane 1
O	Passing road mark 7 on lane 1
A	Passing road mark 1 on lane 2 (motorway lane 1)
S	Passing road mark 2 on lane 2
D	Passing road mark 3 on lane 2
F	Passing road mark 4 on lane 2
W	Passing road mark 5 on lane 2
E	Passing road mark 6 on lane 2
R	Passing road mark 7 on lane 2
4	Start merging, lane code 12
6	End merging, lane code 2
8	Leave motorway lane 1 (lane-changing), lane number 23
2	Enter from motorway lane 2, lane code 32

Table 2.3 Decoded Data

Time	Mark number	lane	Car Id
25349.24	1	2	1
25349.68	2	2	1
25350.08	3	2	1
25350.52	4	2	1
25350.52	1	1	2
25350.88	2	1	2

702cam3mg1.cam
(generated by **CamDataSee,** source file 702cam3.txt)

Table 2.4 Format of Camera Data File

702mg1.txt

Mark Num	Time	Lane Num	Car ID	Mark Num	Time	Lane Num	Car ID	...
1.00	25341.08	2.00	1.00	1.00	25343.32	1.00	2.00	...
2.00	25341.52	2.00	1.00	2.00	25343.68	1.00	2.00	...
3.00	25341.88	2.00	1.00	3.00	25344.04	1.00	2.00	...
4.00	25342.36	2.00	1.00	4.00	25344.40	1.00	2.00	...
5.00	25342.76	2.00	1.00	5.00	25344.76	1.00	2.00	...
6.00	25343.16	2.00	1.00	6.00	25345.04	1.00	2.00	...
7.00	25343.60	2.00	1.00	7.00	25345.44	1.00	2.00	...
...	...	...	...	...	...	...	...	...

(generated by **rmTSych,** source files: 702camXX.cam xx=0--9)

The next step was to combine the data from the 10 cameras. This involved two operations, reference line number conversion and time synchronisation. Absolute reference line numbers was resolved based on camera numbers. For example, the third camera covered reference lines 13-16, so a relative reference line number of 1 is equivalent to an absolute number of 13. The conversion was simply to add an offset of 12 on mark number in the data reduced from camera 3. Time synchronisation was necessary because the accuracy of ordinary camera timers is relatively low and error can accumulate. This was achieved by comparing the recorded event time of passing the reference line at overlapping locations. For example, if a reference line is covered by both camera n and camera $n+1$, and the event time of a vehicle's passing the reference line is registered as t_n and t_{n+1} respectively by the two cameras, the offset time between the two cameras is t_n-t_{n+1}. By adding the offset time to the time field of the data reduced from camera $n+1$, the time base of camera $n+1$ is synchronised to that of camera n. This functionality was implemented in a program (**rmTSych**) and the result saved in a text file. The fields of the file were arranged in such a way that each vehicle occupied four columns. Table 2.4 shows part of the data in a camera data file. The file is named after the trial number and date (e.g. 702mg1 denotes the first merging trial on 2nd of July).

2.2.2 IV Data Reduction

2.2.2.1 Raw Data

Outputs from sensors on the IV were saved in two separated text files every 5 minutes. The sampling rate was 10 Hz, so that there was ten readings recorded every second and each file contains 3000 records. In this research, the outputs from speedometer, front Radar, rear Radar and GPS were used. Table 2.5 shows the selected fields of the sensor outputs. The outputs from some sensors were not all used. For example, GPS can also provide information about speed, satellite status etc, but only those outputs of direct use were incorporated.

The front Radar uses three beams to detect objects; each beam can possibly cover four objects (tracks). Therefore, the total number of tracks is 12. Each detected target is described by three attributes, the range, the relative speed and the signal strength. The Radar also provides a default target selection (Range_13), which has been resolved by the inherent algorithms of the Radar. The rear Radar uses a single narrow beam and only outputs the range of one target. The speedometer also outputs distance travelled between successive sampling instants. This information is redundant under a fixed sampling rate of 0.1 second, which is equal to one tenth of the speed.

Table 2.5 Selected Sensor Outputs

Sensors	Output	Sample Value	Description
PC Timer	Real_Time	51:00.4	Computer time
Speedometer	Speed	30.5	[m/sec]
Rear Radar	Radar_Range(cm)	2416	Range [cm]
GPS	GPS Long	106.3472	Longitude [ddmm.mmmm]
	GPS Lat	5051.114	Latitude [ddmm.mmmm]
	GPS Time	75101	UTC
Front Radar	Range_13	2967	Range [Cm]
	Velocity_13	-17	Relative speed [cm/sec]
	Sel_Beam	3	Default selected beam
	Sel_Track	2	Default selected track
	Range_1	5197	Range (beam 2, track 1)
	Velocity_1	-30	Relative speed (beam2, track1)
	Peak_1	60	signal strength (beam2, track1)
	...	...	...
	Range_12	2964	Range (beam 4, track 4)
	Velocity_12	-28	Relative speed (beam4, track4)
	Peak_12	124	signal strength (beam4, track4)
	Buffer_Size	562	Radar buffer
	Error_Count	126	Error indicator

There is no ambiguity about the speedometer and GPS outputs although errors exist within the data. The rear Radar did not provide extra information about target selection, therefore, further treatment was not feasible. The front Radar outputs 12 range readings, so it was necessary to identify targets of interest such as direct leader, leaders on other lane etc. from raw measurements. Two main factors can affect the target identification in the Radar system. The first is the signal-to-clutter ratio of a target, which is mainly decided by the cross sectional area and the material of the target. The second is the sensor geometry of the Radar system. The IV front Radar used in the experiment has a vertical field of 3^0 and a horizontal field of 8^0 which is divided into three overlapping angular resolution cells (beams). The coverage area is shown in Figure 2.13, where the width of lane is assumed to be 3.65 metres. Objects outside this area cannot be detected (e.g. Target D and E). On certain occasions, problem can arise because of road curvature and gradient. Two Radar beams may detect a target at the same time, while the same target may be detected by different beams at different times. The Radar may also detect vehicles in opposite directions (Target C). The pitch and yaw of the host vehicle can change the direction of sensor and make the situation more complicated. Clutter signals from road surface and other stationary objects such as guardrails, road signs, trees etc, can result in further difficulties in resolving targets.

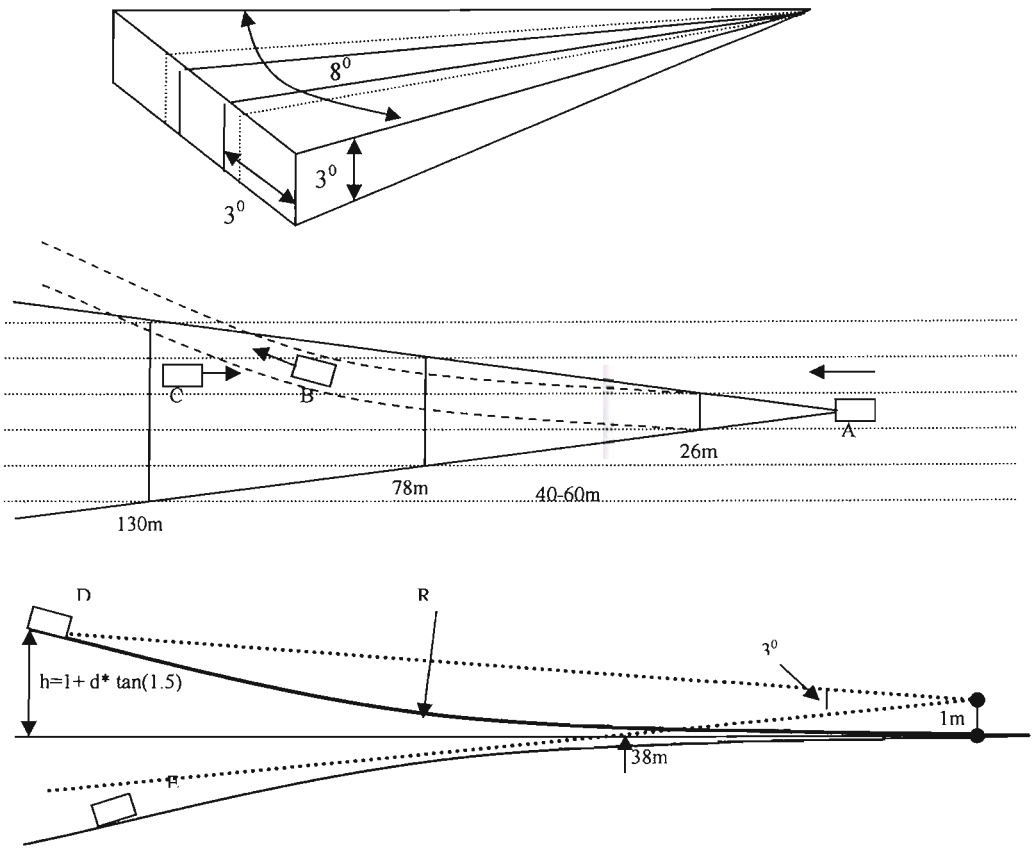

Figure 2.13 Sensor Geometry and Coverage Area of Radar

The range signatures of three tracks, each from a different beam, are shown in Figure 2.14. It can be observed that two tracks (7 and 12) have detected the same target for a short period. Between the ranges of 40-60 metres, clutter signals are registered by all tracks in most occasions. This is likely to be resulted from ground reflections. Although the Radar system contains its own algorithms for resolving the most significant target, it does not always work effectively. If there is no target or the target is distant, the default track will be assigned to a strong reflection that may be from guardrails or vehicles in other lane. It is clear that a Radar-only based sensor system will not be able to resolve targets properly without additional information. In this research, IV camera recordings have been used to help resolving targets covered by the Radar. This function has been integrated in a computer program (IVDataSee) developed as part of this research.

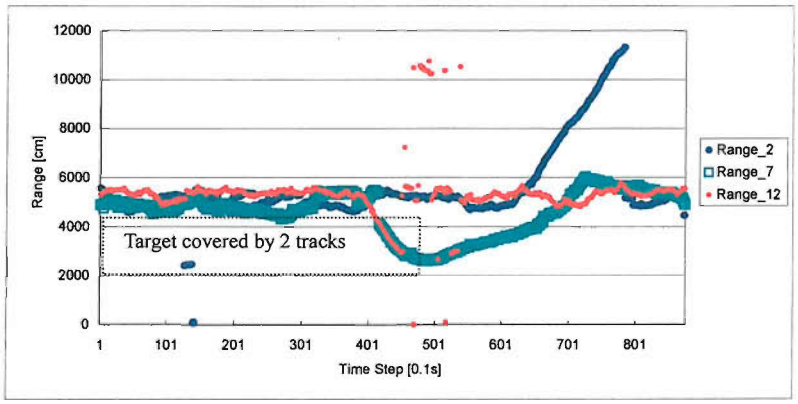

Figure 2.14 Front Target Ranges from Three Tracks

2.2.2.2 IV Data Reduction Using IVDataSee

IVDataSee is a program for visualising and processing IV data. It provides an integrated environment for extracting the desired Radar target range from clustered signals. The program uses IV sensor data as input and allows for direct manipulation on the data. It exports the processed data in text file format. The program supports the following operations:

- Concatenating successive sensor data saved in different files. IVDataSee can read more than one data file exported by the IV computer. This is useful when a process (e.g. car following) has spanned two files.
- Reducing data for a specific road section or time period. IVDataSee can extract data based on user selection, so that only the relevant data on a specific road section based on GPS provided position or during a time segment will be reduced.
- Interactive resolving of Radar targets. IVDataSee provides extensive support for Radar signal processing and target identification, as detailed below.

In order to resolve a target of interest (e.g. leading vehicle) from cluttered signals, IVDataSee provides filtering function and supports interactive manipulation of data using additional visual cues. The filter works on the following thresholds:

- Minimum signal strength
- Absolute maximum relative speed
- Maximum range difference between two successive points of same target
- Minimum number of continuous points to be considered as a target

The first threshold excludes possible false or cluttered reflections that are not directly from a target. The second threshold prevents the inclusion of on-coming vehicles or stationary obstacles that have a relative speed of about the same as or greater than the speed of the host vehicle. The filter first checks whether a data point meets these two thresholds. Any measured points beyond the thresholds will be assigned a range value of –1 as a tag. The filter then looks for points from 12 tracks that can be considered as coming from the same target. A set of points will be assigned to one target if the range differences between successive points are below the third threshold. Possible targets which last longer than minimum number of points (10 points equal to 1 second at 10 Hz sampling rate) are resolved by applying the fourth threshold.

There is a trade-off between threshold settings and number of targets resolved. By setting a higher threshold of signal strength and number of points, there will be fewer resolved targets which are most likely to be the real vehicle targets. However, such a threshold can also result in failure to identify real targets such as distant vehicles with weak reflection and targets with discontinuous data points as a result of interference. Default values of thresholds are provided in the program based on several test data reductions. The default thresholds function reasonably well in most cases but may fail to work properly for data collected in rainy weather. Nevertheless, the threshold-based filter can only exclude part of cluster signals and may fail in resolving a target of interest because of a lack of further information such as relative lateral position.

The second function offered by IvDataSee is to exploit vision features provided by the IV camera. Instead of relying exclusively on the filter, IvDataSee supports the direct manipulation of Radar sensor data interactively. Firstly, targets of interest can be chosen based on video images. For each target selected, the range signature of the target can be estimated from the video data. Similar range signatures are searched for in the Radar data. In practice, it is not difficult to identify a range signature among many others based on visual cues because real targets are well separated longitudinally. The main concern becomes how to reduce a clear range signature from clustered Radar signals. For this purpose, IvDataSee supports the direct manipulation of Radar data from 12 tracks.

A: Associating Range Signatures with Vision

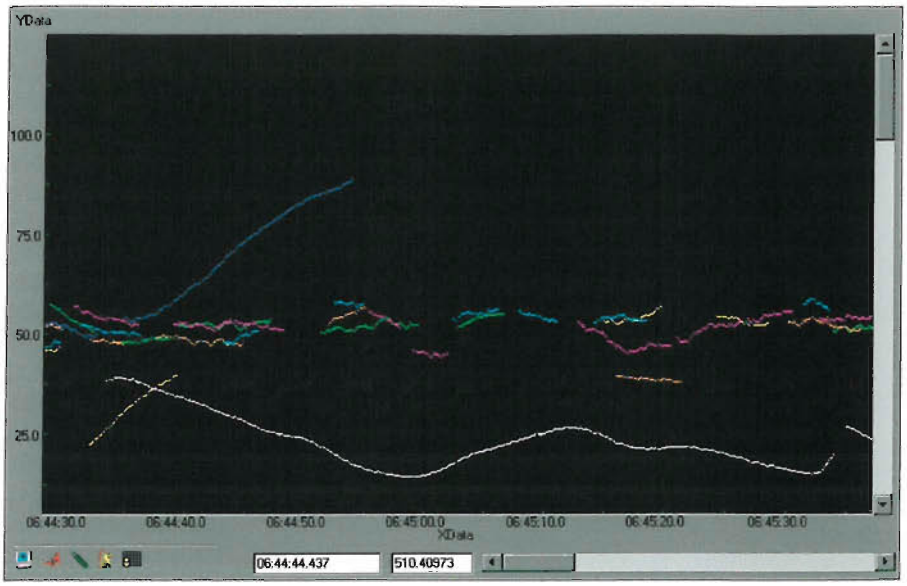

B: After Applying Filter

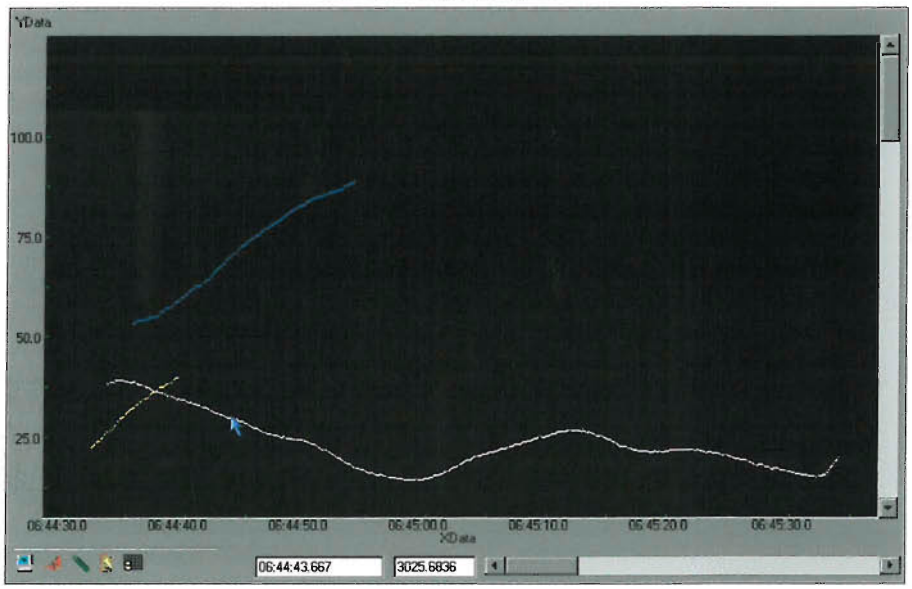

C: Three Targets are Resolved

Figure 2.15 Resolving Radar Targets

Basically, any range signature can be reduced interactively. The operation is outlined in Figure 2.15. IvDataSee can display all range signatures of 12 tracks. By replaying the video recording, the range signature of target of interest can be identified in clustered environment. Noise signals can be excluded by selecting an area within which all data points will be deleted. This area can be as small as a single data point using the zoom function. The display mode can be changed to show only one track at a time to process clustered data track by track. Alternatively, part of the noise signals can be filtered out with

thresholds set in such a way that the interest range signatures are not depressed. The remaining noise can then be excluded manually. For range signatures with discontinuous points as a result of interference, IvDataSee allows the user to add points for continuity. The processed Radar data is several continuous range signatures, each representing an identified target.

The rear Radar data is from a single track. However, data manipulation is similar as for the multi track data in that the user can remove noise points interactively using vision to resolve for interested targets.

2.2.2.3 Data Organisation

An output file from IvDataSee is shown in Table 2.6. The measured speed of the IV, resolved range of leader and follower are arranged in different fields. The time series data is saved in a text data file in matrix form. Up to 6 resolved ranges from the front Radar could be stored at any time. Ranges from different targets, if not overlapping, can also be stored in the same column by a padding tag (-1) between them. Measured relative speed has been discarded because the accuracy (0.5m/s) is not satisfactory compared with that derived from the range reading. Refer to appendix A for a detailed analysis of the accuracy of IV data.

Table 2.6: IV Data Format

No.	Field Name	Value	Description
1	Frame	18970	Record Number
2	Real Time	23437.4	From 00:00:00.0
3	Speed	12.083	m/s
4	F Range	1238	Rear Radar Range Reading[cm]
5	Longitude	109.2495	
6	Latitude	5051.562	
7	UTC	63037	GPS Time [s]
8	Brake Move	0	
9	Throttle Move	48.35	
10	Brake Light	0	
11	L Indicator	0	
12	R Indicator	0	
13	L Range1	2111.333	Front Radar Range Readings [cm]
...	...	...	
18	L Range6	0	

(generated by **IvDataSee**, source file, .os1 and .lr1)

2.3 Integration of Camera Data and IV Data

In the previous section, the process of time-series data reduction and re-organisation has been described. Some data reduced from camera and IV (speed and position) is for the same vehicle. For example, within the coverage of roadside cameras, the speed and position of the IV has been measured

by cameras and IV speedometer, and the reduced data is stored in camera file and IV file respectively. The possible situations include:

- IV: has been measured by Speedometer and Roadside cameras
- Other vehicles: have been measured by Roadside cameras and the IV Radar

The reduced data contains errors from different sources. The sampling bases for camera data (roadside video) and IV data (Speedometer, Radar) are different. The camera data is sampled spatially (i.e., at each reference line) whilst IV data is sampled temporally (i.e., every tenth of second). Where a vehicle is measured by both kinds of sensor, data from different sources needs to be integrated. Data integration is important in merging scenarios where radar is unable to cover all targets of interest all the time.

2.3.1 Data Processing

It is necessary to process the reduced data before integration. Two frequently used data processing procedures are data interpolation and data smoothing

2.3.1.1 Data Interpolation

Two interpolation methods have been used in this research, i.e., linear and Spline interpolation, in order to construct a time series sampled at $[t_0+T, t_0+2T, \ldots, t_0+nT]$ from a time series measured at time $[t_1, t_2, \ldots, t_n]$, and to find a single value from a time series.

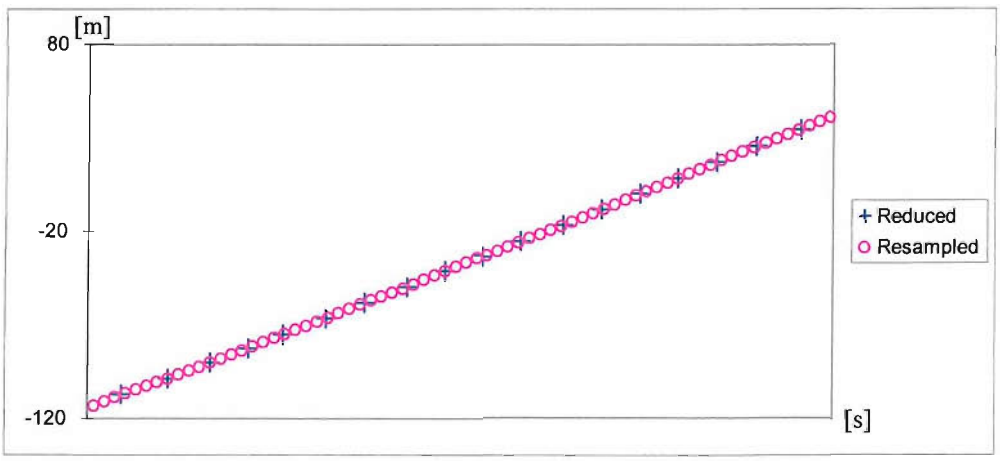

Figure 2.16 Resampling Camera Data Using Spline Interpolation

A function can be approximated locally (i.e., at a small interval) by a polynomial function. Such smooth piecewise polynomial functions are called Spline functions. A function with large intervals can

be approximated by Spline by dividing the larger intervals into several small ones. Interpolation is one common application of Spline. In this research, cubic Spline interpolation has been used in resampling camera data. For example, given a time series measurement, the longitudinal position of a vehicle [t, x], a Spline function can be constructed which takes the value $x(i)$ at the point $t(i)$ for all i. With the known Spline function, any refinement of x can be computed based on a refinement of t, i.e., if tt is a refinement of t, a new vector xx can be obtained based on tt. Using the Spline interpolation function provided in Matlab [11], the original and resampled camera data (longitudinal position) is shown in Figure 2.16. The resampled data has the same sampling basis as that of IV data.

Linear interpolation has been used to find a value between two sampling points. This is frequently required when looking up time discrete data, e.g., to find the merging position through an event time of start merging. Compared with the Spline interpolation method, the linear interpolation is simple and more efficient.

2.3.1.2 Data Smoothing

Noises are always present in any measurement systems and can be introduced by a variety of sources. For example, the pitching of vehicle can introduce measurement errors in the laser speedometer, as can background noise in a Radar system. There are many approaches to removing noise and most measurement systems have implemented noise reduction methods in hardware or software form, e.g. Kalman filter in the Radar system. For remaining noise in the time series data, a data smoothing procedure has been introduced to further improve data accuracy.

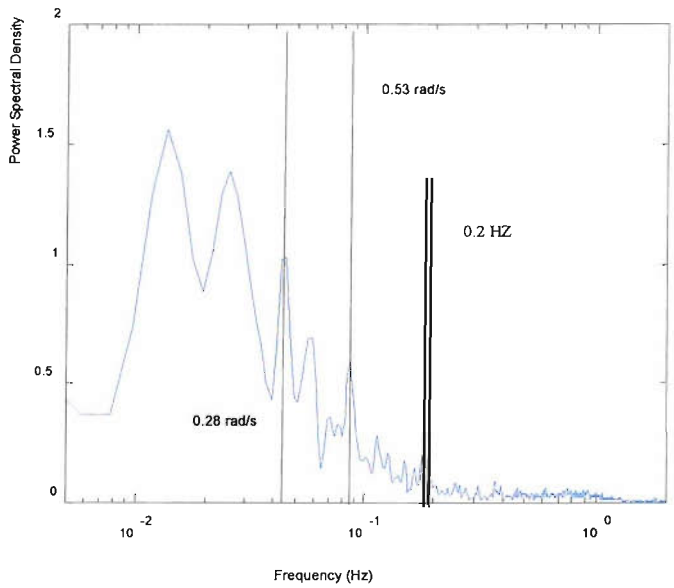

Figure 2.17 Spectrum of Acceleration Rate in Normal Motorway Driving

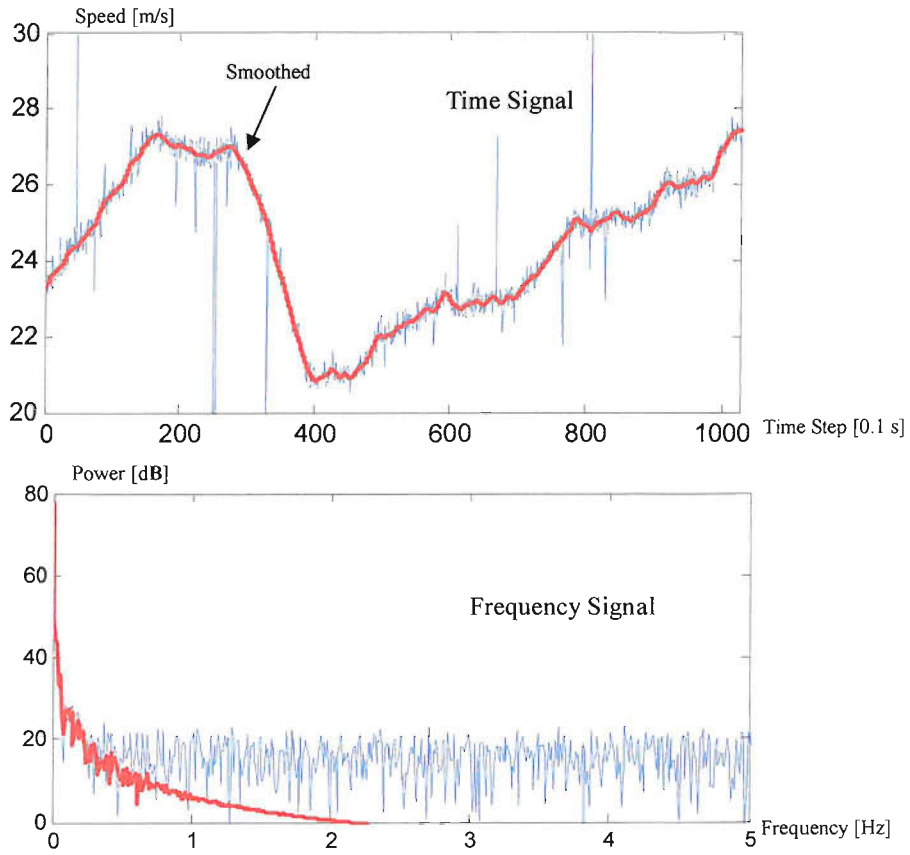

Figure 2.18 Data Smoothing

Data smoothing has been implemented using a Witchworth low pass digital filter. The cutoff frequency of the filter was determined by the performance limitations of drivers. A spectrum analysis of the time-series acceleration data in normal motorway driving revealed that drivers do not respond at a frequency above about 0.2 Hz. For the car following behaviour, Chandler et al., found that the bandwidth of a driver when responding to changes in leading vehicle velocity was 0.37 rad/sec (0.0589 Hz) [18]. This frequency was reported by Allen et al. to be from 0.11 to 0.35 rad/sec with an average of 0.21 rad/sec (0.0334 Hz) for different drivers on the open road [3]. However, it should be noted that the above results are of statistical nature and obtained by fitting to a linear first-order car following model. Slightly more dynamic responses in longitudinal control can be found in a direct spectrum analysis shown in Figure 2.17. This may be attributed to the driver's using another strategy of control through micro-adjustment of throttle. However, considering the performance differences between drivers, and that the mean brake perception reaction time (PRT) in an 'expected' situation is 0.54 seconds (Lerner, et al. 1995, as quoted by Koppa, [51]), responses over 0.5 HZ can be safely treated as 'noise' and removed from the data without losing any useful information. The cutoff frequency of the data

smoothing was thus set at 0.5 HZ so that all the 'noise' which is beyond the human ability to respond could be selectively excluded. Typical data before and after smoothing is illustrated in Figure 2.18. The sharp fluctuations (noise) in the data have been removed. Further details on the accuracy of the processed data are given in Appendix A.

2.3.2 Data Integration

Data integration is the process of combining camera data with IV data. Because the IV measurements are more accurate, IV data is used if a vehicle's time-space trajectory has been registered by both the IV and camera. Where a vehicle's time-space trajectory has been partly registered by both IV and a camera, the IV data was used in the overlapping section. Outside any overlapping sections, camera data was used.

2.3.2.1 Time Synchronisation

As described in Section 2, camera data was reduced based on time information from the first roadside camera timer. Time series data from other roadside cameras was synchronised to this timer. However, the time base of IV data was based on the IV computer clock. Thus, there may have been differences between the time bases of camera and IV data. In order to establish a unified time base for camera data and IV data, the time base of camera data was synchronised with that of IV data through an event time of the passing the merging end by the IV. Supposing that the time of the passing the merging end by the IV is registered as t_c by the roadside camera, and is registered as t_{iv} by the IV front camera, the offset time of camera data from IV data can be calculate according to

$\delta t = t_{iv} - t_c$

By adding δt to the time record of the camera data, time base of camera data became the same as that of IV data. This has been implemented as a module in a computer program for data processing (**GenCmbData**).

2.3.2.2 Distance Measurement Calibration

Problematic situations in combining IV and camera data are illustrated in Figure 2.19. Because of the existence of the measurement error, the trajectory of the same vehicle measured by the IV and cameras is not always identical. If the camera data is directly used outside the overlapping section, the combined data will result in a discontinuity at the end of the overlapping section, which will in turn introduce very large error in calculating time derivatives from the time-space trajectory. The camera data needs to be shifted by δx, calculated based on the difference of two positions at the end of the overlapping section. This process has also been implemented as a module in the **GenCmbData**.

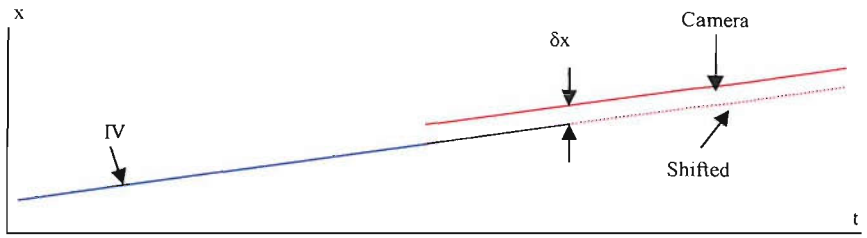

Figure 2.19 Distance Measurement Calibration

A typical combined data (time-space trajectory) is illustrated in Figure 2.20. Each vehicle is described using four state variables: [***Position (x), Speed (x'), Acceleration (x''), Lane Number (y)***], of which, x' is calculated from x if direct measurement of x' is not available. The data smoothing procedure has been applied to increase the accuracy of either direct measurements or their derivatives. The x'' is only available for the IV because the acceleration/deceleration measurement error using camera technology is unacceptable. The result is saved in a combined data file based on each merging (passing) trial. Given the event time (e.g. eye-movement) or position (e.g., at merging end), the corresponding attributes of vehicles, such as speed, position etc., can be obtained through linear interpolation.

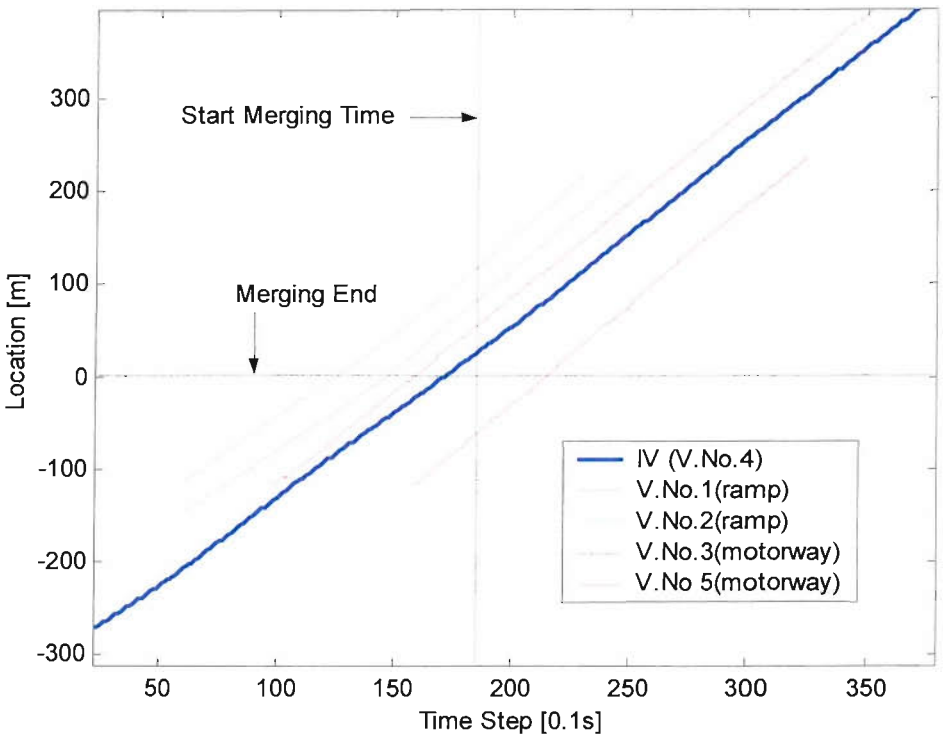

Figure 2.20 Combined Time-Space Trajectories

Chapter 3 Model of Car Following Behaviour

A car-following model describes the follower's acceleration-deceleration behaviour is follow-the-leader situation. Such models are widely used to mimic the longitudinal movement of individual vehicles in microscopic simulation. In merging process, longitudinal movement of both merging and motorway vehicles on the same lane can be described in the context of car following behaviour. Longitudinal control behaviour in follow-the-gap situation described in Chapter 4 is also based on the work described in this chapter.

3.1 A Review of Car Following Models

Car following behaviour is one of the most frequently studied driving task. Many models have been developed in the last half-century [13]. The modelling approaches range from traditional manual control theory to fuzzy logic methods. Several well-known models are briefly reviewed in this section.

3.1.1 General Motor Models

In the late 1950's, the General Motors Research Group developed a series of car-following models. The fundamental concept behind these models was stimulus-response theory. A driver was treated as an information processor, and it was assumed that there existed a stimulus-response relationship that could be expressed as a form of stimulus-response equation:

$$\text{Re}\,sponse = Sensitivity * Stimulus \tag{3.1}$$

The response was generally the acceleration (deceleration) rate of the following vehicle. Chandler et al. obtained a linear stimulus-response equation using relative speed as the argument of the stimulus function and supposing the sensitivity to be a constant, λ.

$$x''_f(t+\tau) = \lambda[x'_l(t) - x'_f(t)] \tag{3.2}$$

where x is the position of vehicle, τ is reaction time, subscript l denoting leading vehicle and f the following vehicle [18].

Gazis et al. proposed that the sensitivity was inversely proportional to the space headway, i.e.

$$\lambda = \frac{\alpha}{x_l(t) - x_f(t)} \tag{3.3}$$

where α is constant [27].

A more general form of the sensitivity term was proposed in 1961, resulting in a generalised representation of the General Motors (GM) car following model:

$$x''_f(t+\tau) = \frac{\alpha [x'_f(t+\tau)]^m}{[x_l(t) - x_f(t)]^n}[x'_l(t) - x'_f(t)] \tag{3.4}$$

where α, m, n are parameters to be determined [28].

The model was first fitted to experimental data at $m=n=0$ by Gazis et al, both sensitivity and reaction time showed high variations between drivers, but the overall goodness of fit was good (R>0.8). Since then, many microscopic calibrations had been made in an attempt to find optimal parameter combinations of the model. However, results have varied considerably across studies [13].

GM models are not full-functioning microscopic simulation models because only speed control behaviour is considered. Another important aspect in car following, i.e., the headway control behaviour, was not modelled. The reason is that human bandwidth (or approximately, gain, λ) in headway control is much lower than that of speed control, so that the headway control term is ignored. This has been experimentally verified and is not a problem when modelling the dynamics of car following behaviour because speed control is dominant in a car following process. However, the only steady state in the model is found at zero relative speed irrespective of the following distance. Headway adjustment at a relative speed of zero will be impossible according to the model, which, of course would result in unrealistic simulation behaviour.

Helly developed a linear model that included additional stimulus term of headway discrepancy between perceived and desired headway, which took the form:

$$x''_f(t+\tau) = k_v[x'_l(t) - x'_f(t)] + k_d[(x_l(t) - x_f(t)) - D_{dsr}(t+\tau)] \tag{3.5}$$

where x is the position of vehicle, τ is reaction time, subscription l denoting leading vehicle and f the following vehicle, k_v and k_d is constant (gain) and D_{dsr} is desired headway of the following vehicle [34].

3.1.2 Crossover Model

The crossover model is identical with the linear form of GM model ($m=n=0$). However, it is based on more generic manual control theory and discussed under frequency domain. For generic close-loop tracking performance, McRuer et al. successfully developed a crossover model by directly looking for the relationships between perceived error ($e(t)$) and system output ($O(t)$) [65]. The underlying

assumption in a crossover model is that the human responds in such a way as to make the total open-loop transfer function behave as a first-order system with gain and effective reaction time. That is:

$$O(t) = k\int e(t-\tau)dt \text{ or } O'(t) = k \cdot e(t-\tau) \quad \textbf{(3.6)}$$

This implies that a human operator is able to adjust his or her performance according to the dynamics of the system to be controlled to achieve a good control over the entire human-machine system.

Allen et al. formulated a simple crossover car following model characterised by crossover frequency (gain, K) and the reaction time (τ) [3], as illustrated in Figure 3.1.

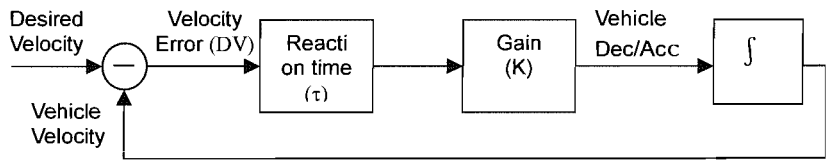

Figure 3.1: Simple Crossover Car Following Model

The open-loop input-output relationship of the driver-vehicle system is modelled as a linear first-order differential equation. The output of the model is acceleration rate and input to model is the perceived relative speed delayed by a time τ. Allen et al. also devised an extended crossover model by taking headway error into account. This was identical to Helly's linear model. Thus, cross-over models have the same advantages and disadvantages.

Another important manual control behaviour model, the optimal control model can also be found in car following literature, e.g., Optimal Control Car Following Model and Heuristic Finite-State Model etc (refer to [5], [6], [7]). They have not seen much application in the microscopic simulation because of the high computational demands,

3.1.3 Stopping-Distance Model

As stopping-Distance Model was derived based on the assumption that a follower always maintains a safe following distance so that he/she could bring his/her vehicle to a safe stop if the leader came to a sudden stop. At any time t, this required a following distance of:

$$s \geq \frac{v_f(t+\tau)^2}{2A_f} + \frac{v_f(t+\tau)+v_f(t)}{2} \cdot \tau - \frac{v_l(t)^2}{2A_l} \quad \textbf{(3.7)}$$

where, v is speed, τ is the reaction time of follower, A_f is the maximum acceleration the follower wishes to undertake, A_l is the maximum acceleration of leader estimated by follower. Subscription f represents for following vehicle and l for leading vehicle [30].

By considering a possible additional delay of $\tau/2$, the model took the form of a safe speed equation:

$$v_f(t+\tau) \le A_f * \tau + \sqrt{A_f^2 * \tau^2 - A_f * (2 * (x_l(t) - D - x_f(t)) - v_f(t) * \tau - \frac{v_l^2(t)}{A_l})} \quad (3.8)$$

where, D is the minimum safe distance between two successive vehicles plus the length of the leading vehicle.

The model has seen widespread use in microscopic simulation because only little calibration is needed, i.e., the expected maximum acceleration the leading vehicle and the maximum acceleration the following vehicle wishes to apply. However, the assumption that a driver always maintains a safe headway is not consistent with empirical observations. The direct control of speed is also unrealistic and a rather too stable result can be achieved.

3.1.4 Action-Point Model

Michaels reporting on human perception of motion, stated that the dominant perceptual factor, or the stimulus, in a car-following situation, was the changing rate of visual angle (angular velocity) [66].

$$\frac{d\theta}{dt} = \frac{4 * W_l}{4 * [x_l(t) - x_f(t)]^2 + W_l^2} [\dot{x}_l(t) - \dot{x}_f(t)] \quad (3.9)$$

where W_l is the width of lead vehicle.

He suggested that a driver would take proper acceleration-deceleration action if the angular velocity were above a threshold. If the driver remained under this threshold, his/her action would be on whether he/she could perceive the change of space between them, i.e. at the 'Just Noticeable Distance'. That is, the driver is only able to modulate the acceleration above that threshold, and will stay with the last acceleration rate until another threshold is broken.

The Mission model was the first microscopic car following model to incorporate perception thresholds [54]. More thresholds were defined such as relative speed threshold for the perception of opening (OPDV) and closing (CLDV) etc. Car following situations were further divided into sub-groups, e.g. uninfluenced driving, closing processes, following processes and emergency situations. A driver was supposed to adopt different acceleration behaviour in different situations if and only if the perceived physical (perception) stimulus exceeded certain minimum values, i.e., the thresholds. For example, in approaching a slower leader, a follower's action above the threshold was assumed to be a constant deceleration:

$$A_f(t+\tau) = -\frac{[\dot{x}_l(t) - \dot{x}_f(t)]^2}{2[x_l(t) - x_f(t) - D]} + A_l(t) \quad (3.10)$$

Where A is deceleration rate, x is the position of vehicle, D is the minimum distance between two successive vehicles plus the length of the leader, subscript l represents for the leader and f for the follower.

The model took into account the human threshold of perception, and thus established a more realistic rationale. However, most calibration efforts were focused on identifying threshold values, while other important aspects, the modulation of acceleration above a threshold had seen less detailed considerations, normally assumed to be a constant or generated from a distribution. In addition, further analysis of model dynamics was virtually impossible, because the model was established on several different behaviours and switching between them is random according to the distribution of the threshold.

3.1.5 Fuzzy Logic Model

Fuzzy logic car following models describes a car following law using linguistic terms and associated rules, instead of deterministic mathematical functions. This is an important advantage since the system can be described in a natural manner that reflects the imprecise and incomplete sensory data provided by human sensory modalities.

McDonald et al. developed a fuzzy logic car-following model based on an implicit speed and headway control assumption, which used relative speed and distance divergence as the principal inputs and acceleration-deceleration rate as output [62]. A rule base in natural language was established to map the input and output space. The model was validated with time-series data collected by an instrumented vehicle and more consistent results had been achieved [102]. Kikuchi et al., on the other hand, assumed the inputs of model to be distance between leading vehicle and following vehicle (DS), relative speed (DV) and acceleration/deceleration rate of leading vehicle (ALV) ([46], [47]). Two models differed in the form of output membership function and their deffuzzification method. The former model used five triangle membership functions while the later used several linear ones.

3.1.6 The Bando Model

Unlike most of the models reviewed above where it was assumed that a following vehicle tried to maintain a safe distance to a leading vehicle mainly by keeping the same speed with the leading vehicle, Bando developed a dynamic car following model based on an idea that each vehicle had a legal velocity (V), which depended on the following distance of the leading vehicle. A driver of a following vehicle controlled his or her acceleration in such a way that he or she could maintain the legal safe velocity according to the motion of the leading vehicle [4]:

$$A_f(t) = a\,[V(x_l(t) - x_f(t)) - \dot{x}_f(t)] \qquad (3.11)$$

where x is the position of vehicle, α is a constant, subscript l denoting leading vehicle and f the following vehicle. V is a legal velocity function.

The stimulus was assumed to be the relative speed between the legal velocity and the actual speed of the following vehicle, and the sensitivity (a) was a constant.

One of the most important properties of the Bando model is that macroscopic traffic performance can be associated with the dynamic car following model. It has been shown that a uniform flow of traffic can lose stability in certain conditions and the model, to some extent, can explain the mechanism for flow breakdown and spontaneous traffic jam formation. However, little research on the validation and calibration based on microscopic data has been reported.

3.1.7 Conclusion

The diversity in car-following models may be a true reflection of multi-dimensional nature of the car following behaviour. Models taking different approaches all showed some ability in describing the phenomenon. Traditional deterministic models, represented by GM series, have a rigid mathematical form, and therefore are convenient for calibration and further analysis, e.g., stability analysis etc. On the other hand, some behavioural oriented models, represented by Action Point Model, still lack practical mathematical tools for the further analysis of model properties.

Only fuzzy logic models have both of the advantages. Such models are behaviourally meaningful because of the simple linguistic form, and is mathematically rigid because several analytical tools have been developed in recent years, which has made possible to explore properties of fuzzy logic model analytically (e.g. [92], [93]). However, an overhead of the fuzzy logic modelling approach is its high computational demand. For this research it was to use fuzzy logic as the main mathematical tool for behavioural modelling.

3.2 Model Identification

Behaviour modelling requires knowledge of human performance. Though driving is relatively simple, there is still much uncertainty surrounding the mechanisms as to how a driver carries out a following task. This has been reflected in the diversities of models of car following behaviour. All the models have established a unique interpretation of the car following behaviour. For example, a driver's role is described as an information processor in GM models, an optimal estimator of state in optimal control models, a safety distance keeper in the stopping distance model and, a state monitor who always wants to keep perceptions below the threshold in action point model. On the other hand, fuzzy logic models treat human operators as a decision-maker who make control decisions based on sensory inputs using fuzzy reasoning.

As human sensory modalities are multi-dimensional, the possible input-output combinations are many. The existed fuzzy logic car following models only represent a very small portion of the possible model formulations, which have been devised based on the developer's interpretation of car following behaviour. A more complete investigation can possibly lead to a more optimal formulation. Thus, the possible sensory inputs and control outputs available to a driver are first investigated through analysis of car following behaviour, and then mathematical tools are determined to meet these requirements. Finally model identified is presented.

3.2.1 Car Following Behaviour

Rasmussen proposed generic human performance taxonomy based on a human information-processing theory, which discriminates three levels of human behaviour: skill-based, rule-based, and knowledge-based. Skill-based behaviour is typified by a performance controlled by stored patterns of behaviour, where the operator reacts to stimuli with little conscious effort or consideration ([78], [79]). Rule based behaviour involves performance in familiar settings, using stored or readily available rules. Knowledge based behaviour is always connected with novel problem solving that is based on a knowledge of the system. This level of behaviour usually requires higher level cognitive processes such as goal setting, strategy selecting, etc.

Lunenfeld and Alexander adopted Rasmussen's three-level performance taxonomy and proposed a similar hierarchy for a driving task, i.e., with three levels: (1) Control, (2) Guidance, and (3) Navigation [56]. They considered the control level of performance to comprise all those activities that involve second-to-second exchange of information and the control inputs between the driver and vehicle. At the guidance level, the driver's main activities involve the maintenance of a safe speed and proper path relative to road and traffic elements. Inputs to the system were dynamic speed and path responses to traffic, roadway geometric, hazards, and the physical environment. Information presented to the driver-vehicle system was continually changing as the vehicle moved along the highway. The driver guided the time-space trajectory of the car based on traffic rules and driving rules. Therefore, guidance level performance was rule-based. The third and highest level, navigation, in which the driver mainly acted as a supervisor, was characterised by such activities as routing selection through his or her own knowledge base, map or road signing. It involved considerable high level cognitive processes and was knowledge-based behaviour.

Lunerfeld's hierarchy of driving behaviour, though conceptual and descriptive, provided a basis for quantitative modelling. Car following behaviour involves both control and guidance level performance. At the control level is the driver's performance in undertaking such tasks as moving feet from throttle to brake etc. The behaviour of negotiating with a leader is clearly at the guidance level. Together with vehicle dynamics, a complete car following model needed to describe the

relationships between a driver's perceived inputs in car following situations and output from driver-vehicle systems as is shown in Figure 3.2.

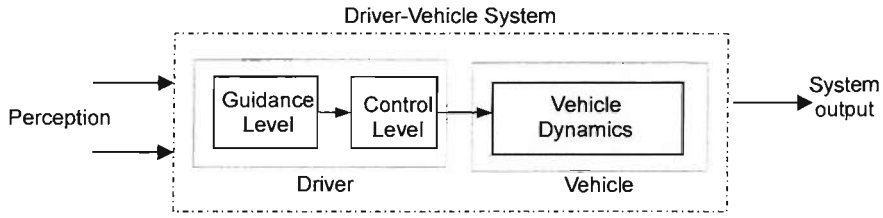

Figure 3.2 Driver-vehicle System

The car following models reviewed above do not explicitly model all components in a detailed way. Instead, they only describe the performance of driver-vehicle system as an entity. The goal in this research was to develop a simulation model, which could be used to mimic the car following behaviour of many vehicles at same time. It is neither practical nor possible for the model to describe every component of a driver-vehicle system in a detailed way. Therefore, it is decided to treat the driver-vehicle system as an entity as in most other car following models. The rationale of doing so has been justified in the crossover model of manual control behaviour where McRuer et al found that the human operators can adjust their performance and respond in such a way as to make the total open-loop transfer function of human-machine system behave as a first-order system. Thus, the behaviour of a driver-vehicle system can be better discussed under the framework of manual control.

A generic description of automobile driving performance can be found in the domain of manual control theory, where it is treated as a typical close-loop tracking task [99]. Car-following behaviour in terms of velocity and headway tracking can be extended as an analogue to this tracking task approach (lateral position control), as illustrated in Figure 3.3.

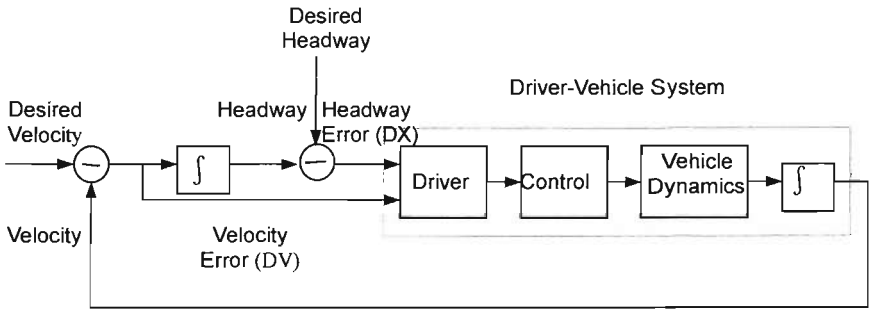

Figure 3.3: The Tracking Loop in Car-following

As a typical manual tracking performance, a conceptual description of car-following can be made like this: when driving a vehicle in car-following situation, the driver can perceive the discrepancy or

error between the desired state and his/her actual state in terms of velocity and headway (DV and/or DX). The driver wishes to reduce this discrepancy by adjusting the accelerator or brake position. This in turn produces a change in driving or braking force, and which in turn causes a change in a vehicle's actual velocity and position, thus forming a closed-loop tracking process. The goal of car following is to maintain a desired following distance and a desired speed. The model describes how a driver controls the driver-vehicle system to achieve this goal.

3.2.2 Fuzzy Logic Car Following Model

Based on the above conceptual representation, car following behaviour can be described using:

- GM Linear Model or Simple Crossover Model if only speed error is considered and the driver-vehicle system behaves in a linear way.
- Helley's Linear Model or Extended Crossover Model if both speed and headway error are considered and the driver-vehicle system behaves in a linear way.

However, both human responses and vehicle dynamics are highly non-linear, and the direct perception of a driver is not limited to speed and headway error. The linear model may be unable to describe car following behaviour sufficiently.

The use of a Fuzzy Inference System (FIS) is a convenient way to map an input space to an output space. The logic can be built on the experience of people who understand the system to be modelled in natural language. The primary mechanism for doing this is a list of if-then statements (i.e., rules). Compared with other input-output mapping tools such as neuro-networks, FIS is built on a very simple concept called 'fuzzy reasoning'. This makes the system natural and suitable to model a human-in-the-loop system (e.g. [84]). A brief introduction to FIS is given below, and a good general introduction can be found in reference [49].

3.2.2.1 A Brief Introduction to Fuzzy Inference Systems

Fuzzy inference systems use IF THEN ELSE rules to relate linguistic terms defined in output space and input space. Every linguistic term corresponds to a fuzzy set. Unlike classical sets that have a distinct and precise boundaries, fuzzy sets have boundaries that are not precise and are described by membership functions that are curves defining how each point in the input space is mapped to a membership grade. The transition from non-membership to membership is gradual rather than abrupt. The fuzzy sets shown in Figure 3.4 represent linguistic terms associated with car following distance of too close, satisfied and too far. The value of the membership is between 0 and 1. A membership degree of 1 represents certainty with respect to an entity belonging to a particular set. It is important to note that the shapes of the fuzzy functions can be arbitrary.

Fuzzy inference is achieved through fuzzy logic operation defined by inference rules, but the method of logical operation is distinct from a traditional one. For example, the union of fuzzy sets (AND) is usually defined as the larger of the two, and intersection (OR) is the smaller of the two. By applying proper implication method (THEN) and rule weight, we obtain the output fuzzy set associated with each rule. The final step is to aggregate all output fuzzy sets from different rules and then resolve a crisp output value from the output fuzzy set (aggregated) using a defuzzification method defined in FIS.

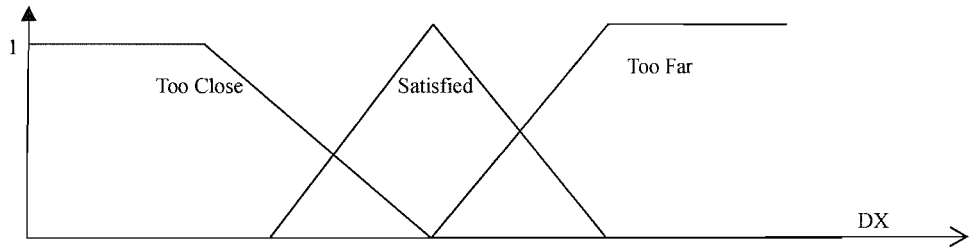

Figure 3.4 Membership Function

Basically, there are two types of inference system, the Mamdani and Sugeno type of fuzzy inference system. The main difference between them is that the output membership functions can only be linear or constant for Sugeno type fuzzy inference. The linear membership function is a linear combination of all input variables and a constant. A typical rule in a Sugeno type system is:

If input x is A and input y is B then output is $x*p+y*q+r$;

where p, q, r are constant and A, B are fuzzy sets.

The output membership function associated with this rule is $x*p+y*q+r$. The constant output membership function is just a singleton spike ($p=q=0$). Because of this distinctive feature, a Sugeno system is very suitable for modelling non-linear systems by interpolating multiple linear models.

The necessary steps in defining a fuzzy system include:

- Selection of input and output variables;
- Fuzzy partition of domains for each variable;
- Selection of linguistic rules, definition of membership functions;
- Selection of operations for inference;
- Selection of a defuzzification methodology.

A tool to design a fuzzy inference system is available in the Fuzzy Logic Toolbox of Matlab [60].

3.2.2.2 A Generic Fuzzy Logic Car Following Model

The generic fuzzy logic car following model that is able to approximate existed models as well as describe new formulations is shown in Figure 3.5 [16]. It is a mapping between variables driver can perceive and variables driver can directly control.

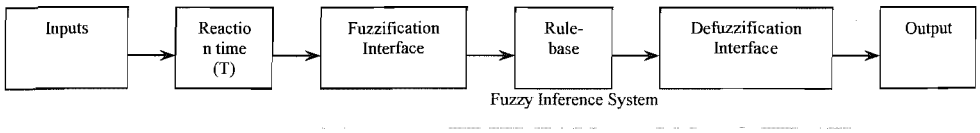

Figure 3.5 A Generic Fuzzy Logic Car Following Model

Input

A driver is able to detect time-to-collision (TTC), relative speed, speed and distance using optic flow information (refer to [36], [37], [71]). Eight candidature variables are identified from some well-established car following models, which can either be directly perceived or estimated from those direct perceptions by drivers.

- V_f: The velocity of the following vehicle
- DX: Distance headway (front to rear)
- DV: Relative speed between the leading and the following vehicle. DV=d(DX)/dt
- V_l: The velocity of leading vehicle. $V_l=V_f+DV$
- T_h: Time headway. $T_h=DX/V_f$
- DV/DX (1/TTC): Reciprocal of time to collision. The variable is a converted form of time to collision (TTC), which will be infinite when DV=0.
- dtheta/dt: Angular velocity. This is calculated based on the following approximate formula: $dtheta/dt=(width*DV)/DX^2$ (The width of leading vehicle is assumed to be 2.5 meters in this research)
- DSSD: Distance divergence. This is calculated according to:

$DSSD = DX/D_{dsr}$, D_{dsr} is the desired headway.

Output

The output variable is assumed to be the acceleration rate of the following vehicle as it is the only direct control available to the driver.

Reaction time

Reaction times of 0, 0.5, 1, ...,3 sec for input variables has been initially hypothesised.

Fuzzy Inference System (FIS)

A Sugeno-type fuzzy inference system has been used. Several specifications about the fuzzy inference system are chosen as follows:

- Type of input membership function: 'gauss' type.
- The number of partition for each input domain: 5
- Implication method: Product
- Defuzzification method: ' weighted average'.

3.2.3 Identified Model Formulation

A large number of model formulations can be represented using the generic fuzzy logic car following model. The optimal is one that gives satisfactory performance and meets other requirements as a microscopic simulation model, which can be identified by comparing the overall performance of different model formulations.

The performance of the fuzzy logic model is usually indicated by the Root Mean Square Error (RMSE) of the model prediction, which is:

$$RMSE = \sqrt{\frac{\sum_{i=1}^{N}[X_i \mid predicted - X_i \mid real]^2}{N}}$$

The key task in model identification is to develop a large number of possible fuzzy logic models, each of which involves such steps as the definition of the membership, construction of the rule base etc. In the past, a single model development has been done by the modeller based on practical experience or the examination of test data, e.g. McDonald, et al., define membership function through 'direct binary' method [62]. However, this approach not feasible when a large number of models are to be constructed. Alternatively, neural fuzzy system can be used to extract the necessary information directly from measurements of car following behaviour as it can directly learn and adapt to the pattern from a large quantity of data. This eliminates the need to devise many fuzzy logic models subjectively. Also, this is a more objective approach and is likely to identify some subtle behaviour that may otherwise be difficulty to find. The approach is especially pertinent when large quantities of time-series data are available. The functionality is available through Adaptive Neural Fuzzy Inference System in Matlab for Suegeno-type fuzzy inference system [60].

Possible model formulations with one, two, three input variables selected from eight candidature ones have been generated and trained using empirical data. The training data was taken from a TRG database, which has been collected on motorways using instrumented vehicle for the validation of FLOWSIM (refer to [64], for a more detailed introduction to data). The data consists of 69 car following traces performed by 8 subjects, totalling 5840 seconds in length. The data processing procedure introduced in section 2.3 has been applied to reduce measurement error.

Table 3.1 Summary of the Data Used in Model Identification

Subject	1	2	3	4	5	6	7	8
Data Length (s)	763	446	1055	596	767	1079	890	243
Traces	10	6	9	7	7	12	9	3

Compared to the data collected in the merging survey, the database used for model identification is relatively small. The reason for using this database was two fold. Firstly, at the time of car following model development, the merging experiment had not started. Secondly, the time needed to train a model is proportional to the size of the training data used. Because of the huge number of the possible model formulations, it would have been impractical to test every model using a large quantity of data. Even using this database which is very large compared with databases used in most past studies, it was estimated that the training could take more than one month. Therefore, the data was further divided into three parts according to the maximum deceleration rate (> 2 m/s^2, 1-2 m/s^2; <=1 m/s^2) used by following vehicle as 'harsh', 'moderate' and 'smooth' group. The 'harsh' data that is 1191 sec in length (11910 data points) is used as the training data because it covers a wider range of car following scenarios. Other data has been used for checking and test purpose.

Using a combination of back-propagation and least square training method, all possible model formulations were tested. The RMSE of the trained model is illustrated in Figure 3.7-9. Because of the large number of combinations for two-input and three input models, only the top 8 (smallest RMSE) have been shown.

3.2.3.1 Single-Input Model

DV or its associated variables (DV, DV/DX, ttheta/td) show better performance than other variables while DV/DX (reciprocal of time to collision) gives the smallest prediction error (Figure 3.6). The results clearly indicate that driver's behaviour is based on a speed difference between the leading and following vehicles. While variables relating to headway (DX, Th, DSSD) alone are unable to explain this behaviour. The velocity of leading or following vehicles (V_f, V_l) alone cannot explain the variations in acceleration rate because car following is an interacting process. The system reaction time is in the range of 1-2 second.

3.2.3.2 Two-Input Model

Of the 28 possible model formulations, three of the top four (DV-T_h, DV-DSSD and DV-DX) are a combination of relative speed and headway (Figure 3.7). This result showed that a combination of speed matching and headway matching strategy is dominant in car following behaviour. Other combinations were composed of reciprocal of time-to-collision (DV/DX) and other variables, an indication that DV/DX will give a good prediction of acceleration/deceleration behaviour. The importance of DV/DX was once again justified. However, the difference between the performance of these models is very marginal, reflecting that similar speed divergence (DV, DV/DX or dthera/dt) or headway (T_h, DX, DSSD) related variables do not show much difference, though some of them such

as DV/DX, dtheta/dt, intrinsically have more behavioural meaning. However, the results clearly show that drivers employ a combination of speed and headway as a basis of their control strategy. The reaction time is in the range of 1 to 2 seconds.

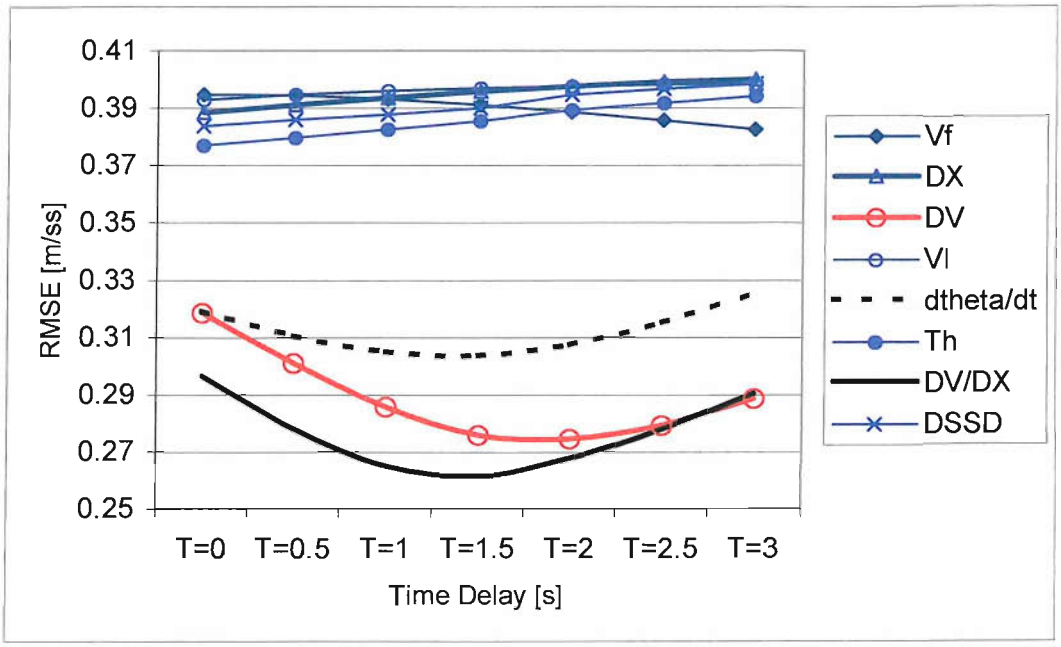

Figure 3.6 RMSE of Single-input model

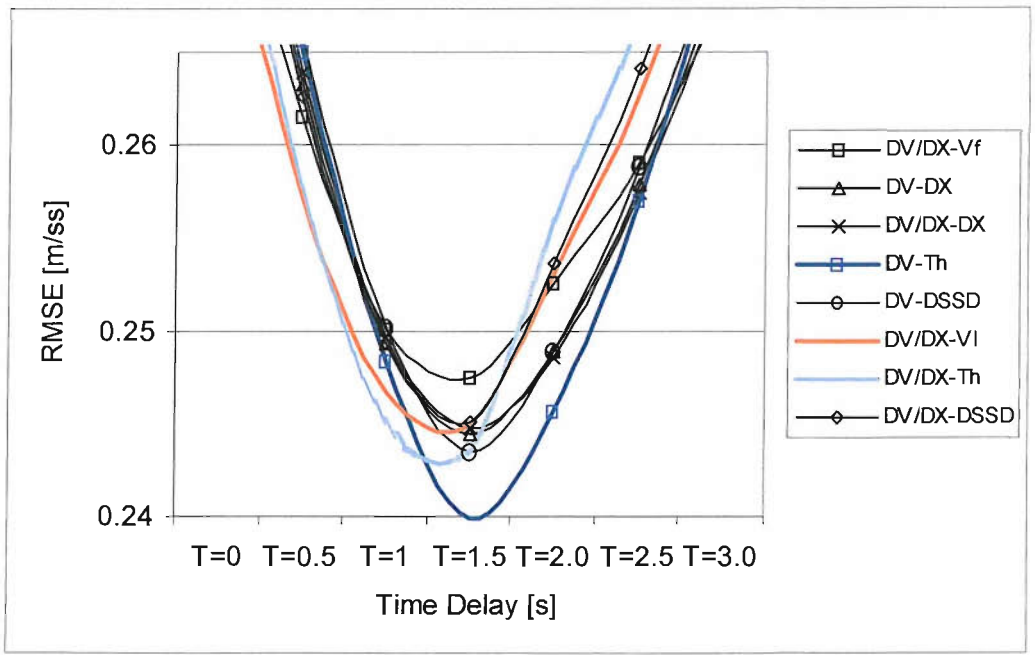

Figure 3.7 RMSE of Two-input model

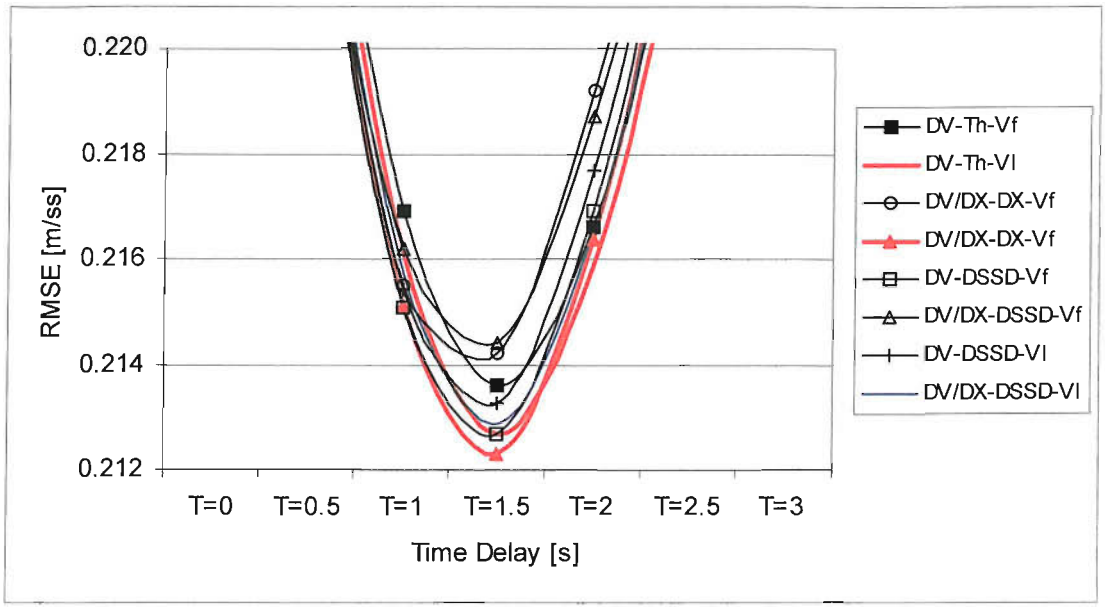

Figure 3.8 RMSE of three-input model

3.2.3.3 Three-Input Model

As shown in Figure 3.8, the top eight combinations all contained relative velocity related factors (DV, DV/DX), headway related factors (T_h, DX, DSSD) and speed related factors (V_f, V_l). The performances are very similar. This result can be interpreted to indicate that an additional speed consideration in the three-input models provide additional ability over two-input models. That is, if the two-input models can predict car following behaviour over the entire speed range, three-input models can predict the car following behaviour within a finer partition of speed than two-input models thus fitting the data more precisely and performing better. It may be seen that the speed partition based on V_f and V_l makes not much difference. This is reasonable because, in car following process, the relative speed between the leading and the following vehicles is kept small. The system delay is in the range of 1to 2 seconds.

The overall RMSE reduction from single-input model to three-input model was significant (0.26150-0.23989-0.21232). However, it should be noted that this has been achieved based on an exponential increase in model complexity. Mathematically, if we consider a one-input model as an interpolation between 5 single-variable linear models, then two-input model is an interpolation between 25 two-variable and a three-input model between 75 three-variable linear models. A slightly lower RMSE can be achieved by using more input variables or finer partitions. However, it is uncertain that a driver would behave based on so many perceptions and the reason based on such a huge rule base. No further investigation were conducted for more complicated models with four or more inputs.

Model simplicity and applicability are important requirements for a microscopic simulation model. Therefore, based on the above, key parameters are relative speed (DV) and distance divergence (DSSD) as input, and acceleration rate as output, because:

- The model incorporating these represents car following behaviour satisfactorily. Although a three-input model gives better performance than a two-input model in terms of RMSE, the difference is marginal.
- The structure of the model is not too complex, and is computationally acceptable.
- The model is applicable to a wide range of car following situations because of the inclusion of a separate headway related term, DSSD.

The selected model formulation can be expressed as:

$$a_f(t)=\text{FUZZY (DV, DSSD)}|t-T_d \qquad \textbf{(3.12)}$$

where FUZZY denotes a fuzzy mapping and T_d is the reaction time.

3.3 Anticipatory Aspects in Car Following Behaviour

The model described above is established on the reactive (compensatory) regime, that is, drivers are assumed to take action when there have been discrepancies between perceived states and their desired states. However, in everyday traffic situations, the detection of relevant information depends not only on perceptual factors, but also on the expectations of drivers. In most cases, small deceleration or accelerations can be anticipated by following drivers based on a range of cues derived from similar traffic settings that the driver is well familiar with. For example, the deceleration of a direct leading car can be anticipated if there is a slower traffic further ahead. The same will hold true for acceleration behaviour if there is an obstructing traffic changing the lane. This kind cue is readily available in the environment.

The existence of anticipatory response in vehicle driving has been recognised by other researchers. Many authors have supposed the existence of two distinct mechanisms in steering control (e.g., [22]). One is anticipatory and the other is compensatory. The fundamental idea behind this two-mechanism approach is the duality of information presented to the driver by the forward view of the road. The visual field of the driver provides information on the instantaneous and future course of the road, so that the driver can not only perceive the present but also extrapolate future 'guidance information'. On the other hand, static and dynamic cues in the visual field contain information on the instantaneous deviations between the vehicle's actual path and its desired path (stabilisation information) [22]. The driver is assumed to respond to both two kinds of information.

There has also been some evidence that support the existence of 'anticipatory response' in car following behaviour. Van Der Hulst, et al. reported on car following behaviour in different visibility conditions (clear or fog) and the predictability of leading car deceleration (predictable or unpredictable) based on a driving simulator experiment [98]. They found that drivers applied a hierarchy of adaptive strategies aimed at the control of time pressure when driving. In normal visibility conditions, drivers adopt an anticipatory driving strategy. When the possibilities for anticipation are reduced, drivers compensate by reducing speed and increasing time headway, in order to increase the time available to react to potential threats (compensatory strategy). When this is impossible or undesirable, drivers have to maintain a high level of alertness in order to react accurately to unpredictable hazardous events. They suggested that 'the adaptation of time headway was related to the difficulty of anticipation, rather than perceptual degradation due to reduced visibility. In another experiment by the same authors, drivers' responses to rather abrupt and more gradual decelerations of the leading car were investigated in a driving simulator where situational traffic cues (e.g., vehicle cutting in) were used to manipulate driver expectations [99]. They concluded that if cues in the environment indicated that the leading car was likely to decelerate, drivers reacted faster. Moreover, drivers increased their headway by decelerating before the leading car actually started to decelerate, which can be considered an anticipatory response.

Biological research has revealed that anticipation is one of the most primitive functions of biological intelligence. Unlike higher cognitive functions, anticipation is deterministic; it does not require that the creature doing the anticipation to make a volitional choice to do so [45]. Based on an extremely sparse set of percepts describing the present state, a creature performs the remarkable feat of recognising a situation, with sufficient time to take corrective action. The mechanism of anticipation has been rigorously justified in mathematical theory by Rosen [82]. The anticipation function of biological intelligence suggests that a driver may be able to recognise the near future state of leading vehicle based on an extremely sparse set of percepts describing the present state, and can take action accordingly.

Though it will be difficult to emulate the anticipation process precisely, it can reasonably be assumed that the near future state of the leading vehicle, characterised by several simple attributes such as velocity etc, can be readily obtained through the anticipation function of biological intelligence. That is to say, the anticipated information, future state of the leading vehicle, may be accessible by driver of the following vehicle because of the existence of this biological intelligence, as long as the cues for anticipation are available. In normal driving, these cues are well presented in front of the driver. In addition, because anticipation is deterministic, drivers will always employ the anticipation function. That is to say, drivers will adopt an anticipatory driving strategy if possible. It may be possible to

improve car following models by taking into account the anticipatory aspect in car following behaviour.

3.3.1 Preliminary Investigation

As has already been noted, drivers mainly use speed information in car following behaviour and the speed information of the leading vehicle should be taken into account in the consideration of anticipation. The anticipatory effect may be verified by assuming a different reaction time in the velocity of the leading vehicle. A new model can be established as illustrated in Figure 3.9. A negative reaction time, T_l, which recognises anticipation of the speed of the leading vehicle, should be expected.

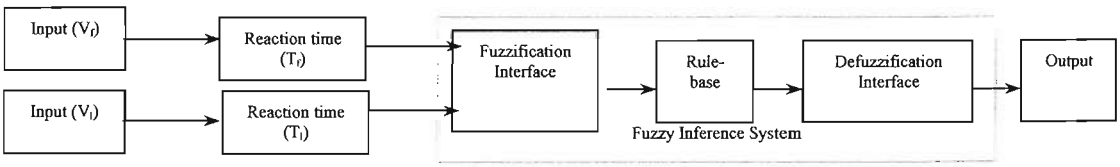

Figure 3.9 Car following Model for Investigating Anticipation

This model, fitted to training data, should be able to identify any relationship between velocity combinations under different reaction time assumptions and the acceleration/deceleration rates. The same data and procedure used in the identification of the compensatory model has been used to obtain RMSE values under different reaction time assumption. The result is shown in Figure 3.10.

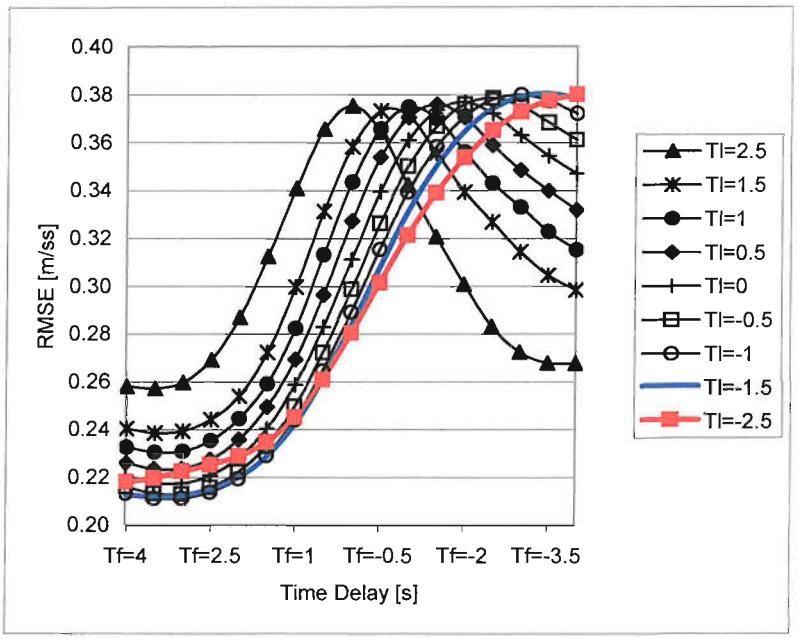

Figure 3.10 RMSE of Anticipatory Car Following Model

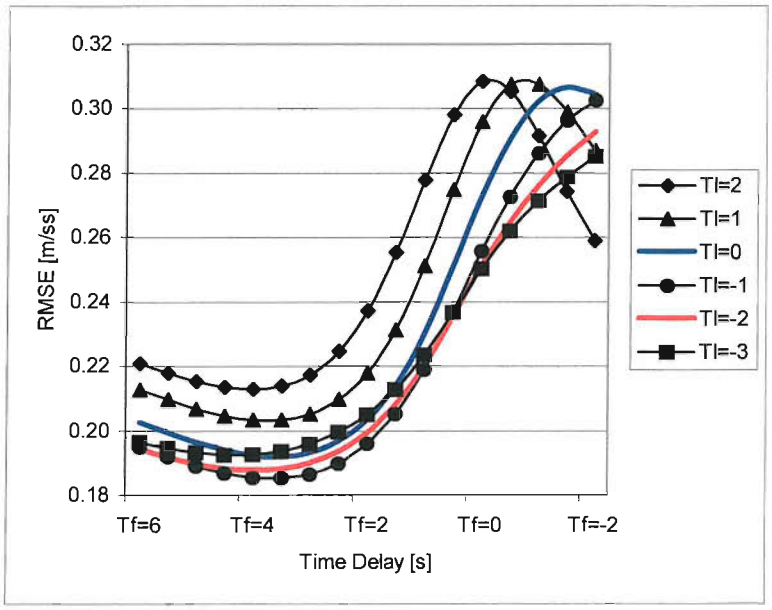

Figure 3.11 RMSE of Anticipatory Model based on 'Medium' Data

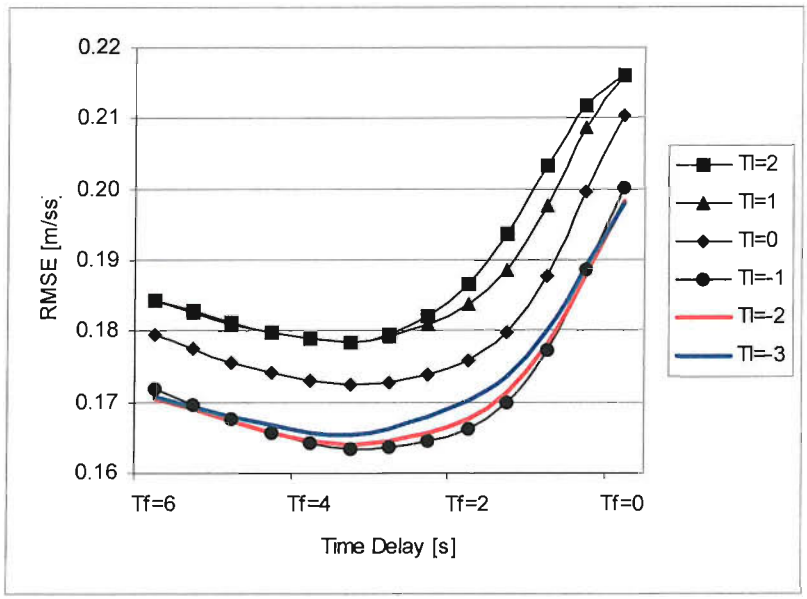

Figure 3.12 RMSE of Anticipatory Model based on 'Smooth' Data

The smallest RMSE has been achieved based on 'harsh' data with a reaction time on the velocity of the leading vehicle of T_l= -1 second, and total reaction time for the velocity of the following vehicle, T_f=3 seconds (RMSE=0.21126). The performance of the model was noticeably improved compared with RMSE obtained under assumption of a uniform reaction time for both inputs, which is: RMSE=0.27234 when $T=T_l=T_f$=1.5 sec and RMSE=0.31127 when $T=T_l=T_f$=0 sec.

The result implies that drivers seem be able to use future information on the leading vehicle, which can be obtained through anticipation. To check the rationale of the above result, the 'medium' (2903 sec) and 'smooth' (1745 sec) time-series data which can be taken as independent as there is no apparent relationship between them, except for using the same subjects and the data being collected on a motorway, is further used to identify the combination of reaction time which leads to the smallest RMSE.

The result based on 'medium' and 'smooth' data is illustrated in Figure 3.11-12. Not surprisingly, the best combination of reaction time is obtained at T_l=-1 sec and T_f=3.5 sec. It should be noted that the reaction time of T_f is in range of 2 - 4 seconds and T_l in range of -0.5- -1.5 seconds shows little difference, although the overall fitted RMSE has been improved noticeably when compared with a uniform reaction time of 0 or 1.5 second under a reactive regime.

Whilst anticipatory behaviour may be the result of a driver's interpreting information available to drivers being followed, such as traffic or geometric conditions, the strength of these relationships would indicate that the concept of anticipation provides a sound 'proxy' of actual behaviour in the situations described.

3.3.2 Anticipatory Model of Car Following Behaviour

To incorporate anticipatory aspect into the car following model, DV is substituted by a new variable, called cognitive velocity divergence (CDV):

$$CDV(t) = V_l(t-T_l)-V_f(t-T_f) \quad \textbf{(3.13)}$$

Based on the identified compensatory model (Equation (3.12)), the corresponding anticipatory car following model can be written as:

$$a_f(t)=FUZZY\,(CDV\,|t,\ DSSD\,|t-T_d) \quad \textbf{(3.14)}$$

where $CDV(t) = V_l(t- T_a)-V_f(t- T_d)$, $T_a = T_l$ *and* $T_d = T_f$ is anticipation time (negative reaction time) and reaction time respectively.

It is assume that drivers try to follow the anticipated future speed of the leading vehicle instead of the past speed. By replacing relative velocity (DV) with this variable, the RMSE has been recalculated for some input combinations using the database. The resulting average RMSE is shown in Figure 3.13. It is very clear that an improvement has been achieved in all cases.

In steady-state conditions, (e.g., v_l≡constant), the anticipatory and compensatory models are the same. There is little previous research as to whether drivers are able to obtain *CDV* information using

perception and anticipation. Studies on the detection of time-to-collision (TTC) and relative speed have all suggested that drivers used the optic flow (refer to [26], [36], [37]). Typically, for TTC detection, two mechanisms, namely cognitive (computational, obtained by calculation) approach and ecological optics approach (directly perceived) have been examined (refer to [87] for a review in this topic). The experimental results seem to favour the later approach, i.e., TTC information is directly available in the optic flow fields and there exists a neural mechanism somewhere in the visual system to process TTC information. It seems unlikely that a driver will or can calculate CDV from anticipated V_l and perceived V_f. However, CDV can also be expressed as: $CDV(t)= (V_l(t-T_a) - V_l(t-T_d)) + DV(t-T_d)$. If drivers are able to anticipate the speed change of a leading vehicle from $t-T_d$ to $t-T_a$, it will be possible for them to obtain CDV information because $DV(t-T_d)$ is readily available from cues in the optical field.

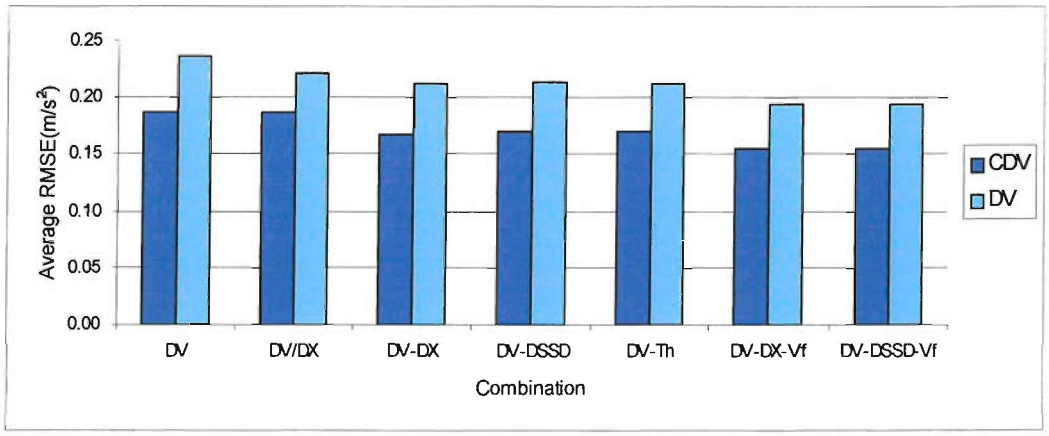

Figure 3.13 A Comparison of RMSE between Compensatory and Anticipatory Model

On the other hand, it can be seen that $V_l(t-T_a) - V_l(t-T_d)$ can be approximately obtained from the acceleration rate of the leading vehicle: $V_l(t-T_a) - V_l(t-T_d) \approx a_l(t- T_d) * (T_d - T_a)$, where a_l is the acceleration rate of the leading vehicle. That is to say, if a driver can perceive the acceleration rate of the leading vehicle, CDV may be obtained. However, behavioural research has revealed that human drivers are unable to perceive the acceleration rate of a leading vehicle accurately (refer to [50] as cited in [51], [96]). Therefore, the future speed of the leading vehicle is more likely to be obtained through a driver's anticipation using other relevant cues. In the case that the acceleration rate of the leading vehicle is available, the anticipatory model is still valid as CDV can be readily obtained from the acceleration rate and perceived DV.

Although the performance of car following behaviour model can be improved by taking into anticipatory aspects into account, the anticipatory model relies on the future state of the leading vehicle, which cannot be obtained in a real time simulation environment. Another predictive model

will be needed to predict the near future state of the leading vehicle based on traffic cues, for which further research is needed. It was decided to use compensatory form of car following model in the simulation model.

3.4 Model Calibration

Model calibration is the process of quantifying model parameters using empirical data. The car following model identified has two sets of parameters, a desired headway (SD) that drivers choose to keep and parameters within the fuzzy inference system describing how drivers keep their speed and headway. The model is calibrated on individual subjects, so that the variations within and between drivers can be explicitly taken into account.

3.4.1 Calibration of Desired Headway

A basic question about the desired headway for car following behaviour is whether there is a constant desired headway over all car following processes and across the driver population. If not, how does it vary with speed, between and within drivers? There is no discrepancy about the variation of the desired headway between drivers. Macroscopic observations of time-headway all suggest a log-normal or negative exponential distribution across the driver population [14] although discrepancies exist between studies regarding the relationship between desired headway and speed. The linear form of the headway-speed relationship assumes that there is a constant desired time headway and the desired headway can be expressed as:

$$SD = C_1 + C_2 * V \tag{3.15}$$

where SD is desired headway, C_1, C_2 (desired time headway) are coefficients, and V the speed (e.g. [21]).

Some researchers have found that time headway is not constant in car following, but increases with speed [100]. Accordingly, some non-linear headway-speed relationships have been proposed, e.g. the quadratic function:

$$SD = C_1 + C_2 * V + C_3 * V^2 \tag{3.16}$$

where C_1, C_2, C_3 are coefficients. Two basic validities about desired headway in car following behaviour will be:

- Desired headway-speed relationship.
- Desired headway distribution of driver and population.

3.4.1.1 Data

The data used was collected during motorway driving in the merging experiment, based on 30 days of observation. Typically, about 40 car-following processes have been identified each day. The car following processes collected on the same day are grouped, which form 30 samples.

3.4.1.2 Result

The desired headway of a driver in one car following process was identified by examining DV-DX (relative speed – following distance) plot. The change of headway in a typical car following process lasting for 2 minutes is illustrated in Figure 3.14. It shows repeated 'goal seeking' cycles on the DV-DX plane. The desired headway was chosen to be the median of headway readings with zero relative speed (cross-over point), and the associated speed can be obtained accordingly. When the number of cross-over points was less than five in a car following process, average values of headway and speed were used.

The speed-headway relationship of a driver was analysed by assuming a fixed minimum separation between moving vehicles of 5 m (C_1 in Equation (3.15)). A speed-headway curve of one subject is shown in Figure 3.15. Each point represents a desired headway identified from one car following process performed by the same driver. The quadratic function (Equation (3.16)) fitted the data better than a linear one (Equation (3.15)). However, the difference was marginal, which implied that a desired time headway could be used to characterise a driver's headway-keeping behaviour. The relatively poor fit (low R value) was an indication that there were other factors affecting a driver's choice of desired headway.

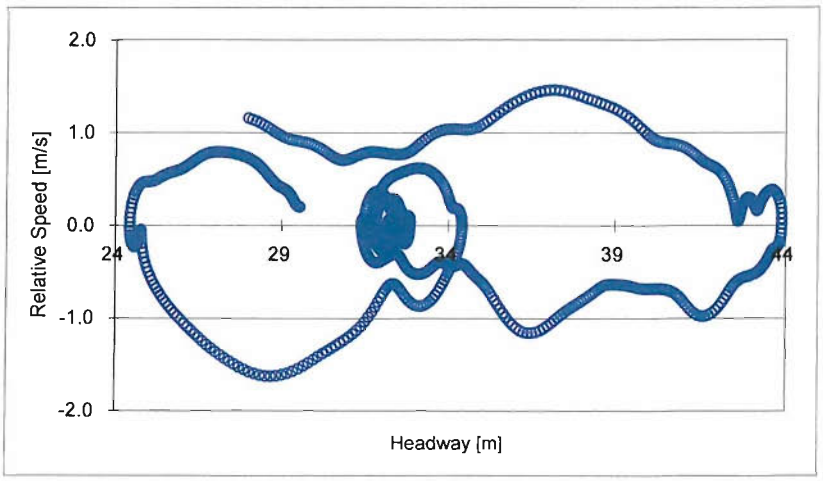

Figure 3.14 Headway in a Typical Car Following Process

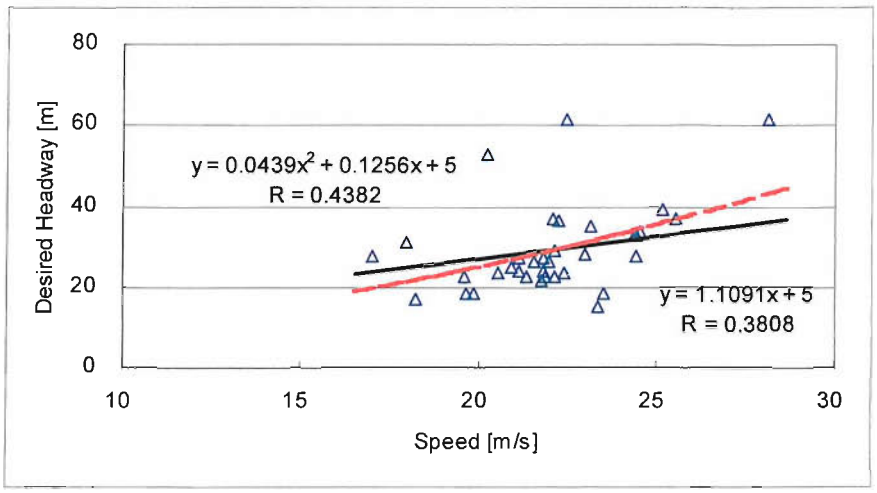

Figure 3.15 Speed – Desired Headway Relationship Based on One Subject

The variations in desired time headway within and between drivers are described statistically. The desired time headway distribution within a typical driver is illustrated in Figure 3.16(a). The distribution of the mean desired time headway between drivers is illustrated in Figure 3.16 (b). A lognormal distribution fitted the data well (Lilliefors test not rejected at the 95% confidence level).

The relationship between the mean and standard deviation of desired time headway from the sample of subjects is shown in Figure 3.17. It is clear that drivers who tend to follow the leader closely show smaller standard deviations in different car following processes.

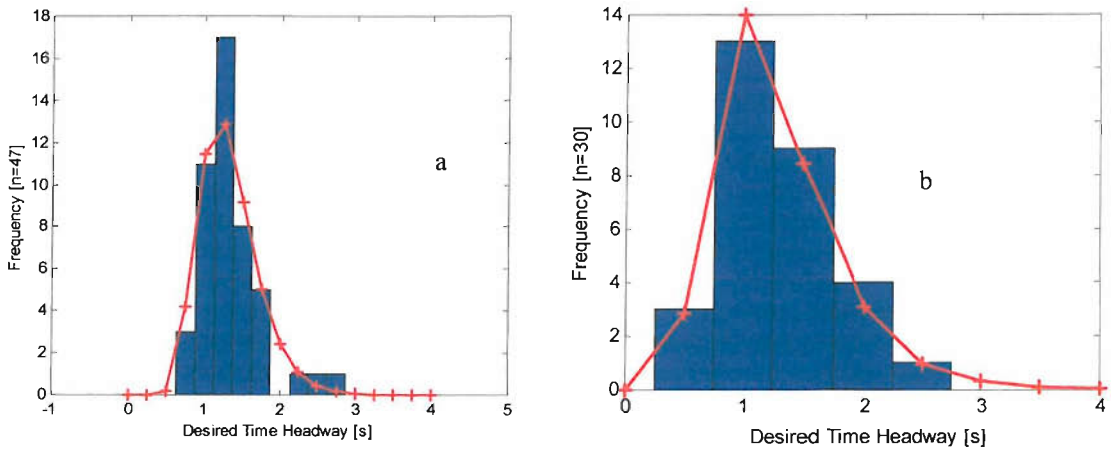

Figure 3.16 Time Headway Distribution within and between Drivers

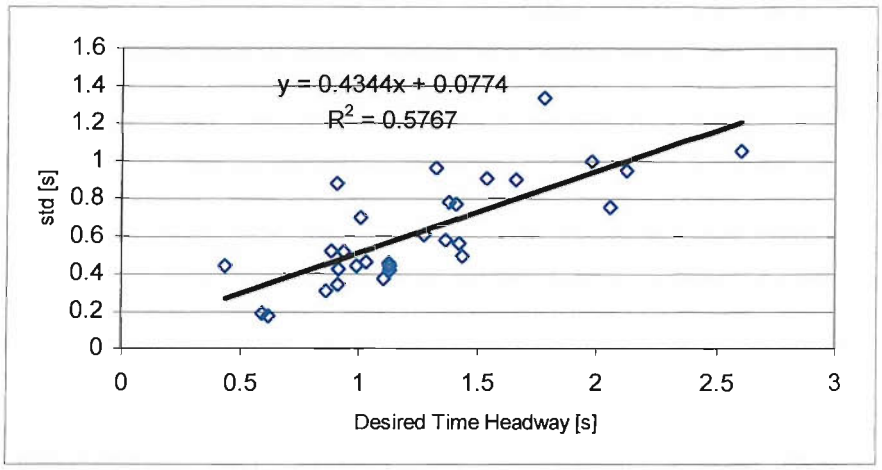

Figure 3.17 Relationship between Mean and Standard Deviation of Desired Time Headway

In conclusion, a driver's desired headway in car following can be approximately described by a constant desired time headway that varies within and between drivers. The mean desired time headway of the sample is distributed lognormally with a mean of 1.26 second and standard deviation of 0.49 seconds (refer to Table 3.3). The desired time headway within a driver is also distributed lognormally, with a standard deviation of:

$$std = 0.4344*m+0.0774 \quad \textbf{(3.17)}$$

where m is the mean desired time headway of the driver.

3.4.2 Calibration of Fuzzy Logic Model

According to model formulation, an open-loop fuzzy logic car following model is characterised by two types of parameters:

- Reaction time (T_d)
- Parameters of Fuzzy Inference System

To calibrate the model these parameters need to be estimated from the empirical data.

3.4.2.1 Data

Two databases were used in calibrating the fuzzy logic model. The first one was collected in a motorway car following experiment for the validation of FLOWSIM described above, and which was used in the model identification. The second one was collected in the merging experiment, which has been used in calibrating the desired headway. In the car following experiment, the subjects are asked to follow the leader, so that the task demand for car following may be higher than that in merging experiment, where no instructions are given to the subject in motorway driving.

3.4.2.2 Procedure

For every car following process, the desired time headway was first calculated with a constant offset of 5 meters. By varying the reaction time T_d , training data was generated for the fuzzy inference system. An adaptive neural fuzzy approach was used to estimate the parameters of the fuzzy inference system, which was analogous to a least squares estimation. 60% of data was used as training data and the remaining 40% as checking data to prevent overfitting. The best fit was obtained when the minimum root mean square error of acceleration rate was achieved. The procedure is detailed as follows:

SD Estimation:
Time-series SD is calculated according to:

$$SD=Th_{dsr}*V_f+5 \quad \textbf{(3.18)}$$

where Th_{dsr} is the desired time headway, which was estimated from empirical data of each car following process by linear regression.

Data Grouping

Data of car following processes performed by the same subject were randomly chosen and grouped into two. One group contained 60% of the processes was used as the training data while the other was used as the checking data.

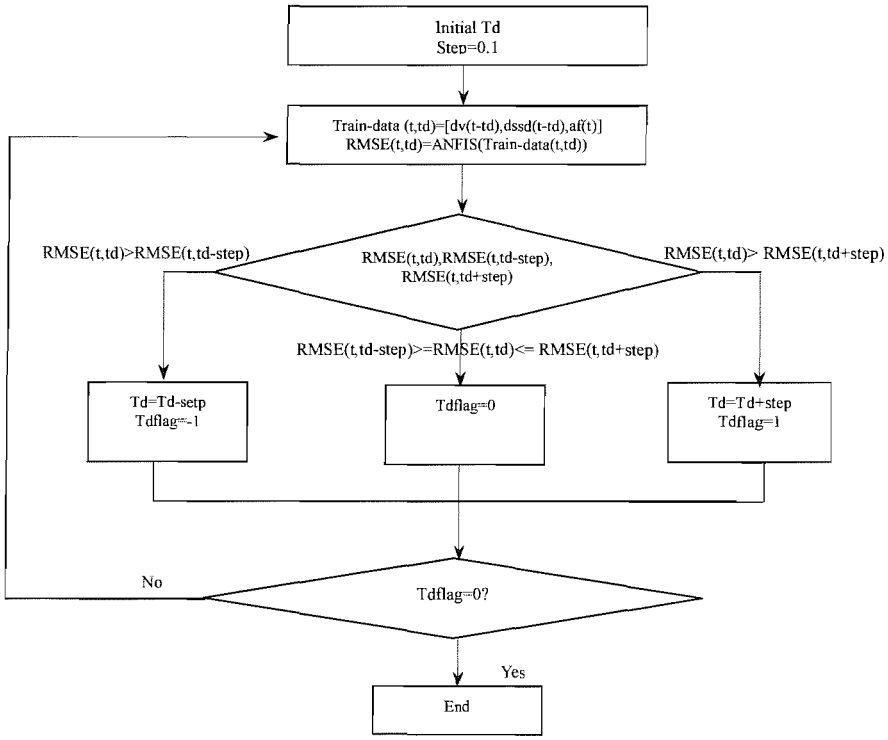

Figure 3.18 Diagram of T_d Estimation Algorithm

Reaction time (Td) Estimation

Reaction time was estimated by comparing the RMSE of the trained fuzzy model. Firstly, training data was constructed based on an initial estimate of T_d, the generated time-series data was then used to train the fuzzy model for a predetermined iteration number. According to several test trials, the RMSE changed little after 5 iterations. Therefore, the RMSE for estimating T_d were based on 5 iterations in training. A fixed step of 0.1 second was adopted to look for the convergence direction of RMSE along T_d. T_d was determined when trained model gave the smallest RMSE. The flowchart for estimation of T_d is illustrated in Figure 3.18.

Parameter Estimation of FIS

Because of the relative importance of speed control in car following, a triangular membership function was adopted with 5 partitions for DV and 3 partitions for DSSD. The output membership function was 15 singletons. The defuzzification method was chosen to be the weighted average.

The initial FIS was generated from training data according to the above specification using grid partition method, where the membership functions of each input were evenly partitioned within the range of the training data. A hybrid learning algorithm was then adopted to adjust membership function parameters of the FIS [60]. In each iteration, the parameters of output membership functions were updated in a forward pass using least-squares method. The inputs were first propagated forward until truth-values based on each rule were obtained. The overall output was then a linear combination of the parameters of output membership functions. The parameters of output membership functions could be estimated based on the training data. The parameters of input membership functions were estimated through back-propagation method in each iteration, where the error signals (the difference between model output and training data) were propagated backwards and the parameters were updated by gradient descent. The parameter optimisation for input and output membership functions were decoupled in the learning process, which was iterated until a stopping criterion had been met (e.g., a error reduction threshold, number of iterations).

The structure of FIS was determined from a comparison between several possible formulations. It was the result of a trade-off between model complexity and model performance. Though it was possible to reduce RMSE by adopting a finer partition of input space or more complex form of membership function, the complexity of the model and the associated computation demand will increase significantly. Considering that the model is targeted to a large-scale simulation, simplicity of model form is of importance to the overall performance of simulation program. The model adopted showed a satisfactory performance in predicting error while its form is relatively simple. The parameters of FIS were initially chosen to be those which gave the lowest RMSE obtained together with T_d in the model training.

Optimisation of Fuzzy Logic Model

The fitted model can be related to driver behaviour through linguistic rules. Because of limitations in training data, some rules generated may be contradictory. In that case, intervention was necessary. The purpose of optimisation was to compensate drawbacks caused by the direct data-driven method. Optimisation of the fuzzy logic model was carried out iteratively. Firstly, the FIS was revised by adjusting the output membership function relating to the contradicting rule in an intuitive way. The RMSE was recalculated. If RMSE had changed only marginally (less than 5%), the model was considered finalised. Otherwise, the model was re-trained and re-optimised, until two requirements, i.e., no contradicting rules and RMSE changes less than 5%, have been met. In the calibration process, only very few cases required optimisation, and slight adjustment of model parameters did not change the RMSE values significantly.

3.4.2.3 Result

A typical calibrated fuzzy model is illustrated in Figure 3.19. The model is described by a parameterised fuzzy inference system and associated reaction time T_d.

The open-loop mapping described by a FIS has more than 40 parameters and is non-linear. For a non-linear system, linear analysis is usually performed to determine qualitative/ quantitative effects of the equivalent linear parameters. This makes it possible to make comparisons. The fuzzy logic model has the same simple linear structure as the linear model (Equation (3.5)) except that the gain is no longer constant. A section plane of a fitted fuzzy logic model at desired headway is illustrated in Figure 3.20. A linearlised speed gain (k) can be calculated near steady-state (DV=0, DX=SD), which was comparable to the λ in linear model. Because headway gain is insignificant compared with the speed gain, only linearised speed gain near steady-state is calculated according to:

$$k = \frac{\partial F(DV, DSSD)}{\partial DV}$$

where F denoting the fuzzy mapping, k is the linealised speed gain of fuzzy logic model.

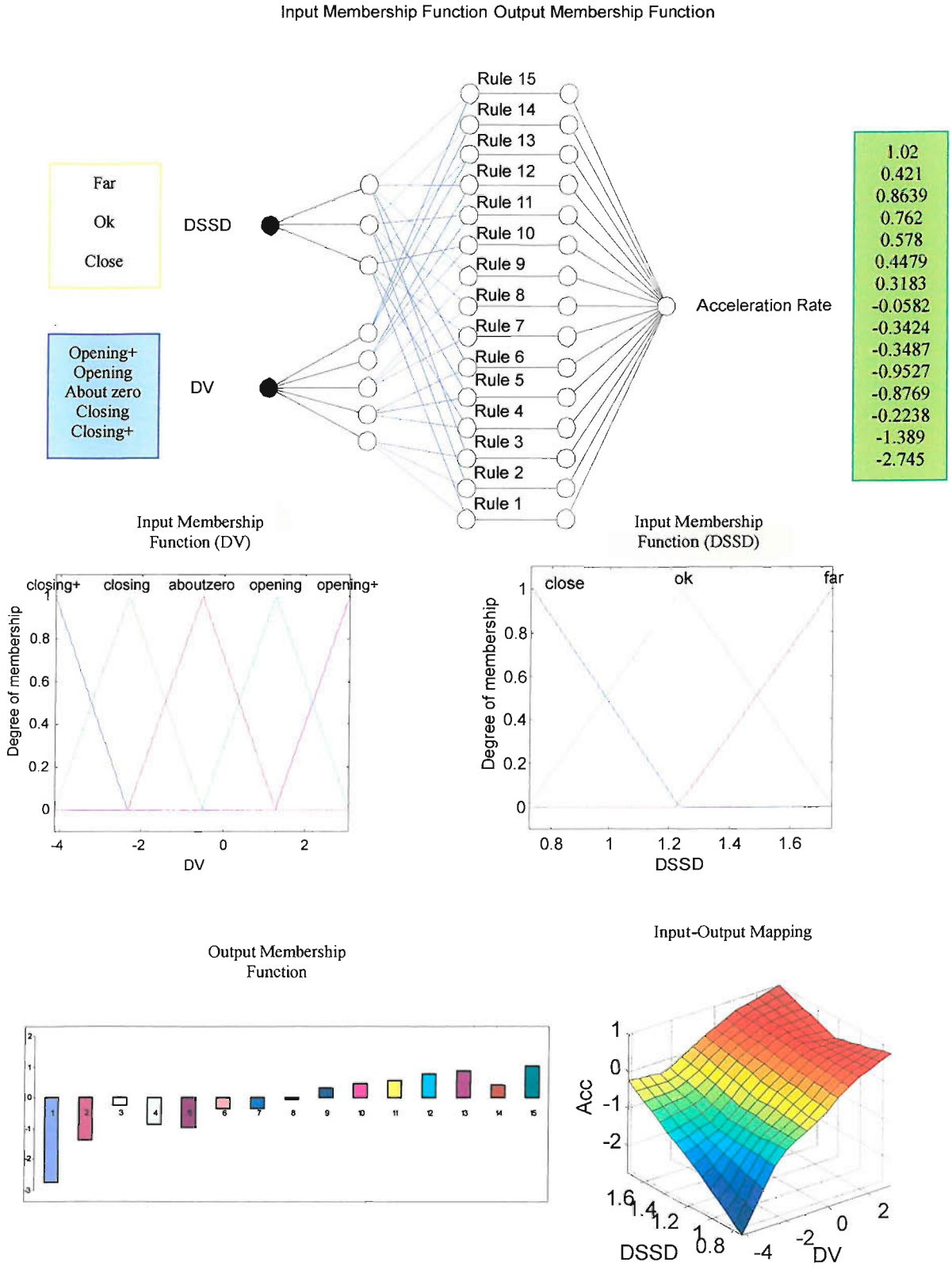

Figure 3.19 A Calibrated Fuzzy Logic Car Following Model

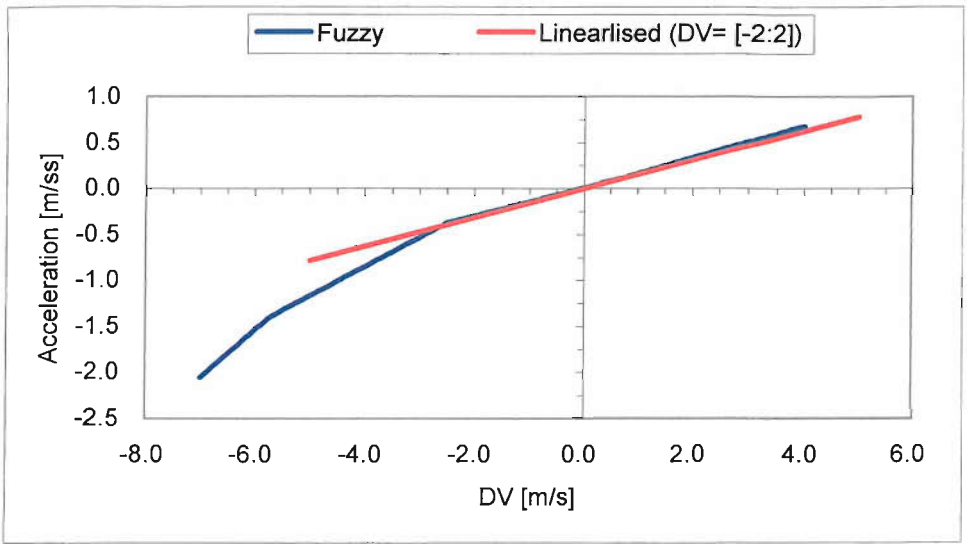

Figure 3.20 Linearlised Speed Gain

The parameters of the calibrated model based on two databases are shown in Table 3.2 and 3.3. The gain k is a linear approximation in DV direction near the steady state.

The identified mean reaction time of 1.75 and 2.49 second is consistent with results from other researchers. For example, when empirical data was fitted to GM model, Chandler, et al reported a reaction time of between 1.0 and 2.2 seconds [18]. Helly et al. found the reaction time to be in the range of 0.5 to 2.2 seconds when fitted to his linear model [34], while Rockwell et al. found that the best fit was achieved when the reaction time was 2 seconds [80]. The speed gain, k was found to be slightly smaller than that from other research. This is because linearlised gain of the non-linear model near the steady-state was used. From Figure 3.20, it can be seen that the gain becomes larger at lower part of the DV partition. If the data would be fitted to a linear model, a larger speed gain would have been obtained. The results of other car following studies are shown in Table 3.4. The parameters obtained in this research are within the variations of the different studies.

Table 3.2 Model Parameters (Car Following Experiment Data)

Sample	Th_{dsr}(s)	k(1/s)	T_d(s)
1	0.5981	0.34	0.1
2	0.6251	0.55	1.4
3	0.9957	0.44	2.0
4	0.7804	0.32	1.9
5	1.9581	0.08	2.9
6	0.8443	0.26	1.6
7	1.8169	0.14	2.5
8	1.8153	0.10	1.6
Mean	1.18	0.28	1.75

Table 3.3 Model Parameters (Normal Motorway Driving Data)

Sample	Th_{dsr}(s)	k(1/s)	T_d(s)
1	0.62	0.27	1.4
2	1.41	0.07	3.6
3	0.86	0.16	3.0
4	0.60	0.23	2.0
5	2.60	0.11	2.5
6	0.91	0.18	2.5
7	1.28	0.13	2.4
8	1.44	0.10	2.5
9	1.13	0.15	3.1
10	0.89	0.19	2.1
11	1.38	0.10	3.9
12	1.36	0.16	1.2
13	0.99	0.19	1.5
14	1.54	0.17	2.9
15	0.94	0.12	2.7
16	1.13	0.23	1.7
17	1.13	0.15	3.3
18	1.98	0.12	4.3
19	1.11	0.16	1.8
20	0.44	0.30	1.0
21	1.78	0.13	3.0
22	1.32	0.15	2.4
23	2.13	0.07	3.5
24	1.01	0.15	1.9
25	1.66	0.13	2.5
26	1.03	0.18	3.3
27	0.92	0.16	1.7
28	2.06	0.16	1.9
29	0.91	0.19	2.5
30	1.42	0.11	2.2
Mean	1.26	0.16	2.49

Table 3.4 Model Parameters of Other Car Following Studies

Observations	T_d (s)	k (1/s)
Chandler, Test Track	1.55	0.368
Forbes, Helly, Tunnel and Open Road	0.983	0.633
Allen, Test Track	3.28	0.21
Allen, Open road	4.96 (4.15*)	0.21

* If an outlier of 11.47 second was excluded

Like the desired time headway, the model parameters calibrated to individual data also vary between drivers. The results of the regression analysis between model parameters and the desired time headway of individual driver is shown in Figure 3.20 and 3.21. It may be seen that parameters describing a driver's dynamic car following behaviour (reaction time and speed gain) can be related to the desired time headway, although any parameters in car following model can take a wide range of values. These relationships between model parameters can be explained by manual control theory.

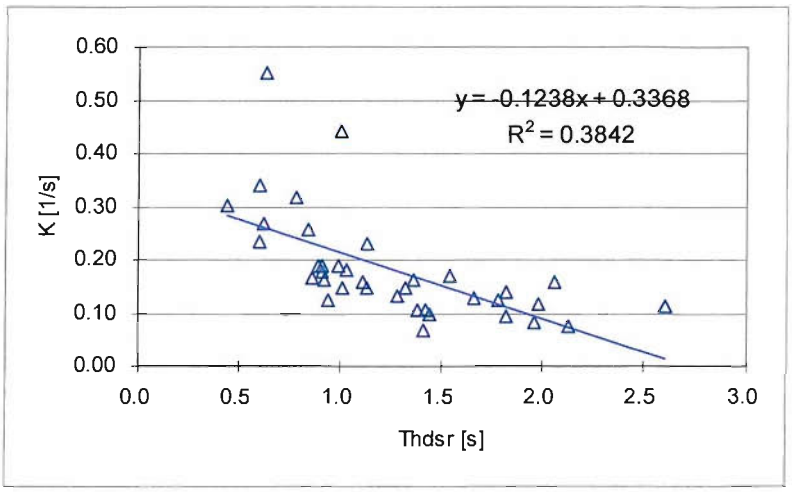

Figure 3.21 Desired Time Headway vs. Linearlised Speed Gain

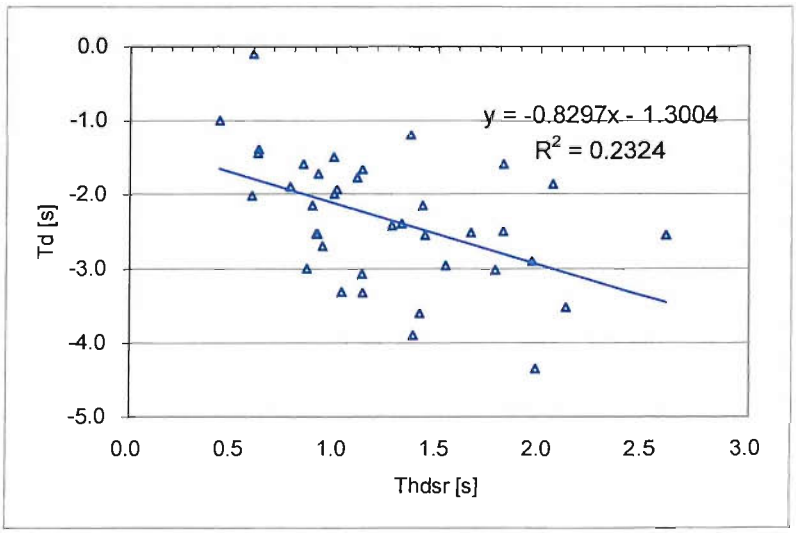

Figure 3.22 Desired Time Headway vs. Reaction time

According to Wickens, the main goal in a manual tracking task is to keep error small and maintain stability [101]. In a car following situation, the following drivers try to keep a desired headway and desired speed. The dynamic behaviour of a driver can be approximately described by two parameters, the reaction time and speed gain, which will determine the headway-keeping errors in car following. Two simulated car following processes with different model parameters are shown in Figure 3.23. Tracking errors can be reduced by employing a large gain and small reaction time.

In the case where a driver has a short desired time headway, the tracking error in car following must be kept small, otherwise a collision may occur, so he/she must use large gain and keep vigilant (i.e., small reaction time). For drivers who keep longer desired time headway, the tracking error will not be

so critical, and the driver can adopt a smoother driving style with small gain and large reaction time. The identified trend that a driver with a small desired time headway also shows a large gain and small reaction time is consistent with the above analysis.

The stability index of the model can be approximated by the product of linearlised speed gain and reaction time (refer to Appendix B). The calibrated model was found to be local stable in all models, but asymptotically unstable in some models. The average T_d and k for reactive models fitted to two databases are shown in Figure 3.24. The identified stability index (k*Td) was similar, which was just in the verge of the asymptotic stability (0.5).

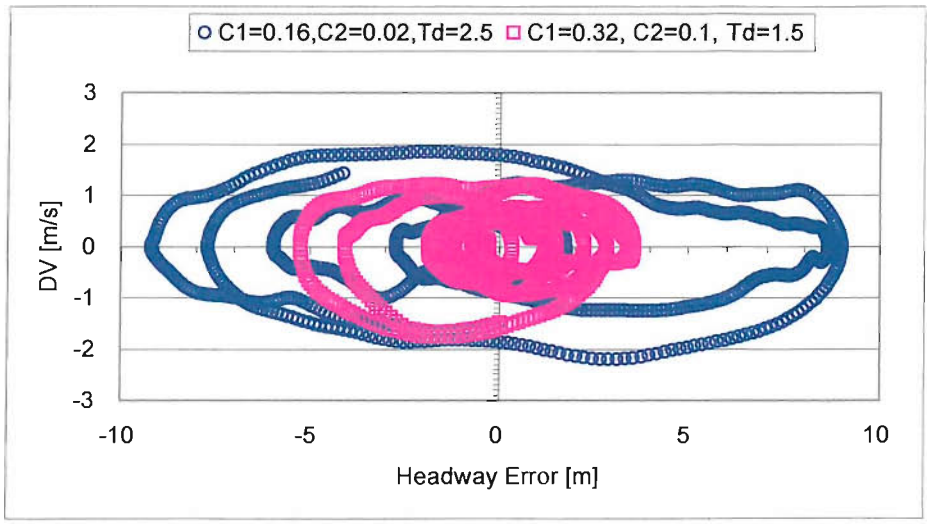

Figure 3.23 Simulated Tracking Errors in Car Following

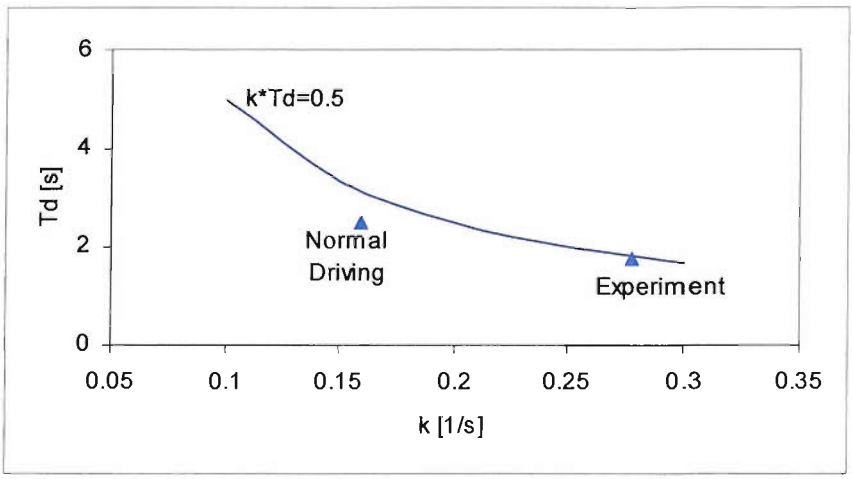

Figure 3.24 Average Calibrated k and Td

3.5 Normalised Fuzzy Logic Car Following Model

In the model calibration process, it has been shown that car following behaviour varies between drivers in a systematic way. The dynamic behaviour can be associated with driver's desired time headway. In the car following experiment, drivers followed the leader more carefully, with larger gain and shorter reaction time than in normal motorway driving. The overall stability index remained nearly constant in all cases. Therefore, it is possible to use a normalised car following model to describe car following behaviour for the driver population. Individual models can then be generated based on the normalised model by varying parameters systematically.

The normalised fuzzy logic car following model was calibrated using selected car following processes with desired time headways of about 1.2 seconds (the average of the sample). The same procedures of model calibration are used. The open-loop mapping of the FIS is illustrated in Figure 3.25. Its linearlised gains are:

k_{norm}= 0.1665 1/s

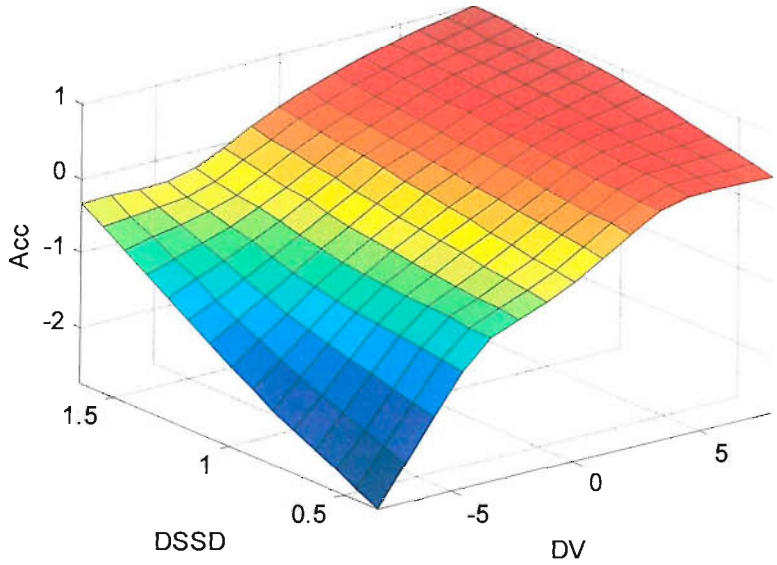

Figure 3.25 Open-loop Mapping of the Normalised Car Following Model

Based on the normalised model, the car following behaviour of individual driver can be described by:

$$a_f(t)=k/k_{norm} * Fuzzy_{norm}(DV, DSSD) \mid t- T_d] \quad \textbf{(3.19)}$$

where k=-0.1238 * Th_{dsr} +0.3368 and T_d= -0.8297 * Th_{dsr} – 1.3004 (refer to Figure 3.21-22)

Th_{dsr} is the desired time headway. This is lognormally distributed within and between drivers as shown in Figure 3.16.

3.6 Model Validation

A number of validation methods have been proposed in the past [55]. Of many different aspects of the car following behaviour, it is necessary to establish that:

- The model can mimic a single vehicle's car following behaviour.
- A number of models can mimic traffic behaviour (a platoon of vehicles each described by a model).

The first can be established by examining the model's behaviour under typical traffic situations. The second can be established by examining the stability of the car following model. Instability can arise within a platoon, which can be frequently observed in form of shock wave. Hence, it is necessary to look at whether the model can reproduce instability under proper situations.

3.6.1 Validation of Single Model Behaviour

As a data-driven approach has been taken to establish and calibrate the model, the model parameters have been derived directly from empirical data. The validity of single car following model in terms of prediction error has been established during model calibration. The average RMSE of the acceleration rate is 0.20 m/s^2.

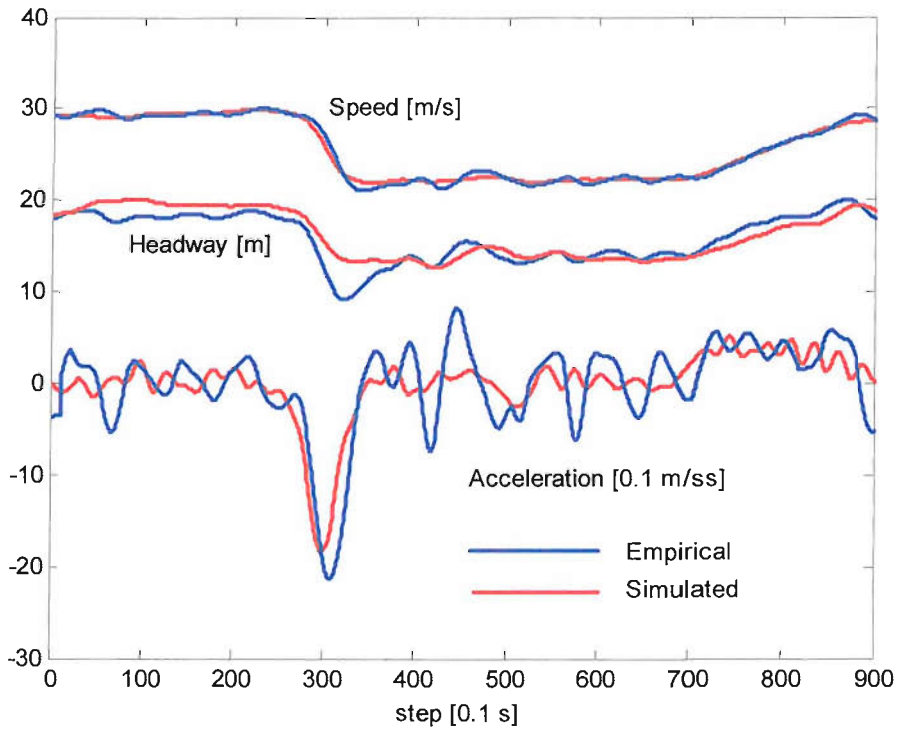

Figure 3.26 A Simulated Car Following Process

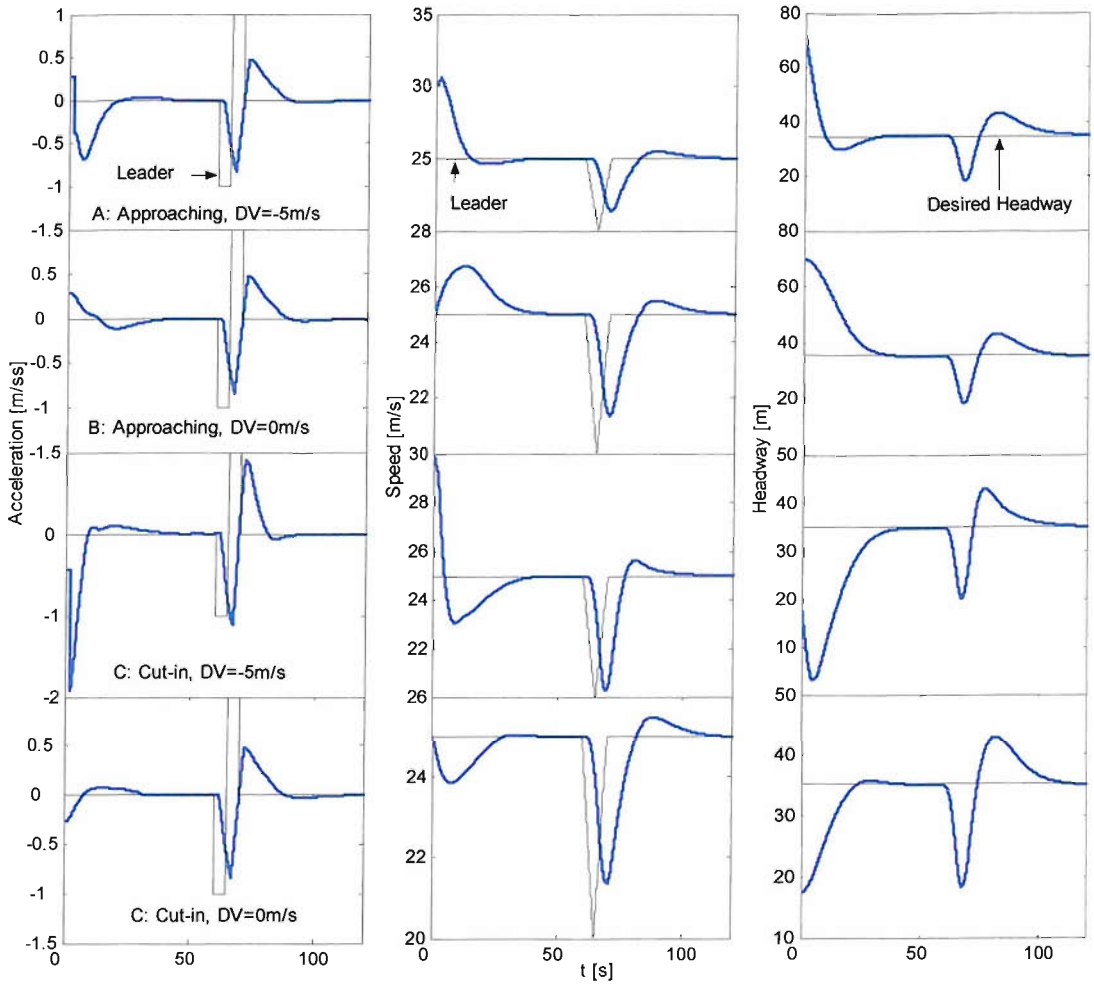

Figure 3.27 Step Responses of the Car Following Model

A typical car following process simulated based on the normalised car following model (k=2*0.1662, T_d=1.5 second) is shown in Figure 3.26. The model can be seen to mimic driver's responses well.

The behaviour of the car following model has been further examined under typical traffic conditions to look at whether a desired headway can be maintained. The test scenarios were step responses to the deceleration of a leading vehicle under different initial conditions. The leading vehicle was maintaining a constant speed of 25m/s before decelerating and accelerating with a constant rate of 1m/s^2 for 5 seconds respectively, and then resumed to its original speed. Initial conditions used in simulation were as follows:

- Approaching (at 2 times of desired headway, A: DV=-5 m/s; B: DV=0)
- Cut-in (at 0.5 times of desired headway, C: DV=-5 m/s; D: DV=0)

The simulation was carried out based on the normalised car following model taking the following parameters:

- Th_{dsr}= 1.2 second;
- T_d=2 second.

The results are shown in Figure 3.27.

The model revealed attractors for headway (the desired headway) and speed (leader's speed, i.e., relative speed=0). Initial deviation from desired headway and speed of the leading vehicle had been finally damped, that is, the modelled vehicles were able to follow the leader under various disturbances.

3.6.2 Validation of Platoon Behaviour

Platoon behaviour can be examined by looking at asymptotic stability, which is concerned with the manner in which fluctuations in the motion of the leading vehicle are propagated down a line of cars. The stability index of the calibrated model varies between drivers. The behaviour of a platoon has been examined using simulation. The behaviour of a uniform platoon composed of identical drivers can serve as a basis in interpreting the behaviour of a platoon composed of different drivers.

The response of a platoon of 20 vehicles to step changes of deceleration/acceleration of a leading vehicle has been investigated. The variation in the leading vehicle's speed was the same as used in the single vehicle model behaviour investigation described above. All the vehicles in platoon take an initial desired headway (SD) and an initial velocity of 25 m/s, the same as the leader.

The test models take the parameters calibrated from two subjects. The linearised stability index of models tested is 0.3934 (A) and 0.6376 (B) respectively. The simulated acceleration, velocity and relative position profile is illustrated in Figures 3.28 and 3.29. The relative positions are based on an assumed vehicle that travels at a constant speed of 25 m/s.

The platoon consisting of vehicles using control law A was asymptotic stable, while platoon consisting of vehicles using control law B was unstable as fluctuation were amplified along the vehicles. A collision can be observed at 9^{th} vehicle in the later case.

The simulation revealed that the fuzzy logic car following model developed in this research could reproduce stable and unstable traffic behaviour. The calibrated models have an average stability index of 0.443, which is just on the verge of asymptotic stability. A platoon consisting of drivers with different stability indexes can become unstable as its length increases. The model is able to produce

'shock waves' under appropriate traffic condition. The simulation also supports the validity of the approximated stability analysis method for fuzzy logic car following model in Appendix B, because two simulations using different stability indexes (stable and unstable) produce the stable and unstable behaviour respectively.

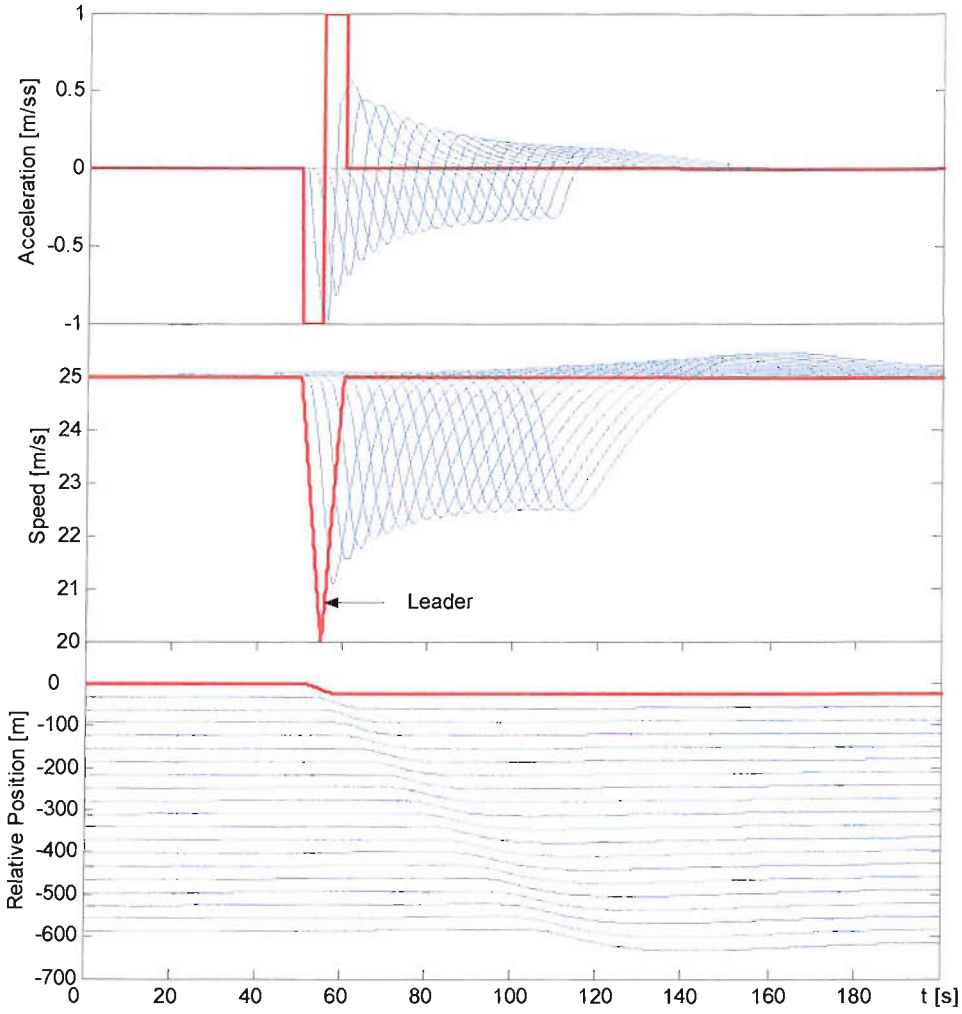

Figure 3.28 Acceleration, Velocity and Relative Position Profile of a Simulated Platoon (Model A)

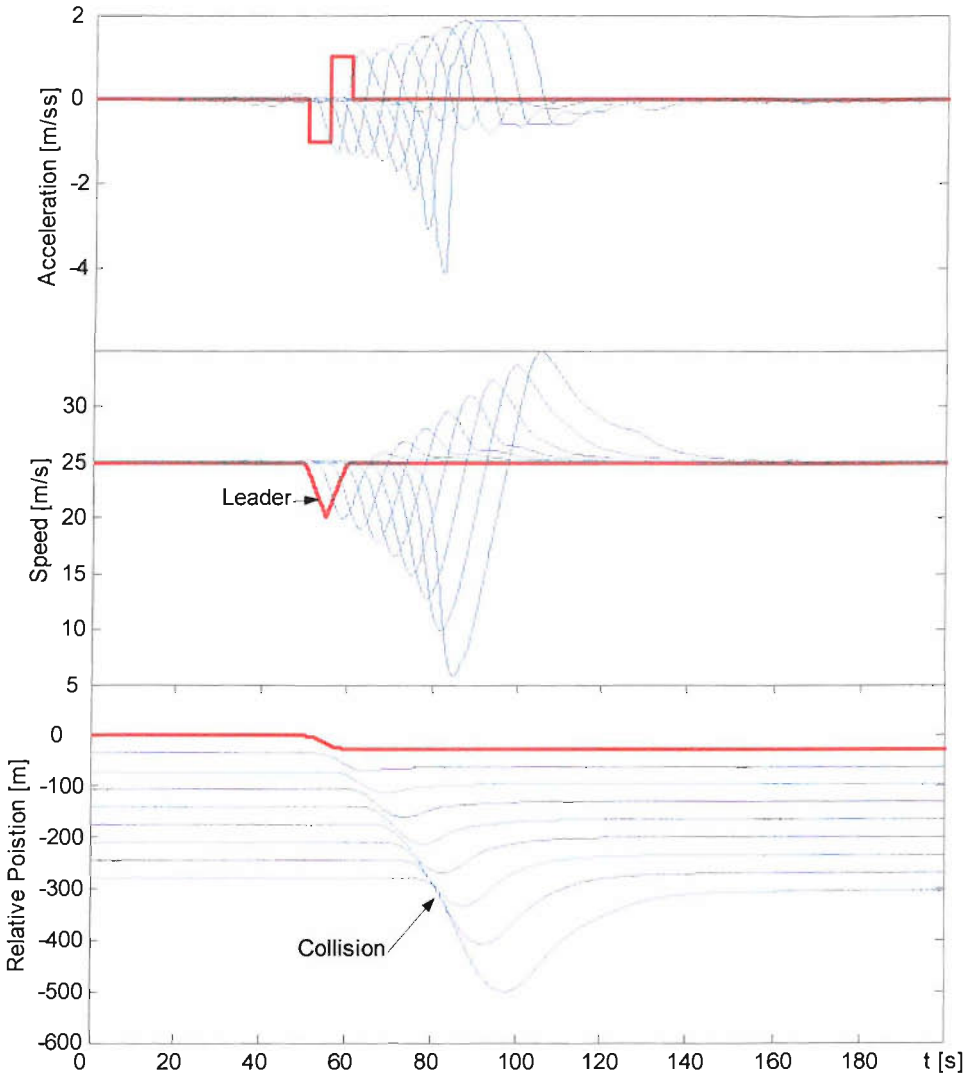

Figure 3.29 Acceleration, Velocity and Relative Position Profile of a Simulated Platoon (Model B)

Chapter 4 Model of Merging Behaviour

This chapter describes development of the model of the behaviour of two interacting traffic streams involved in merging operation. Sub-models have been developed to describe the behaviour of merging vehicles and motorway vehicles and the interactions between the two traffic streams has been integrated in the sub-models. Emphases have been placed on the dynamic aspects of the merging behaviour.

4.1 Merging Process

4.1.1 Sub-tasks in Merging

When merging from an on-ramp, a vehicle moves from the ramp onto the motorway performing two basic types of manoeuvre in the merging process:

- Longitudinal movement control: acceleration/deceleration under constraints of other vehicles and speed limit etc.
- Lateral movement control: steering control in transiting from the ramp onto the motorway, curve tracking etc.

A motorway vehicle on a shoulder lane may also perform two types of manoeuvre when passing merging area:

- Longitudinal movement control: acceleration/deceleration under constraints of other vehicles and motorway speed limit etc.
- Lateral movement control: steering control in changing to outside lane and lane keeping etc.

A driver's steering controls include road curvature tracking, lane keeping, transiting between adjacent lanes (e.g. merging and lane-changing) etc. The low-level, second-to-second lateral control is ignored in this research, as we believe that this detail is not important to the modelling framework. What is important is the decision-level behaviour of drivers in lateral control, e.g., when moving from an acceleration lane to a motorway shoulder lane. Therefore, the lateral movement control considered has been limited to cross-lane situations. The process when a vehicle moves from one lane to another is represented by a momentum event of merging or lane-changing (both involve accepting a gap). Based on this simplified representation, the behaviour of a merging vehicle will be the acceleration control

(including stop at the end of acceleration lane if necessary) and gap-acceptance. For a motorway vehicle, this behaviour will be acceleration control and lane-changing.

Acceleration control is a continuous task and has been modelled as a time continuous process in most car following models. Although there is some evidence that human behaviour is discontinuous, the existence of inertia both in the driver and vehicle creates the smoothness and continuity of the observed time-space trajectory, which make the time-continuous approach suitable [83]. The lateral movement into a gap on a target lane cannot be carried out instantaneously; it involves a discrete decision and a steering manoeuvre. A driver with a desire to move into a gap must first evaluate the gap structure, accept it and then initiate the necessary steering manoeuvre. Ignoring the low-level details, this process is represented by a discrete choice of accepting a gap, which can be directly observed when a vehicle crosses the separation line between lanes. Gap acceptance in merging and lane-changing is nearly identical except that the desire to accept a gap is different. Merging is a forced lane-changing, where a merging vehicle has to accept a gap while on the acceleration lane. Except for the case of merging vehicles stopped at the end of acceleration lane, gaps are accepted whilst the vehicles are moving. Within the obvious complexity of a merging operation lie two basic types of driver behaviour, continuous acceleration control and discrete gap acceptance.

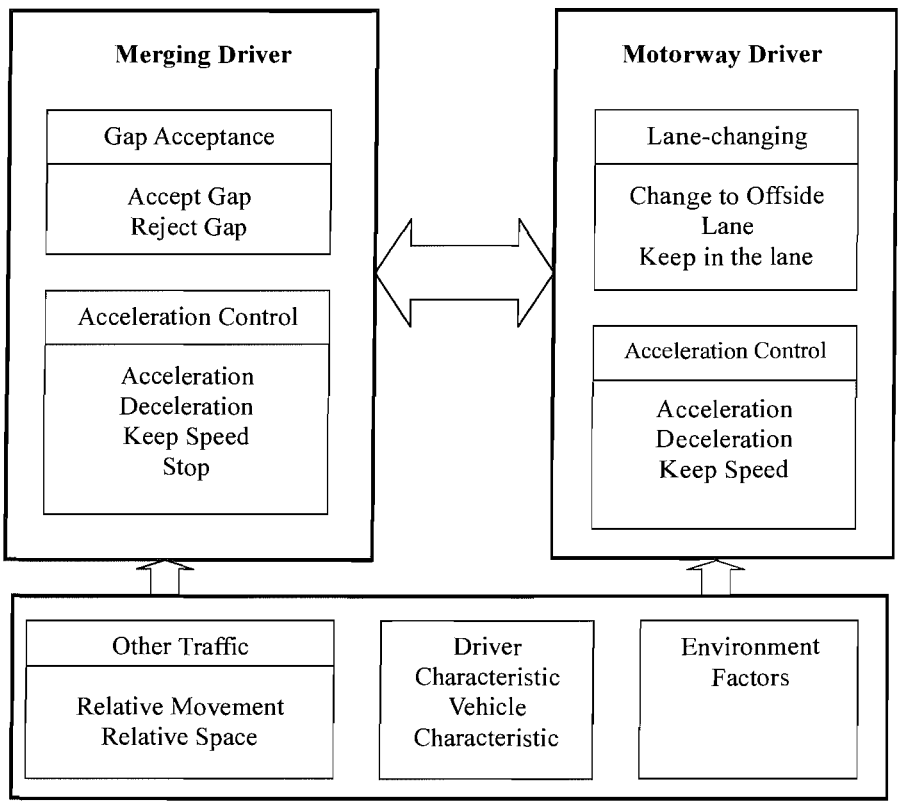

Figure 4.1 Possible Driver Actions and Affecting Factors

The possible actions of merging and motorway drivers during a merging process are illustrated in Figure 4.1. Many internal and external factors can influence the behaviour of both ramp and motorway vehicles and the interactions are complex. Basically, a driver's manoeuvre is constrained by two kinds of external factors, other vehicles (moving) and road geometry (fixed).

4.1.2 Geometrical Constraints

A merging process can be spatially divided into three zones according to the geometric features of a merging area:

- ✧ Zone I: upstream of the sight point on the ramp, i.e., where merging drivers cannot see relevant motorway traffic;
- ✧ Zone II: from sight point to merging end, where merging drivers can see motorway traffic but cannot yet merge because of physical barriers;
- ✧ Zone III: from the merging end to the end of acceleration lane, where merging drivers can merge onto the motorway.

A schematic division of three zones is shown in Figure 4.2. The sight point is the position where a merging driver can first see the parallel motorway section which contains the vehicles relevant to his/her downstream merge. Also, motorway vehicles can see a merging vehicle after it has passed the sight point. The geometric constrains on a driver's actions are as follows:

- The interaction is only possible after a merging driver has been in Zone II.
- Merging is only allowed in Zone III (on acceleration lane).
- A merging vehicle is free to change lane after merging.
- A motorway vehicle can choose to change lane in any zones.

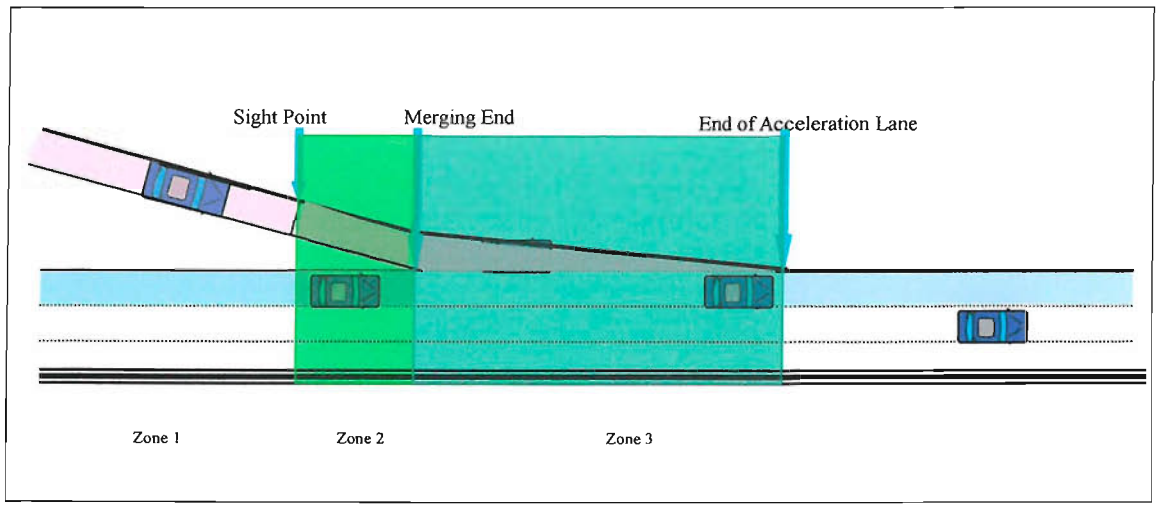

Figure 4.2 Spatial Division of a Merging Process

4.1.3 Constraints from Other Vehicles

As illustrated in Figure 4.3, a merging vehicle C may be constrained by motorway vehicles B and D which bound a gap in motorway traffic during the merging process. The motorway vehicle B may be constrained by his/her direct leader on motorway shoulder lane (D), and also the existence of the merging vehicle C can influence his/her behaviour.

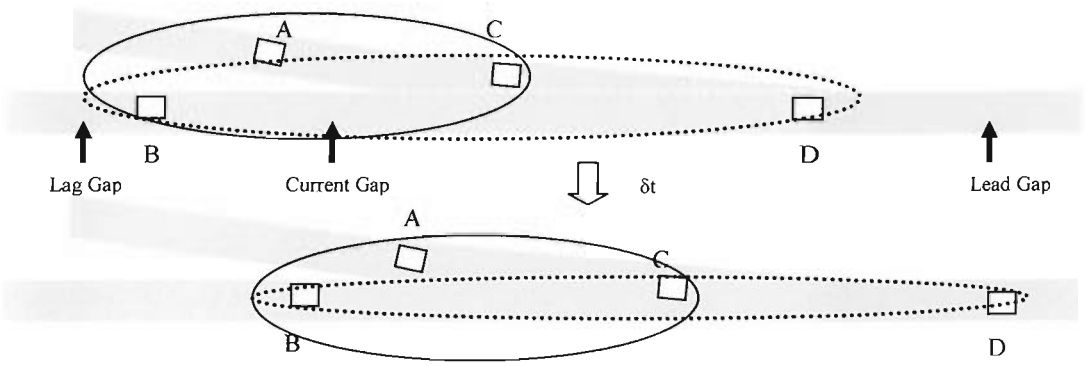

Figure 4.3 A Merging Vehicle and a Gap forms a Unit of Analysis

The situation becomes more complicated in multiple merges, when more than one vehicle (e.g., A and C) merge into a single large motorway gap. For example, the merging vehicle C forms a direct constraint on the other merging vehicle A as overtaking is not allowed. That is, a merging vehicle may be directly constrained by a leading vehicle either on the motorway shoulder lane or acceleration lane, and by a following vehicle on the motorway shoulder lane. On the other hand, a motorway passing vehicle (B) is directly constrained by his/her direct leader on motorway and may be influenced by the closest merging vehicle in front, if any.

At any time during the merging process, a merging vehicle can adjust his/her relative position to a gap or shift to another gap by acceleration control, but cannot change the gap size. A motorway lag vehicle, on the other hand, can change the gap size by acceleration control to facilitate or prevent a merge manoeuvre. Therefore, microscopic merging behaviour can be examined by focusing on a merging vehicle and a gap.

The term 'gap' usually refers to a motorway gap, which is the time or distance interval between successive motorway vehicles. This has been widely used in most models, especially analytical ones, because gap distribution can be easily generated based on flow rate. However, in microscopic behaviour analysis, a gap that is formed by a leader either on the motorway shoulder lane or on the

ramp and a follower on the motorway shoulder lane is more relevant as they constitute the direct physical constraints as explained. Terms relating to the gap have been defined as follows:

Let x_A be the longitudinal position of a merging vehicle A, x_B be the longitudinal position of vehicle B on motorway shoulder lane and x_C be the longitudinal position of vehicle C either on the ramp or the motorway shoulder lane,

A **(current) gap** for the merging vehicle A is the time or distance interval between vehicle B and C only and if only: $x_B<x_A<=x_C$ and there are no other vehicles between B and C on the motorway shoulder lane.

A **(current) motorway gap** is the time or distance interval between B and C, if and only if B-C forms a current gap and C is on the motorway shoulder lane.

A **lead gap** is the motorway gap directly in front of the current motorway gap, i.e., a gap consists of the gap leader and his/her leading vehicle.

A **lag gap** is the motorway gap directly behind the current motorway gap, i.e., a gap consists of the gap follower and his/her following vehicle.

A gap with reference to a merging vehicle can be a motorway gap or part of it depending on whether there are other merging vehicles. Accordingly, 'gap leader' and 'gap follower' refer to the leading and following vehicle with reference to a merging vehicle in a gap. In this way, a merging vehicle and a gap forms a unit of analysis, e.g. A-B-C and C-B-D all forms a unit of analysis.

Microscopically, the merging process can then be described as a dynamic interacting process between a merging vehicle and a gap. The goal of a merging vehicle is to accept a gap before reaching the end of the acceleration lane. In order to accept a gap, a merging driver must try to position him/herself properly relative to the gap. A merging driver may not be able to accept a first selected gap, then he/she must select another gap. The iterations last until a gap is finally accepted. The motorway lag vehicle (as the gap follower) can choose to maintain his/her desired following distance or desired speed as in normal car following situation, or he/she can take actions to facilitate or prevent merging by changing the gap size or by changing lane. Such interactions are only possible when motorway and merging drivers can view each other, and so it is limited to Zones II and III.

4.2 Merging Behaviour Analysis

In the previous sub-section, a framework to describe the dynamic merging process has been established. A detailed understanding of driver behaviour in this process is necessary to model how drivers perform such sub-tasks as acceleration control and gap acceptance etc.

4.2.1 Data

The data used in this stage of the research was collected with metering-off, i.e., the results obtained are based on un-controlled merging operation. It has been assumed that the basic behaviour of drivers will not change under different control schemes (e.g. ramp metering). Thus, if the model developed for un-controlled situations captures the characteristics of merging behaviour, it should be able to represent merging under controlled conditions.

15 subjects carried out 79 merging and 58 passing operations with metering-off, typically 9 trials each day by one subject. Passing trials in which no vehicle merged directly in front or behind the IV have been discarded because of the lack of direct interactions. Data from four merging trials were found to be incomplete because of sensor errors, so had to be discarded. The final reduced data included 75 merging trials and 23 passing trials.

4.2.2 Behaviour of Merging drivers

Historically, merging behaviour analysis had focused on the gap-acceptance behaviour of merging vehicles (e.g. [2], [23]), in which a merging driver is assumed to judge the motorway gap structure once he/she is on the acceleration lane. If an appropriate motorway gap was available, the driver accepted it and merged into the main traffic stream. Otherwise, he/she had to wait for another motorway gap while travelling on the acceleration lane.

In this research, the behaviour analysis has been based on the complete merging process with the scope of analysis extended to include behaviour in Zone 2 for the reason explained in the previous sub-section. Although the gap is accepted on the acceleration lane (Zone 3), the preparation for gap-acceptance may have started before a merging vehicle arrives at the merging end. In addition, no assumptions about the decision point of accepting/rejecting a gap were made. So, the accepted/rejected gaps observed at a fixed point (e.g. merging end) are not going to be used to characterise a driver's gap-acceptance behaviour, accepted gap is analysed instead. Driver's eye-movement was also analysed in detail in an attempt to find useful explanatory information.

4.2.2.1 Acceleration/Deceleration Behaviour

The speed profiles of five merging processes performed on the same day by one subject are shown in Figure 4.4. If there are no constraints from other traffic, the driver is free to accelerate and then merge at any section of the acceleration lane. Trial 1 is typical of this situation in which the process is characterised by an acceleration to achieve the driver's desired speed or motorway traffic speed. In the

presence of other traffic either on the ramp or on the motorway, the patterns are more variable as indicated by the plot of the other four trials.

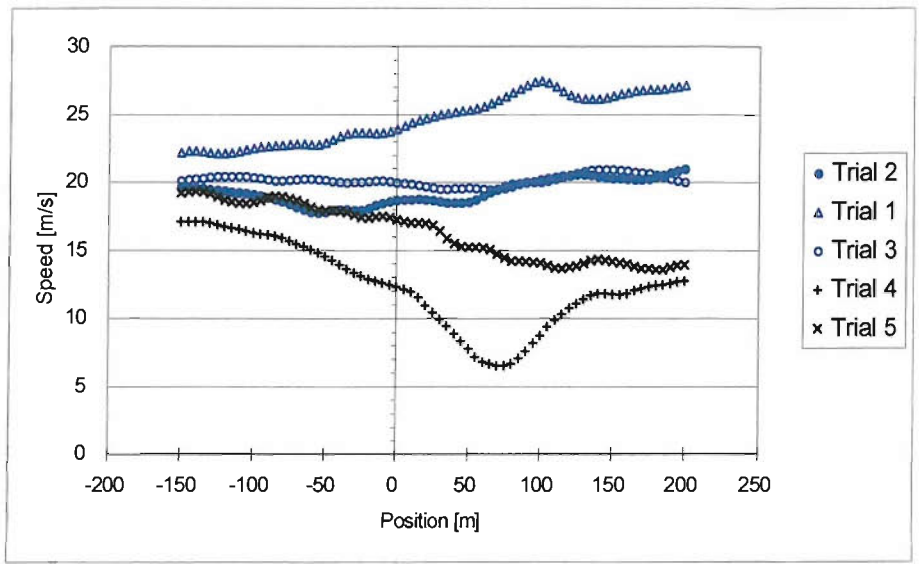

Figure 4.4: Speed Profiles of Merging vehicles (position of merging end is 0m)

It is clear that the longitudinal control of a merging driver is not an open-loop type of behaviour. Intuitively, a merging driver can be influenced by three factors. The first is the current gap leader. A 'safe' headway must be always maintained in order to avoid collision. The second is the gap. In order to merge into a gap, merging drivers must position themselves appropriately or select another gap by controlling acceleration. For example, if a merging driver wishes to accept a lag motorway gap because the current gap is unacceptable, he/she may slow down. The third is the distance to the end of the acceleration lane. The merging driver must make sure that the vehicle can be properly stopped at the end of acceleration lane if necessary.

The average speed of merging and passing vehicles is shown in Figure 4.5. The overall tendency is that merging drivers try to accelerate up to the motorway traffic speed (and approximately, the gap speed). It is noticeable that the effect of the existence of the end of acceleration lane (182m) cannot be clearly identified from this speed plot. This may be attributed to the fact that most vehicles can merge early so that the possible speed reduction of later merged vehicles, if any, does not contribute much to the average.

It is not possible to identify the acceleration behaviour of merging drivers by simply examining the speed change pattern. It was therefore decided to describe the longitudinal control of merging vehicle as a close-loop behaviour of tracking a gap. The detail will be described in the model development.

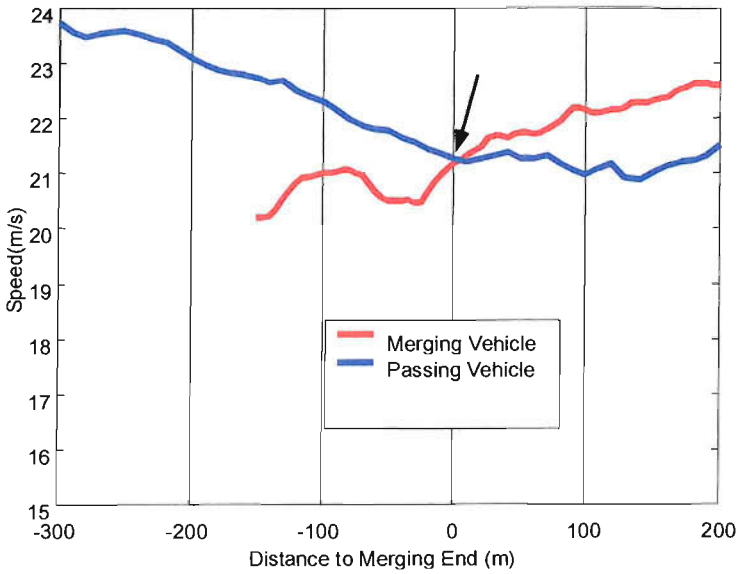

Figure 4.5 Average Speed of Merging and Passing Vehicles

4.2.2.2 Gap-Acceptance Behaviour

Merging drivers accept a gap when they start to merge. The accepted gap and the corresponding states of the merging vehicle have been summarised in Table 4.1 and Table 4.2. Though this represents only a snapshot state of the vehicles involved, the information is believed to be an important index of overall merging behaviour. Averages are only calculated for those gap leaders and followers that have a headway of less than 100 meters (or time headway of 4 second) because outside this range, the influences are assumed to be insignificant. Because of the limitations of camera coverage and the Radar detection range, not all gap leaders and followers could be covered in the observation. For those vehicles outside the observation area at the merging moment, headway of 150 meters for identification has been assigned, but was not used in calculating the average.

The front to rear headway or time headway as defined in Section 1.1 is used in this Chapter unless otherwise stated. This is more suitable for behavioural analysis as the drivers are more concerned about the net separation between vehicles rather than the bumper to bumper separation (including the length of the vehicle).

Merging Position

80% of drivers start to merge in the first 50 meters of the acceleration lane. The average start and end merging position are 35.4 m and 90 m from merging end respectively. The distribution of merging position is shown in Figure 4.6. A comprehensive regression analysis between merging position and other attributes does not give definitive conclusion (with a R^2 less than 0.1). This had also been reported by Kou, et al. where merging position was found to be independent of merging speed, lag time, lead time, relative speed etc.

Table 4.1 States of Merging Vehicle

Percentile	Merge Speed (m/s)		Merge Position(m)		Acceleration Rate (Average, m/s^2)
	Start	End	Start	End	
Max	30.91	30.37	75.03	184.98	1.37
80%	23.65	23.70	48.47	109.82	0.42
60%	22.48	22.59	38.76	98.96	0.33
40%	20.32	20.79	30.46	78.75	0.13
20%	18.74	19.37	18.47	65.20	-0.11
Min	7.43	7.33	3.52	23.95	-1.12
Average	21.10	21.45	35.41	90.02	0.11

Table 2.2 Accepted Gap-Structure

Percentile	Gap Lead				Gap Follower			
	Headway+ (m)	Time Headway (s)	Relative Speed (m/s)	Angular Velocity (rad/s)	Headway (m)	Time Headway (s)	Relative Speed (m/s)	Angular Velocity (rad/s)
Max	>=100	>=4	8.18	0.147	>=100	>4	4.91	0.114
90%	(87.8%)	(83.7%)	3.12	0.026	(78.9%)	(77.10%)	2.62	0.043
80%	64.15	3.20	1.73	0.0065			2.3	0.0065
70%	55.21	2.52	1.36	0.0033	67.94	3.54	1.07	0.0025
60%	41.93	1.97	1.06	0.0018	62.36	2.91	0.51	0.0005
50%	36.60	1.56	0.54	0.0008	49.55	2.29	0.32	0.0001
40%	32.01	1.35	0.24	0.0002	34.44	1.60	0.09	0
30%	20.55	0.99	-0.29	-0.0001	18.64	0.98	-0.22	-0.0008
20%	15.7	0.81	-0.67	-0.0025	12.06	0.67	-1.93	-0.0017
10%	12.16	0.63	-1.53	-0.0076	8.87	0.41	-2.26	-0.0059
Min	4.76	0.25	-7.33	-0.0209	6.13	0.34	-4.04	-0.0619
Average*	35.62	1.52	0.68	0.0085	39.2	1.81	0.24	0.0045

* Average is only calculated for those below a headway (front to rear) of 100m and a time headway of 4 second.

+ Headway and Time Headway is measured from front to rear bumpers

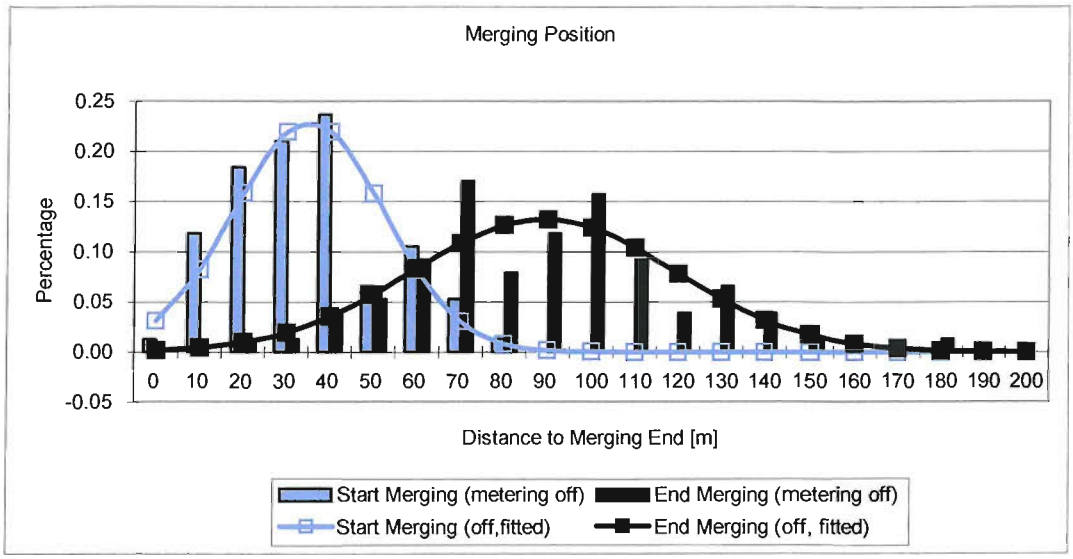

Figure 4.6 Merging Position (Interval=10m)

Accepted Gaps

Accepted gaps show large variations from trial to trial. The observed lag time and angular velocity are compared to Michaels et al in America and Tafti in UK, on which the average accepted lag time headway is 1.895 second (Tafti), and the average lag angular velocity is 0.0043 (Michaels) and 0.0044 (Tafti) respectively (refer to [67] and [91]). The accepted gaps and the average calculated from those with a headway (front to rear, both lead (positive value) and lag (negative value)) of less than 100 meters are shown in Figure 4.7.

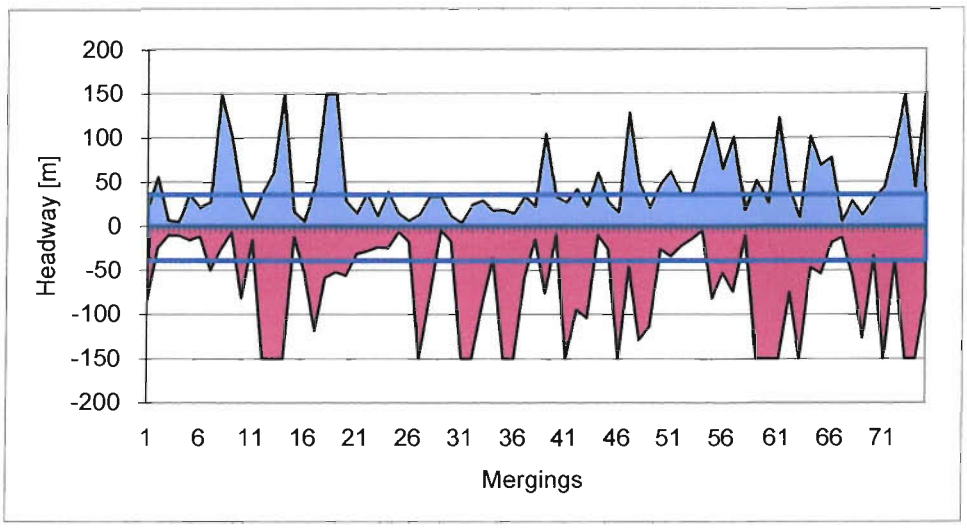

Figure 4.7 Accepted Gaps

Analysis of accepted gaps was focused on deriving distributions of accepted gaps and regression analyses between accepted gap size and other influencing factors such as relative speed and merging position. The distribution of accepted gaps (Table 4.2) is motorway flow rate related, and so it could vary considerably. For example, the average lead and lag time observed at medium flow rate is reported to be 2.2 and 4.0 second ([88], M5/M6, 1982) respectively, which is much higher than that observed at peak hours in this research. Regression analysis did not reveal definitive relationships between accepted gap and other attributes such as relative speed, acceleration rate and merging speed.

Under more constrained situations, some relationships between influencing factors were found to be more definitive. The first is the relationship between merging speed and accepted gap size. The result is illustrated in Figure 4.8, which is based on gaps smaller than 100 m. Better regression result can be obtained by further excluding gaps larger than 80 m. However, the subdivision of lead and lag times did not improve the goodness of fit. The result suggests that minimum acceptable gap size increases with merging speed. This is intuitively reasonable, as a driver needs more manoeuvring room at higher speed, except for the minimum separation to the gap leader and/or the gap follower. The minimum acceptable gap was small compared with the desired headway in car following situations (gap size is about twice that for car following headway). This may be explained by the fact that the merging vehicle and its gap leader/ follower are still in separate lanes at the moment when merging starts, and the gap size can increase during the time from the start of merge to the end of merge.

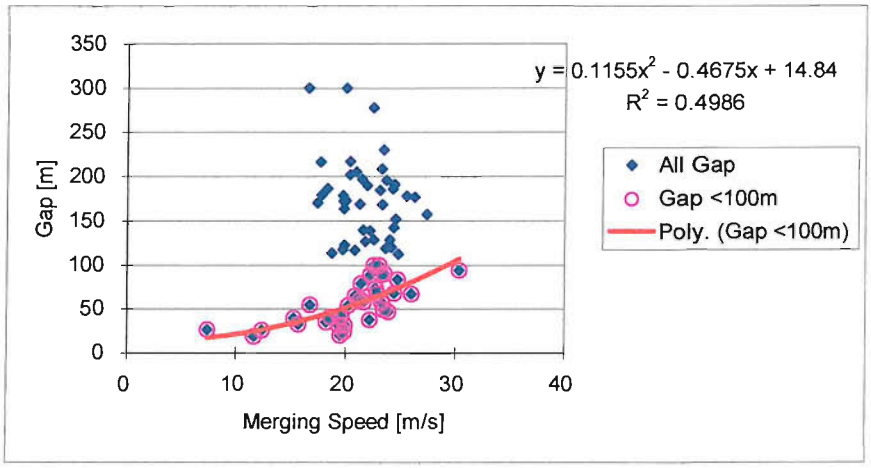

Figure 4.8 Merging Speed Affects Minimum Acceptable Gap

Another relationship found was between the acceleration of merging vehicle and the relative speed to the gap leader. For close gap leaders (headway < 55m), merging driver acceleration/deceleration was found to be based on speed difference, which is very similar to that in car following situations. This is

an indication that a merging vehicle tries to follow a gap by following a gap leader in constrained situations. Similar relationships were not been found for gap follower.

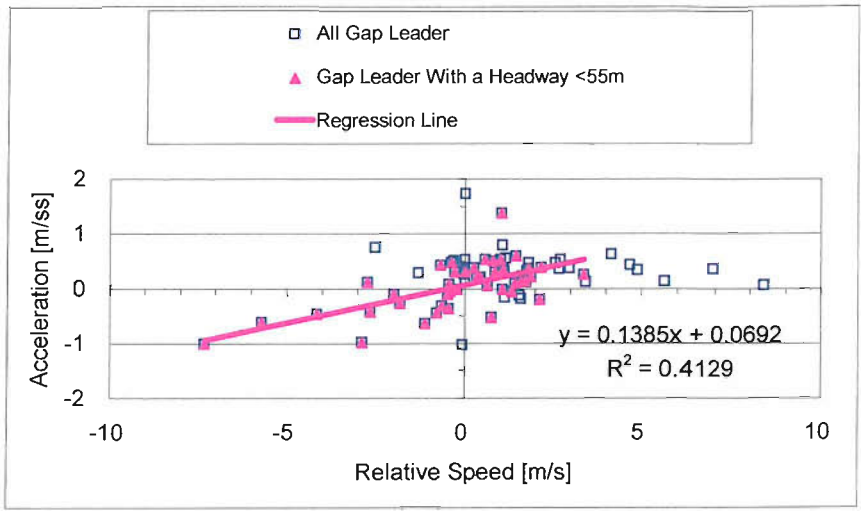

Figure 4.9 Merging Vehicle Accelerate/Decelerate to Follow the Gap Leader

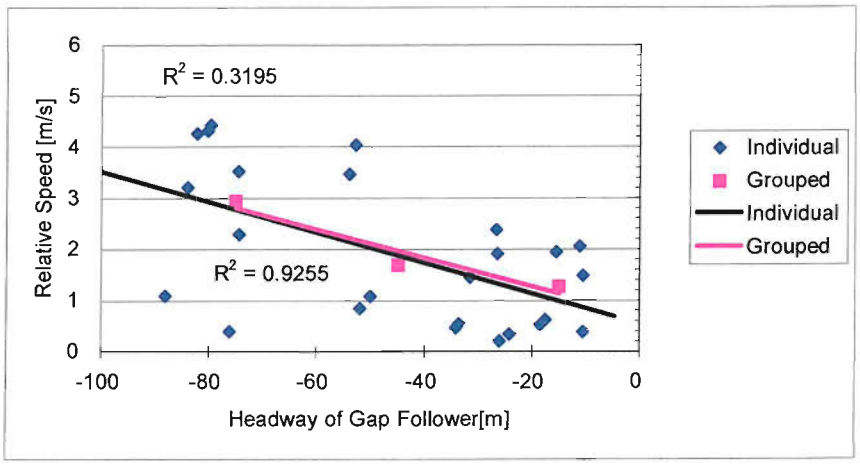

Figure 4.10 Accepted Distance Lag vs. Relative Speed

A third relationship was between the relative speeds and headways of gap followers. Only the gap followers within 90 m that were faster than the merging vehicles were included because they formed a potential collision harzard. These data was further grouped into three intervals according to headway lag size (0-30m, 31-60m, 61-90m) and the average calculated for relative speed within each group. The result of the regression analysis is shown in Figure 4.10. Overall, the headway lag of an accepted gap was larger if the gap follower was approaching faster. The result seems to indicate that a merging driver when accepting a gap tries to leave a TTC(DV/DX) for his/her gap follower in order to prevent forming a critical situation. No conclusive relationship was identified between headway lead and the

relative speed to the gap leader. This was expected as the merging driver was controlling his/her vehicle continuously with reference to a gap leader, so that at the moment of accepting the gap, TTC to the gap leader will no longer be a serious constraint.

Dynamic Changes of Gap Size

The dynamic changes of the time headway during merging processes observed at 50 meters interval are shown in Figure 4.11. The observed profile is the result of interaction between the merging vehicle and the gap. The merging end is located at 0 meter. The overall pattern of the time headway change is a closing and then expanding process. The merging driver maintains reduced time headway to the gap leader, and the gap follower undertakes co-ordinated behaviour by slowing down. After merging, both the merging vehicle and the gap follower resume their desired time headway. This is a dynamic gap-acceptance process. It should be noted that because of reaction time, the headway change pattern of the gap follower illustrated in Figure 4.11 is a typical deceleration process, i.e., a closing and then expanding pattern.

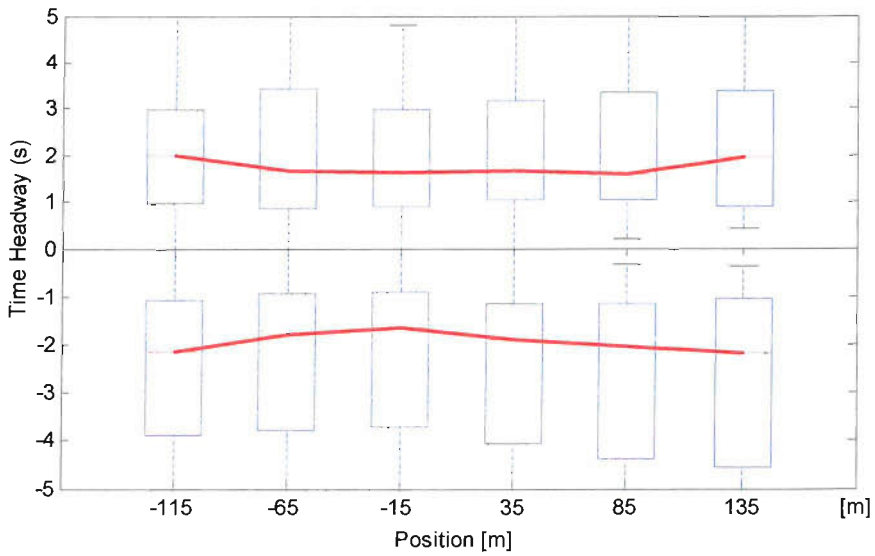

Figure 4.11 Time Headway During Merging

4.2.2.3 Eye-movement

Analysis of an accepted gap cannot obviously identify the point of decision, nor the gap rejection behaviour of a driver. However, eye-movement records can give information about where and when a merging driver obtains information of the gap follower. In this research, eye-movement refers to the

event when a driver changes his/her direction of vision towards a rear-view mirror or right-rear direction as measured from in-vehicle cameras.

The distribution of the number of eye-movements in each merge is shown in Figure 4.12, and the distribution of the position of each eye-movement is shown in Figure 4.13. The number of eye-movement in each merging ranged from 2 to 7 with an average of 3.88, which is approximately distributed evenly between 2 to 5. Spatially, 86.75% of eye-movements happened before a merging driver reached the merging end.

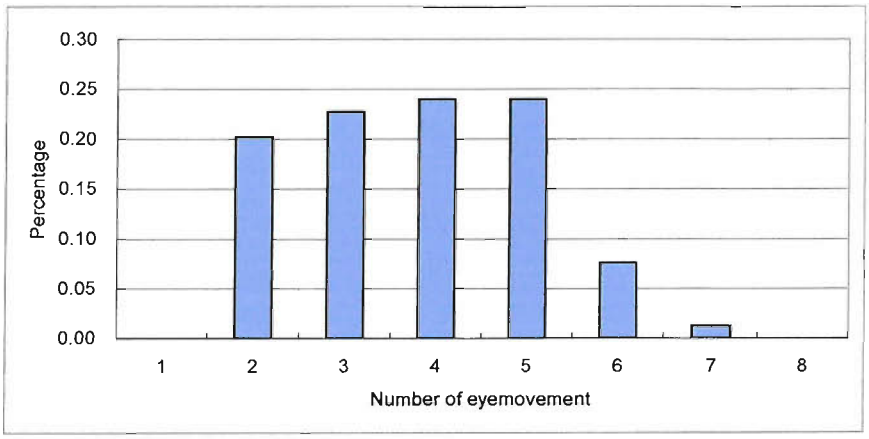

Figure 4.12 Distribution of the Number of Eye-movement in a Merging

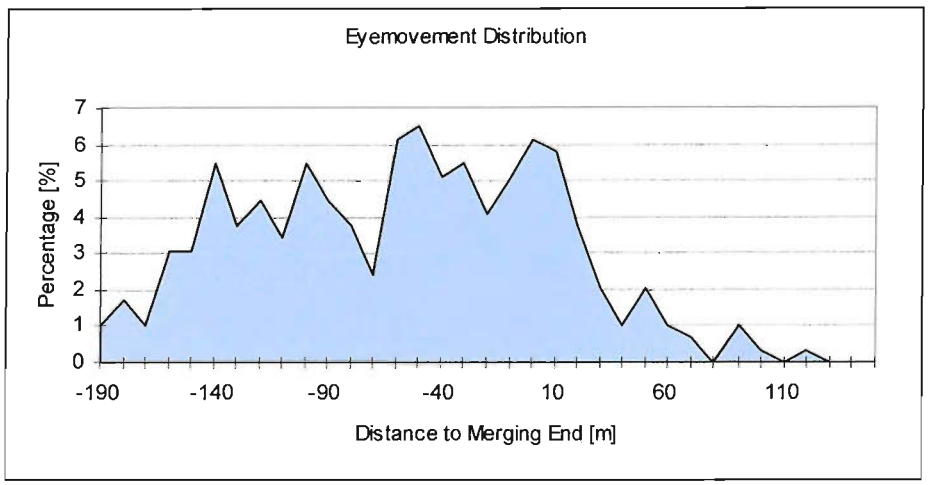

Figure 4.13 Spatial Distribution of Eye-movement

The cluster centre of eye-movements using fuzzy cluster analysis based on the average number of the eye-movement in a merge is shown in Figure 4.14. The most likely positions of eye-movement are -133, -69, -13 and 47m from the merging end. The first location coincided with the point where ramp

traffic can first sight relevant motorway traffic (about –140 m). A high percentage of drivers looked to the rear side twice, before reaching the merging end as the high cluster density indicates. This is a reflection that the interaction between the two traffic streams was very important at this stage. The fourth eye-movement occurred at the start of merge, a reflection that some drivers needed to have a final check at this stage. The speed change tendency associated with each eye-movement identified is also logical. The slight decrease in speed at the third eye-movement location may be an indication that the cognitive demand to look-back was so high as to temporarily distract the driver from speed control.

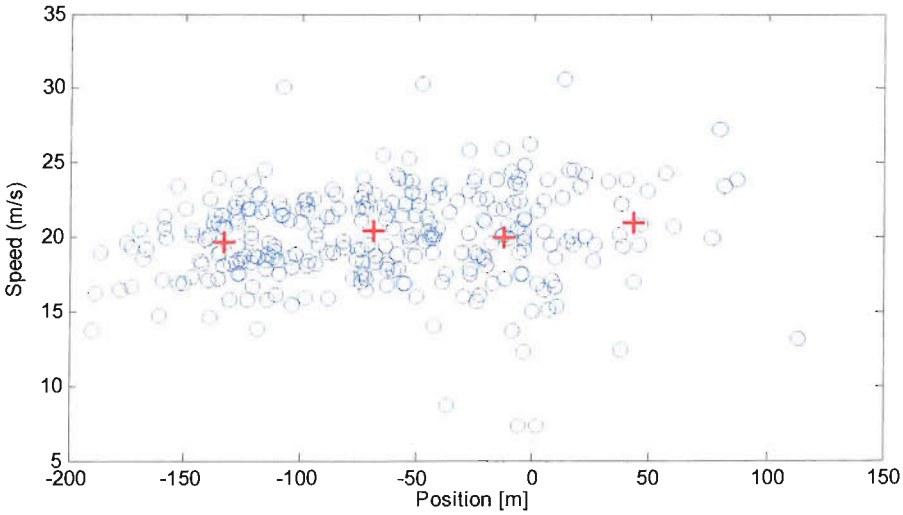

Figure 4.14 Speed and Location of Eye-movement Event ('+' denotes cluster centre)

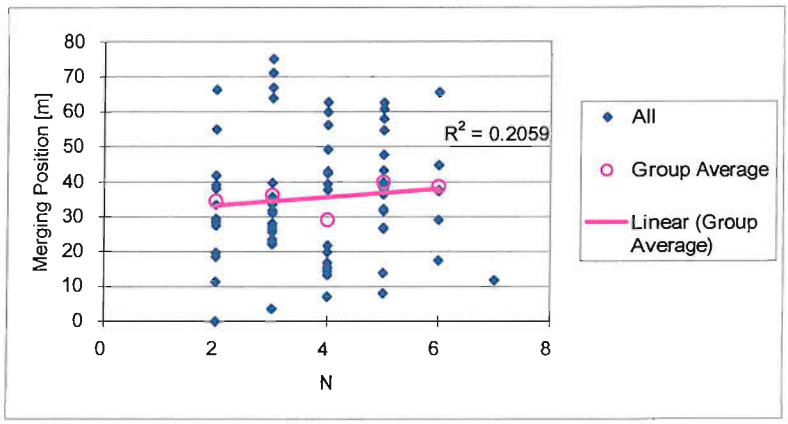

Figure 4.15 Number of Eye-movement vs. Merging Position

No definitive relationship between merging position and number of eye-movement was identified (Figure 4.15). However, the number of eye-movement during a merging has a close relationship with the accepted gap structure as shown in Figure 4.16. This has been analysed by grouping the data

according to the number of eye-movements (The only merge that had 7 eye-movements was included in the group of 6 eye-movements). The result suggests that a merging driver may look back more frequently if the gap leader is distant. It appears logical because drivers need to share perception resources between the tasks of looking forward and looking back. Frequent looking back, i.e., more eye-movements, is likely to affect following performance and drivers will compensate by keeping a larger headway to the gap leader. However, this effect is very marginal as indicated in Figure 4.16. For the gap follower, the results suggested that merging drivers pay more attention to a closer gap follower by looking back more frequently as indicated by the first half of the curve. Interestingly, drivers seemed to be able to achieve a larger headway to the gap follower by looking back more frequently as the second half of the curve suggests.

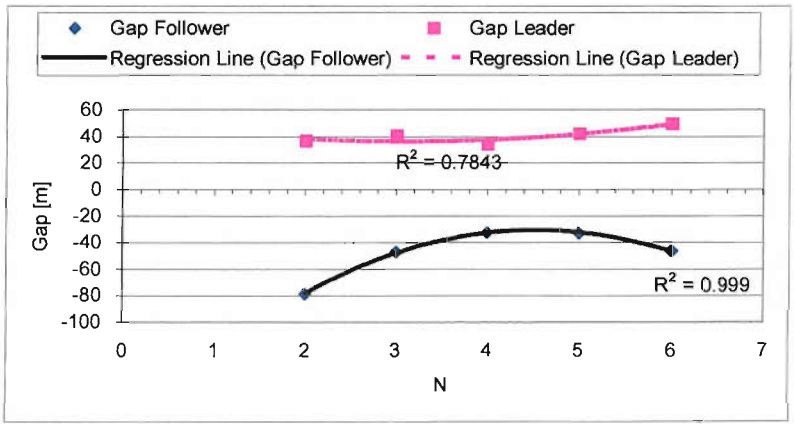

Figure 4.16 Number of Eye-movement vs. Accepted Gap

What the pattern of eye-movement demonstrates is that merging drivers evaluate the state of their gap follower and other lag vehicles regularly during a merging process. By looking-back regularly, he/she regularly gets refreshed information on the gaps. This information is used to guide acceleration control in order for the merging driver to position him/herself properly within a gap, or to guide gap selection. Once a merging driver is on the acceleration lane, the information can be used for the gap-acceptance decision.

4.2.2.4 Gap-Selection Behaviour

Eye-movement cannot be interpreted as the decision point of accepting/rejecting a gap as most eye-movements happen on slip road where gap-acceptance is still impossible. The decision point of accepting a gap may be taken to be the moment of start of merging, which can be directly observed. The decision point of rejecting a gap (selecting another gap) cannot be readily identified by observing eye-movements. However, rejected gaps can be directly observed by comparing the original gaps presented to a merging vehicle at a reference point and the final accepted gaps. Two typical merging

processes are shown in Figure 4.17. In the top graph, the final accepted gap is the original gap at the sight point, while in the lower graph, another has been accepted. Setting different reference points for observing the original gap will result in a different number of rejected gaps. The finally accepted gap compared with the original one observed at the sight point is illustrated in Figure 4.18. It can be seen that most drivers (87%) are able to merge into the original gap while few drivers overtake or are overtaken to accept another gap. As shown in Figure 4.19, the selection of another gap (rejecting original gap) mostly happened upstream the merging end and this accounted for 81.2% of all rejected gaps. After passing the merging end, merging drivers seldom rejected any gap, which is less than 3% (18.8%* 13%). The result is consistent with those from other research. It was reported that only 6.39% merging drivers rejected one gap and 0.46% rejecting two on the acceleration lane according to [52].

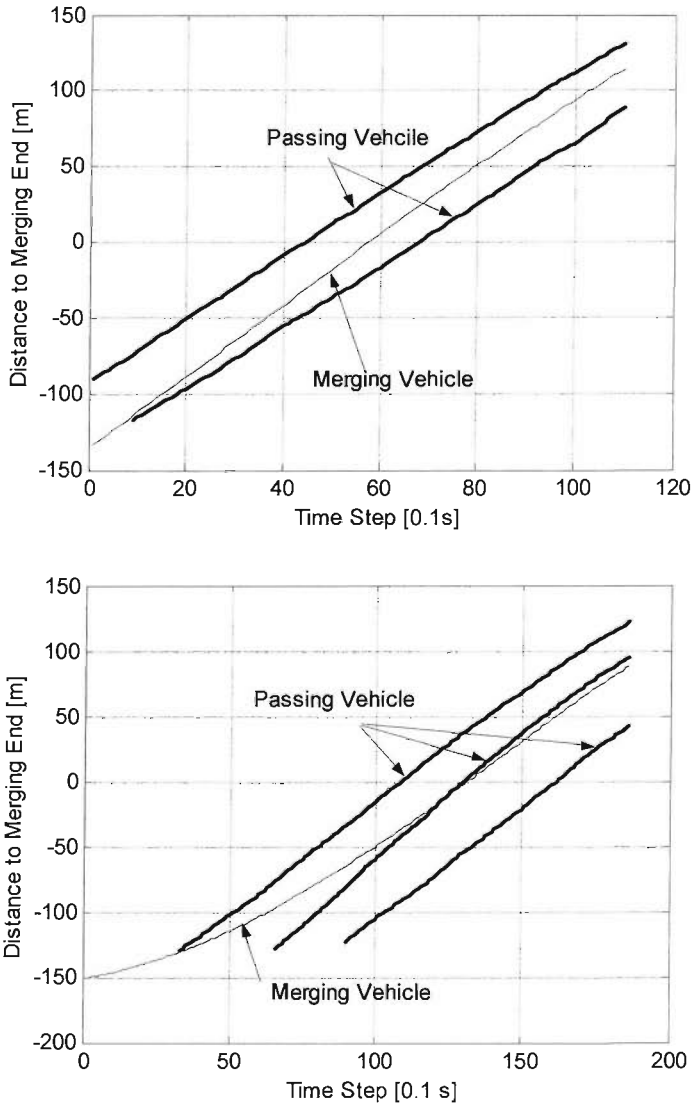

Figure 4.17 Merging into the Original Gap/Selecting Another Gap

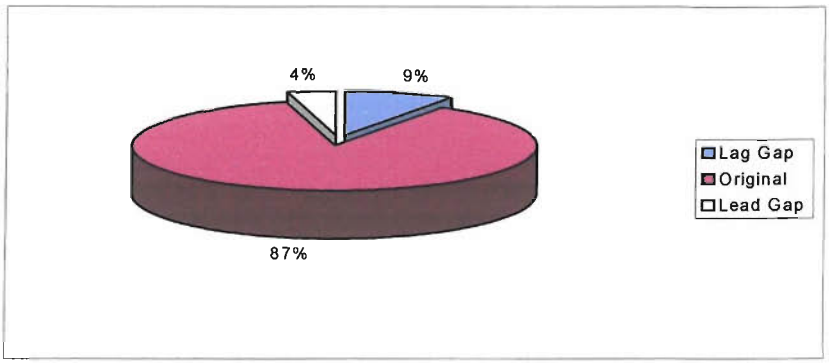

Figure 4.18 Distribution of Accepted Gaps

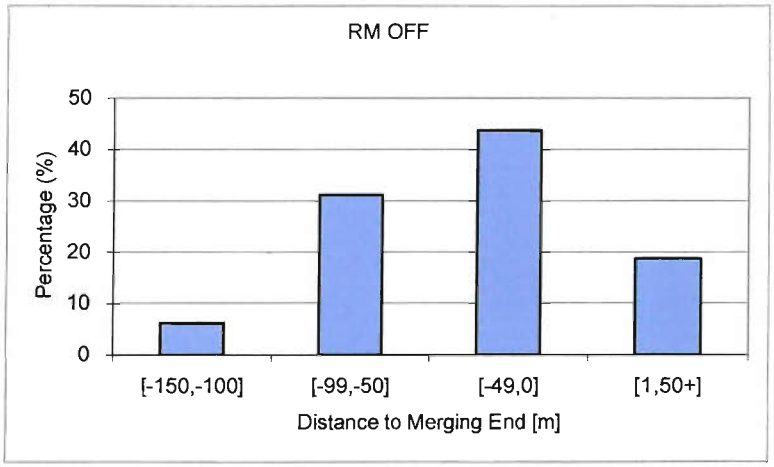

Figure 4.19 Geographical Distribution of Gap Rejection

The final accepted gap was very dependent on the initial traffic arrival condition. If a merging vehicle arrived at the sight point at a much slower speed than that of the motorway traffic, he/she could do little other than fall into lag gaps.

Alternatively, the phenomena of the change of the current gap can be described as gap selection behaviour. A merging driver faces several consecutive motorway gaps at any time during the merge. They must select one gap to guide their control behaviour. The analysis of the accepted gap reveals that most merging drivers select the current gap and finally merge into it. For those merges where the finally accepted gap was different from the original gap, there were two possibilities. The first was that the merging driver selected the original gap as the target gap, but failed to accept it either because the gap was unacceptable or he/she was unable to catch up to the gap. The second possibility is that he/she selected another gap as the target gap.

It will be difficult to judge whether the merging driver has selected the current gap as the target gap or not. However, for speed control purposes, the merging driver may be considered to be most likely to select the current gap as the target gap because optical flow information is easier to perceive for the close target. Basically, the merging driver tries to achieve two goals before reaching the end of the acceleration lane. One is to reach a similar speed to the motorway traffic, and the other is to position him/herself into a proper gap. This second goal is easier to achieve before reaching the merging end where the relative speed between the merging and the passing traffic is normally large so that relative position between vehicles can be adjusted quickly at high relative speed. It will be difficult to adjust the relative position on the acceleration lane as the relative speed between the merging and passing traffic has become smaller. This may explain why nearly all the merging vehicles merge into the current gap after passing merging end. Therefore, it can be reasonably assumed that merging vehicles select the current gap as the target gap during merging process. The current gap can change because of the existence of the relative speed between the merging vehicle and the gap, which is initially condition dependent, and most likely happens upstream of the merging end. Once on the acceleration lane, the merging drivers just simply try to merge into the current gap.

4.2.3 Behaviour of Motorway Drivers

The behavioural analysis of motorway drivers is focused on the acceleration/deceleration behaviour of passing vehicle. Theoretically, a passing vehicle has the right of the way and is only constrained by its motorway leader. The assumption that merging vehicles have no influence on motorway traffic has been established based on this belief. However, the rationale for this assumption needs to be justified.

Lane-changing behaviour is complicated as the motivation to change lane cannot be observed directly. However, the lane-changing of a gap follower (passing vehicle) will create a gap that is large enough for merging vehicles, and so the lane changing rate could be an important index. Therefore, the analysis has focused on the lane-changing rate of passing vehicles on the motorway shoulder lane.

4.2.3.1 Acceleration/Deceleration Behaviour

The speed distribution measured at six different reference-points in 100m intervals are shown in Figure 4.20. Clearly, the speeds measured at the merging end are significantly different form those measured upstream (a side-by-side comparison of two notched box plots is the graphical equivalent of a t-test). A constant speed assumption about the passing vehicle is invalid at least at high flow rate on which the text observations are based on.

The acceleration rate is significantly different upstream and downstream of the merging end as shown in Figure 4.21. The overall trend is deceleration followed by acceleration. The turnover point is about 100 meter downstream of merging end where all merging vehicles have been begun to merge or have merged. The acceleration rate measured at –100m was found to be significantly lower than 0 (a comparison between a notched box and fixed value is equivalent to a t-test).

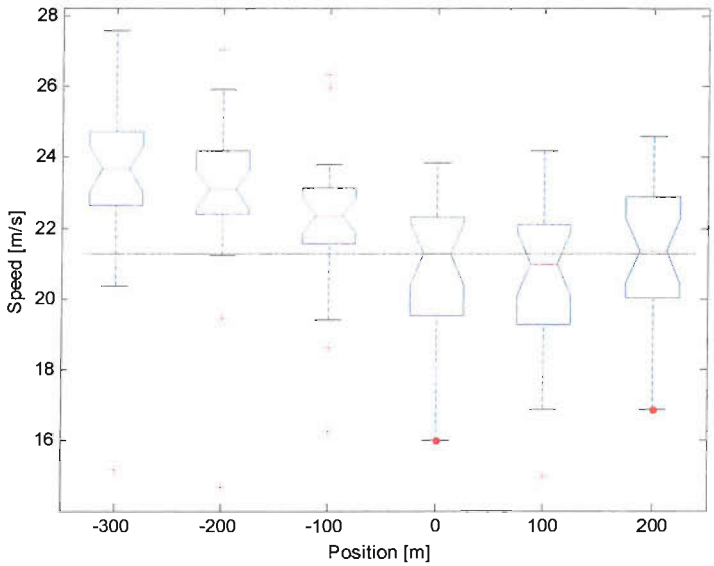

Figure 4.20 Speed of Passing Vehicle

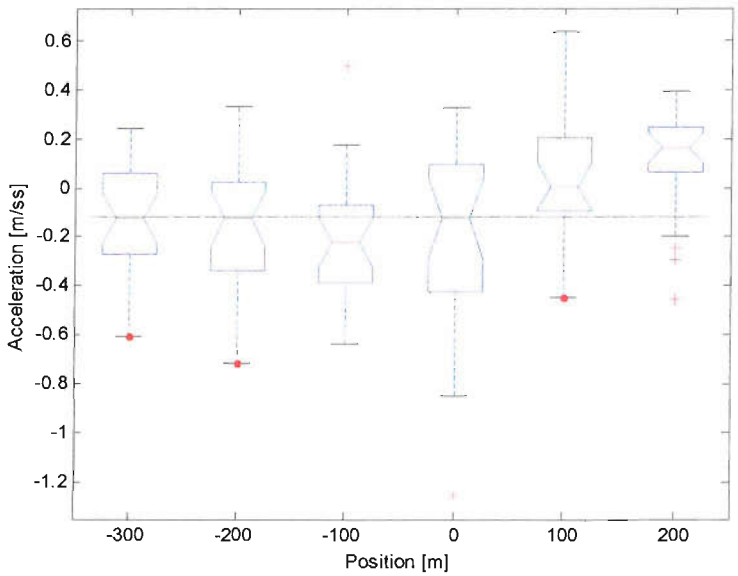

Figure 4.21 Acceleration of Passing Vehicle

The deceleration of a passing vehicle can be caused by the presence of a immediately merging vehicle or by constraint from a motorway gap leader decelerating because the existence of another merging vehicle in front of it. The direct or chained influences from merging traffic result in the observed pattern in the vicinity of the merging area. Of significance is that the variations of speed and acceleration measured at the merging end (0m) were larger than those measured at other positions. This may be explained by the fact that direct interactions in merging manoeuvre between ramp and motorway traffic are most frequent there.

The overall deceleration pattern can be interpreted as a co-operative behaviour of passing traffic. Though a passing driver has the right of the way, he/she can still take co-operative action by slowing down to reduce the speed difference with the merging traffic. The reason for taking co-operative action may be complex, and not all drivers are willing to do so. However, on average passing drivers decelerated before reaching the merging end (the maximum deceleration rate was measured at −100m). The pattern of speed change identified is logical, as critical situations can be formed in forced merging by slow merging vehicles if the passing vehicle maintains a higher speed. It should be noted that complete information on a gap follower may be hard to perceive by a merging vehicle in the limited number of look-backs. To some extent, it may be easier for a passing vehicle to avoid a safety critical situation by taking co-operative action.

4.2.3.2 Lane-changing Behaviour

The lane-changing behaviour of passing vehicles on the shoulder lane was analysed in two ways. The first was based on the merging trials performed by the IV in which the lane-changing rate of the motorway gap leader and gap follower was examined. The second was based on all vehicles on the shoulder lane within a section 250 meter upstream of the merging end from which average lane-changing rates were calculated.

The lane-changing rate of the motorway gap leader and follower in 75 merging trials is shown in Figure 4.22. Most passing vehicles remained on the motorway shoulder lane. For those changing lane, lane-changing upstream of the merging end was more frequent.

The average lane-changing rate observed upstream of the merging end when ramp metering was switched off is shown in Figure 4.23. Lane changing was counted every 5 minutes from 7:05 to 9:55 am. Some 9.2 vehicles changed to outside lane in each 5 minutes on average, representing 6.63% of all vehicles. The regression analysis suggests that the proportion of vehicles changing to an outside lane (the ratio of lane changing count to 5 minutes flow count) decreased with an increase in traffic flow, as

there would have been less opportunity to do so. Overall, only a small proportion of the vehicles changed lane upstream the merging end, especially in high flow rate.

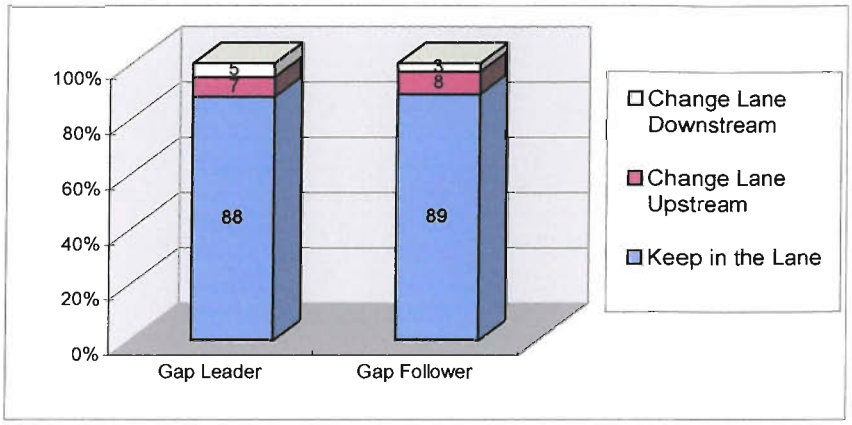

Figure 4.22 Lane Changing Rate of Gap Leader and Follower

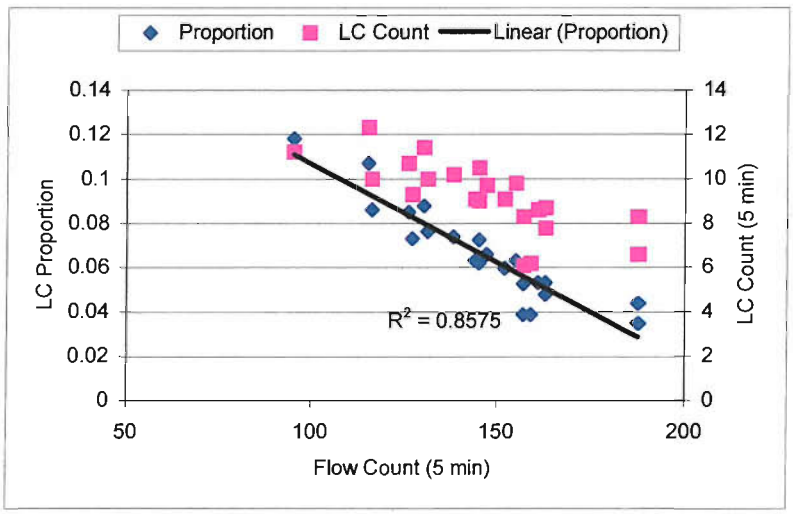

Figure 4.23 Lane Changing Rate Upstream Merging End

The statistics of lane changing do not explain why or how a passing driver changes lane. A lane-changing model is usually used to describe the lane-changing behaviour of passing drivers using such indexes as motivation and opportunity of lane-changing. The results of the analysis are a reflection of the motivation and/or opportunity of lane-changing for passing vehicles.

4.3 Model of Merging Behaviour

Based on the behaviour analysis, a conceptual description of the merging process can be made as: "when arriving at sight point, a merging driver initiates a gap search and selects a target gap (first eye-movement), then he/she follows the gap in order to merge. During this process, he/she can update information about the gap by looking-back regularly (second and third eye-movement, etc). Once on the acceleration lane, he/she accepts the gap and merges at proper time if he/she manages to achieve a satisfactory gap-structure. Otherwise, he/she has to select another gap and repeat the process. On the other hand, a gap follower on the motorway can see the merging vehicle on ramp/acceleration lane, and can either facilitate or prevent a possible merge through acceleration/deceleration control or lane-change".

The merging driver selects a gap and tries to accept it by his/her own decision. The gap follower controls the vehicle by his/her own action too. There is no direct communication between the merging driver and the gap follower (a motorway gap follower may signal a merging vehicle to let him/her into the stream of traffic, but this is not considered here). However, actions by both drivers result in a change in gap structure.

The model has been established on the basis of gap and merging vehicles (unit of analysis) in the merging area. The gap leader is the forcing term (the model input) and will not be affected by the other two elements in the unit of analysis. The merging vehicle and the gap follower interact with the gap leader and each other. In case there is no merging vehicle with reference to a motorway gap, the gap follower follows the leader as usual. It should be noted that a gap leader with reference to one gap could be the gap follower or merging vehicle of another gap, so the interactions are chained. In total, five sub-models are needed to describe merging behaviour:

- Acceleration Control of Merging Driver (ACM model)
- Gap Selection of Merging Driver (GSM model)
- Gap Acceptance of Merging Driver (GAM model)
- Acceleration Control of Passing Driver (ACP model)
- Lane Changing of Passing Driver (LC model)

4.3.1 Model of Acceleration Control Behaviour (ACM and ACP)

The models describing the acceleration control of merging (ACM Model) and passing (ACP Model) vehicles are similar to the motorway car following model described in Chapter 3. Acceleration control is treated as a close-loop manual tracking behaviour incorporating the ramp-motorway effect. The

merging driver follows a gap dynamically in order to merge into it, so he/she is constrained by gap leader and gap follower as well as the length of acceleration lane. The passing driver follows the gap leader, but is also influenced by a merging vehicle that may merge into the gap by his/her own decision. Taking these additional constraints into account, the models take the general form of:

$$x_r''(t+\tau_r) = f[(x_l'(t)-x_r'(t)),(x_l(t)-x_r(t)),(x_f'(t)-x_r'(t)),(x_f(t)-x_r(t)),(x_r(t)-x_e)] \quad \textbf{(4.1)}$$

$$x_f''(t+\tau_f) = g[(x_l'(t)-x_f'(t)),(x_l(t)-x_f(t)),(x_r'(t)-x_f'(t)),(x_r(t)-x_f(t))] \quad \textbf{(4.2)}$$

where $x_l(t)$, $x_r(t)$ and $x_f(t)$ is the position of gap leader, merging vehicle and gap follower at time t, x_e is the position of the end of the acceleration lane. τ is reaction time, f and g are appropriate functions.

Based on the behavioural analysis in the previous section, it was found that the two traffic streams try to achieve the same speed during a merging process. The adjacency to the end of acceleration lane was not found to affect the speed of merging vehicle significant at this site. Headway (both headway lag and lead with reference to a merging vehicle) did not show conclusive relationships with other variables. These findings are consistent with the results from studies in manual tracking performance. As discussed in Chapter 3, empirical research on manual car-following performance has revealed that driver's headway control bandwidth is very low compared to the speed control bandwidth [3]. In more general manual tracking problem, McRuer et al. found that humans responded in such a way as to make the total open-loop transfer function behave as a first-order system with gain and effective reaction time [65]. That is, in order to track a leading vehicle, or in the merging case, to track two vehicles, drivers mainly behave based on speed information rather than headway information. This can be easily verified by looking at the large variations in headway and small variations in relative speed of accepted gaps. Therefore, it was decided not to include separate headway terms in the model formulation, as their influences are insignificant.

For the reasons explained in the development of car following model, Fuzzy Logic was selected as the mapping tool that has been successfully used in describing dynamic manual tracking behaviour. The reciprocal of Time To Collision (1/TTC, or DV/DX) was chosen as the decision variable because it has been found that drivers are more sensitive to 1/TTC among possible relative speed related variables [107]. Accordingly, the model can be expressed as:

$$x_r''(t+\tau_r) = FUZZY[(x_l'(t)-x_r'(t))/(x_l(t)-x_r(t)),(x_f'(t)-x_r'(t))/(x_f(t)-x_r(t))] \quad \textbf{(4.3)}$$

$$x_f''(t+\tau_f) = FUZZY\ [(x_l'(t)-x_f'(t))/(x_l(t)-x_f(t)),(x_r'(t)-x_f'(t))/(x_r(t)-x_f(t))] \quad \textbf{(4.4)}$$

where $FUZZY$ denotes a fuzzy logic mapping expressed as a fuzzy inference system, other variables are the same as in equation (4.1) and (4.2).

The above formulation does not have steady states in terms of headway, which may result in unrealistic behaviour such as collisions between two vehicles and exceeding the acceleration lane (merging vehicle) if it is directly implemented in simulation. This problem will be solved in the gap-acceptance model, where a minimum distance separation between vehicles must be satisfied if a gap is accepted by a merging vehicle. Before a gap is accepted, the merging vehicle and gap follower remain on different lanes, and any relative longitudinal position will not lead to a collision. In the case of multiple merges where a gap leader may be another merging vehicle, it will be ensured that a minimum headway lead will be maintained all the time in simulation. To avoid a merging vehicle from running out of acceleration lane, it will be made sure that a merging vehicle can safely stop at the end of acceleration lane using maximum deceleration if the current gap is unacceptable. That is:

$$a_r(t)==A_r; \quad for\ x_r(t)>X_c = x_e - v(t)^2/2A_r\ and\ if\ the\ gap\ is\ unacceptable \tag{4.5}$$

where X_c is the critical point where a merging driver must start maximum deceleration in order to avoid running out of the acceleration lane, A_r is the maximum deceleration rate of ramp vehicle.

Equation (4.5) was established in an intuitive way and cannot be verified easily as stopping at the end of the acceleration lane is rare. The equation will less likely take effect in simulation because:

(1) If a gap is unacceptable, a merging driver may have selected another gap and follow that gap before reaching the X_c. The gap-selection behaviour will be described in the next sub-section.

(2) If a gap is acceptable, equation (4.5) does not take effect.

Therefore, the treatment of the effect of the end of acceleration lane, though subjective, is consistent with the observed facts that merging drivers very rarely stop at the end of acceleration lane. A comparison of longitudinal control behaviour in car following and merging is summarised in Table 4.3.

Table 4.3 Comparisons of Follow-the-leader and Follow-the-gap

	Follow-the-Leader	Follow-the-Gap
Constraints	Leader	Gap leader and gap follower
Desired States	Desired Speed, Desired headway, can be achieved by follower's own actions	Desired Speed, Minimum distance separation, may be unable to achieve by merging vehicle's own actions, depending on the gap follower's action and available length of acceleration lane
Lateral position	In the same lane with leader	In different lane with gap follower, in same or different lane with gap leader

The fuzzy logic models for dynamic control of merging and passing driver behaviour were trained using empirical data collected with ramp-metering-off, using the same procedure introduced in section 3.3. The number of partitions for inputs was selected to be 3. Sugeno type of fuzzy inference system was adopted. The input-output mapping of the calibrated model is shown in Figure 4.24.

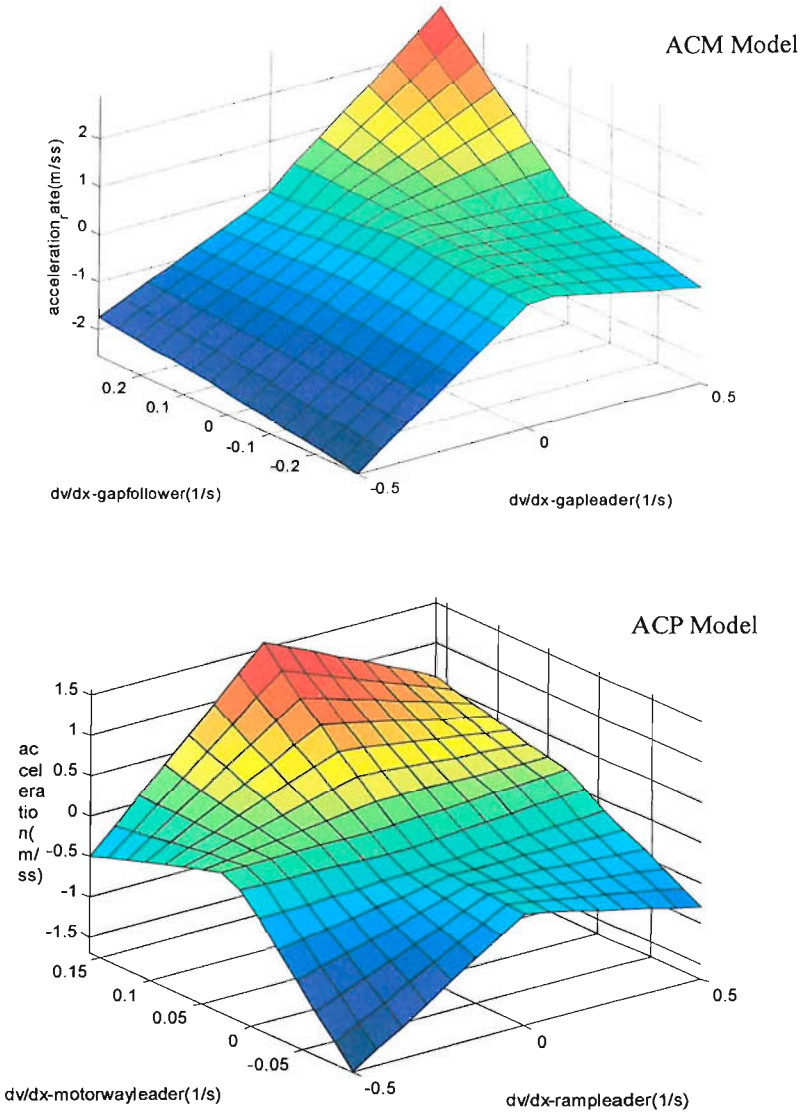

Figure 4.24 Input-Output Mapping of Dynamic Control Model

The logic revealed by the model is intuitively reasonable. The ACM has a speed attractor where the gap leader and the gap follower have the same speed. That is, a merging vehicle will finally reach the gap speed. The ACP does not have the similar speed attractor. The mapping shows a dominant region of deceleration.

The identified reaction time is about 1 second for the ACM model and 2 seconds for the ACP model as shown in Figure 4.25. The reaction time in the dynamic control of merging drivers is slight smaller than the reaction time in car following behaviour. This may be necessary in order to follow a gap

without much manoeuvring room. The difference in reaction time compared with that in car following behaviour and for passing driver are similar. Because the dynamic control of merging and passing drivers is a transient process covering only part of the tracking loop, the RMSE of fitted models are slightly larger than those of the car following model.

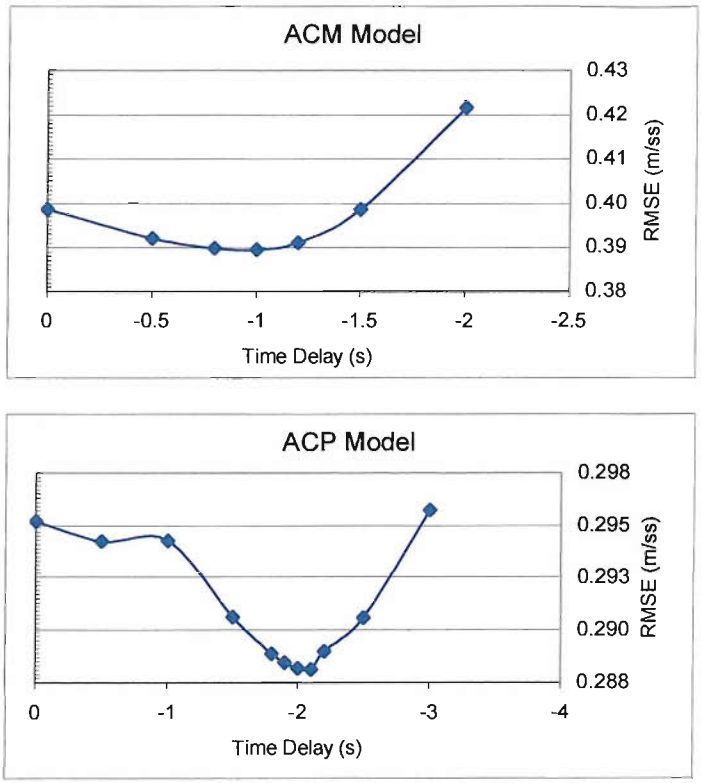

Figure 4.25 Reaction time

4.3.2 Models of Gap Selection and Gap Acceptance Behaviour (GSM and GAM)

Gap acceptance and gap-selection behaviour of merging drivers can affect the acceleration control of both gap followers and merging vehicles. Models describing these two behaviours have been formulated separately.

Gap Selection

A merging driver must select a gap. The selected gap is assumed to be the current gap as most drivers finally accepted their original gap. A merging driver may need to select another gap if the current gap has changed or the current gap has become unacceptable during the merging process. For example, a slow merging vehicle may be unable to follow a gap; he/she will either fall into a lag gap (current gap change) or become too close to the gap follower (gap unacceptable). The same holds true for a fast merging vehicle. Because gap-acceptance is only possible on the acceleration lane, a merging driver is

assumed to select another gap when the current gap has become unacceptable on the acceleration lane. In the case when a current gap has changed, the selected gap will be the new current gap. In case that a current gap becomes unacceptable, the selected gap is the lag gap.

Gap Acceptance

A step function has been used to describe gap acceptance behaviour:

$$\alpha\ (t) = \begin{cases} 1, t \geq Gc \\ 0, t < Gc \end{cases} \quad \textbf{(4.6)}$$

where G_c is the critical attribute of the gap, which can be in the form of headway, time headway, lead time, lag time etc. For the gap acceptance behaviour in motion, a merging driver must keep a safe distance to both gap leader and gap follower if he/she wants to accept the gap. The gap size also constrains the possible manoeuvring room available to the merging driver. Three thresholds based on distance separation have been selected to describe the gap acceptance behaviour of merging drivers:

(1) Gap Size : The critical gap size (front to rear bumper) is the function of the speed of the merging vehicle as shown in Figure 4.26, and can be expressed as:

$G_s = 4.253 \cdot e^{0.0968 v_m}$, where G_s is the critical gap size and v_m is the speed of the merging vehicle.

(2) Lead Separation (LG_c) and Lag Separation (RG_c): The critical lead and lag distance separation (front to rear) is the function of the relative speed as shown in Figure 4.27-28, and can be expressed as:

$LG_c = 6.7553 \cdot e^{-0.2684(v_l - v_m)}$, and , $RG_c = 5.3472 \cdot e^{0.5104(v_f - v_m)}$

for $(v_f - v_m) > 0$ and $(v_l - v_m) < 0$.

where v_l, v_m, v_f is the speed of gap leader, merging vehicle and gap follower respectively.

(3) A mimimum separation of 5 meters has been applied elsewhere as the minimum observed separation is 4.76 meters.

All thresholds were derived from the minimum gap accepted under critical situations. The reason is that a fixed decision point cannot be assumed because the decision point for rejecting a gap is unknown. G_c, in whatever form cannot be derived by examining the gap that is accepted and rejected by the same number of drivers in a decision point. However, merging behaviour analysis revealed a simple fact that nearly every merging driver accepts the current gap after passing merging end regardless of the gap size. That is to say, G_c should be very close to the minimum accepted gap size observed. The concept is explained in Figure 4.29. Therefore G_c can be approximately derived based on the minimum accepted gap of merging drivers.

If the gap is accepted while the merging vehicle is at a stop, traditional gap-acceptance theory developed for intersections can be applied. G_c can be directly derived by observing the accepted/rejected gaps [20]. However, gap acceptance at a stop is very rare in motorway merging scenarios, and so the same G_c was used as in [88]. That is, G_c=4 second in terms of time headway for all drivers.

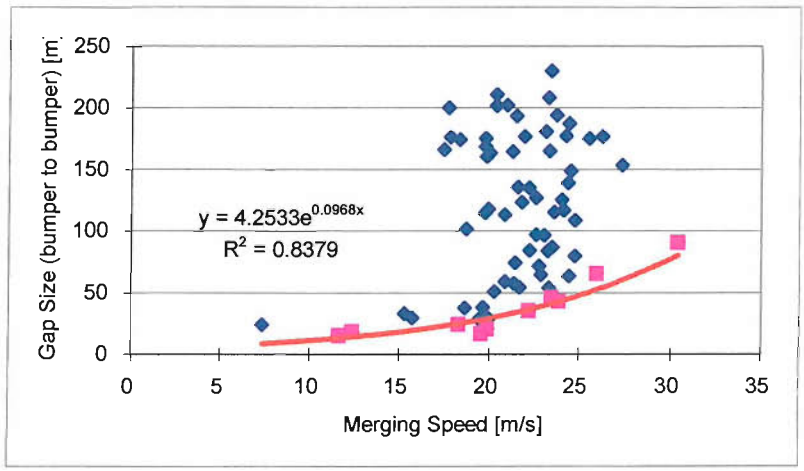

Figure 4.26 Gap Size Threshold

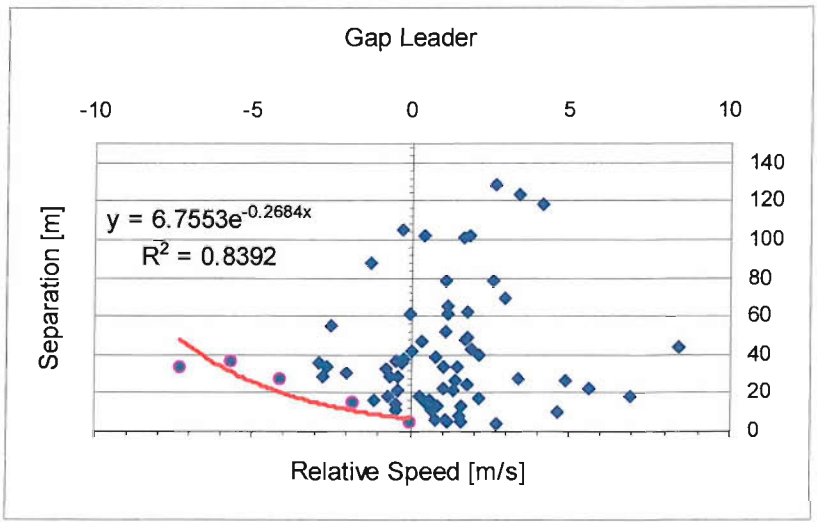

Figure 4.27 Lead Separation Threshold

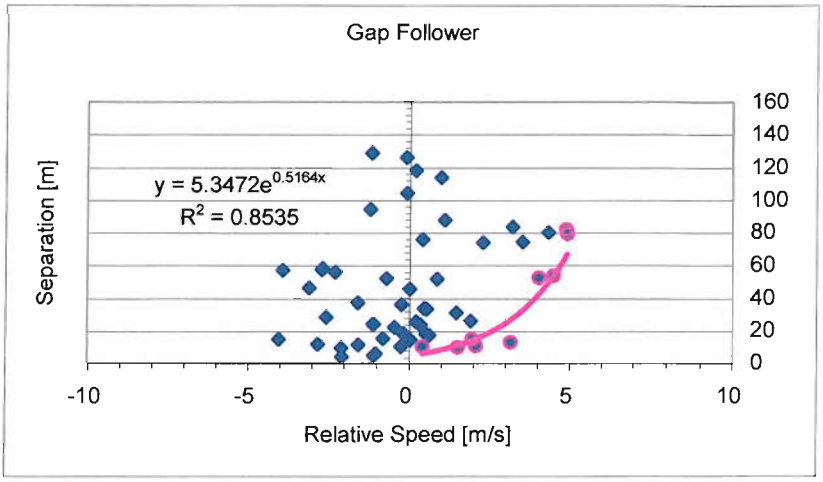

Figure 4.28 Lag Separation Threshold

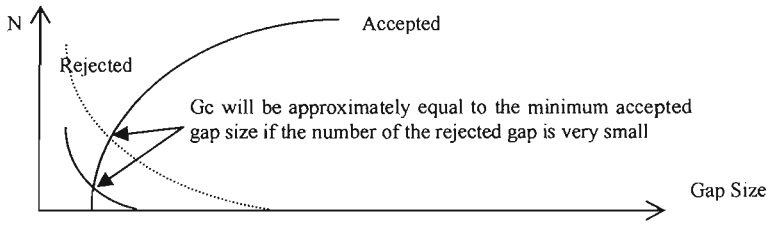

Figure 4.29 Concept of Critical Gap and the Minimum Accepted Gap

4.3.3 Model of Lane-changing Behaviour

Lane-changing is a frequent phenomenon in multilane motorways. Models describing this behaviour are the basic components in microscopic simulation.

Analytical Models

Analytical models use a heuristic approach in defining lane-changing behaviour based on well held beliefs about the lane-changing decision process. Skabardonis developed a simple lane-changing model in his traffic flow simulation [88]. The main reason for lane-changing was assumed to be the speed difference between vehicles. When faster vehicles caught up the slower ones, a 'catching-up distance' would be reached at which a lane-changing would occur if the proper gap structure was available. Gap acceptance behaviour in lane-changing was described by two thresholds, lead and lag time. Sultan developed a more detailed lane-changing model for his microscopic simulation model of motorway operation [9]. The model used many thresholds to describe the motivation and opportunity for a lane-changing, most of which were derived from empirical data. Lane change was modelled as a

sequence of three steps: decision to consider a lane change, choice of left or right lane, and search for an acceptable gap to execute the decision, in Gipps's structure model [31].

Fuzzy Logic Model

Wu et al. developed a lane-changing model based on fuzzy logic as part of the FLOWSIM motorway simulation model [103]. They assumed that a lane-changing decision was based on a driver's motivation to change lane and the opportunity available for such changing. Two different sub-models were used for lane-changing in FLOWSIM, lane change to offside (LCO) and lane change to nearside (LCN) as the motivation was considered to be different from these manoeuvres. The LCO model had two premise variables, 'overtaking benefit' and 'opportunity'. The 'overtaking benefit' was measured by the speed gain when a LCO was carried out, while the 'opportunity' concerning the safety and comfort of the lane change, was measured by the time headway to the nearest approaching vehicle from the rear on the offside lane. The LCN model used 'pressure from rear' and 'gap satisfaction' as inputs. The variable 'pressure from rear' was measured as the time headway of the following vehicle, while 'gap satisfaction' was measured by the period of time for which it would be possible for the vehicle to stay in the available gap in the nearside lane without reducing speed. The rule base was constructed on well-accepted beliefs and the model represented an encouraging approach towards complex calibrated and validated behaviour modelling.

In the merging scenario, the lane-changing behaviour of motorway vehicles is likely to be affected by merging operations. However, the basic features of lane-changing may be considered to be the same for drivers either within or outside the merging area, and lane-changing of motorway vehicles is not forced. The motorway lane-changing model could therefore be directly applied in describing lane-changing behaviour of vehicles passing the merge. In this research, the fuzzy logic lane-changing model of FLOWSIM has been used.

4.4 Model Validation

Validation can be regarded as the act of determining whether a simulation model reasonably represents or approximates a real system for its intended use [55]. Although validation is problem-dependent [77], two fundamental elements in model validation are generally considered:

1. Data: representing real-world scenarios that should be different from that used in the model calibration.
2. Indicators: representing the basis for the comparison between model and real-world system performances that could be macroscopic or microscopic.

The intended use of the merging behaviour model developed in this research was to mimic driver's merging behaviour (together with other behavioural models) in a host simulation package, through which many applications could be made. Although it is possible to validate the model to a specific application by comparing aggregated indexes relevant to that application, a microscopic validation that is application independent may be more appropriate. The advantage is that the fundamental behaviour (instead of the aggregated performance) of the model can be verified explicitly and exclusively by comparing second-to-second responses of the model with the observed time-series data. The validity established in this approach is rigid and generic.

4.4.1 Data for Model Validation

Time-series data collected with ramp metering in operation was used in the validation of the model. The microscopic behaviour data was reduced from 87 merging and 71 passing trials carried out by 15 subjects, of which passing trials without a vehicle merging directly in front or rear of the IV and merging trials without a gap follower, and incomplete datasets were excluded. The final reduced data includes 37 merging trials and 35 passing trials.

4.4.2 Validation Method

Models were tested on two ways:

- Subjective judgement of the model performance
- Quantitative examination in terms of RMSE of the prediction errors.

The subjective judgement could establish the validity of the model behaviour in an intuitive way. This has been carried out by characterising model behaviour such as speed control and gap acceptance from visual animation outputs and simulation results.

The model performance was tested by using simulation to examine the behaviour of vehicles controlled by the behavioural models in measured scenarios. The quantitative validity of the model was established by comparing whether the simulated and observed time-series trajectories agreed well.

4.4.3 Results

4.4.3.1 Qualitative Validation Result

Animation

A valid merging model should be able to produce reasonable merging operation, understandable by drivers according to their experience. Obviously unrealistic behaviour, such as rejecting very large gaps, accepting very small gaps at high relative speed, could be identified from the animation generated by computer simulation.

The overall performance of the model was examined by looking at the animation of the merging operation produced by mmSIm (Implementation details in Chapter 5). Two snapshots from an animated merging process showing a merging vehicle successfully merging into a gap are shown in Figure 4.30. It is noticeable that the gap structure is changing during the merging process, which is consistent with the observed phenomena.

The simulation has been run for a wide range of traffic scenarios. Several features observed in the real merging operation have been also found in the simulation:

- Only very few vehicles stop at the merging end, even with high traffic flows.
- Merging vehicles do not accept gaps at a fixed point (e.g. merging end).
- The accepted gap (compared to the original one), varies depending on the arrival condition.
- The passing vehicle reveals co-operative behaviour.
- The two traffic streams tend to reach a similar speed.

The conclusion was that the merging operation produced in simulation was intuitively reasonable.

Speed Control

The speed control of the merging and passing vehicle is illustrated in Figure 4.31, where the gap leader maintained a constant speed of 25m/s (a random noise with std=0.1 was added) and a slower merging vehicle (20 m/s) was going to merge into a gap of 50 meters. This represents a typical merging scenario. From the speed profiles, it could be seen that the merging vehicle and the gap follower would tend to reach a similar speed, which was close to that observed in real traffic (Figure 4.5). The time-series positions of modelled vehicles confirmed that the two traffic streams were able to reach similar speed around the merging end.

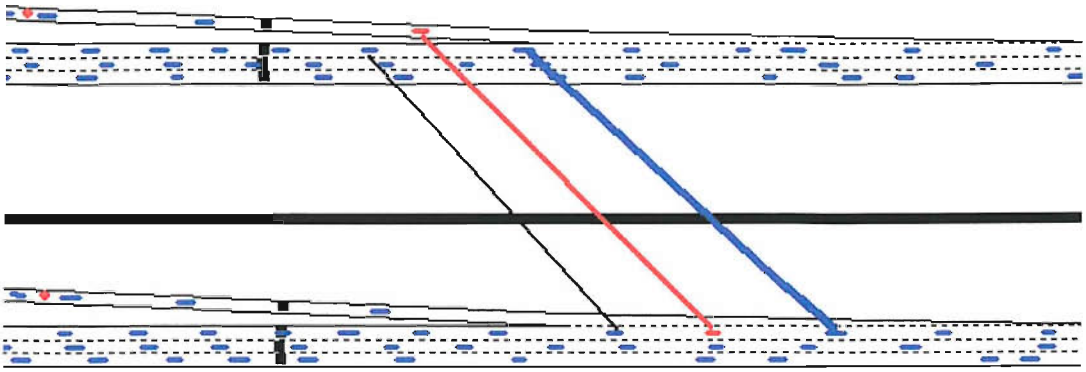

Figure 4.30 Animation of Merging Operation (color reversed)

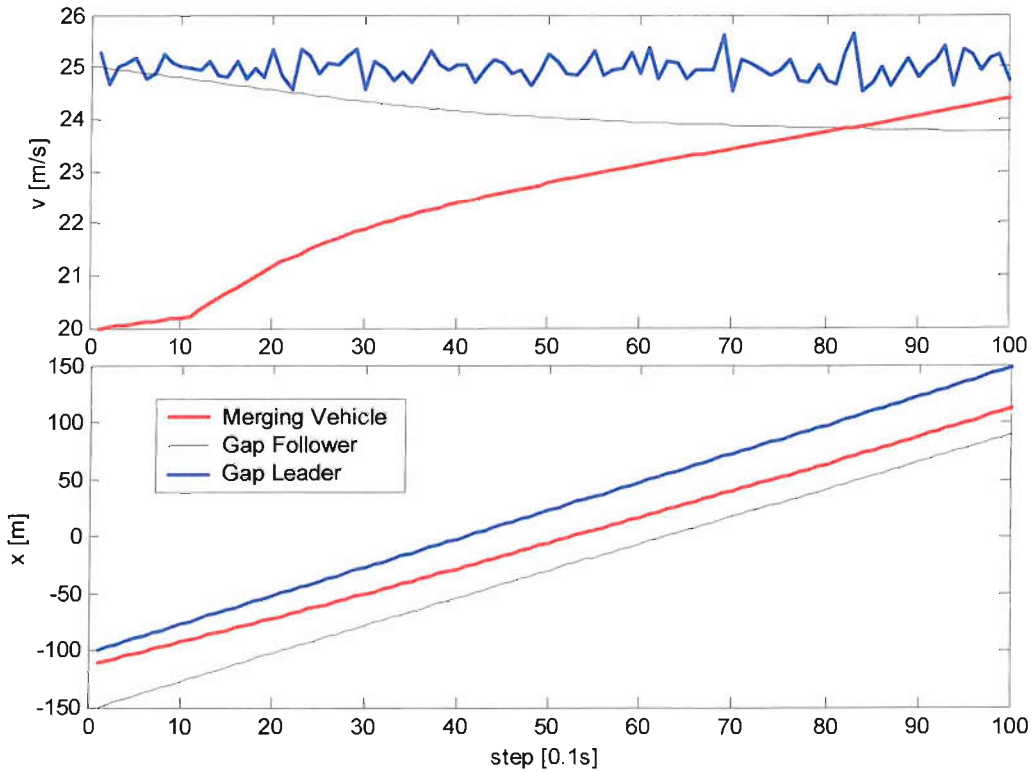

Figure 4.31: Speed and Position Profiles of a Simulated Merging

Gap-acceptance

Simulated time-space trajectories under different initial conditions are shown in Figure 4.32. The gap leader was programmed to travel at a constant speed of 25 m/s. The initial gap size was 50 meters (2 seconds) and the initial speed of the gap follower was 25 m/s. With varying arrival speeds of the merging vehicle, it can be seen that the merging vehicle accepted different gaps, including the current

gap, the lead gap, and the lag gap. The modelled vehicle was able to accept different gaps depending on the initial conditions.

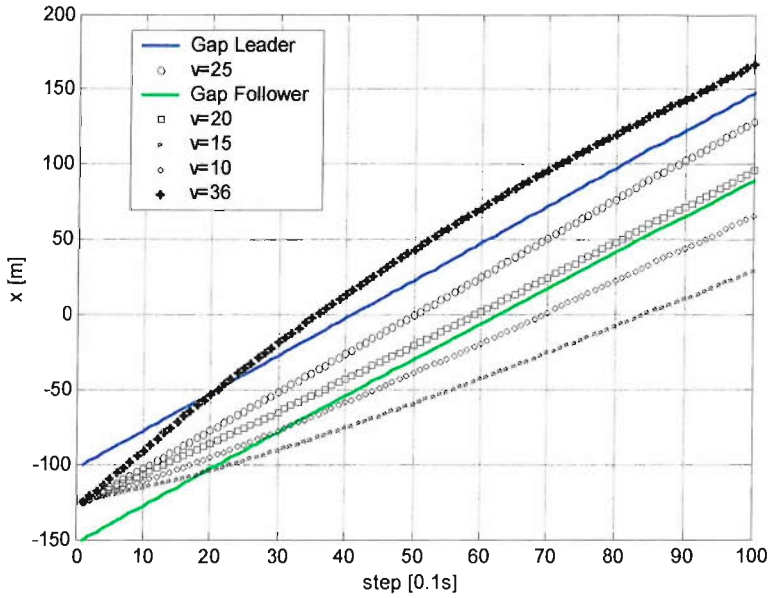

Figure 4.32 Merging Trajectories Under Different Initial Speed

4.4.3.2 Quantitative Validation Result

As behavioural models were developed taking a data-driven approach, the RMSE of models had been obtained in parameter estimation, which was 0.39 and 0.29 m/s^2 for the ACM model and ACP Models respectively (Figures 4.25). The validity of behavioural models was further examined to see whether time-series trajectories of modelled vehicles could be reproduced.

The merging and passing vehicle under the control of the behavioural models have been simulated in measured traffic scenarios. The simulation was carried out for three settings.

- The merging vehicle was controlled by the model. Time-space trajectories of the gap leader and the gap follower were empirically measured.
- The gap follower was controlled by the model. The others were empirically measured.
- Both the merging vehicle and gap follower were controlled by the model, and the gap leader was empirically measured.

The first two settings were designed to validate two interactive sub-models, i.e., ACP and ACM. This was considered necessary as an initial step, as any unrealistic merging behaviour could have been caused by sub-models, or their combinations. In this way, the effects of each sub-model could be separated. The third setting represented the combined behaviour of two interacting sub-models. This was similar to the use of the model for traffic simulation.

Results from three simulation runs under typical traffic situations are shown Figure 4.33. In most cases, the simulated trajectories mimicked the measured ones well under all settings. However, problematic situations existed where gap selection could not be easily decided. Figure 4.34 shows two such scenarios. In the first case (A), the simulated merging vehicle merged into a lead gap while he/she actually took the current one based on observation. The second showed a contrary situation (B). The observed gap follower applied significant deceleration to create a gap for the merging vehicle while the simulated one did not. As a result, the merging vehicle took a lag gap according to simulation instead of the current one. However, this cannot be simply interpreted that the simulated merging (or passing) trajectories were unrealistic as the gap selection under both simulated and observed condition were possible and practical. The RMSE would not be a reliable indicator of model performance under that case because comparison of trajectories under different gap selection is meaningless. The average RMSE of the modelled trajectories was 4.72 m excluding trials with different gap selection between simulated and observed trajectories. The performance of the model was considered satisfactory.

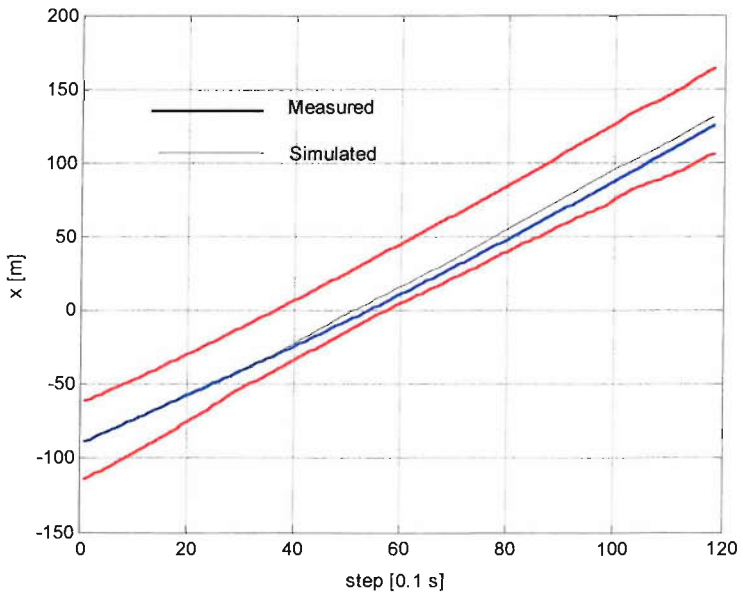

Figure 4.33(a) Typical Simulated Merging Processes (setting 2)

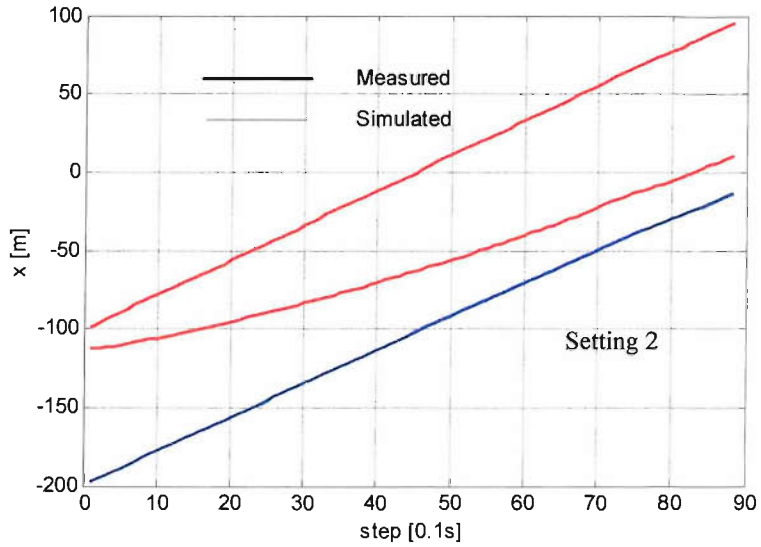

Figure 4.33(b) Typical Simulated Merging Processes (setting 1)

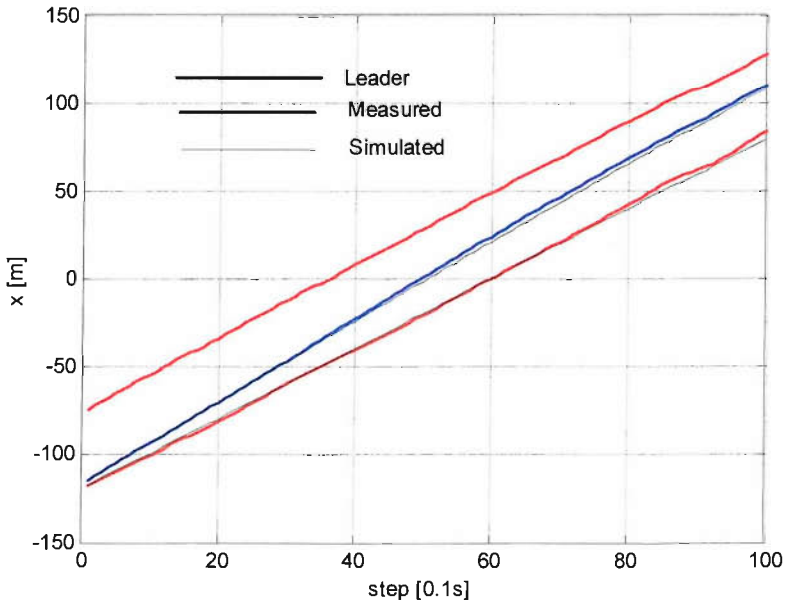

Figure 4.33(c) Typical Simulated Merging Processes (setting 3)

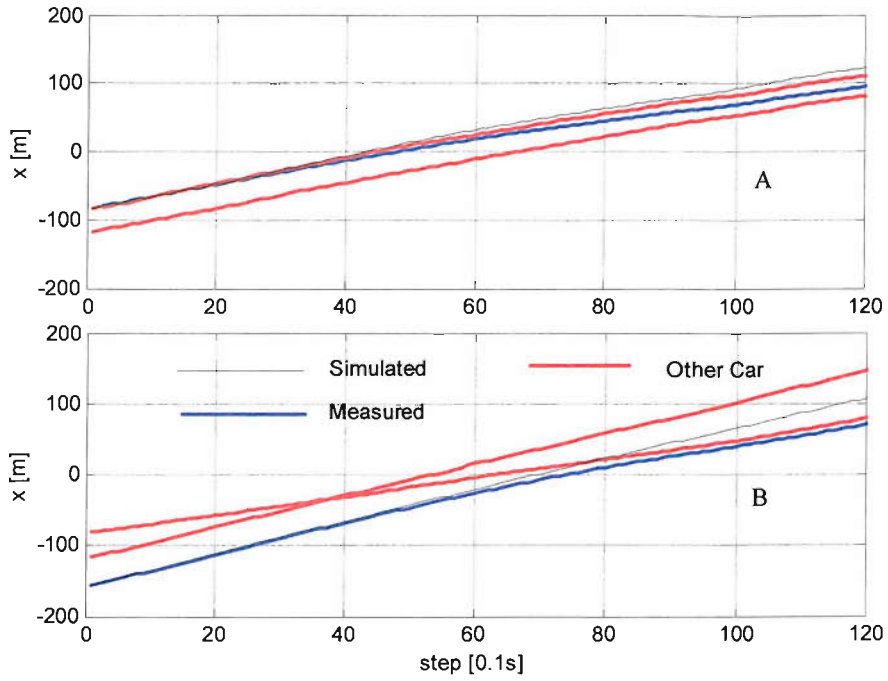

Figure 4.34 Simulated Merging Processes with Different Gap Selection

Chapter 5: Simulation

The use of computer simulation in transportation dates back to the 1950s ([29] and [59]). Since then, developments in this field have been substantial. Computer simulation has now become one of the most widely used tools for transportation practitioners and researchers [24].

Many simulation models developed so far have been microscopic in nature. Some commercial simulation products are quiet comprehensive and can be used for network-wide analysis. Other research oriented simulation programs are normally special-purpose with limited application areas. Although some commercial simulation tools provide some sorts of API (application programming interface) to allow users to change the behaviour logic within the simulation environment, it is still not possible to implement user defined behaviour models in most packages. Research oriented simulation programs are usually designed to be application-specific, which makes it difficult to add new behavioural modules or road components into the original program framework. It was decided to implement simulation of motorway merging operation as a self-containing program in this research. The program is named mmSIm, which denotes Motorway Microscopic SImulation of Merging operation.

5.1 Framework

Advances in computer hardware and programming methodology have influenced computer simulation tremendously in the last fifty years. PCs have become the most popular hardware platform with high performance-to-cost ratios. Object-oriented languages (e.g., SMALLTALK, C++, JAVA) are gaining prominence since they support the concept of reusable software by defining objects to solve a programming task. The PC was chosen as the hardware platform and Object-Oriented Programming (OOP) method for software development. The main programming language was chosen to be JAVA as it was hardware platform independent and fully supporting OOP.

The framework of the simulation program is shown in Figure 5.1, which specifies the main user-interfaces (UI) of the program and simulation input-output (IO). NET-EIDTOR allows user to construct, amend the roadwork environment, adding the controls (e.g. ramp metering, VMS etc) and

setting virtual detectors (e.g. loop etc). SIMULATION-SETTINGS provides UI for the management of simulation parameters, allows users to change the properties of drivers and/or vehicles. Input/Output (IO) is another important part of the program whereby vehicles can be generated according to traffic flow input and relevant results can be exported from detectors for further analysis. The program also provided animation to facilitate visual examination.

NET-EDITOR and SIMULATION-SETTINGS were implemented in two different modules. They served as the UI for setting properties of the network and driver-vehicle systems. The visual animation and IO was implemented in another module SIMMAIN. The core algorithms were also implemented in this module, which controlled the generation and movement of driver-vehicle systems within the simulated environment. Simulation output visualisation was also implemented in this module to provide an integrated and user-friendly interface. Three screen-shots when running different modules are shown in Figure 5.2.

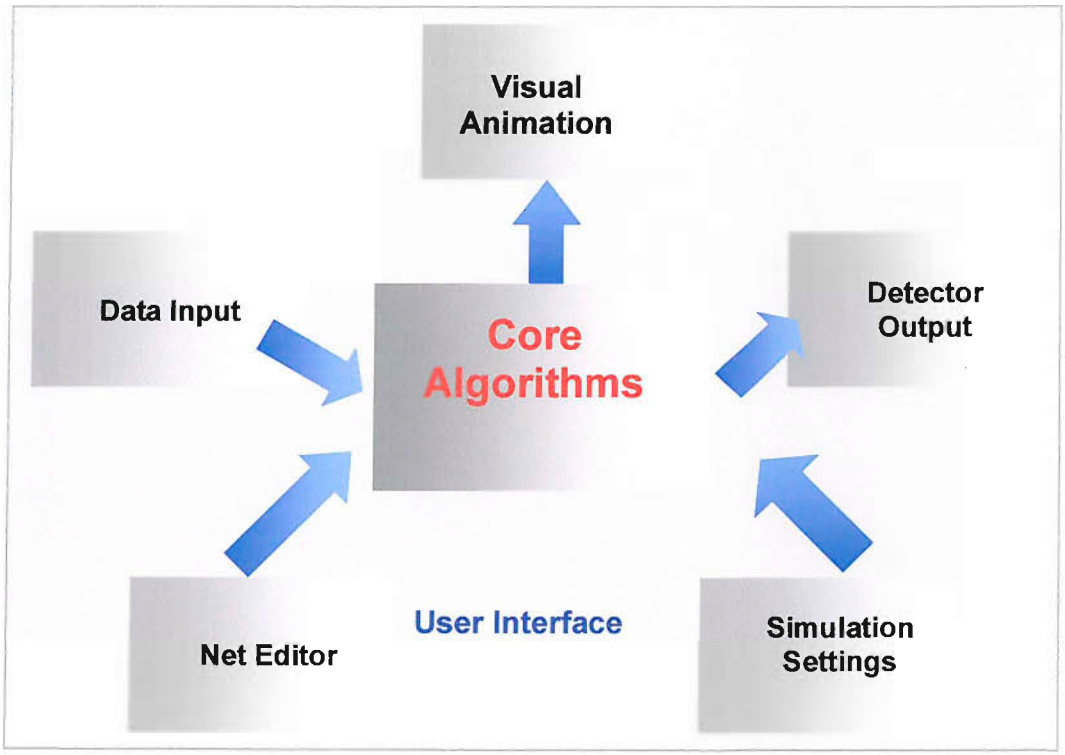

Figure 5.1 Framework

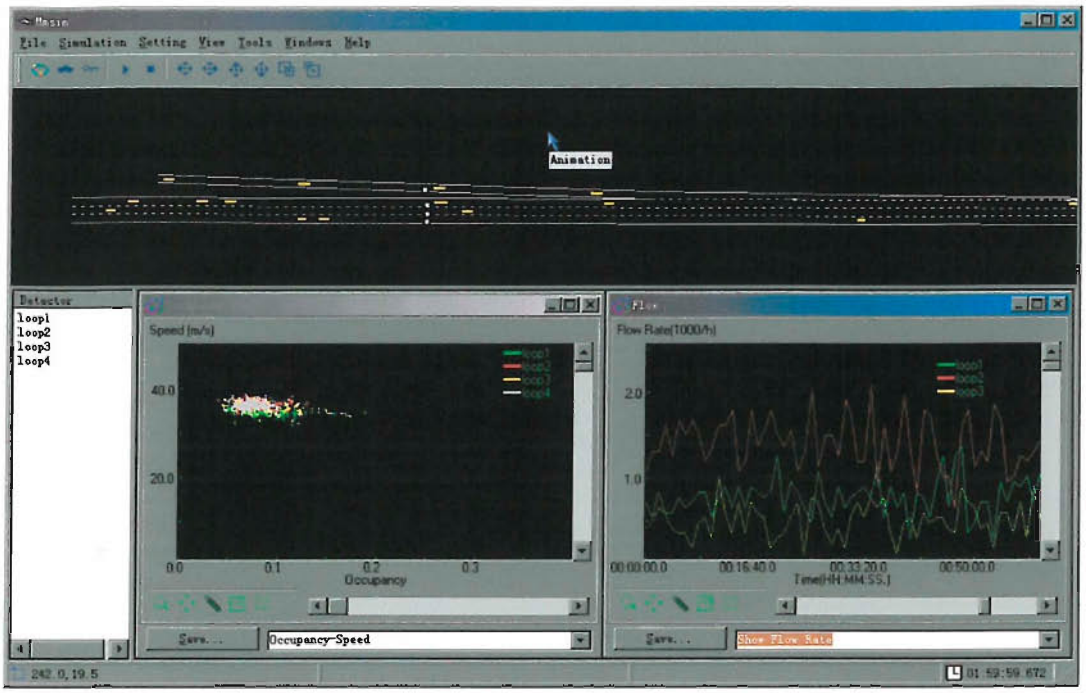

A: SIMMAIN

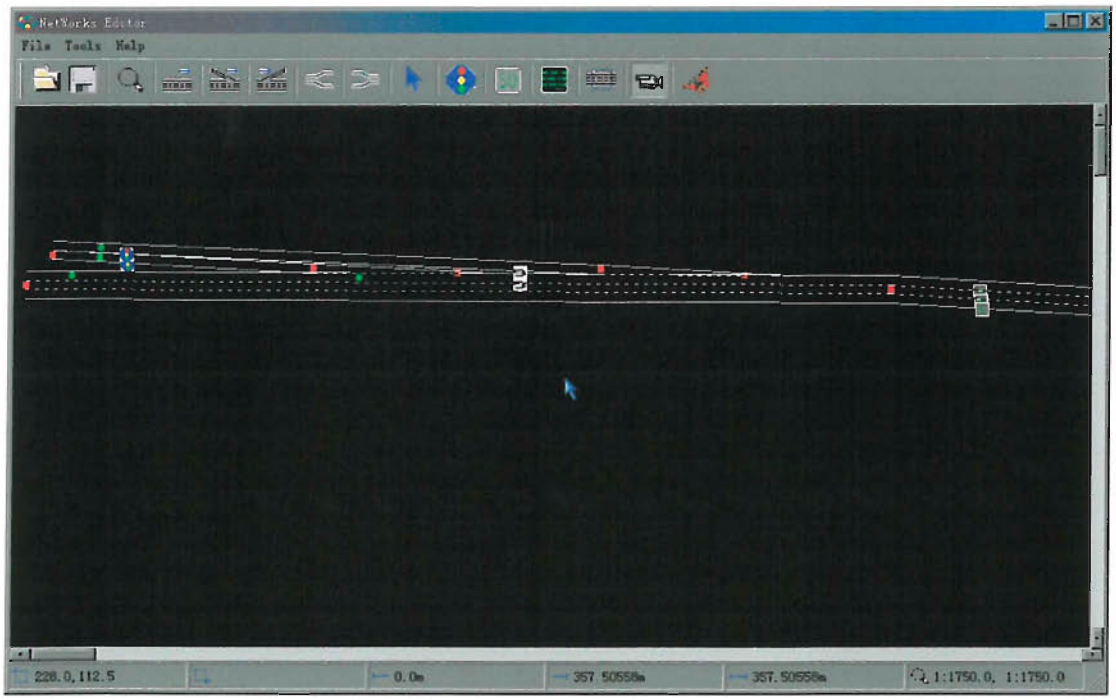

B: NET-EDITOR

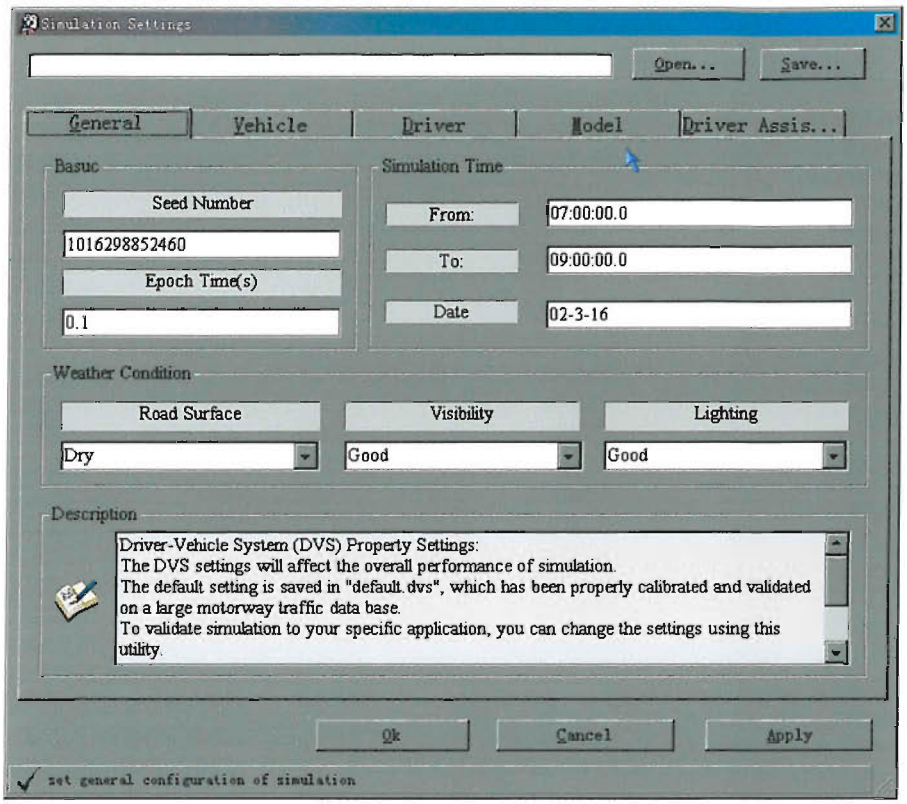

C: SIMULATION-SETTINGS

Figure 5.2 Screenshots from mmSIm

5.2 Core Algorithms

Transportation systems are a collection of driver-vehicle elements moving on physical networks, each element interacts with other elements and the environment. Behavioural models govern the movement of the driver-vehicle element. Object-oriented programming is very suitable in describing a great number of similar elements in traffic. Accurate traffic behaviour is produced by programming objects to interact in a natural way. Of the many objects defined in the simulation program, the most important is the driver-vehicle system. This sub-section introduces core algorithms in generating and moving these basic elements.

5.2.1 Vehicle Generation

At the outset of a simulation run, vehicles are generated at origins, usually at the periphery of the analysis network, according to some headway distribution based on specified volumes. A vehicle and its driver forms an entity that can be defined in terms of its relevant attributes:

- Vehicle: length; width; acceleration limit; deceleration limit; type; etc.
- Driver: aggressiveness; reaction time; desired headway; desired speed; model parameters etc.

Each attribute must be represented by the analyst, some by scalars (e.g. vehicle length); some by a functional relationship (e.g., maximum vehicle acceleration as a function of its current speed); some by a probability distribution (e.g., desired headway).

5.2.1.1 Traffic Arrival

Traffic arrival is stochastic in nature, which can be described by a time headway distribution model. Models representing single-lane time headway distributions are of two main types: simple models of a single statistical distribution and mixed models representing headway distributions of following and non-following vehicles in appropriate proportions.

Simple Model

One of the important distributions in a simple model is the Lognormal Distribution.

$$f(t) = \frac{1}{\sigma t \sqrt{2\pi}} e^{-\frac{(Ln(t)-\mu)^2}{2\sigma^2}} \quad \textbf{(5.1)}$$

This model gave a good fit to following vehicle headway data obtained at high flows. It has been found that the introduction of a minimum headway of 0.3 sec improved the fit of the log-normal distribution [95].

Mixed Model:

Generalised Queuing ([68]) and Semi-Poisson Models ([15]) are based on the assumption that constraints imposed by stability and safety considerations, and the lack of overtaking opportunities prevents traffic in a single lane from behaving as a random phenomenon. In a Queuing Model, the distribution is assumed to be:

$$f(t) = \psi g(t) + (1 - \psi) h(t) \quad \textbf{(5.2)}$$

Where: $f(t)$ is the p.d.f of all headways;

$g(t)$ is the p.d.f of following headways;

$h(t)$ is the p.d.f of non-following headways;

ψ is the proportion of following vehicles.

Non-following headway t was the sum of a following headway x drawn from the p.d.f $g(x)$ and a gap $(t-x)$ which was negative-exponentially distributed with parameter λ, the flow rate. The proportion of following vehicles was defined by:

ρ = mean following headway/mean headway (traffic intensity), thus obtained:

$$f(t) = \rho g(t) + (1-\rho)\lambda \exp(-\lambda t) \int_0^t g(x) \exp(\lambda x) dx \quad \textbf{(5.3)}$$

In Semi-Poisson Model, each non-following headway was obtained by comparing an exponential headway with a following headway:

$$f(t) = \psi g(t) + (1-\psi) \frac{\lambda \exp(-\lambda t) G(t)}{g^*(\lambda)} \quad \textbf{(5.4)}$$

where $g^*(\lambda)$ is the Laplace transform of $g(t)$ and $G(t)$ is c.d.f of $g(t)$.

Branston fitted the model using data from M4 and Indiana site with a following headway distribution, $g(x)$, using normal, log-normal (only in Queuing Model) , and gamma distributions. He concluded that the Queuing Model, when using a log-normal distribution for following headway, gave the best overall fit to data [14].

For the purpose of this research, non-random models were considered, which could generate traffic arrival under different traffic volumes. The Queuing Model with a log-normal distribution of following headway, which had been used in several microscopic simulations, has been adopted for both motorway and ramp traffic generation. When density is very high, the headway distribution in a Queuing Model relaxed to a log-normal (ψ=1), which has been reported to give a good fit to following vehicle headway data.

Time Headway Distribution

Given the flow rate of λ^* vehicle/second, the distribution of the following headway that is independent of the flow rate will be:

$$g(t) = LogNormal(\mu, \sigma)$$

Typical parameters given by Branston are:

m=E(g(t))=1.6 second, s=Std(g(t))=0.4 second for slow motorway lane, and

m=E(g(t))=1.3 second, s=Std(g(t))=0.4 second for fast motorway lane [14].

The proportion of following vehicle (ψ) and the parameter for non-following headway distribution ($1/\lambda$) are traffic volume dependent, which has been given in [14]:

$$\lambda = \lambda^* - 0.5\lambda^{*1.5} \quad \textbf{(5.5)}$$

$$\psi = \rho - 0.5(\rho - 1)\lambda^{*0.5} \quad \textbf{(5.6)}$$

where: the traffic intensity $\rho = \dfrac{m}{1/\lambda^*}$

The flow diagram for generating the single-lane time headway distribution using Queuing Model is shown in Figure 5.3.

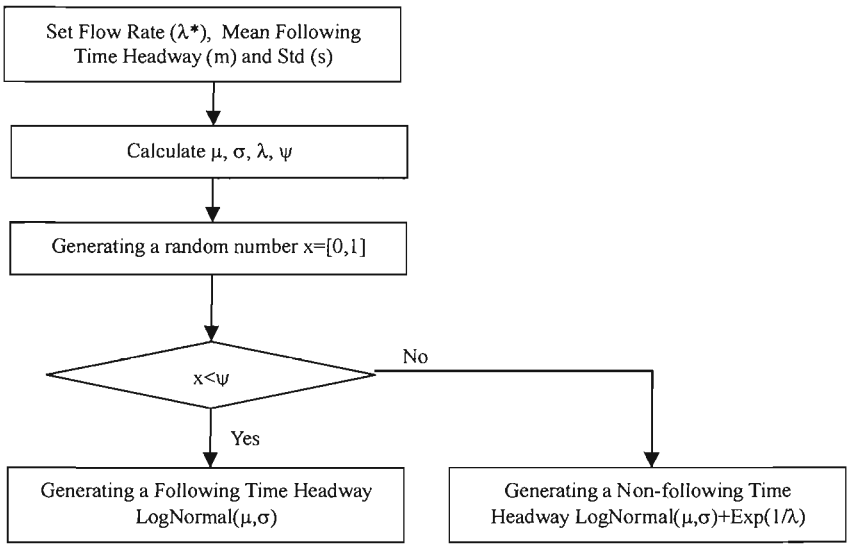

Figure 5.3 Generation of Arrival Time Headway Based on Queuing Model

Lane Distributions

If the total flow rate of a multi-lane motorway is provided, it is necessary to distribute traffic flow across each lane. The regression result from 5-minute loop data collected upstream merging end for a period of two month in this research is shown in Figure 5.4. The proportion of traffic in each lane of the three-lane motorway can then be calculated by Equation 5.7-9.

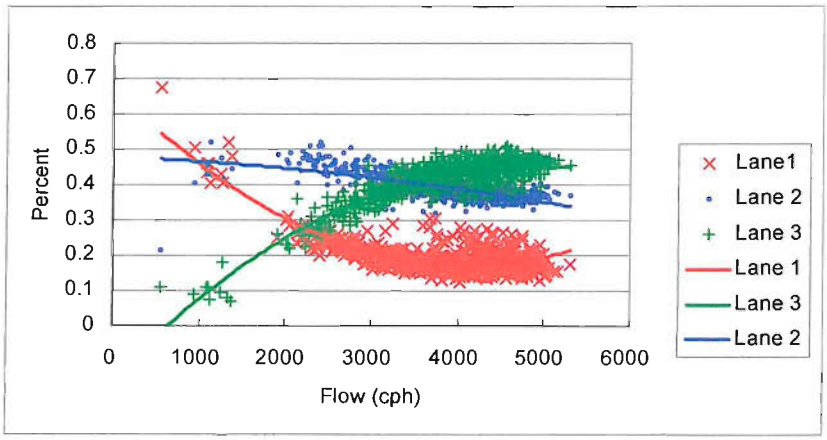

Figure 5.4 Lane Distribution

$$Lane\ 1\ Proportion = -2.6284E\text{-}08q^2 + 2.5220E\text{-}04q - 1.5061E\text{-}01 \quad \textbf{(5.7)}$$

$$Lane\ 2\ Proportion = -3.018E\text{-}09q^2 - 1.052E\text{-}05q + 4.795E\text{-}01 \quad \textbf{(5.8)}$$

$$Lane\ 3\ Proportion = 2.9302E\text{-}08q^2 - 2.4168E\text{-}04q + 6.7106E\text{-}01 \quad \textbf{(5.9)}$$

where q is the total flow rate for a three-lane motorway.

The proportion of H.G.V. on the three-lane motorway was calculated according to the following equations in [39]:

$$P_1 = \frac{1200P \cdot q}{(1200 + P \cdot q) \cdot q_1} \quad \textbf{(5.10)}$$

$$P_2 = \frac{(P \cdot q)^2}{(1200 + P \cdot q) \cdot q_2} \quad \textbf{(5.11)}$$

$$P_3 = 0$$

where P is the total proportion of the H.G.V, q is the total flow rate, q_1 and q_2 denotes flow rate on lanes 1 and 2 .

For the lane distribution of multi-lane ramp or other multi-lane motorway, this simulation model does not provide default algorithms and a user must provide traffic flow rate and proportion of H.G.V for each lane.

5.2.1.2 Vehicle Attributes

The following attributes are assigned to a vehicle when it is generated. Extensive reference has been made to the previous PhD research work at TRG reported by Skabardonis and Sultan in deciding some of the default values (refer to [9] and [88]). However, the program is designed to be able to take user defined vehicle generation parameters, which can vary between applications.

Vehicle Type

The number of vehicular types is user-defined in our implementation. There is no limitation to the number of types that a user can define. However, for each vehicular type defined, a user needs to specify the corresponding attributes. By default, two vehicular types are defined: Car and Heavy Goods Vehicle (H.G.V).

Vehicle Lengths

Empirical observation has revealed that the variations of vehicle lengths can be described by normal distributions based on vehicular types [97]. The default value used in this research, shown on Table 5.1, is the same as that used by Skarbardonis.

Table 5.1 Default Distribution of Vehicle Length

Vehicle Type	Mean [m]	Std
Car	4	0.6
H.G.V.	11	2.4

For a finer partition of vehicular types, users are requested to provide type and parameters of the length distribution for each type of vehicle defined. A vehicle's length is sampled from the corresponding distribution according to its type.

Maximum Acceleration Rate

The maximum acceleration rate is dependent on speed. The maximum acceleration-speed relationship for Car (up) and H.G.V (lower) used in the simulation based on [43] is shown in Figure 5.5.

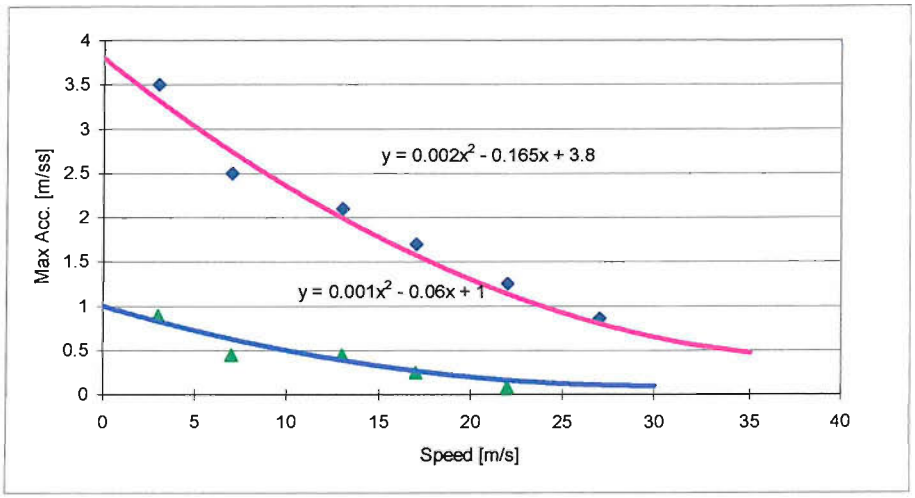

Figure 5.5 Maximum Acceleration Rate-Speed Relationships

Maximum Deceleration Rate

The maximum deceleration rate used in the simulation is 4.0 m/s^2, which is decided based on the highest deceleration rate observed in car following experiment of this research.

5.2.1.3 Driver Attributes

The following attributes are assigned to a driver regardless of the vehicle type.

Desired Time Headway (Th_{dsr})

The desired time headway is closely related with the driver's desired headway (SD) in a car following situation as described in Chapter 3. The bumper to bumper time headway can be derived from Th_{dsr} using:

Th= Th_{dsr}+ $(5+ L)/v$, where L and v are the length and speed of the vehicle.

According to the car following experiment, the desired time headway of the driver sample is distributed lognormally with [m=1.26s, std=0.49s]. With an average vehicle length of 4 m and a typical speed of 30 m/s, this equates to an average bumper to bumper time headway of 1.56 s. The

lognormally distributed following time headway used in the Queuing Model gives [1.6, 0.4] for the slow lane and [1.3, 0.4] for the fast lane. Clearly, the results from this microscopic observation are larger for the fast lane time headway distribution. This may be explained by the fact that the result from the car following experiment is based on all lanes and using a small sample size (population of part of TRG). To remain compatible with the traffic generation model used, the desired time headway has been converted from the time headway:

$$Th_{dsr} = T_h - (5+L)/v \quad \textbf{(5.12)}$$

where T_h is the generated time headway of traffic arrival, L is the length of the vehicle and v is the speed.

Aggressiveness:

Aggressiveness of a driver is defined as the ratio between linearlised speed gain and that of the normalised driver so that a normalised driver has an aggressiveness attribute of 1.

Awareness

Awareness is defined as the ratio between time delay and that of the normalised driver so that a normalised driver has an awareness attribute of 1.

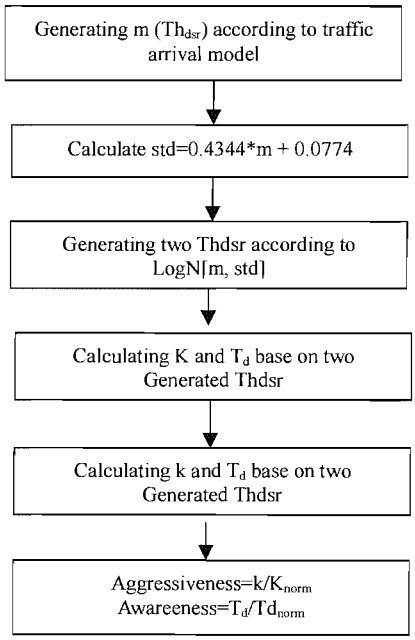

Figure 5.6 Flow Diagram for Assigning Aggressiveness and Awareness

The generation of aggressiveness and awareness has been based on regression results obtained in the car following behavioural analysis reported in Chapter 3, based on driver's desired time headway:

(1) Linearlised gain:

$k = -0.1238 * Thdsr + 0.3368$

(2) Time delay

$T_d = 0.8297 * Thdsr + 1.3004$

(3) Standard deviation of the desired time headway within driver

$std = 0.4344 * m + 0.0774$, where m is the mean desired time headway of a driver

The procedure of generating aggressiveness and awareness is illustrated in Figure 5.6

Desired Speed

A driver's desired speed is the free speed at which each driver wishes to travel. The mean desired speed can be estimated from speed-flow relationship at the volume of 300 vph/lane according to the definition by Duncan [25]. The mean desired speed in this research has been estimated using 5 minutes loop data (upstream the merging end) as shown in Figure 5.7. Standard deviation has been estimated based on the relationship proposed by Burrows [17] and confirmed by Sultan [9], that is: $\sigma = 2/3$ s, s is the difference of mean desired speed between adjacent lanes. The result is summarised in Table 5.2.

Table 5.2 Desired Speed Distribution

Lane	Mean (m/s)	s=4.5 (m/s)	Range
1	u-s=28.3	σ=2s/3=3	[u-3s, u+s]
2	u=32.8		[u-2s,u+2s]
3	u+s=37.2		[u-s, u+3s]

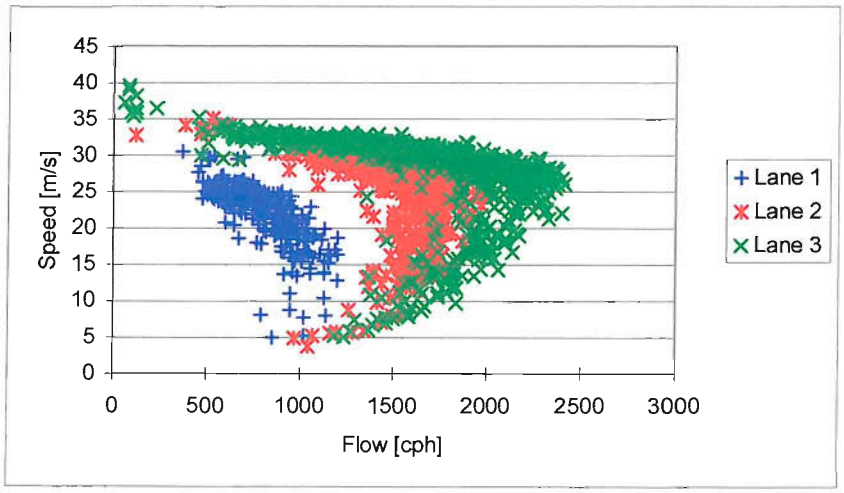

Figure 5.7 Flow-Speed Relationship Observed Upstream Merging End

5.2.2 Vehicle Movement

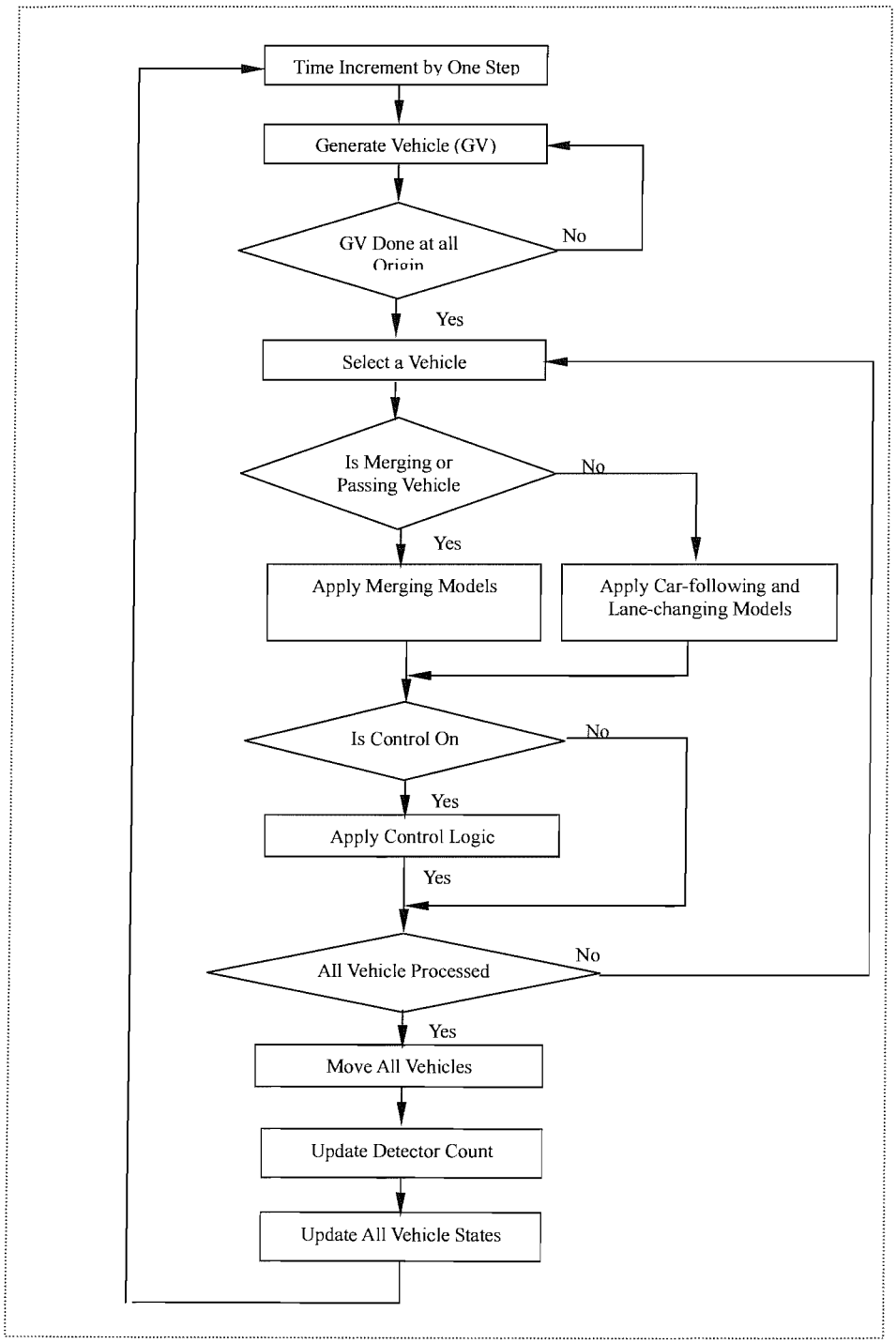

Figure 5.8 Simulation Step

The driver-vehicle systems are handled in succession in a fixed time step. The default time step is 0.1 second. The state of each driver-vehicle element is updated in accordance with the relevant behavioural models in each step. The flow diagram for updating driver-vehicle elements in each simulation step is shown in Figure 5.8.

5.2.3 Implementation of Fuzzy Logic Model

The key task in each step is to calculate the output for different behavioural models. Most behavioural models developed in this research were established on fuzzy logic in which a fuzzy inference system (FIS) has been used to map the inputs to outputs.

Fuzzy logic models can take different forms, e.g. single input single output, multi-inputs single output etc., and can use different types of FIS, e.g. Sugeno or Mamdani etc. A generic FIS to meet different requirements has been implemented in this research.

The implementation is basically established on the stand-alone program of FIS in Matlab [44], re-written in JAVA using the OOP method. To retain compatibility with the Matlab development environment, an interface was also implemented to read FIS files created using Matlab. Through this, any FIS developed using Matlab can be directly implemented in this simulation.

A typical FIS has several inputs and outputs, each input or output is described by several membership functions. Inputs and outputs are associated using logical operations based on a linguistic rule-base. Implementation of FIS involves manipulation of many linguistic terms, such as type of membership function, logical operation, which make the data structure complicated. A Fis class has been established to define the data structure and operation of the data (methods).

5.2.3.1 Membership Function

The membership function is a parametric representation of the shape of a fuzzy set. Symmetrical triangular fuzzy sets, for instance, are defined by the two parameters that specify their width and the position of the peak. Ten types of popular membership functions have been implemented including triangular, Sigmoid, Gauss, PI etc. The data structure was defined as an inner class (Mfnode) of Fis as follows:

```
class Mfnode
        {
                .....
                String sLabel="";
```

```
        String sType="";
        int mfFcnTag;

        float[] af_Para= new float[4];
        float fValue=0;//for Sugeno only
        float[] af_SugenoCoef;//for sugeno only
        float[] af_ValueArray; //for Mamdani only, array of MF values
        boolean userDefined; //true if the MF is user-defined
        .....
}
```

The basic attributes of a membership function are 'sType' and 'af_Para', which holds Type and Parameters. The maximum number of parameters for a membership function is four.

5.2.3.2 Input / Output

A single input/output domain can be partitioned for a finer description, e.g., relative speed can be closing, about zero and leaving etc. Another inner class (Ionode) has been used to describe the collection of fuzzy sets belong to the same input/output. The data structure is defined as follows.

```
class Ionode
{
        .....
        String sName="";
        int iMfNum; //number of MF
        float af_Bound[]; // universe of discourse
        Mfnode[] Mf; // MF array
        float fValue; //holding crisp value
        .....
 }
```

Figure 5.9 is a graphical representation of the above definition. Any crisp input value can be converted to associated linguistic terms with some degree of truth through fuzzification, and fuzzy reasoning can then be applied.

5.2.3.3 If-Then Rules

The rule list was implemented using arrays in Fis class:

```
.....
public int[][] ai_RuleList; // Rule list
```

```
public float[] af_RuleWeight; //Weight of rules
public int[] ai_AndOr;      /* AND-OR indicator, and=1, or=0*/
.....
```

ai_RuleList is a integral matrix, each row denotes a rule. The column number is associated with inputs and outputs. For example, a rule of [1 2 1] denotes 'If Input 1 is membership function 1(a fuzzy set, e.g. closing) and/or (denoted by ai_AndOr) input 2 is membership function 2 then output is membership function 1'. The number of inputs, outputs and number of rules are also defined in Fis class:

```
.....
public int iInNum=0; //Number of Inputs
public int iOutNum=0; //Number of Outputs
public int iRuleNum=0; // Number of Rules
.....
```

In this way, inputs and outputs in a rule can be properly resolved.

Interpretation of If-Then rules is implemented in several private methods defined in Fis class. Using fuzzy logic car following model as an example, three steps in the process are illustrated. Figure 5.10 shows how a rule 'if DV is closing and DX is satisfactory then deceleration' has been interpreted.

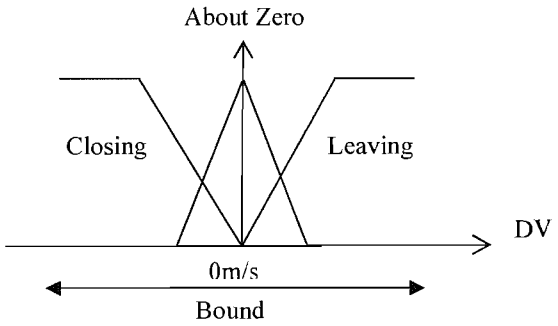

Figure 5.9 An Input / Output of FIS (Relative Speed)

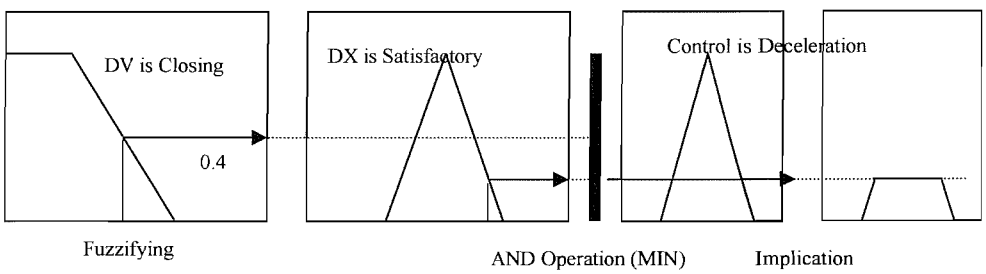

Figure 5.10 Interpreting a Rule

Step 1: Fuzzify Input

The task was to compute membership value of fuzzy set s for a crisp input x, that is, to evaluate $\mu_s(x)$ (μ is the membership function). The implementation is different for different types of membership function. The following code is used to compute triangle membership function value.

```
private float fisTriangleMf(float x, float para[])
{
        float a = para[0], b = para[1], c = para[2];

        if (a>b)
                fisError("Illegal parameters in fisTriangleMf() --> a > b");
        if (b>c)
                fisError("Illegal parameters in fisTriangleMf() --> b > c");

        if (a == b && b == c)
                return ((x == a)? 1 : 0);
        if (a == b)
                return ((c-x)/(c-b)*(((b<=x) ? 1 : 0)*((x<=c) ? 1 : 00)));
        if (b == c)
                return ((x-a)/(b-a)*((a<=x) ? 1 :0 )*((x<=b) ? 1 : 0));
        return(fisMax(fisMin((x-a)/(b-a), (c-x)/(c-b)),0));
}
```

Step 2: AND/OR Fuzzy Logic Operation

In the case that the antecedent of a rule has more than one part joined by a fuzzy operator, the truth-value of a rule is computed by applying fuzzy logic operation:

$$\alpha_r = T(\mu_{s_1^r}(x_1), \mu_{s_2^r}(x_2), ..., \mu_{s_n^r}(x_n))$$

where T denotes a fuzzy logic operation.

Basically, any number of well-defined methods can fill in for the AND operation or the OR operation. Two AND methods, min and product, and two OR methods, max and probor (probabilistic or) have been implemented. The following code is the implementation of probor method.

```
private float fisProbOr(float x, float y)
{
        return(x + y - x*y);
}
```

The truth-value of a rule can be computed by iterative using of this method if there are more than two parts in an antecedent.

Step 3: Apply Implication

The truth-value of a rule was then applied to the output membership function using the implication method, which resulted in the output of a rule denoted by a truncated fuzzy set. Two commonly used application methods are MIN and Product.

5.2.3.4 Fuzzy Inference

The implementations of a fuzzy inference system for Mamdani and Sugeno type of FIS are slightly different. For a Sugeno type of FIS, the output is directly computed according to:

$$output = \frac{\sum_{r=1}^{n} \alpha_r \cdot k_r}{\sum_{r=1}^{n} \alpha_r}$$

where, for each rule r, k_r is the output membership function, in most cases a singleton or the linear function of the input variables. α_r is the truth-value of the rule r.

For Mamdani type of FIS, the fuzzy sets resulting from the activated rules are first combined (aggregation), the final output fuzzy set is obtained by applying aggregation methods to the rule outputs. Three aggregation methods implemented are 'MAX', 'SUM' and 'PORBOR'. The final step in fuzzy inference is to obtain a crisp output value using defuzzification method. Most of the common defuzzification methods in Fis class have been implemented. The use of 'MAX' aggregation method and 'Centre of Gravity' defuzzification method in resolving a crisp output value is shown in Figure 5.11.

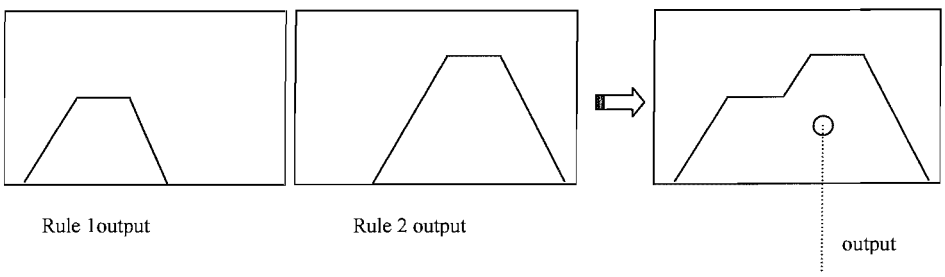

Figure 5.11 Aggregation and Defuzzification

5.3 Evaluation of Local Impact of Ramp Metering on Merging Operation

Through the work introduced so far, the merging operations could be reproduced on computer simulation using behavioural models developed in this research and other studies. It was then possible to carry out computer simulation experiments to provide useful information on the what-if problems related with the merging operation.

A promising application area is the evaluation of ramp metering operations. Ramp metering is considered to be an increasingly important advanced transportation management system (ATMS) measure to improve traffic flow on motorways. The metering only allows traffic to enter the motorway at a rate dependent on the conditions of the motorway traffic to keep the main traffic moving at a reasonable speed, thus effectively reduce mainline congestion.

In metering, ramps are controlled in a similar manner as surface street intersection traffic signals. The control plan can be fixed, local traffic responsive based on volume, occupancy or speed obtained by the local detectors. Ramp metering may also be controlled from a central system based on ramp and mainline traffic conditions within an area. Adaptive or traffic responsive control is achieved by utilizing ramp metering algorithms. Most metering employs a fixed green time of 2 seconds to allow for one vehicle to pass in each phase (one car per green time principle)[102], and some others use a longer green time to allow more than one vehicle to pass in each phase (e.g., at this survey site, 3 cars each phase, at Junction 10 of M27, 2 cars each phase). By varying cycle time, different metering rates can be achieved. The entry traffic sometimes has to stop at a metering point so that discharging traffic characteristics on to the acceleration lane could be different at metering junctions.

Ramp metering has demonstrated effectiveness in increasing mainline speed and reducing travel time, congestion and accidents in several before-and-after studies (refer to [33], [73] and [92]). These improvements are generally believed to have been achieved through keeping mainline traffic density below a critical level and by breaking up platoons in merging traffic. While a system-wide effect is clearly determined by a combination of many factors such as control strategies etc., the local impact of ramp metering is relatively isolated and the benefits, if any, may come from minimising the disturbance to flow on the motorway caused by platoons of merging vehicles. Little research work has been reported on this topic.

It is also possible that the implementation of ramp metering could affect the operational efficiency at the ramp junction because of the reduced discharge speed of the merging traffic. This may result in

insufficient merging speed and could have an adverse effect on the motorway passing traffic as a result of the interaction. Once again, little research has been done on this issue.

5.3.1 Evaluation Study

A comprehensive observation for a ramp-metering junction has been carried out as part of this research as described in Chapter 2. A before-and-after evaluation has been made for the investigated junction using some indicative measures.

The evaluation study starts with a before-and-after comparison of merging operation at the observed on-ramp junction based on empirical data, and then it is extended to include a wider range of traffic scenarios using computer simulation. The result from empirical evaluation has also been used to check the validity of the result from simulation evaluation for the observed scenarios.

5.3.1.1 Measure of Impact (MOI)

There are several indexes that can be used to measure the quality of traffic operations. The most appropriate one may be the average speed or travel time as this is directly associated with the level of service that a road transport system can provide. Roess et al. has identified that the most significant impact of merging operations is in the merging influence area of about 1500 ft long (457.2m) in lanes 1 and 2 of the motorway as well as the acceleration lane [81]. An influence area has been defined as:

(1) For motorway passing traffic (on the shoulder lane): 200 meter upstream to 450 meter downstream of the merging end.

(2) For merging traffic: metering point to 450 meter downstream of merging end.

The area defined longitudinally covers the merging influence area suggested by Roess et al., and has been extended to include the section upstream of the merging end. This was decided based on the following two considerations:

(1) The motorway passing traffic on the shoulder lane starts to decelerate before arriving at the merging end as has been revealed in Chapter 4, so it is appropriate to include an upstream section in average speed calculation. The passing traffic on lane 2 has not been included in this (local) evaluation because the interaction between merging traffic and passing traffic on lane 2 is indirect.

(2) The merging traffic may be delayed by the ramp metering light, which is mainly decided by metering rate and ramp traffic demand, etc. To compare the local impact on the merging operation, it is more suitable to focus on travel speed after passing the metering point so that the operational effect of ramp metering can be evaluated exclusively.

The standard deviation of passing traffic speed within the selected area was also chosen to be a measure of impact, i.e., an indicator of disturbance introduced by the merging operation. The measures of impact selected in this evaluation are summarised in Table 5.3.

Table 5.3 Measure of Impact of Ramp Metering on Merging Operation

Measure of Impact
Average Speed Improvement of Passing Traffic (DV_p)
Change of Standard Deviation of Speed of Passing Traffic (std V_p)
Average Speed Improvement of Merging Traffic (DV_m)

5.3.1.2 Evaluation Scenarios

The aim of this evaluation study has been to compare the before-and-after operational effect of ramp metering. This can be achieved by comparing measures of impact under certain traffic conditions. The traffic conditions adopted in this evaluation study are shown in Table 5.4. The main variable is traffic volume. A 3-car-per-cycle principle was used to simulate ramp-metering operation, which is the same as used in the Junction 11. Fixed cycle times of 15, 12 and 10 seconds were used at metering rates of 700, 900 and 1100 vph. A 34-second queue override cycle (20 s for green, 2 s for each amber and 10 s for red) was also used when the number of queuing vehicles reached ten. The effect of other variables, such as proportion of HGV, gradient of the roadway etc., can all be converted into the equivalent traffic volume. Overall, there are 24 different combinations.

Table 5.4 Evaluation Scenarios

Metering	On and Off
Merging Traffic Volume (metering rate)	700 – 1100, increment 200 vph
Passing Traffic Volume	600 – 1500, increment 300 vph
Proportion of HGV	Fixed 5%

5.3.1.3 Simulation

The network configuration for this evaluation study is shown in Figure 5.12. Mainline traffic is generated 1000 m upstream the merging end for 'warming up' purpose. Merging traffic is generated 250 m upstream of the merging end. The metering point is 135 m upstream the merging end and the view-point is assumed to be at –130 m. The length of the acceleration lane is 185 meters. The traffic can discharge freely downstream. Traffic volume varies according to the scenarios to be modelled. The measure of impact was calculated by averaging the MOI within the evaluation area. Two simulations are run for each scenario using different seed number, each simulation lasts for 1 hour.

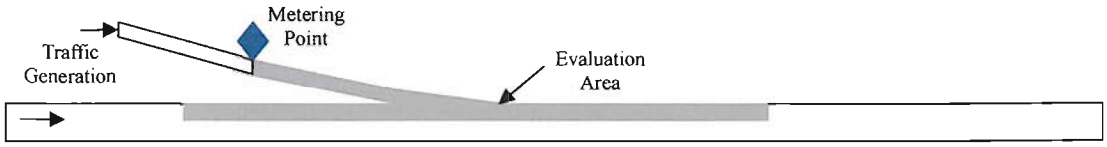

Figure 5.12 Network Configuration of Simulation (not to scale)

5.3.2 Results from Observation

As described in Chapter 2, The observation was based on the taper merge, which is connected with the offside lane of the slip road. The data used for the impact evaluation is from two sources. The first is time-series data based on trials performed using the IV as a probe vehicle. The second is from the loop detectors. The locations of loops are shwon in Figure 5.13.

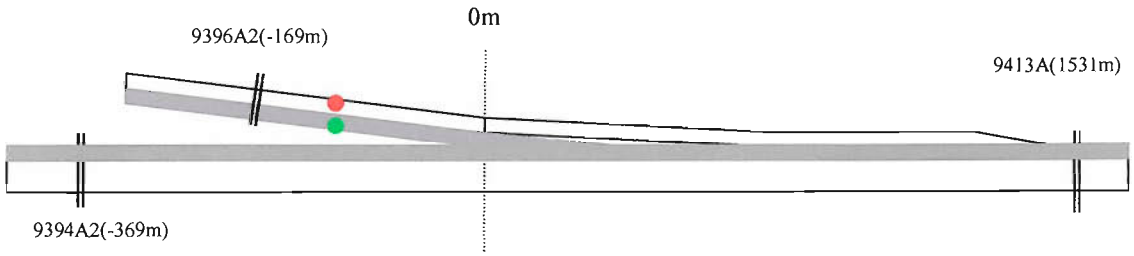

Figure 5.13 Location of Loops

The basic operation of the ramp metering can be outlined using the loop data. The traffic volume (5-minute) at the slip road (loop 9396A2) is shown in Figure 5.14. The entry traffic volume was high but stable. Before 7:30 am, the mainline traffic volume was relatively low (Figure 5.15), so that merging was easy. As a result, the majority of drivers chose to merge from the offside taper merge, the traffic volume on the offside lane of the slip road was significantly higher than that of inside lane. After 7:30 am, the entry traffic volume becomes stable. The average entry traffic volume at the taper merge between 7:30 to 8:45 am was 932 vph (metering off, 16 days) and 911 vph (metering on, 16 days) respectively, based on 32 days of observation. The passing traffic volume on the shoulder lane is shown in Figure 5.15, which was a 5-minute rate based on loop 9394A2. The peak flow volume between 7:40 to 8:30 am varied considerably not only as a result of the variation in traffic demand, but also the bottleneck effect of the recurrent congestion, which limited the the maximum passing traffic volume.

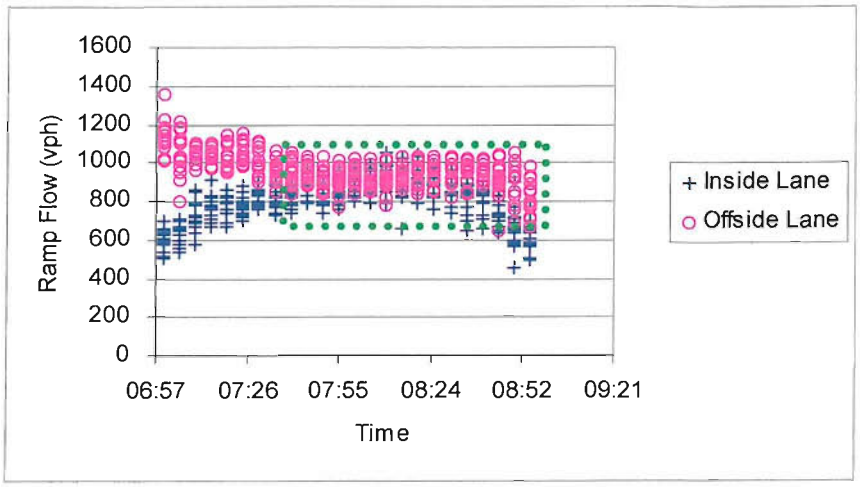

Figure 5.14 Entry Traffic Volume

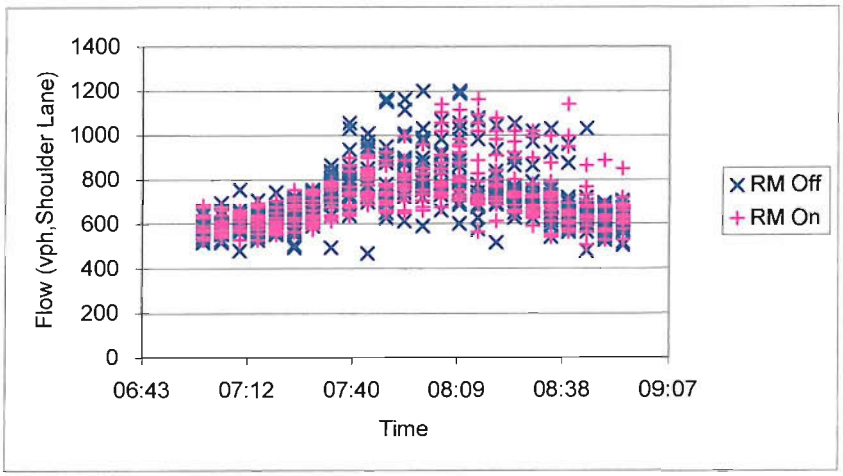

Figure 5.15 Passing Traffic Volume (Shoulder Lane)

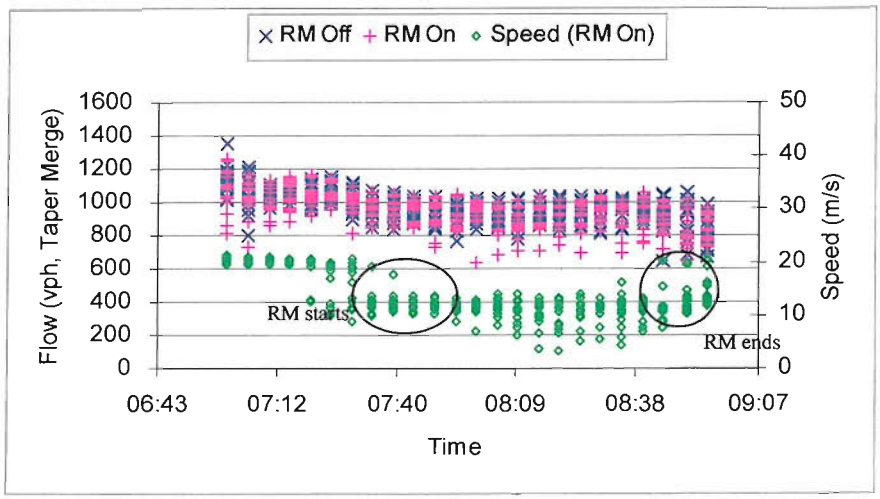

Figure 5.16 Start and End Time of Ramp Metering

The ramp metering implemented at this site was a local traffic responsive one using ALINEA algorithms [72]. A three-car-per-cycle principle (i.e., within each cycle, the duration of the green was sufficient to allow three vehicles per lane to pass) with variable cycle times of 10, 12, 15, 20, 24 and 30 seconds (i.e., metering rate of 1080, 900, 720, 540, 450 and 360 vph) was used. A 34-second queue override cycle (20 s for green, 2 s for each amber and 10 s for red) was triggered when the occupancy at the entrance to the slop road exceeds a preset value in order to release the queue. The metering was set to operate between 7:00 and 9:00 a.m., and was switched on and off during that time using speed and flow thresholds. From Figure 5.16, it can be seen that the start and end time of ramp metering varies from day to day. The earliest time of turning ramp metering on was 7:20 am, while the earliest turning off time was 8:45 am.

The MOI of ramp metering on merging operation was calculated based on trials performed using the IV. Corresponding merging and passing traffic volume was obtained from 5-minutes loop data (9394A2 for passing traffic and 9396A2 for merging traffic) based on the time of IV trials. The outcome is shown in Figure 5.17 and Table 5.5 (The speed illustrated was 5-minute average speed measured by loop 9396A2).

It can be seen from Figure. 5.17 that the average speed of both merging and passing traffic was lower under ramp metering. At the higher passing traffic volume, the speed reduction on the passing traffic was greater. On the other hand, the standard deviation of the speed of the passing traffic was significantly lower with metering-on (1.97 m/s) than that with metering-off (2.41m/s) (Table 5.5).

These results are subject to both the context and the limited number of samples using the IV as a probe vehicle. The volume of merging traffic under metering on and metering off at the observed site were mostly between 800 and 1050 vph, and the average volume only differs by 21 vph between metering off and metering on situations. The results represent a ramp metering application involving little diversion of merging traffic.

Table 5.5 T test of std V_p of Passing Traffic

	RM Off	***RM On***
Mean (m/s)	2.406684	1.967814
Variance (m/s)	1.077232	1.324396
Observations	55	71
t Stat	2.244296	
P(T<=t) one-tail	0.013316	
t Critical one-tail	1.657545	
P(T<=t) two-tail	0.026631	
t Critical two-tail	1.979765	

Overall, it seems that although the passing traffic becomes more stable (with small standard deviation of the speed) under ramp metering, the operational performance (average speed) in the merging influence area is degraded.

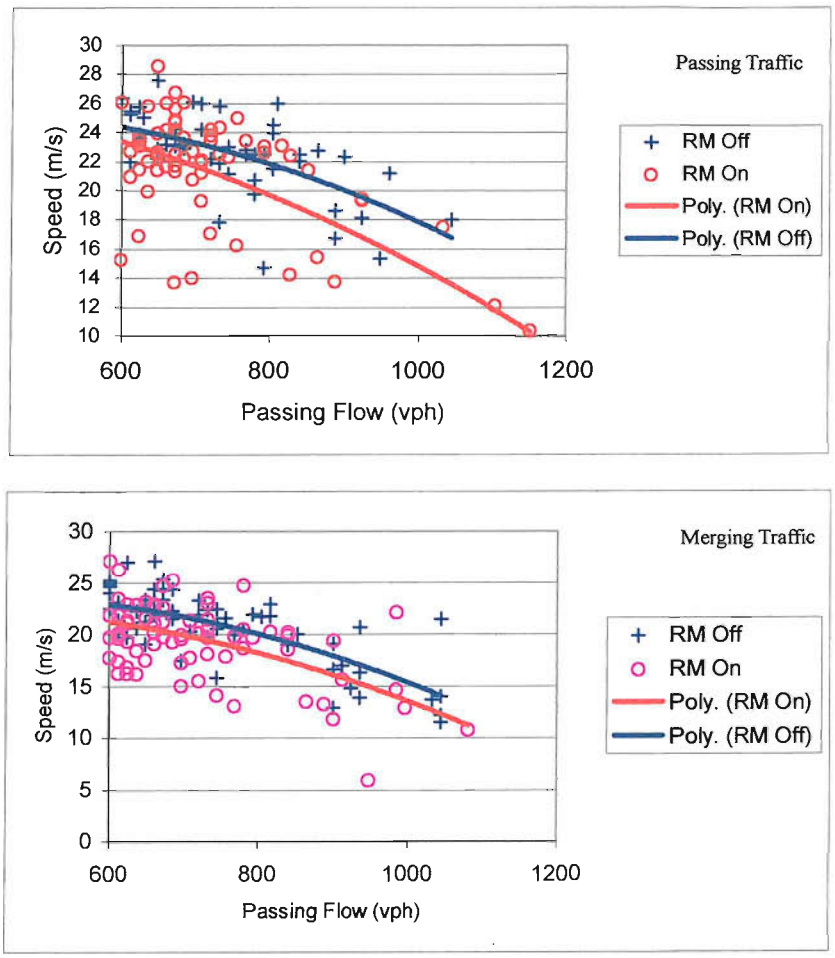

Figure 5.17 Average Speed under Metering-off and Metering-on

5.3.3 Results from Simulation

The predicted speed improvement under ramp metering, which is the difference of the average speed between ramp metering off and ramp metering on is shown in Figure 5.18. Two empirical points were based on the passing traffic volume of 600 and 900 vph, where the corresponding average merging traffic volume was 930 vph. The simulation results at the merging traffic volume of 900 vph agree well with the empirical observation (Empirical results under other traffic scenarios cannot be obtained because of the limitations of the observed traffic operation at the experiment junction and the limited number of probe trials as described in the last section).

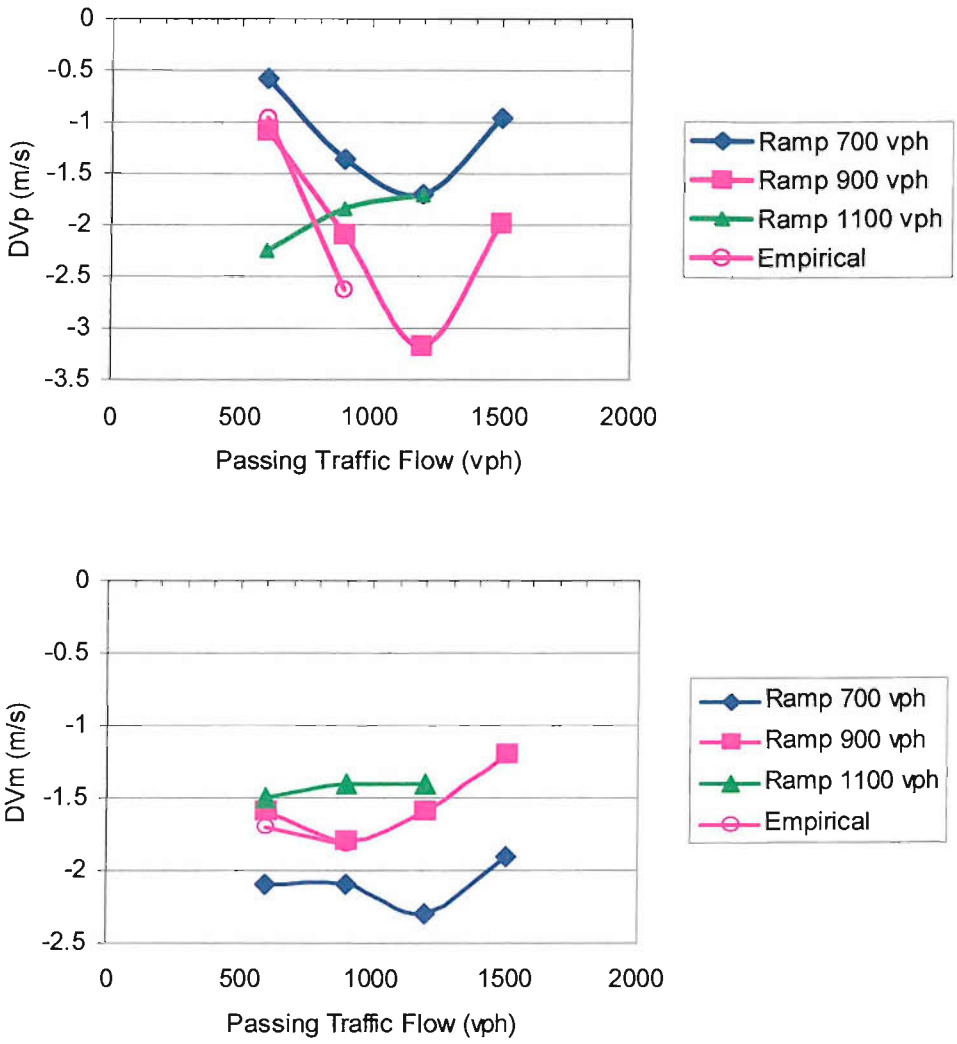

Figure 5.18 MOI of Ramp Metering – Simulation Results

It can be seen that speed changes as a result of ramp metering are consistently negative, that is, the average speed of both merging traffic and passing traffic decreases under ramp metering within the evaluation area. This effect is understandable for the merging traffic, because under ramp metering control, many merging vehicles have to stop at the metering point so that the discharge speed at metering point has been reduced. The result also shows that, at a lower metering rate, the speed reduction of the merging traffic is more significant. This is intuitively reasonable as the red time increases with the decrease of the metering rate, so merging vehicle is more likely to stop at the metering point when the metering rate is low.

The patterns revealed by the speed changes of the passing traffic suggest that at lower merging and passing traffic volumes, the speed reduction is smaller. At either very high merging or passing traffic volumes, speed reductions tend to be smaller. This may be explained by the decrease of interactions between two traffic streams when any traffic is dominant. In addition, the ramp metering will be operated on the queue override algorithm at some cycles when the merging traffic demand is high (at very high merging traffic volume), then traffic operation will be similar between metering-on and metering-off, so the speed reduction as a result of ramp metering could be small.

The speed reduction as a result of ramp metering may have been caused by the reduced discharge speed of merging traffic at the metering point (as shown in Figure 5.16). The behavioural observations indicated that motorway passing traffic could take cooperative action to match the speed of merging traffic when approaching merging area. A reduction in the average speed of the passing traffic can be expected if the speed of the interacting merging traffic has been reduced because of ramp metering. Overall, the implementation of ramp metering does not improve the local efficiency of the merging operation.

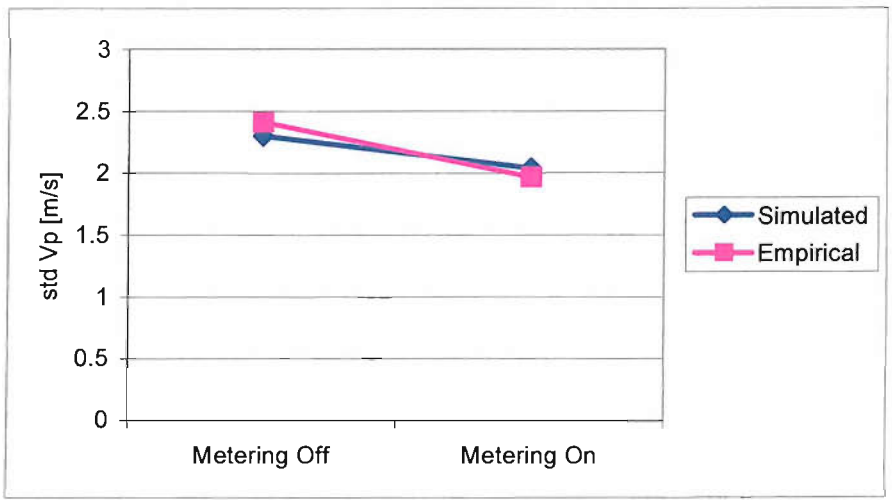

Figure 5.19 Mean Standard Deviation of Passing Traffic Speed

The mean standard deviation of the speed of passing traffic is shown in Figure 5.19. The simulation result is consistent with the empirical observation at this site. The reduction in the variation of the passing traffic speed is evident. As the standard deviation of the speed of passing traffic is a reflection of the speed variations when passing the merging influence area, smaller variations indicate that traffic operation is generally smoother under metering-on. This may partly explain the decrease of the accident rate as a result of ramp metering reported in literatures (e.g. [19] and [70]).

The evaluation has been based on a local merging influence area and the simulation was conducted based on a fixed metering rate for each traffic situation. The effect of control dynamics for a specific ramp metering algorithm under varying traffic demands has not been considered. In addition, both observation and simulation are based on a specific site. For other sites with significantly different geometry and traffic conditions, the effect of ramp metering on the traffic operation could be different. For example, the distance from the metering point to the merging end is relatively short (135 m) at the observed site (so that merging vehicles being stopped at the metering point may unable to achieve a desirable merging speed when reaching the merging end, and the speed reduction as a result of ramp metering may be more significant), and the downhill slope on the ramp and the uphill slope on motorway near merging area may all affect the merging operation. So the result may not be indicative of the general effectiveness of ramp metering, for which, there is already an abundance of evaluation research. The focus here is on analysing operational effect of the ramp metering on the observed local junction to arrive at general results, rather than on either evaluating specific control algorithms or network benefits under specific ramp metering strategies. For site and algorithm specific evaluations, the simulation model and the algorithms need to be configured and validated to specific applications.

The conclusion is that implementation of ramp metering may cause marginal reductions in the average speed on both merging and passing traffic under same traffic conditions at some sites. This implies that ramp metering does not necessarily improve motorway traffic operation in all conditions. However, the finding does not contradict some more favourable conclusions regarding the effectiveness of ramp metering from other studies. By using proper adaptive control tactics, it is possible to improve motorway traffic operation. Zhang et al. has shown that the effectiveness of the ramp metering can be achieved at (and is restricted to) traffic conditions that have the potential to switch between congested and non-congested situations [104].

If the change of the local operational characteristic as a result of ramp metering, as identified in this evaluation, can be taken into account in the ramp metering algorithms, more precise metering tactics (switch time) can be targeted and the benefits of the ramp metering may be further enhanced. For the change of the operational characteristics, additional observations from the upstream and downstream loop data may be made. Figure 5.20 shows the 5-minute flow-speed curve measured by loop 9394A2 on the upstream traffic while Figure 5.21 shows that of loop 9413A on the downstream traffic. The general pattern is much the same as that measured by probe vehicle merging trials or from simulation. The average speed is reduced under ramp metering for the same traffic conditions. However, the downstream traffic condition shows smaller differences between metered and unmetered cases. This can be explained as most ramp metering algorithms are targeted to optimise the downstream traffic condition rather than the upstream one.

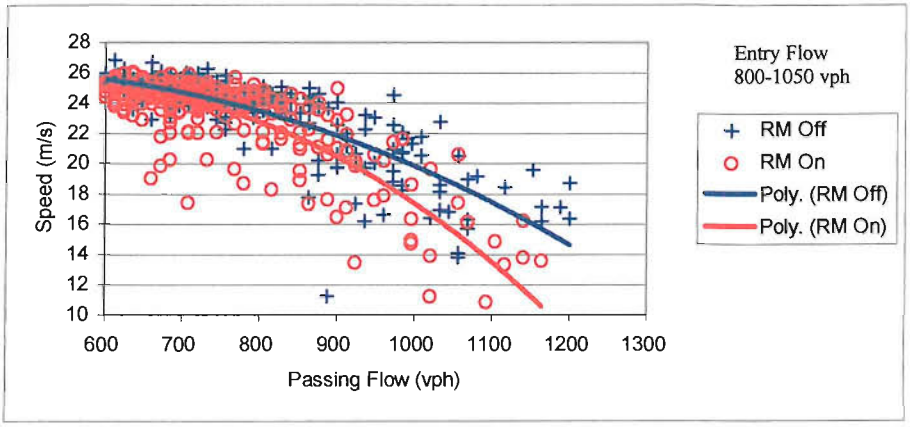

Figure 5.20 Average Speed of Upstream Passing Traffic

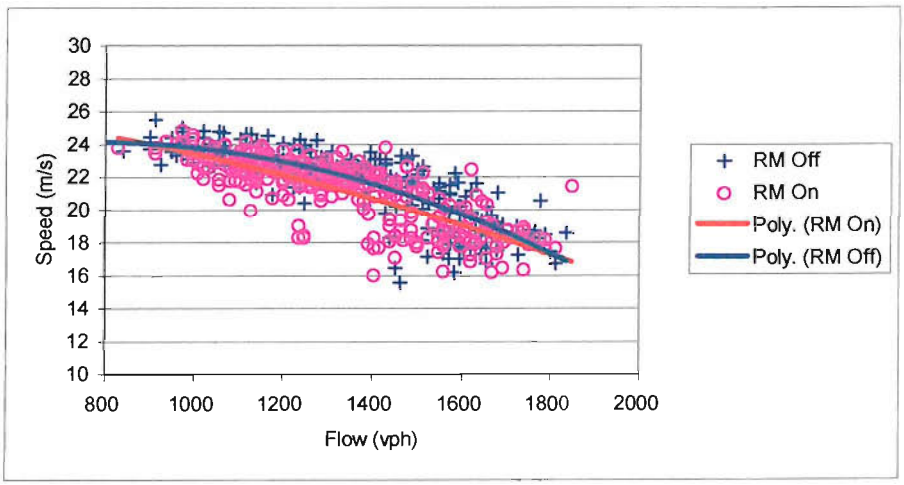

Figure 5.21 Average Speed of Downstream Passing Traffic

Chapter 6 Conclusion

The objective of the research described in this thesis has been to develop a computer simulation model capable of reproducing realistic merging operation at motorway on-ramps. This has been achieved by using several interacting behavioural sub-models, each describing one sub-task of overall motorway driving. Emphasis has been paid to the fundamental study of the dynamic control behaviour of a driver in response to a leader or a gap consisting of two vehicles.

A data-driven approach has been adopted in the development of behavioural models, to ensure that the understanding of behaviour is directly derived from observation. Two types of behaviour have been analysed and modelled. The first is dynamic control behaviour in performing such tasks as follow-the-leader in car following and follow-the-gap in merging situations. They have been modelled as a continuous, compensatory manual control behaviour using fuzzy theory with model parameters estimated from empirical time-series data. The second is discrete choice behaviour in performing such tasks as gap selection and gap acceptance using traffic dependent thresholds. For merging behaviour, the dynamic control and discrete choice are considered as an interacting process so that one of them can influence the other. The performance of the model is satisfactory in terms of prediction error (RMSE) when validated to empirical time-series data.

Compared with most existing models, the merging model developed in this research has the advantage that traffic dynamics in merging operation are modelled explicitly. A merging vehicle will first try to achieve a similar speed with the target gap and position him/herself appropriately relative to the gap through dynamic control, then gap acceptance on the acceleration lane becomes a very natural part over the dynamic control process. This will not result in an unrealistically abrupt merge onto the motorway traffic lane because the merging vehicle has been guided by the gap before accepting it. In addition, the cooperative behaviour of motorway passing vehicles has been modelled explicitly. As a result, unrealistic model behaviour such as an excessive number of vehicles stopping at the end of the acceleration lane and shockwaves caused by the sudden cut-in of a slow merging vehicle etc. (i.e., the drawbacks of models using simple gap acceptance logic) can be generally avoided. The ability of the model to reproduce traffic dynamics is enhanced

The modelling approach of dynamic control behaviour has been first established based on a car following scenario, and then extended to the merging situation where constraints are from both front and rear side. Adaptive neuro-fuzzy system has been used as the main mathematical tool in model development. The model has been established on fuzzy logic, which has the advantage of tolerance for imprecision, uncertainty and partial truth while still being able to achieve tractability and robustness. From the model performance, it can be concluded that fuzzy logic well reflects the human imprecision reasoning process in performing driving tasks, and hence, is suitable to model human behaviour.

A better understanding of driver behaviour in car following and merging scenarios has been achieved through a comprehensive observation and analysis. The car following model shows satisfactory performance. It has been found, as shown in section 4.2, that the majority of speed adjustment and gap selection, as well as the eye-movements, are carried out by the merging driver on the slip road upstream the merging end. This represents the most dynamic interactions between two traffic streams, which has been ignored in most of previous studies. The dynamic merging behaviour model established based on the complete merging process is able to mimic the merging behaviour well.

The model has been successfully implemented in a computer simulation, which can be run as a stand-along program for merging operation related applications. An evaluation of ramp metering on the merging operation shows satisfactory model performance against measured data. By varying traffic condition systematically, the impact of ramp metering on merging operation has been evaluated in terms of speed reduction of motorway traffic. Ramp metering can result in a change in junction operation and cause marginal speed reduction to the interacting traffic streams in the observed site.

Motorway merging is one of the operations where two interacting traffic streams travelling in same direction forms a single stream. Microscopically, this kind of operation all involves a moving vehicle dynamically interacting with a gap on the target lane. The framework established in this research can be applied in a variety of similar situations such as lane-loss, lane-closure and lane changing manoeuvre, as a guide for behavioural analysis or as a prototype for the model development. The more direct and immediate use of this research work may be found in traffic simulation where behavioural representation is still identified as a weak point [8].

2.1 Contributions

This research presents the first comprehensive investigation and modelling work of dynamic merging operation at motorway on-ramps. The dynamic control behaviour of follow-the-leader has also been investigated in depth. The main contributions are as follows:

1. Establishment of the in-depth understanding of merging behaviour through analysis of complete merging process covering slip road and acceleration lane, based on accurate time-series data collected using a combination of camera technology and Instrumented Vehicle.
2. Development of the fuzzy logic car following model taking into account of difference between and within drivers, using data-driven method with anticipatory aspects investigated.
3. Design and development of the microscopic model of merging behaviour incorporating two interacting traffic streams with dynamic control explicitly modelled using fuzzy logic and validated to time-series empirical data.

This thesis establishes a model framework to describe dynamic merging behaviour. The computer simulation model implemented demonstrates satisfactory performance in reproducing dynamic microscopic behaviour, and hence can work robustly in large scale traffic simulation models.

2.2 Directions for Future Work

Several improvements are possible in collecting and reducing empirical data. As discussed in section 2.2, time-series data derived from camera recordings suffers from low sampling rates with limited accuracy and requiring tremendous efforts in data reduction. An alternative method is to upgrade the IV Radar with a wide horizontal field of view (HFoV) where geometric conditions do not cause additional constraints (e.g., obstruction of the field of view). This will relieve the need for camera data where targets are lost. Even in partly obscured geometric configurations, use of range sensor with a wide HFoV could reduce the number of cameras needed. Recently, a laser Radar has been installed on the IV at TRG, which has a maximum HFoV of 270^0. In addition, the accuracy of speed measurement can be increased by using more advanced speed sensors. One promising system is VBox that makes use of Doppler shift measurement on GPS carrier phase, and is able to measure the ground speed at an accuracy of 0.1 km/h [108].

It has not been possible to look at the difference within and between drivers and their distribution through a prolonged observation in this study. This additional knowledge may be accomplished through follow-up projects using more advanced data collection methods.

The gap selection logic identified in this research is very simple, as the observed gap change rate is very low on the acceleration lane at the selected experiment site. It will be desirable to further look at the behaviour at different site with different geometric configurations.

It has been shown that the performance of the merging behaviour model is satisfactory under most situations when validated to time-series data. But in certain circumstances, the gap selection is difficult to predict when a merging vehicle is very close to either a gap leader or a gap follower so that two gaps could both be the target gap. The problem may be remedied by considering two consecutive gaps in the gap selection logic and dynamic control model of the merging vehicle. However, this will significantly complicate the model and requires higher computational resource if implemented in simulation. Alternatively, a new gap selection logic could be developed to help choose one gap from two consecutive gaps based on certain attributes. However, only marginal improvement can be expected as the occasions with difficult gap selection appear to be small in number.

Within the computer simulation model of merging operation, several components (e.g., lane-changing model) are taken from other studies. The performance of a simulation model is not only decided by the quality of the behavioural models themselves but the compatibility with different models. It is possible that a lane changing decision made by the lane-changing model creates a situation that is impossible for the car following model to handle, e.g., a slow and close cut-in in front of a fast vehicle. Further research is required to investigate the compatibility between different behavioural models.

The merging operation can be generalised to a variety of traffic operations involving a forced lane changing caused by the termination of a lane, e.g. lane closure because of road-work, lane-loss etc either on motorway or urban road where a capacity critical situation is likely. The traffic dynamics will be extremely important near capacity as disturbance resulting from frequent interactions between competing traffic streams cannot be easily absorbed. This may lead to flow breakdown. If traffic simulation is to be used as a tool in managing these near capacity situations, a dynamic model developed based on detailed empirical data will certainly be an advantage. The research in this direction is likely to be extended to urban road situations in the near future.

With increasing concerns on the traffic congestion, there is a strong interest in evaluation and control of merge-related operations and the associate computer simulation technology. Through the pilot scheme of ramp metering in Southampton, advanced access control has been introduced into motorway operation in UK. It is quite likely that behavioural modelling and computer simulation application in merging-related operations will be further intensified in the near future.

Appendix A: IV Measurement Error

A.1 Accuracy of Direct Measurements and Derivatives

The IV sensor outputs contain measurement errors. For the two direct measurements, IV speed measured by Laser Speedometer and range to leading or following targets measured by Radar, their measurement error can be assumed to be normally distributed (N) with a mean measurement error of zero (Gaussian White Noise).

Let ε_v and ε_r be the random measurement error of speed and range respectively,

$$\varepsilon_v \sim N(0,\sigma_v) \quad \textbf{(A.1)}$$

$$\varepsilon_r \sim N(0,\sigma_r) \quad \textbf{(A.2)}$$

The error of the acceleration rate of IV calculated from speed measurement ($a=dv/dt$, sampling rate 10 HZ) will be ten times of the convolution of the speed measurement error:

$$\varepsilon_a \sim N(0,10*\sqrt{\sigma_v^{\,2}+\sigma_v^{\,2}}) \quad \textbf{(A.3)}$$

Accordingly, the error of calculated range rate and speed of leading vehicle (the same for the following vehicle) will be:

$$\varepsilon_{dr} \sim N(0,10*\sqrt{\sigma_r^{\,2}+\sigma_r^{\,2}}) \quad \textbf{(A.4)}$$

$$\varepsilon_{lv} \sim N(0,\sqrt{\sigma_v^{\,2}+\sigma_{dr}^{\,2}}) \quad \textbf{(A.5)}$$

where σ_{dr} is standard deviation of calculated range rate error ($dr=d(range)/dt$), ε_{lv} is the error in speed of leading vehicle ($lv=v+dr$).

Based on equipment manufacturer's specification (95% probability, $\pm 2\sigma$), the accuracy of raw measurements and theoretical accuracy of the direct derivatives calculated using equation (A.3-5) have been summarised in Table A.1.

Table A.1 Theoretical Accuracy

Item	Accuracy (2* σ)
Speed (v)	0.278 m/s
Range (r)	0.2 m (at 100 m)
Range Rate (dr)	2.83 m/s
Acceleration (a)	3.93 m/s^2
Speed of Leading Vehicle (lv)	2.84 m/s

A.2 Accuracy of the Processed Data

It has been shown in the theoretical analysis that the accuracy of derivatives is very large compared with the raw measurements. The data was further processed using a low pass filter to exclude the high frequency components.

The accuracy of the processed data is mainly determined by the cutoff frequency of the filter used in data smoothing. If only the white noise in raw measurement is concerned, using lower cutoff frequency will exclude more noisy components as the white noise is distributed in the whole spectrum. However, the human response that is higher than cutoff frequency will also be excluded, which will cause deformation on the measured time-series. The cutoff frequency in data smoothing has been chosen to be 0.5 Hz based on spectrum analysis of human response, which is much higher than typical human response frequency in everyday driving (about 0.05 Hz). Figure A.1 shows the error introduced in the smoothing process (cutoff frequency 0.5Hz) as a function of the base frequency of the sinusoid signal to be filtered. It can be observed that for the 0.05 Hz sinusoid signal, the error introduced in the data smoothing process is ignorable.

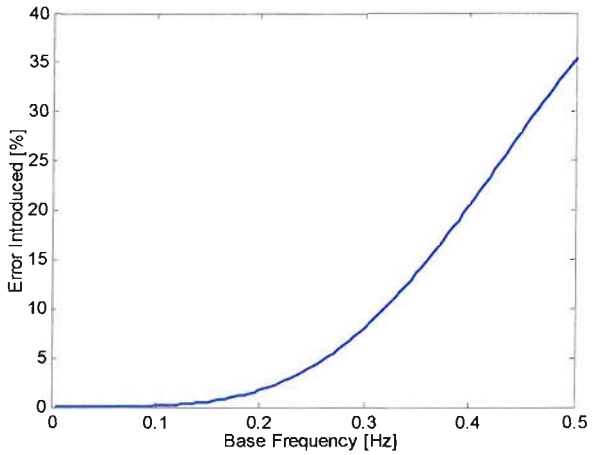

Figure A.1 Error Introduced in Data Smoothing Process

The accuracy of the processed data using the proposed method (low passing filter at 0.5 Hz) was analysed using simulation. Two 3000-point 0.05 Hz sinusoid signals (300 seconds) were generated to represent accurate speed (v [m/s] =15+5sinωt) and range (r [m] =25+10sinωt) respectively. The measured speed and range were generated by adding white noises with the amplitude specified in Table A.1 (ε_v, ε_r). Other derivatives, such as acceleration, range rate etc, were then generated from the noised range and speed data. The noise speed and range, together with other derivatives calculated from them, were then processed using data smoothing procedure. By comparing the processed data with the accurate one, the remaining error distribution in the processed data can be examined.

There is two-way to process derivatives such as acceleration rate, range rate:

- Calculate derivatives from direct measurements, then smooth.
- Calculate derivatives from smoothed direct measurements, then smooth again (optional).

It can be shown except for some boundary points, derivatives calculated from smoothed measurement is the same as the smoothed derivatives calculated from direct measurement. Supposing *x(k)* is the direct measured time-series, *y(k)* is the smoothed time-series. The z-transform Y(z) of the digital filter's output *y(k)* is related to the z-transform X(z) of the input *x(k)* by

$$Y(z) = H(z)X(z) = \frac{b_1 + b_2 z^{-1} + ... + b_{n+1} z^{-n}}{a_1 + a_2 z^{-1} + ... + a_{m+1} z^{-m}} X(z) \qquad \textbf{(A.6)}$$

where H(z) is the filter's transfer function. The constants *b(i)* and *a(i)* are the filter coefficients and the order of the filter is the maximum of *n* and *m*. The difference equation form of the z-transform relation shown in equation (A.6) is:

$$y(k) = b_1 x(k) + b_2 x(k-1) + ... + b_{n+1} x(k-n) - a_2 y(k-1) - ... - a_{m+1} y(k-n) \qquad \textbf{(A.7)}$$

Let *dy(k) = y(k+1) - y(k), dx(k) = x(k+1) - x(k),* it can be observed that:

$$\begin{aligned} y(k+1) - y(k) &= b_1(x(k+1) - x(k) + b_2(x(k) - x(k-1)) + ... + b_{n+1}(x(k-n+1)x(k-n)) \\ &\quad - a_2(y(k) - y(k-1)) - ... - a_{m+1}(y(k-n+1) - y(k-n)) \\ &= b_1 dx(k) + b_2 dx(k-1) + ... + b_{n+1} dx(k-n) - a_2 dy(k-1) - ... - a_{m+1} dy(k-n) = dy(k) \end{aligned}$$

That is, $DY(z) = H(z)DX(z)$.

The boundary points (k<order or k>N-order) were different based on two procedures. For example, if the derivative was calculated before applying smoothing procedure, the *dy(1)* would be:

$$dy(1) = b_1 dx(1) = b_1(x(2) - x(1))$$

While the calculated derivative from smoothed x(k) was:

$$dy(1) = y(2) - y(1) = b_1(x(2) - x(1)) + b_2 x(1) - a_2 b_1 x(1)$$

In this research, the derivatives were calculated from the smoothed measurements. This was because very large error existed in the time derivatives calculated from direct measurement (each time derivative calculation amplified the error more than ten times for data sampled at 10 Hz). The data smoothing process could not effectively reduce the error at boundary points, so that very large error still existed in the smoothed derivatives that were calculated from direct measurement. On the other hand, by first applying smoothing process on the direct measured data, the accuracy of the data used for derivative calculation would be significantly improved. As a result, the accuracy of the derived data at the boundary points could be improved.

The accuracy of the processed data based on simulation is summarised in Table A.2. The distribution of the remaining error is shown in Figure A.2-6. It can be observed that the accuracy ($2*\sigma$) of the derivatives calculated from direct measurement is identical with that obtained in theoretical analysis. In all cases, the accuracy of the processed data has been greatly improved.

The real-world human response may contain higher frequency components than assumed in this analysis. However, from Figure A.1, it is evident that the data smoothing procedure will not introduce significant error into signals with a frequency lower than 0.1 Hz. For the empirical measured time-series containing higher frequency components, the cutoff frequency of the filter should be increased accordingly.

Table A.2 Accuracy of the Processed Data

Measured	Items	Raw	After Smooth	
	Speed [m/s]	0.278	**0.08**	
	Range [m]	0.2	**0.06**	
Derived	Items	Calculated From Raw Measurement	Calculated From Smoothed Data	After Smooth
	Acceleration [m/s^2]	3.9	0.16	**0.12**
	Range Rate [m/s]	2.8	0.11	**0.08**
	Leading Vehicle Speed [m/s]	2.9	0.13	**0.11**

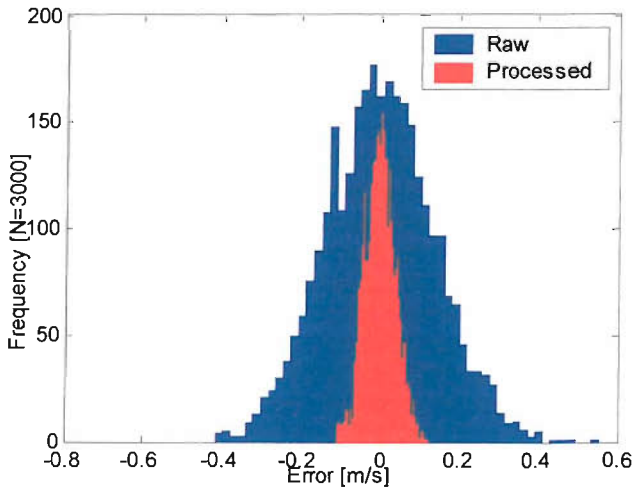

Figure A.2 Distribution of Speed Error

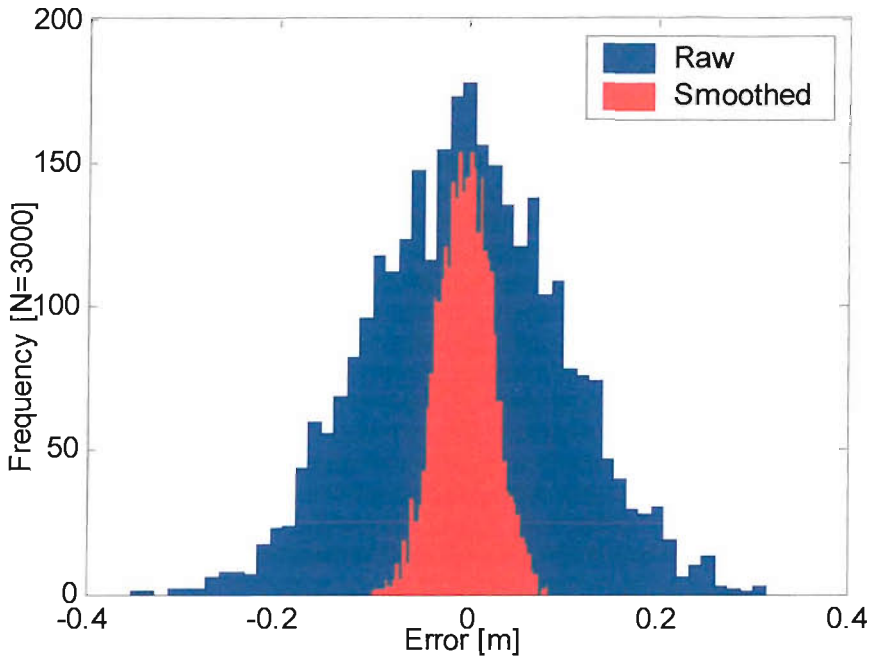

Figure A.3 Distribution of Range Error

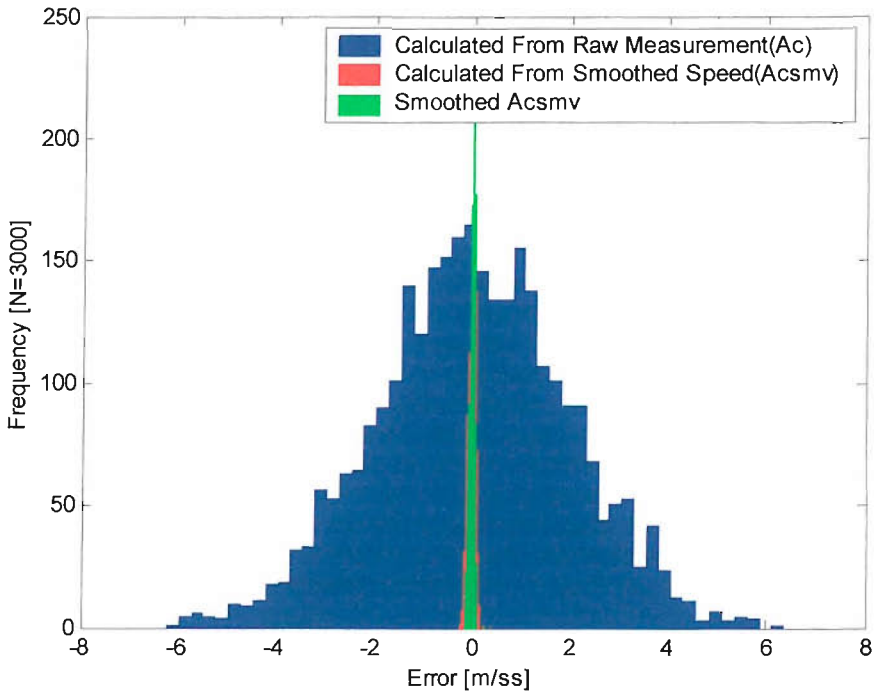

Figure A.4 Distribution of Acceleration Rate Error

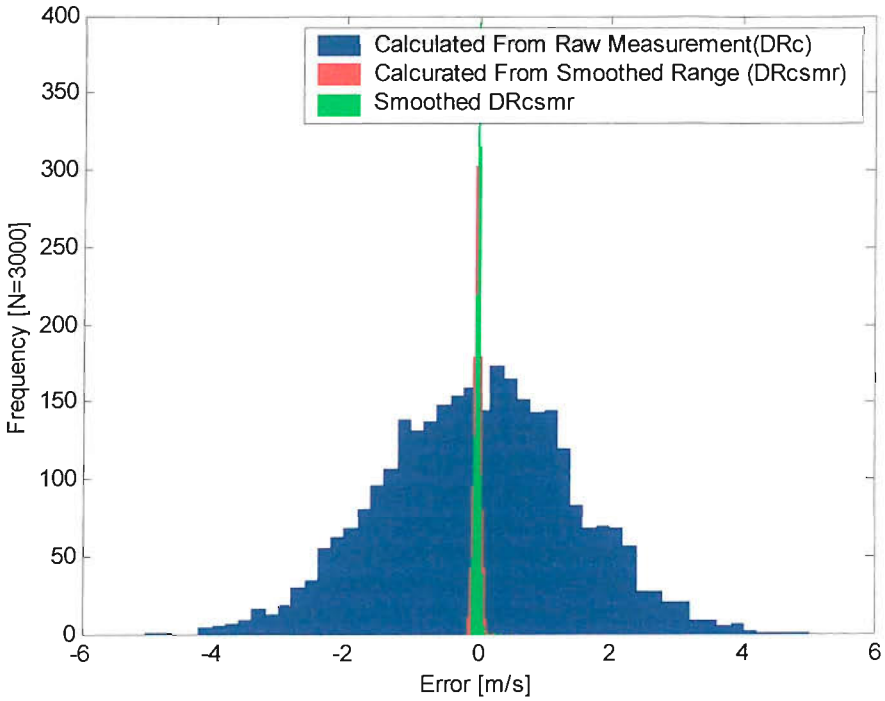

Figure A.5 Distribution of Range Rate Error

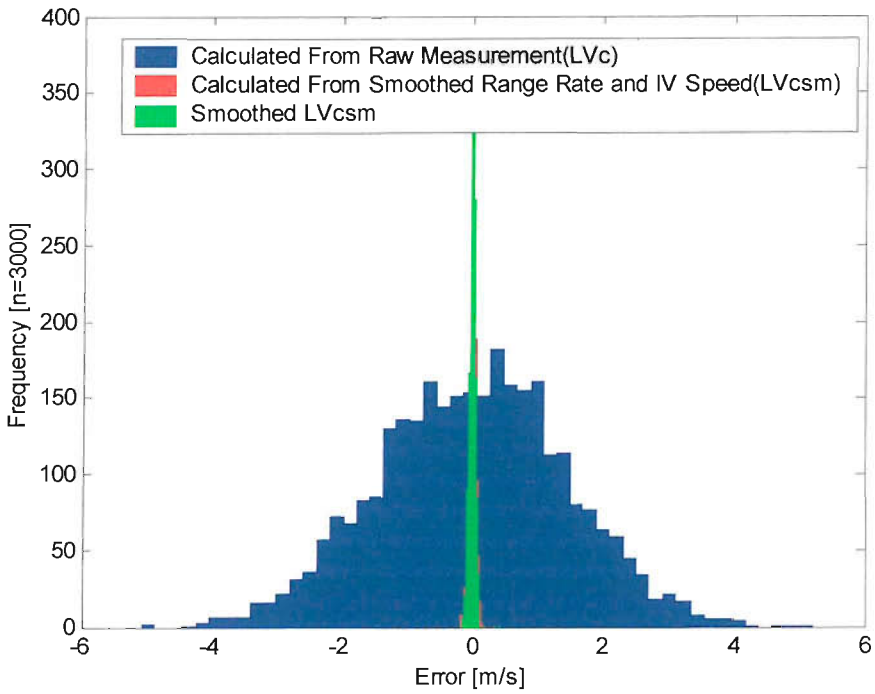

Figure A.6 Distribution of Leading Vehicle Speed Error

Appendix B: Stability Analysis

B.1 Stability of Classic Car-Following Model

Stability analysis of classic car-following model can be reduced to the problem of evaluation of properties of solutions to the equivalent differential equation with time delay. For the linear GM model, with an equivalent differential equation:

$$x''_{n+1}(t) = \lambda(x'_n(t-\tau) - x'_{n+1}(t-\tau)) \quad \textbf{(B.1)}$$

where x_n, x_{n+1} $(n=1,\ldots, N)$ represent the position of leading and following vehicle, ' denotes time derivatives, λ is coefficient and τ is time delay.

The stability of steady-state has been found to be:

$\lambda\tau > \pi/2$, the solution is oscillatory with increasing amplitude

$\lambda\tau = \pi/2$, the solution is oscillatory with constant amplitude

$\lambda\tau < \pi/2$, the solution is oscillatory with damped amplitude;

$\lambda\tau <= 1/e$, the solution is non-oscillatory and damped

$\lambda\tau < 1/2$, the oscillation in solution alone a line of vehicles is damped (refer to [18], [35]).

The physical meaning of this stability criteria is that fluctuation in acceleration (the same for velocity and spacing) introduced into a platoon of vehicles will be settled down to steady state in different manners or amplified alone the vehicles. For a two-vehicle platoon, speed fluctuation will be settled down if $\lambda\tau < \pi/2$, and for an arbitrary length of platoon, it should be $\lambda\tau < 1/2$.

The stability criteria for non-linear form of GM model (reciprocal space model), with a governing equation,

$$x''_{n+1}(t) = \frac{\alpha(x'_{n+1}(t))}{(x_n(t-\tau) - x_{n+1}(t-\tau))}(x'_n(t-\tau) - x'_{n+1}(t-\tau)) \quad \textbf{(B.2)}$$

was derived through linearisation around the equilibrium point by considering $\lambda'\tau$,

$$\lambda' = \frac{\alpha(x'_{n+1}(t))}{(x_n(t) - x_{n+1}(t))} | equilibrium \quad \textbf{(B.3)}$$

then the stability analysis was the same as for the linear model (refer to [38], [105]).

The analysis of stability for car following model has been further extended to non-autonomous situation for linear model. Zhang et al evaluated stability of a platoon by considering an oscillation forcing term in leading vehicle:

$x_1(t)=Fsin(\rho t-\varphi_1)$, ρ is the angular frequency, and φ_1 the initial phase.

The explicit condition for the stability over cars was obtained as:

$\lambda_i\tau_i < [\rho\tau_i/2\sin(\rho\tau_i)]$, if $|\rho\tau_i|<2.3138$,

$\lambda_i\tau_i < \pi/2$, if $|\rho\tau_i|>2.3138$,

for i=2, 3, …,N.

It was shown that low frequency oscillations in the forcing term were more dangerous [105].

If physical constraints, such as nonnegative velocity and bounded spacing (on one side by collision and on other non-car-following situation) was considered, then the stability condition would depend on initial condition of headway and relative speed etc. between vehicles. Though it is possible to consider the physical constraints in the stability analysis of linear model by solving the differential equation explicitly, the conclusions reached will be not generic.

B.2 Stability of Fuzzy Logic Car Following Model

In proposed fuzzy logic car following model:

$$x''_{n+1}(t) = FUZZY(DV, DSSD)_n \quad \textbf{(B.4)}$$

Two input variables are relative speed (*DV*) and headway divergence (*DSSD*).

$$DSSD = (x_n(t-T_d)-x_{n+1}(t-T_d))/(SD_{n+1}) \quad \textbf{(B.5)}$$

where,' represents time derivative, *SD* is the desired headway, T_d is time delay.

The fuzzy mapping expressed as the fuzzy inference system is time independent, the output will be decided only on the input values, which is equivalent to one specific conventional linear system at any point. Malki, et al revealed that a fuzzy inference system:

$$o(t)=FUZZY[e'(t), e(t)] \quad \textbf{(B.6)}$$

which take e(t) and e'(t) as input, and o(t) as output had the same simple linear structure as that expressed in PD control law:

$$o(t)=c_1*e'(t)+c_2*e(t) \quad \textbf{(B.7)}$$

except that the two gains (c_1 and c_2) were no longer constant [58]. More generally, Thathachar et al. had proven the equivalence of stability properties of fuzzy systems and linear time invariant switching system [94]. Therefore, stability of fuzzy logic car following model can be discussed around any steady-state in a traditional way by examining equivalent linealised gain (c_1 and c_2) of fuzzy inference system.

The fuzzy logic car following model had the same linear structure as:

$$x''_{n+1}(t) = c_1(x'_n(t-T_d) - x'_{n+1}(t-T_d)) + c_2\left(\frac{x_n(t-T_d) - x_{n+1}(t-T_d)}{SD}\right) \quad \textbf{(B.8)}$$

Noticing that c_2/SD is constant in the stability calculation, it can be replaced with c_2'.

Though proper transformation,

$t=T_d*\tau$,

$\beta_1=c_1*Td$

$\beta_2=c'_2*Td$

equation (B.8) can be converted into:

$$x''_{n+1}(\tau)=\beta_1((x_n'(\tau-1)-x_{n+1}'(\tau-1))+\beta_2((x_n(\tau-1)-x_{n+1}(\tau-1)) \quad \textbf{(B.9)}$$

Through Laplace-Transform of (B.9), obtain:

$$X_{n+1}(s)=[(s\beta_1+\beta_2)/(e^s s^2+\beta_1 s+\beta_2)]X_n(s) \quad \textbf{(B.10)}$$

where $X(s)=L(x(t))$.

Empirical fitting results has revealed that $\beta_2<<\beta_1$, (e.g., [18], this research), by assuming $\beta_2=0$, equation (B.10) can be reduced to:

$$X_{n+1}(s)=[\beta_1/(e^s s+\beta_1)]X_n(s) \quad \textbf{(B.11)}$$

Follow the Herman's way [35], it can be observed that local stability criteria is the same as in classic linear car following model when fluctuation of acceleration, velocity or position is considered, that is:

(1) $\beta_1> \pi/2$, the solution is oscillatory with increasing amplitude

(2) $\beta_1= \pi/2$, the solution is oscillatory with constant amplitude

(3) $\beta_1< \pi/2$, the solution is oscillatory with damped amplitude;

(4) $\beta_1<= 1/e$, the solution is non-oscillatory and damped

where $\beta_1=c_1*T_d$.

If β_2 is considered explicitly, the analytical analysis of equation (B.10) will be not possible. However, it is clear that the effect of headway control term is insignificant as $\beta_2 << \beta_1$. Therefore, the conclusion obtained without considering headway control term should be reasonably representative.

It can be concluded that the local stability of proposed fuzzy car-following model could be analysed by examining the product of time delay and equivalent gain of fuzzy inference system round the steady state. The later is solely determined by the structure of fuzzy logic inference system and its parameters.

Theoretical analysis of the asymptotic stability or stability under non-autonomous condition is not possible for non-linear fuzzy logic car following model. However, fitting result shows that c_1 is nearly constant in the fuzzy input domain near steady state. The fuzzy logic model can be approximated with a linear model in asymptotic stability analysis with $\beta'_1=c'_1*Td$, c'_1 is the linealised speed gain of fuzzy model.

The asymptotic stability of a platoon of N vehicles can be considered under $\beta_2=0$,

$$sX_{n+1}(s)=s[(\beta'_1)^{(n)}/(e^{s}s+\beta'_1)^{(n)}]X_1(s) \qquad \textbf{(B.12)}$$

n=1,2, ..., N,

The same approaches of stability analysis by Chandler or Zhang can be applied ([18], [105]), which leads to the approximate asymptotic stability criteria of:

$\beta'_1< 1/2$.

Appendix C: Source Code

The source codes of some important sub-routines were listed below. Sub-routines have been chosen based on their relationship with the merging behavioural models. The purpose for doing so was to facilitate implementation of the behavioural models developed in this research in other simulation package. Other common implementations, such as car following behaviour model implementation, network representation, manipulation of the vehicle references etc. may vary in different simulation packages, were not included.

C.1 Model Initialisation

The initialisation of fuzzy logic models was implemented in the constructor for the MmsimCore class (core algorithms). A fisReader class have been implemented, through which fuzzy logic model file could be directly read into the memory to initialise the fuzzy inference system object. The fuzzy logic model file is compatible with the '.fis' file format defined in Matlab, so any fuzzy logic model developed in Matlab can be directly used in this simulation program.

```
public MmsimCore()
{
        ……
        /********* initialising fuzzy logic model*/
        // normalised fuzzy logic car following model
        fisCfModel= fisReader.readFisFile("...dvdssdnor.fis");
        //other fuzzy logic model, lane changing model; merging model
        fisLcOModel= fisReader.readFisFile("...LCoff.fis");
        fisLclModel= fisReader.readFisFile("...LCin.fis");
        fisMgModel= fisReader.readFisFile("...mgmd.fis");
        fisPsModel= fisReader.readFisFile("...psmd.fis");
        ……
}
```

C.2 Simulation Step

The manipulation performed in each simulation step corresponding to the flow diagram in Figure 5.8 was listed here. A two-step procedure was implemented to progress driver-vehicle system within the network, i.e., calculation and then move. So updating of the state of the driver-vehicle system was performed in the 'move' method. For the merging behaviour, the gap acceptance behaviour was implemented in the latitudinal movement step method and follow-the-gap behaviour was implemented in the longitudinal movement step.

```
private void simStepForward()
{
        if (bPause) // paused
                return;
        genDVS(); //traffic generation
        lcCalOneStep(); //latitudinal movement calculation
        lcMoveOneStep(); // latitudinal movement and updating
        cfCalOneStep(); //longitudinal movement calculation
        cfMoveOneStep(); //longitudinal movement, detector counting and updating
}
```

C.3 Merging Behaviour Related Implementation

The merging behaviour related implementation is shown as follows. For easy understanding of the model parameters, some scalars were used to describe model parameters, which were variable names in the program. Also a few lines of conditional code, long notes and debugging code were omitted for easier reading.

```
/*****************************************
 * Gap Acceptance
 * ***********************************/
private void gapAcpCalOneStep(DVS vh, absLane lane, float mgend, float len)
{
        if ((vh.x<mgend)||(vh.x<=vh.fMgPos*len+mgend))//has not passed the merging end
        return;
                assignGapLF(vh,lane);
                float xl,xf,vl,vf;
                if (null==vh.offgapIder)
                {
                        xl=MAXSEP+vh.x;
                        vl=vh.v;
                }
                else
                {
                        xl=vh.offgapIder.x;
                        vl=vh.offgapIder.v;
                }
                if (null==vh.offgapflwer)
                {
                        xf=vh.x-MAXSEP;
                        vf=vh.v;
                }
                else
                {
                        xf=vh.offgapflwer.x;
                        vf=vh.offgapflwer.v;
                }
                float ldv=vl-vh.v;
                float ldx=xl-vh.x-carLen(vh.offgapIder);
                float fdv=vh.v-vf;
                float fdx=vh.x-xf-vh.fCarLen;

                if (ldx<=MINSEP||fdx<=MINSEP) //too close
```

```
                return;

        if (vh.v<=SLOWV)//the vh is slow
        {
                if (fdx/(vf+0.1)<STOPTH)
                        return;
                else
                {
                        vh.fMgScore=1;
                        return;
                }
        }
        else//vh is fast
        {
                if (ldv<0) //the leader is slower
                {
                        float lgc=(float)(6.7553*Math.exp(-0.2684*ldv));
                        if (vh.x>mgend+DISTRD*len) //later merging Trds decrease
                                lgc=lgc*0.8f;
                        if (lgc>ldx)
                        return;
                }
                if (fdv<0) //the follower is faster
                {
                        float rgc=(float)(5.3472*Math.exp(-0.5104*fdv));
                        if (vh.x>mgend+DISTRE*len)
                                rgc=rgc*0.8f;
                        if (rgc>fdx)
                        return;
                }
                float gc=(float)(4.253*Math.exp(0.0968*vh.v));//gap size threshold
                if (vh.x>mgend+DISTRE*len)
                        gc=gc*0.8f;
                if (gc>xl-xf)
                        return;
                vh.fMgScore=1;
        }
}
```

```
/*****************************************
* Passing Vehicle Control
* ***********************************/
private void psOneStep(DVS vh, absLane lane, float viewpos, float accend)
{
        if ((vh.x<=viewpos)||(vh.x>accend))//not in merging influence area
                cfCalOneStep(vh,lane);
        else
        {
                DVS rampId=lane.vlist.findInGapL(vh);
                DVS mld=vh.getLeader();
                if (null==rampId)
                        cfCalOneStep(vh,lane);
                else
                {
                        if (null==mld)// both rampleder and motorway leader is absent
                        {
                                cfCalOneStep(vh,lane); //follow the leader
                        }
                        else
                        {
                                if ((rampId.x>=mld.x)||(rampId.x-vh.x<=DISTTHD))//ramp
                                leader is in front
                                        cfCalOneStep(vh,lane);
                                else// using passing model here
                                {
                                        float ttcr,ttcm;
                                        ttcr=(rampId.v-vh.v)/(rampId.x-vh.x);
                                        ttcm=(mld.v-vh.v)/(mld.x-vh.x);
                                        if (rampId.x-vh.x-
                                        rampId.fCarLen<0.8f*(vh.fDsrTh*vh.v+MINSEP))
                                        vh.newacc=fisCfModel.fisComputer(rampId.v-
                                        vh.v,(rampId.x-
                                        vh.xc)/(vh.fDsrTh*vh.v+MINSEP));
                                        else
                                        vh.newacc=fisPsModel.fisComputer(ttcr,ttcm);
                                }
                        }
                }
        }
}
```

```
/*****************************************
* Merging Vehicle Control
* ************************************/
private void mgOneStep(DVS vh, absLane lane,float viewpos, float accend)
{
        /**********************************
         * initialising the ramp vehicle
         *********************************/
        DVS ld=vh.getLeader();
        if (vh.carWaiting)//the car is waiting, need to start
        {
                if (null==ld) //there is no leader
                {
                        //start without a leader
                        vh.carWaiting=false;
                        vh.v=(float)rand.getNextNorm(vh);//parameter can be changed
                }
                else //there is a leader
                {
                        if (ld.carWaiting)//the leading car is also waiting
                                return;//can not start
                        else
                        {
                                if (vh.x+ld.v*vh.fDsrTh*0.8f+MINSEP>ld.x)//leading car is
                                too close
                                        return;//can not start
                                else
                                {
                                        //start with a leader
                                        vh.carWaiting=false;
                                        if (ld.x>=vh.x+MAXSEP)
                                                vh.v=(float)rand.getNextNorm(vh);
                                        else
                                        {
                                                vh.v=ld.v+(ld.x-vh.x-
                                                ld.fCarLen)*SHGAIN;//speed equal to
                                                the leader
                                                float
                                                sspeed=(float)rand.getNextNorm(vh);
                                                if (vh.v>sspeed)
                                                        vh.v=sspeed;
                                                if (vh.v<0)
                                                        vh.v=0;
```

```
                                        }
                                    }
                                }
                        }
                        for (int i=0; i<vh.dVBuffer.length;i++)
                        {
                                vh.dVBuffer[i]=vh.v;
                                vh.dXBuffer[i]=-i*vh.v*clock.getSimStep();
                                vh.dABuffer[i]=0;
                        }
                }
                /*******************
                 * Calculating one step
                 *******************/
                // three sections, 1:before control, 2: before viewpos; 3: before acc end
                if (bRCOn)//ramp metering is on
                {
                        if (vh.x<=fRCPos && vh.x>fRCPos-ANTICIDIST)//still not passing the
                        metering line
                        {
                                if (null==ld || ld.x>fRCPos)
                                {
                                        if (iRCLight==IntGeneral.REDPHASE)
                                        {
                                                if (vh.x==fRCPos)
                                                        vh.newacc=0;
                                                else
                                                {
                                                        if (vh.v<=VTHD)//slow vehicle
                                                                vh.newacc=NORMACC;
                                                        else
                                                                vh.newacc=-
                                                                vh.v*vh.v/2/(fRCPos-vh.x);
                                                }
                                                return;
                                        }
                                        else
                                        {
                                                if (vh.x>=fRCPos-vh.v* fTimeGo)
                                                {
                                                        vh.newacc=maxACC(vh.v,vh.iDVSType);
                                                        return;
                                                }
                                                else
```

```
                                        {
                                                if (vh.v<=VTHD)
                                                        vh.newacc=NORMACC;
                                                else
                                                vh.newacc=-vh.v*vh.v/2/(fRCPos-vh.x);
                                                return;
                                        }
                                }
                        }
                }
        }

        if ((!vh.carWaiting)&& vh.x<=viewpos)
        {
                cfCalOneStep(vh,lane);
                return;
        }
        if (stopACC(vh,accend))
        {
                return;
        }

        //find gap leader and gap follower
        vh.offgapIder=lane.vlist.findOffGapL(vh);
        if (null!=vh.offgapIder)
                vh.offgapflwer=vh.offgapIder.getFollower();
        else
                vh.offgapflwer=lane.vlist.findOffGapF(vh);
        DVS ldr=vh.getLeader();
        if (null==ldr)
                vh.dvs_GapLeader=vh.offgapIder;
        else
        {
                if (null==vh.offgapIder)
                        vh.dvs_GapLeader=null;
                else if (vh.offgapIder.x<ld.x)
                        vh.dvs_GapLeader=vh.offgapIder;
                else
                        vh.dvs_GapLeader=ldr;
        }

        vh.dvs_GapFollower=vh.offgapflwer;

        if (null==vh.dvs_GapLeader)
```

```
                cfCalOneStep(vh,lane);
        else
        {
                if (null==vh.dvs_GapFollower)
                {
                        cfCalOneStep(vh,lane);//with the gap leader
                }
                else//apply merging model
                {
                        if (vh.x>=accend-vh.v*vh.v/2/vh.fMinAcc)
                                vh.newacc=vh.fMinAcc;
                        if (gsCal(vh,vh.dvs_GapLeader,fisCfModel,-1));//stick to gap?
                                return;
                        float ttcl,ttcf;
                        //debug
                        if (vh.x>=accend-getStopD(vh)) //switching gap
                        {
                                ttcl=(vh.v-vh.dvs_GapLeader.v-
                                vh.v)/(vh.dvs_GapLeader.x-vh.x);
                                ttcf=(vh.v-vh.dvs_GapFollower.v)/(vh.x-
                                vh.dvs_GapFollower.x);
                        }
                        else //follow the gap
                        {
                                ttcl=(vh.dvs_GapLeader.v-vh.v)/(vh.dvs_GapLeader.x-
                                vh.x);
                                ttcf=(vh.dvs_GapFollower.v-vh.v)/(vh.x-
                                vh.dvs_GapFollower.x);
                        }
                        vh.newacc=fisMgModel.fisComputer(ttcl,ttcf);
                }
        }

}
```

Reference

[1] Ackroyd, L. W. and A. J. Maddern. J. S. R. Ernest. 1973. 'A Study of Vehicle Merging Behaviour At Rural Motorway Interchanges.' *Traffic Engineering Control*, No. 15, 192-5.

[2] Ahmed, K. D. and A. M. Ben. H. N. Koutsopoulos. R. G. Mishalani. 1996. 'Models of Freeway Lane Changing and Gap Acceptance Behaviour.' *Proceedings of the 13th International Symposium on Transportation and Traffic Theory* (Ed. Lesort, J. B.). 501-15.

[3] Allen, R. W. and R.E Magdaleno. C. Serafin. S. Eckert. T. Sieja. 1997. 'Driver Car Following Behaviour Under Test Track and Open Road Driving Condition.' SAE Paper 970170, SAE.

[4] Bando, M. and K. Hasebe. A. Nakayama. A. Shibata. Y. Sugiyama. 1995. 'Dynamical Model of Traffic Congestion and Numerical Simulation'. Physical Review, Vol. 51(2), 1035-42.

[5] Baron, S. and D. Kleinman. W. Levison. 1970. 'An Optimal Control Model of Human Response.' *Automatica*, No 5, 337-369.

[6] Bekey, G. A. and G. O. Burnham. J. Seo. 1977. 'Control Theoretic Models of Human Drivers in Car Following.' *Human Factors*, Vol. 19(4), 399-413.

[7] Burnham, G. O. and G. A. Bekey. 1976. 'A Heuristic Finite-State Model of the Human Driver in a Car-Following Situation.' *IEEE Transactions on Systems, Man and Cybernetics*. SMC(8), 554-562.

[8] Bernuer, E. and L. Breheret. S. Algers. M. Boero. C. D. Taranto. M. Dougherty. K. Fox. J. Gabard. 'Smartest – Review of Micro-Simulation Models.' University of Leeds, 1998.

[9] Beshr, S. 2000. The Study of Motorway Operation Using A Microscopic Simulation Model, PhD Thesis, University of Southampton.

[10] Blumenfeld, D. E. and G. H. Weiss. 1971. 'Merging from an Acceleration Lane.' *Transportation Science*, Vol. 5(2), 161-168.

[11] Boor, C. MathWorks Inc. 1999. 'Spline Toolbox User's Guide (version 2).' MathWorks Inc.

[12] Brackstone, M and M. McDonald. B. Sultan. 1999. 'Dynamic Behavioural Data Collection Using An Instrumented Vehicle.' *Transportation Research Record*, No. 1689, 9-17.

[13] Brackstone, M. and M. McDonald. 2000. "Car Following: A Historical Review." *Transportation Research (F)*, Vol. 2(4), 181-196.

[14] Branston, D. 1976. 'Models of Single Lane Time Headway Distributions.' *Transportation Science*, Vol. 10(2), 125-148.

[15] Buckley, D. J. 1968. 'A Semi-Poisson Model of Traffic Flow.' *Transportation Science*, Vol. 2 (2). 107-133.

[16] Buckley, J.J. 1993. 'Sugeno Type Controllers are Universal Controllers.' *Fuzzy Sets and Systems*, No. 53, 299-304.

[17] Burrow, I. J. 1974. 'Speed of Cars on Motorways in England.' Transport and Road Research Laboratory, LR 663.

[18] Chandler, F.E. and R. Herman. E.W. Montroll. 1958. 'Traffic Dynamics: Studies in Car Following.' *Operations Research*, Vol. 6, 165-184.

[19] Cleavenger, D. K. and J. Upchurch. 1999. 'Effect of Freeway Ramp Metering on Accidents: The

Arizona Experience.' *ITE Journal*, Vol. 69(8), pp. 2.

[20] Daganzo, C. F. 1981. 'Estimation of Gap Acceptance Parameters Within and Across the Population from Direct Roadside Observation.' *Transportation Research (B)*, Vol. 15(1), 1-15.

[21] Daou, A. 1966. 'On Flow Within Platoons.' *Journal of Australia Road Research*, Vol. 2(7), 4-13.

[22] Donges, E. 1978. 'A Two-Level Model of Driver Steering.' *Human Factors*, Vol. 20(6), 691-707.

[23] Drew, D. 1967. 'Gap Acceptance Characteristics for Ramp-freeway Surveillance and Control.' *Highway Research Record*, No. 157, 108-143

[24] Druitt, S. 1998. 'Some Real Applications of Micro-simulation.' *Traffic Engineering and Control*, Vol. 39(11), 600-7.

[25] Duncan, N. C. 1976. 'Rural Speed-Flow Relations.' Transportation and Road Research Laboratory, LR 705.

[26] Evans, L. and R. Rothery. 1974. 'Detection of the Sign of Relative Motion when Following a Vehicle.' *Human Factors*, Vol. 16, 161-173.

[27] Gazis, D.C. and R. Herman. R.B. Potts. 1959. 'Car-following Theory of Steady-State Traffic Flow.' *Operations Research*, Vol. 7, 499-505.

[28] Gazis, D.C. and R. Herman. R.W. Rothery. 1961. 'Non-linear Follow the Leading Models of Traffic Flow.' *Operations Research*, Vol. 9(4), 545-67.

[29] Gerlough, D. L. 1956. 'Simulation of Freeway Traffic by an Electronic Computer.' *Highway Research Board Proceedings*, Vol. 35, 543-547.

[30] Gipps, P. G., 1981. 'A Behavioural Car-following Model for Computer Simulation.' *Transportation Research (B)*, Vol. 15, 105-111.

[31] Gipps, P. G. 1986. 'A Model for the Structure of Lane-changing Decisions.' *Transportation Research (B)*, Vol. 20(5), 403-414.

[32] Glickstein, A. and S. L. Levy. 1961. 'Application of Digital Simulation Techniques to Highway Design Problems.' *Western Joint Computer Conference*, 39-50.

[33] Haj-Salem, H. and M. Papageorgiou. 1995. 'Ramp Metering Impact on Urban Corridor Traffic: Field Results.' *Transportation Research (A)*, Vol. 29(4), 303-19.

[34] Helly, W. 1959. 'Simulation of Bottlenecks in Single Lane Traffic Flow.' *Proceedings of Symposium on Theory of Traffic Flow*, 207-238.

[35] Herman, R. and E. W. Montroll. R. B. Potts. R. W. Rothery. 1959. 'Traffic Dynamics: Analysis of Stability in Car Following.' *Operational Research*, No. 7, 86-106.

[36] Hoffmann, E.R. and R.G. Mortimer. 1994. 'Drivers' Estimates of Time to Collision.' *Accident Analysis and Prevention*, Vol. 26(4), 511-520.

[37] Hoffmann, E.R. and R.G. Mortimer. 1996. "Scaling of Relative Velocity Between Vehicles." *Accident Analysis and Prevention*, Vol. 28(4), 415-421.

[38] Holland, E. N. 1998. 'A Generalised Stability Criterion for Motorway Traffic.' *Transportation Research (B)*, 32(2), 141-154.

[39] Hollis, E. R. and R. Evans. 1976. 'Motorway Traffic Patterns.' Transport and Road Research Laboratory, LR 705.

[40] Hounsell, N. B. and S. R. Barnard. M. McDonald. 1992. 'An Investigation of Flow Breakdown and

Merge Capacity on Motorways.' TRL Contractor Report (CR 338)

[41] Hounsell, N. B. and S. R. Barnard. M. McDonald, 1994. 'Capacity and Flow Breakdown on UK Motorways.' *Proceedings of the Second International Symposium on Highway Capacity*, Vol. 1, 277-94.

[42] Huberman, M. 1982. 'The development and Evaluation of a Technique for Measuring Vehicle Acceleration on Highway Entrance Ramps.' *Proceedings of the Roads and Transportation Association of Canada Forum.* Vol. 4(2), 90-96.

[43] ITE. 1976. 'Transportation and Traffic Engineering Handbook.' Washington DC.

[44] Jang, R. 1994. 'Stand-alone C Codes for Fuzzy Inference Systems.' MathWorks, Inc.

[45] Kercel, S. W. and W. B. Dress. 1995. 'Anticipatory Pre-crash Restraint Sensor Feasibility Study: Final Report.' Oak Ridge National Lab.

[46] Kikuchi, S. and P. Chakroborty. 1992. "Car-following Model Based on Fuzzy Inference System." *Transportation Research Record*, No.1365, 82-91.

[47] Kikuchi, S. 1996. 'Fuzzy Inference-based Driver Decision Processes and Traffic Flow Simulation.' ITS-IDEA Program Project Final Report, Transportation Research Board, USA, pp 27.

[48] Kita, H. 1999. 'A Merging-giveway Interaction Model of Cars in a Merging Section: a Game Theoretic Analysis.' *Transportation Research (A)*, Vol. 33, 305-312

[49] Klir, G. J. and B. Yuan. 1995. *Fuzzy Sets and Fuzzy Logic: Theory and Applications.* Prentice Hall PTR.

[50] Boff, K. R. and J. E. Lincoln. 1988. 'Engineering Data Compendium.' USAF, H. G. Armstrong Medical Research Laboratory, Wright-Patterson AFB, Ohio, (Section 8.1).

[51] Koppa, R. J. 1999. "Human Factors". In *Traffic Flow Theory*, TRB Special Report 165

[52] Kou, C. C. and R. B. Machemehl. 1997. 'Modelling Driver Behaviour During Merge Manoeuvres.' Southwest Region University Transportation Centre Report (SWUTC/97/472840-00064-1), pp305

[53] Kou, C. C. and R. B. Machemehl. 1997. 'Modelling Vehicle Acceleration-Deceleration Behaviour during Merge Manoeuvres.' *Canadian Journal of Civil Engineering*, Vol. 24, 350-358.

[54] Leutzbach, W. and R. Wiedemann. 1986. 'Development and Applications of Traffic Simulation Models at the Karlsruhe Institute fur Verkehrwesen.' *Traffic Engineering and Control*, Vol. 27(5), 270-278.

[55] Lieberman, E. and A. K. Rathi. 1999. 'Traffic Simulation.' In *Traffic Flow Theory*, TRB Special Report 165.

[56] Lunenfeld, H. and. G. J. Alexander. 1990. 'A User's Guide to Positive Guidance (3rd Edition).' Federal Highway Administration, Washington, D.C.

[57] Makigami, Y. and T. Matsuo. 1991. 'Evaluation of Outside and Inside Expressway Ramps Based on Merging Probability.' *Journal of Transportation Engineering*, Vol. 117(1), 57-70.

[58] Malki, H. A. and H. Li. G. Chen. 1994. 'New Design and Stability Analysis of Fuzzy Proportional-Derivative Control Systems.' *IEEE Transactions on Fuzzy Systems*, Vol. 2 (4), 245-254.

[59] Mathewson, J. H. and D. L. Trautman. D. L. Gerlough. 1955. 'Study of Traffic Flow by Simulation.' *Highway Research Board Proceedings*, Vol. 34, 522-530.

[60] MathWorks Inc. 1999. 'Fuzzy Logic Toolbox User's Guide (version 2).' MathWorks Inc.

[61] McDonald, M. and M. A. Brackstone. 1997. 'The Role of the Instrumented Vehicle in the Collection of Data on Driver Behaviour.' *IEE Proceedings of Monitoring of Driver and Vehicle Performance Colloquium*

[62] McDonald, M. and J. Wu. M. Brackstone. 1997. "Development of a Fuzzy Logic Based Microscopic Motorway Simulation Model." *Proceedings of the IEEE Conference on Intelligent Transport Systems.* Boston, USA.

[63] McDonald, M. and M. Brackstone. B. Sultan. 1998. 'Instrumented Vehicle Studies of Traffic Flow Models.' *Proceedings of the Third International Symposium on Highway Capacity*, Vol. 2, 755-773.

[64] McDonald, M. and M. Brackstone. B. Sultan. C. Roach. 2000. "Close Following on the Motorway: Initial Findings of an Instrumented Vehicle Study." *Vision in Vehicles VII* (Ed. Gale, A. G.), Elsevier, North Holland, Amsterdam.

[65] McRuer, D. T. and E.S. Krendel. 1959. "The Human Operator as a Servo System Element." *Journal of the Franklin Institute*, Vol. 267, 381-403.

[66] Michaels, R. M. 1965. 'Perceptual Factors in Car-following.' Proceedings of the Second International Symposium on the Theory of Road Traffic Flow, 44-59.

[67] Michaels, R. M. and J. Fazio. 1989. 'Driver Behaviour Model of Merging.' *Transportation Research Record*, No. 1213, 4-10.

[68] Miller, A. J. 1961. 'A Queuing Model for Road Traffic Flow.' *Journal of Royal Statistical Society*, Series B. Vol. 23(1), 64-75.

[69] Mine, H. and T. Mimura. 1969. 'Highway Merging Problem with Acceleration Area.' *Transportation Science*, Vol. 3(3), 205-213.

[70] Traffic Management Centre. 1998. 'Trunk Highway 169 – Dynamic Ramp Metering Evaluation.' Minnesota Department of Transportation, Metropolitan Division, pp58.

[71] Monen, J. and E. Brenner. 1994. "Detecting Changes in One's Own Velocity from the Optic Flow." *Perception*, Vol. 23, 681-690

[72] Papageorgiou, M. and H. Hadj-Salem. F. Middelham. 1991. 'ALINEA: A Local Feedback Control Law for On-ramp Metering.' *Transportation Research Record*, No.1320, 58-64.

[73] Papageorgiou, M. and H. Haj-Salem. J.M. Blosseville. 1997. 'ALINEA Local Ramp Metering: Summary of Field Results.' *Transportation Research Record*, No.1603, 90 – 98.

[74] Perchonok, P. A. and S. L. Levy. 1960. 'Application of Digital Simulation Techniques to Freeway On-ramp Traffic Operations.' *Proceedings of the 39th Highway Research Board Annual Meeting*, Vol. 39. 506-523

[75] Polus, A. and M. Livneh, 1985. 'Comments on Flow Characteristics on Acceleration Lanes.' *Transportation Research (A)*, 21(1), 39-46.

[76] Polus, A. and M. Livneh. 1987. 'Vehicle Flow Characteristics on Acceleration Lanes.' *Journal of Transportation Engineering*, Vol. 111(6), 595-606.

[77] Rao, L. and L. Owen. 2000. 'Validation of High-Fidelity Traffic Simulation Models.' *Proceedings of the 79th Annual Meeting of Transportation Research Board,* Washington D. C.

[78] Rasmussen, J. 1983. 'Skills, Rules, Knowledge: Signals, Signs and Symbols and Other Distinctions in Human Performance Models.' *IEEE Transactions: Systems, Man & Cybernetics*, SMC(13), 257-67.

[79] Rasmussen, J. and A. Pejtersen. L. Goodstein. 1992. *Cognitive Engineering -- Concepts and Applications, Part1: Concepts.* John Wiley, New York.

[80] Rockwell, T. H. and R. L. Ernst. A. Hanken. 1968. 'A Sensitivity Analysis of Empirically Derived Car Following Models.' *Transportation Research*, Vol. 2(4), 363-73.

[81] Roess, R. B. and J. M. Ulerio. 1994. 'New Capacity Analysis Procedures for Ramp-freeway Terminals.' *Proceedings of the Second International Symposium on Highway Capacity*, Volume 2, 503-22

[82] Rosen, R. 1985. *Anticipatory systems: Philosophical, Mathematical, and Methodological Foundations.* Pergamon Press, Oxford.

[83] Rothery, R. W. 1999. 'Car Following Models.' In *Traffic Flow Theory*, TRB Report 165.

[84] Rouse, W. B. 1983. 'Fuzzy Models of Human Problem Solving.' *Advances in Fuzzy Set, Possibility Theory and Application* (Ed: Wang, P. P.), Plenum Press, New York.

[85] Schofield, M. J. and L. Neal. T. Mclean. 1999. 'Ramp Metering – 10 Years on. ' *Proceedings of Seminar D at the AET European Transport Conference*, Vol. P432, 305-16, Cambridge.

[86] Shih, T. Y. and M. Yang. 2001. 'The Performance of GPS Standard Positioning Service Without Selective Availability.' *Survey Review*, Vol. 36 (281), 192-201.

[87] Sidaway, B. and M. Fairweather. H. Sekiya. J. Mcnitt-Gray. 1996. "Time-to-Collision Estimation in a Simulated Driving Task." *Human Factors*, Vol. 38(1), 101-113.

[88] Skabardonis, A. 1981. 'A Model of Traffic Flow at Ramp Entries.' PhD Thesis, University of Southampton.

[89] Skabardonis, A. 1985. 'Modelling the Traffic Behaviour at Grade-Separated Interchanges.' *Traffic Engineering & Control*, Vol. 26(9), 410-415.

[90] Szwed, N. and N. M. H. Smith. 1974. 'Gap Acceptance and Merging.' *Proceedings of Australian Road Research Board*, Vol. 7(4), 126-151.

[91] Tafti, M. F. 2000. 'Observations of Traffic Behaviour at Two Merge Sites on British Motorways'. *Proceedings of UTSG Conference*, Vol. 3, Oxford

[92] Taylor, C. and D. Meldrum. 2000. 'Evaluation of a Fuzzy Logic Ramp Metering Algorithm: A Comparative Study Among Three Ramp Metering Algorithms Used in the Greater Seattle Area.' Report No. WA-RD 481.2, Washington State Department of Transportation

[93] Tanaka, K and M. Sugeno. 1992. 'Stability Analysis and Design of Fuzzy Control Systems.' *Fuzzy Sets and Systems*, Vol. 45, 135-156.

[94] Thathachar, M. A. L. and P. Viswanath. 1997. 'On the Stability of Fuzzy Systems.' *IEEE Transactions on Fuzzy Systems*, Vol. 5(1), 145-151.

[95] Tolle, J. E. 1971. 'The Lognormal Headway Distribution Model.' *Traffic Engineering and Control*, Vol. 13(1), 22-24.

[96] Torf, A. S. and L. Duckstein. 1966. 'A Methodology for the Determination of Driver Perceptual Latency in Car Following.' *Human Factors*, Vol. 8(5), 441-447.

[97] Van AS, S. C. 1979. 'Traffic Signal Optimisation – Procedures and Techniques.' PhD Thesis, University of Southampton.

[98] Van der Hurlst, M. and T. Rothengatter. T. Meijman. 1998. 'Strategic Adaptations to Lack of Preview in Driving.' *Transportation Research (F)*, Vol. 1(1), 59-75.

[99] Van der Hurlst, M. and T. Meijman. T. Rothengatter. 1999. 'Anticipation and the Adaptive Control of Safety Margins in Driving.' *Ergonomics*, Vol. 42(2), 336-345.

[100] Vermijs, R.G.M. 1991. 'The Use of Micro Simulation for the Design of Weaving Sections.' *Proceedings of International Symposium on Highway Capacity*, 419-27.

[101] Wichens, C.D. 1992. *Engineering Psychology and Human Performance (2nd Edition).* HarperCollins Publishers Inc., New York.

[102] Wisconsin Department of Transportation. 2000. 'Ramp Metering (Chapter 3).' Intelligent Transportation Systems (ITS) Design Manual.

[103] Wu, J. and M. Brackstone. M. McDonald. 2000. 'Fuzzy Sets and Systems for a Motorway Microscopic Simulation Model.' *Fuzzy Sets and Systems*, Vol. 116, 65-76.

[104] Zhang, H. M. and S. G. Ritchie. W. W. Recker. 1996. 'Some General Results on the Optimal Ramp Control Problem.' *Transportation research(C),* Vol. 4(2), 51-69.

[105] Zhang, X. and D. F. Jarrett. 1997. 'Stability Analysis of the Classic Car-Following Model.' *Transportation Research (B)*, Vol. 31(6), 441-462.

[106] Zheng, P. 1997. 'Objective Assessment System on Navigation Simulator.' *Chinese Navigation*, Vol. 38(1), 46-52

[107] Zheng, P. and M. McDonald, 2001. 'Identifying Best Predictors for Car Following Behaviour from Empirical Data.' *Proceedings of 13th European Simulation Symposium*, 158-165.

[108] Strategic Test Scandinavia AB. 2002. *VBOX - Non-Contact Speed Measurement Using GPS* [WWW]. http://www.strategic-test.com/support/download/vbox_literature.pdf (12 August 2002)